A NOPALINE-TYPE *OVERDRIVE* ELEMENT, AND ITS INFLUENCE UPON *AGROBACTERIUM*-MEDIATED TRANSFORMATION FREQUENCY AND T-DNA COPY NUMBER IN *NICOTIANA TABACUM*

A Thesis presented in partial fulfilment of
the requirements for the degree of
Doctor of Philosophy in Molecular Genetics
at Massey University, Palmerston North,
New Zealand/Aotearoa

ANDREW GILBERT GRIFFITHS

1996

Dedication

This Thesis is
dedicated to my parents

Juliet, Merv and Pauline

and to Tina

ABSTRACT

Overdrive is an enhancer element located outside and adjacent to the right border of the T-DNA in *Agrobacterium tumefaciens* octopine-type tumour-inducing (Ti) plasmids. This element is necessary for maximal enhancement of T-strand production and subsequent *A. tumefaciens*-mediated plant transformation frequency, and only the octopine-type *overdrive* had been characterised in any detail. A putative *overdrive* has been identified in the nopaline-type Ti-plasmid pTiT37 on the basis of its homology with known octopine-type *overdrive* sequences, particularly the eight base-pair so-called *overdrive* consensus core. The putative nopaline-type *overdrive* core, however, is only 75% homologous to that of all known *overdrive* core regions. Furthermore, as there are other sequences throughout the nopaline-type T-region that share 75% homology with the *overdrive* consensus core, the precise location of the nopaline-type *overdrive* is undetermined, although all nopaline-type T-region fragments exhibiting *overdrive*-like activity contained the putative *overdrive* core adjacent to the right border. The role of this particular putative core in T-DNA transfer has never been established.

Deletions were made in the putative nopaline-type *overdrive* consensus core adjacent to the right border of a binary plant transformation vector derived from pTiT37. This was to establish whether this putative *overdrive* core does have a role as a transmission enhancer as proposed (Peralta *et al*., 1986; Van Haaren *et al*., 1988; Culianez-Macia and Hepburn, 1988). Two deletions were selected for the full study. The first encompassed the putative nopaline-type *overdrive* core flanked by 3 bp (5′) upstream, and 4 bp (3′) downstream, and was located in pANDY9. The other, located in pANDY10, encompassed the putative consensus core plus the entire region sharing homology with the octopine-type *overdrive*. This second deletion was to determine whether the core alone could account for *overdrive*-like activity, or whether further sequences are necessary to produce the effect. The vector with no deletions in the putative nopaline-type *overdrive* region was pANDY8.

As determined by quantitative *Nicotiana tabacum* transformation assays, both deletions of the putative nopaline-type *overdrive* core (pANDY9, pANDY10) equally decreased the rate at which calli appeared, and equally decreased transformation frequency by 47% compared with that of pANDY8. That deletion of the putative core influenced plant transformation frequency provided strong evidence that it was indeed an *overdrive*-like core. Furthermore, in a *virC2* mutant environment, the plant transformation frequency was reduced markedly for all three plasmids (approximately

90% reduction compared to when in the wild-type *vir* environment). However, there was no difference in the plant transformation frequencies of the pANDY8-10 series in a *virC2* environment. This indicated that the mechanism by which the deletions influenced plant transformation frequency did not act independently of the *virC* operon, which is further evidence of *overdrive*-like activity.

The type of *vir* regulon influenced the effect of the deletions in the putative *overdrive*. The transformation frequency of the plasmid with the intact putative *overdrive* region (pANDY8) was very similar in both an octopine-type *vir* environment (21.7 organogenic calli per 10 leaf discs in LBA4404) and a nopaline-type *vir* environment (18.7 organogenic calli per 10 leaf discs). However, in an octopine-type *vir* environment, deletions in the putative core resulted in a 47% decrease in transformation frequency, whereas in a nopaline-type *vir* environment the deletions had no effect upon transformation frequency. This may be due to a higher level of *vir* gene products (a feature associated with nopaline-type *vir* regulons), particularly VirD1 and VirD2 compensating for the lack of a fully active putative *overdrive.*

Southern analysis of plants arising from the transformation experiments (in an octopine-type *vir* environment) revealed that removal of the putative nopaline-type *overdrive* core halved the incidence of multiple T-DNA insertion events from 34.7% (pANDY8, intact nopaline-type *overdrive*) to 12.2% (pANDY9) and 14.3% (pANDY10). Deletion of the nopaline-type *overdrive* core also restricted the insert number to a maximum of two, rather than four or more. This is the first time that deletions in the regions outside the T-DNA have been shown to influence T-DNA copy number.

ACKNOWLEDGEMENTS

I wish to thank my supervisors, Dr Derek White and Professor Barry Scott for encouragement and guidance through the course of this project. I would particularly like to thank Dr Derek White for the use of facilities and resources in the Plant Molecular Genetics Laboratory at AgResearch Grasslands, as well as financial assistance for the preparation of this thesis. I am also grateful for the financial assistance provided by a University Grants Committee post-graduate scholarship, and a William Georghetti scholarship, during the course of this study.

I would like to thank Professor Paul Hooykaas for the gift of *Agrobacterium tumefaciens* strains, MOG1010 and MOG1010-C, and Paul Sanders for the gift of *Arabidopsis thaliana* ecotype, No-0, and particularly Donald Kerr for the generous gift of his promoter-tagging vector, pBIN19/GTG.

Thanks to Nick Ellison for brilliant Mac support, and Helen Dick for the generous loan of a computer, and both Helen and Bob Fletcher for statistical guidance. And to Steven, Ann, Sarah and Barbara of the CRI Campus Library-thanks for your efforts and humour-they don't pay you enough!!

A special thanks to Peter Spring, as well as Derek Charlton for photographic work.

And to all those past and present comprising the Plant Molecular Genetics Laboratory: Derek, Jacqui, Donald, Roy, Thomas, Marg (Xena), Feri, Brigi, Shashi, Erika, Nick, Dale, Alicia, Kez, Dorothy, Don and Trish, and especially Fran, Anya and Blackie, Lorelle, Bron and Andrew, Wendy and Sarah (honourary members). I wish to thank you all for your knowledge, friendship and encouragement, and for helping make science a fun place to be.

A special thank you to Mum, Dad, Pauline, Gran, Dean, Nils, John and Kaisu, just for being there.

Thanks too to the Voisey clan: Hilly, Peter, Jane, Pole, Lindy, Susie and Graham, (and Oscar!!) for the generous welcome, and for bravely leaving a daughter/sister/aunt on this side of the planet.

And I am especially grateful to my partner in crime and in life, Dr Christine Voisey, not only for her excellent proofing skills, but for her support, encouragement and love.

ABBREVIATIONS

A	ampere
A_{260}	absorbance [$\log(I_0/I)$] in a 1 cm light path at 260 nm
Ap	ampicillin
ATP	adenosine 5′-triphosphate
BAP	6-benzylaminopurine
bla	gene encoding β-lactamase which confers resistance to ampicillin and carbenicillin
bp	base-pair
BSA	bovine serum albumin
°C	degree Celcius
Cb	carbenicillin
Ci	curie (3.7×10^{10} nuclear disintegrations s^{-1}; 37 GBq)
cpm	counts per minute
CTAB	hexadecyltrimethylammonium bromide
2,4-D	2,4-dichlorophenoxyacetic acid
dATP	2′-deoxyadenosine 5′-triphosphate
dCTP	2′-deoxycytidine 5′-triphosphate
DEAE	diethylaminoethyl
DMF	dimethyl formamide
dGTP	2′-deoxyguanosine 5′-triphosphate
DMSO	dimethyl sulphoxide
DNA	deoxyribonucleic acid
DNase	deoxyribonuclease
DTT	dithiothreitol
dTTP	2′-deoxythymidine 5′-triphosphate
EDTA	ethylenediaminetetraacetic acid
EDTA(Fe)	ethylenediaminetetraacetic acid, ferric-sodium salt
EDTA(Na_2)	ethylenediaminetetraacetic acid, disodium salt
EGTA	ethylenebis(oxyethylenenitrilo)tetraacetic acid
g	gram
g	acceleration due to gravity (9.81 m s^{-2})
GUS	β-glucuronidase
gusA	gene encoding β-glucuronidase (syn. *uidA*)
h	hour
HEPES	4-(2-hydroxyethyl)-1-piperazineethanesulphonic acid
Hoechst 33258	2′-[4-hydroxyphenyl]-5-[4-methyl-1-piperazinyl]-2,5′-bis-1H-benzimidazole; bisbenzimide
IAA	indole-3-acetic acid
IBA	indole-3-butyric acid
2ip	6-(γ-γ-dimethylallylamino)purine
IPTG	isopropyl-β-D-thiogalactopyranoside

kΩ	kiloohm
kb	kilobase-pairs
Kinetin	6-fufurylaminopurine
Km	kanamycin
kV	kilovolt
LB	left border from T-DNA of *Agrobacterium tumefaciens*
l	litre
M	Molar, moles per litre
mcs	multiple cloning site
mcs-P_{35S}-*nptII*	an NPTII-encoding gene under the control of a P_{35S} promoter with a pUC18 mcs located 5′ of the P_{35S}
MES	2-[N-morpholino]ethanesulphonic acid
μF	microFarad (capacitance) (A s V^{-1})
μg	microgram
μm	micrometre
mg	milligram
min	minute
MilliQ water	water that has been purifed by passing through a MilliQ ion exchange column
mM	millimolar
mm	millimetre
mol	mole
M_r	relative molecular mass (g mol^{-1})
ms	millisecond
ng	nanogram
nptII	gene from Tn5 coding for neomycin phosphotransferase
NPTII	neomycin phosphotransferase which confers resistance to kanamycin
OD	*overdrive*
OD_{600}	optical density at 600 nm in a 1 cm light path
Ω	ohm (electrical resistance) (V A^{-1})
*ocs*3′	transcription-termination sequence of the octopine synthase gene
oriV	origin of replication
P_{35S}	the promoter of the Cauliflower Mosaic Virus 35S RNA subunit
P_{35S}-*nptII*	an NPTII coding gene under the control of the P_{35S} promoter
P_{nos}	the promoter of the plant-expressed nopaline synthase gene from *Agrobacterium tumefaciens*
P_{nos}-*nptII*	an NPTII coding gene under the control of the P_{nos} promoter
PEG	poly(ethylene glycol)
PVP	polyvinylpyrrolidone
RB	right border from T-DNA of *Agrobacterium tumefaciens*
Rf	rifampicin
RNA	ribonucleic acid
RNase	ribonuclease
rpm	revolutions per minute

s	second (time)
SDS	sodium dodecyl sulphate
Sm	streptomycin
Sp	spectinomycin
SSPE	saline, sodium phosphate, and EDTA buffer
Tc	tetracycline
TE	Tris (10.0 mM), EDTA (1.0 mM) pH 8.0
TEMED	*N,N,N′,N′*-tetramethylethylenediamine
Tm	timentin
Tris	tris(hydroxymethyl)aminomethane
Triton X-100	octylphenoxy polyethoxyethanol
U	units
UV	ultraviolet light
UV-A	near UV (315-400 nm)
V	volt (m^2 kg s^{-3} A^{-1})
v/v	volume per volume
vol	volume
W	watt (m^2 kg s^{-3}) or (V A)
w/v	weight per volume
X-gal	5-bromo-4-chloro-3-indolyl-β-D-galactopyranoside
X-gluc	5-bromo-4-chloro-3-indolyl-β-D-glucuronide
Zeatin	6-(4-hydroxy-3-methyl-but-2-enylamino)purine

TABLE OF CONTENTS

Page

ABSTRACT iii
ACKNOWLEDGEMENTS v
ABBREVIATIONS vi
TABLE OF CONTENTS ix
LIST OF TABLES xvi
LIST OF FIGURES xvii

CHAPTER 1 INTRODUCTION 1
OVERVIEW 1

1.1 *AGROBACTERIUM TUMEFACIENS*: GENETIC COLONISER . . . 4

1.2 *A. TUMEFACIENS*: PLANT GENETIC ENGINEER 7

1.3 *A. TUMEFACIENS*-MEDIATED PLANT TRANSFORMATION . . . 8
1.3.1 Ti-plasmid Structure 8
1.3.2 Induction of *vir* Genes 11
1.3.3 T-DNA Generation 17
1.3.4 T-complex Transfer 19
1.3.5 Nuclear Localisation 20
1.3.6 Integration into Plant Nuclear DNA 22

1.4 THE *OVERDRIVE* T-DNA TRANSMISSION ENHANCER 23
1.4.1 Discovery of *Overdrive* 23
1.4.3 Characterising *Overdrive* 26
1.4.4 Role of *Overdrive* 28
1.4.5 *Overdrive* and the *virC* Operon 29
1.4.6 Is There a Nopaline-type *Overdrive*? 31

1.5 *OVERDRIVE* AND MULTIPLE T-DNA COPIES IN TRANSGENIC PLANTS 35

1.6 AIMS 36

CHAPTER 2 MATERIALS AND METHODS 37
2.1 BACTERIAL PROCEDURES 37
2.1.1 Growth of Bacteria 37
2.1.2 Bacterial Strains and Plasmids 37
2.1.3 Transformation of *A. tumefaciens*: Tri-parental Mating 37
2.1.4 Transformation of *A. tumefaciens*: Electroporation 40
2.1.5 Preparation of Electrocompetent *A. tumefaciens* Cells 41
2.1.6 Transformation of *E.coli*: $CaCl_2$ Method 41
2.1.7 Preparation of Competent *E. coli* Cells with $CaCl_2$ 41
2.1.8 Transformation of *E. coli*: Electroporation 42
2.1.9 Preparation of Electrocompetent *E. coli* Cells 43

2.2 DNA PROCEDURES 43
2.2.1 Plasmid Isolation from *A. tumefaciens*: Alkaline Lysis 43
2.2.2 Plasmid Isolation from *E. coli*: STET Method 44
2.2.3 Plasmid Isolation from *E. coli*: Large Scale Alkaline Lysis . . 44
2.2.4 Precipitation of DNA 45
2.2.5 DNA Quantification by Spectrophotometry 45
2.2.6 DNA Quantification by Serial Dilution on Agarose Gels 45
2.2.7 DNA Quantification by Fluorometry 46
2.2.8 Determining DNA Fragment Size 46
2.2.9 Agarose Gel Electrophoresis of DNA 46
2.2.10 DNA Recovery from Agarose Gels: DEAE-Cellulose Method . 47
2.2.11 DNA Recovery from Agarose: Silica Powder Method 48
2.2.12 DNA Recovery from Agarose: Spin-Column Method 48
2.2.13 Restriction Digestion of Plasmid DNA 49
2.2.14 Partial *Eco*RI Digestion of *Hin*dIII-linearised Plasmid DNA . . 49
2.2.15 Exonuclease BAL 31 Deletions in pANDY6 49
2.2.16 End-filling 5′ Overhangs 50
2.2.17 Recessing 3′ Overhangs 51
2.2.18 CAP-Treatment of Vector DNA 51
2.2.19 DNA Ligation 51
2.2.20 Screening Recombinant Plasmids: β-Galactosidase Method . . . 52
2.2.21 Screening Recombinant Plasmids: Rapid Colony Lysis 52
2.2.22 DNA Sequence Analysis: Sequencing Reactions 52
2.2.23 DNA Sequence Analysis: Sequencing Gels 53

2.3 PLANT PROCEDURES 54
2.3.1 Growth of *Arabidopsis thaliana* 54
2.3.2 *A. thaliana*: Bulk Seed Production 54
2.3.3 *A. thaliana*: Seed Sterilisation and Germination 54
2.3.4 *A. thaliana*: Producing Root Explants 55
2.3.5 Growth of *Nicotiana tabacum* 55
2.3.6 *N. tabacum*: Producing Leaf Disc Explants 55
2.3.7 Plant Transformation 55
2.3.8 Plant Transformation: *Arabidopsis thaliana* 56
2.3.9 Plant Transformation: *Nicotiana tabacum* 57

2.4 SOUTHERN ANALYSIS 58
2.4.1 Isolation of *N. tabacum* Genomic DNA 58
2.4.2 Restriction Digestion and Electrophoresis of Genomic DNA . . 58
2.4.3 Southern Blotting: Conventional Alkaline Transfer 59
2.4.4 Southern Blotting: Downward Alkaline Transfer 59
2.4.5 Preparing [^{32}P]-Labelled Probe DNA 60
2.4.6 Purifying [^{32}P]-Labelled Probe DNA 61
2.4.7 Hybridisation: SSPE Method 61
2.4.8 Hybridisation: SDS Method 62
2.4.9 Stripping Blots 62

CHAPTER 3 RESULTS 63
PART I VECTOR CONSTRUCTION 63
3.1 DELETING THE PUTATIVE *OVERDRIVE* CORE 63
3.1.1 Overview 63
3.1.2 Optimising Partial *Eco*RI Digestion of pBIN19/GTG 63
3.1.3 Removal of P_{nos}-*nptII* fusion to create pANDY6 68
3.1.4 Optimising BAL 31 Reaction Conditions 68
3.1.5 Identifying Clones with Putative Deletions in *Overdrive* 73
3.1.6 Sequencing Deletions in the Putative *overdrive* Region 73

3.2 MODIFYING P_{35S}-*nptII* PLANT SELECTABLE MARKER 78
3.2.1 Overview 78
3.2.2 Preparing P_{35S}-*nptII* Fusion for Attachment of an mcs 78
3.2.3 Attaching pUC18 mcs to P_{35S}-*nptII* Fusion 82

3.2.4 Preparing mcs-P_{35S}-*nptII* for Insertion into pANDY6, pANDYOD⁻ Vector Series 85
3.2.5 Sequencing Junctions of mcs-P_{35S}-*nptII* in pANDY4 87

3.3 COMPLETION OF pANDY VECTOR SERIES 92
3.3.1 Overview 92
3.3.2 Construction of pANDY8, pANDY9, and pANDY10 92
3.3.3 Sequencing Junctions of mcs-P_{35S}-*nptII* in pANDY8 to pANDY10 92
3.3.4 Transferring pANDY8-10 Series to *A. tumefaciens* 97

3.6 SUMMARY OF VECTOR MODIFICATIONS 100

PART II PLANT TRANSFORMATION EXPERIMENTS 101
3.7 *OVERDRIVE* AND PLANT TRANSFORMATION 101
3.7.1 *N. tabacum* Transformation Experimental Design 101
3.7.2 *Overdrive* and Callus Production in *N. tabacum*: a Time-Course 101
3.7.3 The *overdrive* and Production of Callus, Green Callus, and Organogenic Callus in *N. tabacum* 103
3.7.4 *Overdrive* and Other Strains of *A. tumefaciens* 106
3.7.5 *Overdrive* and *vir* Environment 106
3.7.6 *Overdrive* and the *virC* Operon 111
3.7.7 *Overdrive* and *Arabidopsis thaliana* 111

3.8 DETERMINING T-DNA COPY NUMBER IN *N. TABACUM* . . 114
3.8.1 Determining T-DNA Copy Number 114
3.8.2 T-DNA Copy Number 123
3.8.3 Spread of T-DNA Copy Number 123

CHAPTER 4 DISCUSSION 126
4.1 ANALYSING THE PUTATIVE NOPALINE-TYPE *OVERDRIVE* 126
4.1.1 Identification of Regions Necessary for Function of the Putative Nopaline-type *Overdrive* 127
4.1.2 The Putative Nopaline-type *Overdrive* does not Influence Processes after T-DNA Transfer 128
4.1.3 Nopaline vs Octopine-type *vir* Environment 129

4.1.4 Was Putative Nopaline-type *Overdrive* Activity Abolished? . 130
4.1.5 Importance of Sequences between the Right Border and the *Overdrive* Region 133
4.1.6 Importance of the *Overdrive* Consensus Core 136
4.1.7 Is the Putative Nopaline-Type *Overdrive* Core an *Overdrve* Core? 136
4.1.8 Biological Significance of *Overdrive* 138a
4.1.9 *Overdrive* in other DNA Transfer Systems 138a

4.2 INFLUENCE OF *OVERDRIVE* ON T-DNA COPY NUMBER . . 139

4.3 IMPLICATIONS OF T-DNA COPY NUMBER 142
4.3.1 T-DNA Copy Number and Transformation Frequency in Plant Transformation Systems 142
4.3.2 T-DNA Copy Number and Transformation Frequency in Gene-Tagging 143

4.4 FUTURE DIRECTIONS 145

4.5 SUMMARY 145

REFERENCES 146

APPENDICES 163
APPENDIX 1: BACTERIAL MEDIA 163
A1.1 AB Minimal Medium 163
A1.2 LB (Luria-Bertani) Medium 163
A1.3 SOB Medium 163
A1.4 SOC Medium 163
A1.5 TY Medium 164
A1.6 YEB Medium 164
A1.7 YM Medium 164

APPENDIX 2: PLANT MEDIA 165
A2.1 GM Medium 165
A2.2 ARM Media Base 165
A2.3 ARM I Medium 165
A2.4 ARM II Medium 165

A2.5 ARM III Medium 166
A2.6 ½MS Medium 166
A2.7 Nic I Medium 166
A2.8 Nic II Medium 166
A2.9 Nic III Medium 166

APPENDIX 3: MEDIA STOCK SOLUTIONS 167
A3.1 Antibiotics 167
A3.2 Phytohormones 167
A3.3 MS Stock Solutions 167
A3.4 Acetosyringone 168

APPENDIX 4: SOLUTIONS AND BUFFERS FOR DNA 169
A4.1 1 M Tris-HCl, pH 8.0 169
A4.2 0.5 M EDTA(Na_2), pH 8.0 169
A4.3 TE Buffer 169
A4.4 DNase-Free RNase-A 169
A4.5 Cell Resuspension Buffer 169
A4.6 Cell Lysis Solution 169
A4.7 STET Lysis Buffer 169
A4.8 Equilibrated Phenol 170
A4.9 TNE Fluorometry Buffer 170
A4.10 DNA Fragment Size Standards 170
A4.11 TAE Buffer 170
A4.12 SUDS 170
A4.13 GLB 171
A4.14 DEAE Elution Buffer 171
A4.15 Restriction Endonuclease Dilution Buffer 171
A4.16 5× Blunt End Ligation Buffer 171
A4.17 2× Cracking Buffer 171
A4.18 TBE Buffer for Sequencing Gels 171
A4.19 40% Acrylamide Solution 171
A4.20 Nucleotide TLC Phosphate Buffer 172
A4.21 TE-Equilibrated Sepharose CL-6B Resin 172
A4.22 20× SSPE 172
A4.23 100× Denhardt's Solution 172
A4.24 SSPE Hybridisation Solution 172
A4.25 Fragmented Herring Testes DNA 172

A4.26 2× SSPE Wash 173
A4.27 1× SSPE Wash 173
A4.28 0.1× SSPE Wash 173
A4.29 1 M Disodium Phosphate Buffer, pH 7.2 173
A4.30 SDS Hybridisation Solution 173
A4.31 SDS Wash Solution 173
A4.32 Genomic Extraction Buffer 173

APPENDIX 5: SEQUENCE DATA FROM pANDY4 174
A5.1 Sequence data from the junction of pMTL25P through the pUC18 mcs to the $P_{mas2'}$ promoter of the mcs-P_{35S}-*nptII* fusion 174
A5.2 Sequence data from the junction of pMTL25P through to the *ocs*3′ terminator of the mcs-P_{35S}-*nptII* fusion 175

APPENDIX 6: PLASMID MAPS 176
A6.1 pBIN19/GTG 176
A6.2 pANDY6 177
A6.3 pANDYOD^{-}2 and pANDYOD^{-}3 178
A6.4 pSLJ491 179
A6.5 pMTL22P 180
A6.6 pMTL25P 181
A6.7 pUC18 182
A6.8 pANDY1 183
A6.9 pANDY2 184
A6.10 pANDY3 185
A6.11 pANDY4 186
A6.12 pANDY8, pANDY9, and pANDY10 187
A6.13 pJIT166 188

APPENDIX 7: SOUTHERN ANALYSIS DATA 189

LIST OF TABLES

		Page
Table 1.	Bacterial strains and plasmids used in this study.	38
Table 2.	Southern analysis using a [^{32}P]-labelled *nptII* left border probe with *Hin*dIII and *Eco*RI-digested genomic DNA from plants transformed with pANDY8.	189
Table 3.	Southern analysis using a [^{32}P]-labelled *nptII* left border probe with *Hin*dIII and *Eco*RI-digested genomic DNA from plants transformed with pANDY9.	192
Table 4.	Southern analysis using a [^{32}P]-labelled *nptII* left border probe with *Hin*dIII and *Eco*RI-digested genomic DNA from plants transformed with pANDY10.	194
Table 5.	Southern analysis using a [^{32}P]-labelled *gusA* right border probe with *Hin*dIII and *Eco*RI-digested genomic DNA from plants transformed with pANDY8.	195
Table 6.	Southern analysis using a [^{32}P]-labelled *gusA* right border probe with *Hin*dIII and *Eco*RI-digested genomic DNA from plants transformed with pANDY9.	196
Table 7.	Southern analysis using a [^{32}P]-labelled *gusA* right border probe with *Hin*dIII and *Eco*RI-digested genomic DNA from plants transformed with pANDY10.	197

LIST OF FIGURES

		Page
Figure 1A-B.	Comparison of the octopine and nopaline-type Ti-plasmids. . . .	9
Figure 2.	Overview of the molecular processes involved in *Agrobacterium tumefaciens*-mediated plant transformation. . .	13
Figure 3.	Comparison of *overdrive*-like sequences in right border regions of the octopine-type pTiA6NC T_L- and T_R-DNA, the nopaline-type pTiT37, and the *Agrobacterium rhizogenes* pRiA6 T_L-DNA.	24
Figure 4.	Characterising the octopine-type *overdrive*.	27
Figure 5.	Comparison of *overdrive*-like sequences in right border regions of a range of Ti- and Ri-plasmids.	32
Figure 6.	Summary of construction of pANDY6, pANDYOD$^-$2, and pANDYOD$^-$3.	64
Figure 7.	Fragments generated by a partial *Eco*RI digestion of *Hin*dIII-linearised pBIN19/GTG.	65
Figure 8.	Establishing the optimal *Eco*RI concentration for production of partially *Eco*RI-digested fragments of *Hin*dIII-linearised pBIN19/GTG.	67
Figure 9A-B.	Identification of pANDY6.	69
Figure 10A-C.	Optimising BAL 31 reaction conditions.	71
Figure 11.	Identification of clones with deletions in the putative nopaline-type *overdrive* core.	74
Figure 12A-B.	Sequence data detailing various deletions centred upon the putative nopaline-type *overdrive* core of the pANDYOD$^-$ series.	76

Figure 13. Summary of modification of the P_{35S}-*nptII* fusion prior to its insertion 79

Figure 14A-C. Determining orientation of the P_{35S}-*nptII* insert with regard to the pUC18 mcs during construction of pANDY2. 83

Figure 15. Restoration of the *Eco*RI site during the construction of pANDY4. 88

Figure 16A-C. Nucleotide sequence of the junctions of the mcs-P_{35S}-*nptII* fusion with pMTL25P in pANDY4. 90

Figure 17. Summary of construction of pANDY8, pANDY9, and pANDY10 93

Figure 18A-D. Identification of plasmids pANDY8, pANDY9, and pANDY10. 95

Figure 19A-D. Identification of *A. tumefaciens* strain LBA4404 colonies harbouring either pANDY8, pANDY9, or pANDY10. 98

Figure 20. Deletions in the putative nopaline-type *overdrive* region of plant transformation vectors, and their influence upon mean cumulative callus production (calli per 10 leaf discs) plotted against time (days after cocultivation). 102

Figure 21. Deletions in the putative nopaline-type *overdrive*, and their influence upon the production of callus, green callus, and organogenic callus (transformation frequency), after a 60 day cultivation period on a selective medium. 104

Figure 22. Deletions in the putative nopaline-type *overdrive*, and their influence upon the proportion (%) of *N. tabacum* calli that became green, and the proportion (%) of green calli that became organogenic, after a 60 day cultivation period on a selective medium. 104

Figure 23A-C. Deletions in the putative nopaline-type *overdrive* region of the plant transformation vectors (pANDY8-10), and their influence upon callus production in *N. tabacum*, when harboured by LBA4404. 107

Figure 24A-C. Deletions in the putative nopaline-type *overdrive* region of the plant transformation vectors (pANDY8-10), and their influence upon callus production in *N. tabacum*, when harboured by MOG1010. 109

Figure 24D-F. Deletions in the putative nopaline-type *overdrive* region of the plant transformation vectors (pANDY8-10), and their influence upon callus production in *N. tabacum*, when harboured by LBA4404, MOG1010, GV3101, and MOG1010-C. 110a

Figure 25A-C. Deletions in the putative nopaline-type *overdrive* region of the plant transformation vectors (pANDY8-10), and their influence upon callus production in *Arabidopsis thaliana*, when harboured by LBA4404. 113

Figure 26A-C. Determining T-DNA copy number with *Hin*dIII digested plant genomic DNA. 115

Figure 27. Representative *Hin*dIII digest of *N. tabacum* genomic DNA. 117

Figure 28. Representative autoradiograph of *Hin*dIII-digested *N. tabacum* genomic DNA hybridised with [^{32}P]-labelled *nptII* probe. 118

Figure 29A-C. Determining completeness of genomic digestion using *Eco*RI. 120

Figure 30. Representative autoradiograph of *Eco*RI-digested *N. tabacum* genomic DNA hybridised with [^{32}P]-labelled *nptII* probe. . . 122

Figure 31. The effect of deletions in the *overdrive* region upon the incidence of multiple T-DNA insertion events in transgenic *N. tabacum.* 124

Figure 32. The effect of deletions in the *overdrive* region upon the range of T-DNA copy number in transgenic *N. tabacum.* 125

Figure 33. The top and bottom strand sequence of the T_L-DNA right border and *overdrive* region of the octopine-type Ti-plasmid pTiA6 that is protected by VirC1 in DNase I footprint analysis. 135

CHAPTER 1 INTRODUCTION

OVERVIEW

The advent of *Agrobacterium tumefaciens*-mediated plant transformation has revolutionised both plant genetic engineering and plant development research. Many plants are now routinely transformed by the introduction of genes to improve resistance to viral, fungal or insect pathogens, to produce plastics, improve the protein quality of feedstuffs, or to produce antibodies or drugs. Furthermore, powerful tools to study plant developmental biology, such as gene-tags (Feldmann, 1991), or enhancer/promoter traps (Fobert *et al.*, 1991; Kertbundit *et al.*, 1991; Lindsey *et al.*, 1993) have been designed for use with *Agrobacterium tumefaciens*-mediated transformation procedures.

In the wild, the soil-borne *A. tumefaciens* causes crown gall disease in susceptible plants by transferring a portion of DNA (the T-DNA) to the host plant. The DNA to be transferred is produced from within the delimiting left and right borders on a tumour-inducing (Ti) plasmid in the bacterium, and transferred to the plant cell where it is integrated into the genome. The T-DNA contains genes for the *in planta* production of phytohormones and unusual sugar/amino acid derivatives (opines). The ensuing phytohormone imbalance leads to plant cell proliferation and the formation of a tumour (gall) that produces the encoded opines, which are thought to provide a unique nutrient source for the bacteria (reviewed in Greene and Zambryski, 1993). The particular opine-type (such as octopine or nopaline) produced in a plant tumour depends upon which type of Ti-plasmid is harboured by the infecting *A. tumefaciens* strain.

Transformation of the plant (T-DNA generation, transfer and integration into the plant genome), and subsequent tumour development and opine production, is a complex and multi-stepped procedure (reviewed in Hooykaas and Schilperoort, 1992; Kado, 1991; Ream, 1989; Winans, 1992; Zambryski, 1992; Zupan and Zambryski, 1995). Effective plant transformation requires efficient production and transfer of T-DNA from the bacterium into cells of the host plant. A T-DNA transmission enhancer, located outside the T-DNA and adjacent to the right border, has been found to be necessary for efficient T-DNA transfer in octopine-type Ti-plasmids (Peralta *et al.*, 1986; Van Haaren *et al.*, 1987b; Shurvinton and Ream, 1991). A functional 24 bp oligonucleotide of this octopine-type T-DNA transmission enhancer was synthesised and called *overdrive* (Peralta *et al.*, 1986). A search for similar sequences in the

regions flanking the right borders of other Ti- and root-inducing (Ri) plasmids used the octopine-type *overdrive* as a template. An 8 bp sequence was discovered which was highly conserved among the seven right border regions analysed (Peralta *et al.*, 1986; Shurvinton and Ream, 1991). This conserved sequence, the *overdrive* consensus core, is often flanked by sequences that share little homology with the octopine-type *overdrive* (Peralta *et al.*, 1986; Shurvinton and Ream, 1991).

Only the *overdrive* activity of octopine and nopaline-type Ti-plasmids has been studied in any detail, and while the 24 bp octopine-type *overdrive* has been well characterised (Peralta *et al.*, 1986; Shurvinton and Ream, 1991; Toro *et al.*, 1988; 1989; Van Haaren *et al.*, 1987b; 1988), *overdrive*-like activity in nopaline-type Ti-plasmids has been little studied. Analysis of the region adjacent to the nopaline-type right border revealed a sequence with 75% homology to the *overdrive* consensus core (Peralta *et al.*, 1986). This putative *overdrive* core is flanked by sequences with little homology to the 24 bp octopine-type *overdrive*. Analysis of a similar 24 bp region of nopaline-type Ti-plasmids reveals that only 5 bp in the 16 bp outside the putative core share homology with the octopine-type *overdrive* region. Furthermore, the putative *overdrive* core of the nopaline-type Ti-plasmid is the only consensus core detected thus far that is not 100% homologous to that of the octopine-type *overdrive* (Peralta *et al.*, 1986; Shurvinton and Ream, 1991). As the putative nopaline-type *overdrive* core has only 75% homology (6 out of 8 bp) with the octopine-type *overdrive* consensus core, and since such 6 bp homologies occur throughout the nopaline-type T-region, Wang *et al.* (1987) proposed that this putative *overdrive* core region is unlikely to play a significant role in T-DNA transfer. There is, however, evidence of *overdrive*-like activity associated with the region adjacent to the nopaline-type right border in both octopine and nopaline-type *vir* environments (Culianez-Macia and Hepburn, 1988; Jen and Chilton, 1986b; Van Haaren, 1988; Wang *et al.*, 1987). Whether any of the *overdrive*-like sequences are an integral part of nopaline-type *overdrive* activity has yet to be determined, although the putative *overdrive* core has been associated with all the nopaline-type Ti-plasmid fragments studied thus far that exhibit *overdrive*-like activity. Furthermore, any sequences involved in nopaline-type *overdrive* activity have yet to be precisely identified, as the smallest portion of the nopaline-type Ti-plasmid yet studied that exhibits *overdrive*-like activity, is a 103 bp fragment (Culianez-Macia and Hepburn, 1988).

The aim of this thesis was to determine whether deletions centred upon this putative *Agrobacterium tumefaciens* nopaline-type *overdrive* core influence T-DNA transmission to plant cells. In this way, sequences required for nopaline-type

overdrive activity may be precisely identified, as well as possibly elucidating any role the putative *overdrive* core may have in T-DNA transmission. This was the first time that precise deletions were to be made within the native sequence of a putative *overdrive* element, rather than performing large scale deletions from outside the enhancer. Furthermore, the influence of these deletions on T-DNA copy number in transgenic *Nicotiana tabacum* was also to be determined.

1.1 *AGROBACTERIUM TUMEFACIENS*: GENETIC COLONISER

Agrobacterium tumefaciens is a Gram-negative, obligately aerobic, soil-borne phytopathogen. It is the causative agent of the tumourigenic crown gall disease at wound sites of many gymnospermous, dicotyledonous, and some monocotyledonous plants (De Cleene and De Ley, 1976). During infection of the plant, a segment of DNA (the transferred or T-DNA) from the large (200 kb) extrachromosomal bacterial tumour-inducing (Ti) plasmid is processed, transferred to the plant cell, and then stably integrated into the plant cell genome (Reviewed by Hooykaas and Schilperoort, 1992; Ream, 1989; Zambryski, 1992).

This process is a form of genetic colonisation (Hooykaas and Schilperoort, 1992), as the T-DNA contains genes under the control of eukaryotic promoter sequences indigenous to the bacterial DNA, that direct the plant cell to:
a) synthesise phytohormones, such as auxins and cytokinins, resulting in hormone imbalance and subsequent tumourigenesis (Nester *et al.*, 1984);
b) synthesise and excrete low molecular weight amino acid/sugar derivatives (opines), that are not normally synthesised by plant cells (Hooykaas and Schilperoort, 1992).

At least 20 opines have been described, although most are members of four families, the octopine, nopaline, mannopine, and agrocinopine families (Dessaux *et al.*, 1993; Winans, 1992). The particular opines produced in a plant tumour depends upon which Ti-plasmid (such as an octopine or nopaline-type) is harboured by the inciting *A. tumefaciens* strain. Furthermore, a strain which directs the synthesis of a particular opine has, almost without exception, a corresponding non-transferred gene able to direct the transport and catabolism of the same opine (Winans, 1992).

The tumour, therefore, provides an ecological niche. Not only do the tumour-inciting bacteria harbour the Ti-plasmid genes required to import and catabolise opines (a source of carbon, nitrogen and sometimes phosphorus (Winans,1992)), but tumourigenesis increases the number of plant cells producing opines (Greene and Zambryski, 1993). The opines support growth of *A. tumefaciens* cells harbouring the appropriate Ti-plasmid, and are hypothesised to provide a selective advantage over other bacteria in the rhizosphere (Petit and Tempé, 1985). However, various *Pseudomonas* and *Rhizobium* isolates are also able to catabolise opines, thus competing with *A. tumefaciens* for this nutrient source (Bergeron *et al.*, 1990).

Recent evidence, however, has challenged the bacteriocentric view that *Agrobacterium* genetic colonisation of plants is a parasitic relationship solely for the benefit of the

bacteria. Opines may, in fact, be beneficial not only to the bacteria, but also the plant, as opines (such as mannopine and mikimopine) produced in plants transformed with *Agrobacterium rhizogenes*, exhibit allelochemical properties (Sauerwein and Wink, 1993). Although untested under natural conditions in the field, these opines have been shown to not only inhibit the growth of herbivorous lepidopteran larvae (*Manduca sexta*), but to also exhibit allelopathy against weed seeds (*Lepidium sativum*, Brassicaceae), retarding seedling growth by 90% (Sauerwein and Wink, 1993). Furthermore, in crown galled plants, opines are not restricted only to the tumours, but are translocated throughout the plant and exuded into the rhizosphere as a component of plant root exudates (Savka *et al.*, 1996). Since opines, which may have an allelochemical role in the wild, can translocate throughout the plant, Sauerwein and Wink (1993) proposed the *Agrobacterium*-plant interaction to be a form of mutualism, and that the opines produced may be more important to both partners than previously recognised.

In the plant/soil environment, the Ti-plasmid is generally lost from *A. tumefaciens* populations because propagation of a Ti-plasmid confers a selective disadvantage on bacteria when opines are not available (Guyon *et al.*, 1993). Therefore, on an established crown gall, opines support growth of a dense *A. tumefaciens* colony, of which a proportion do not harbour the appropriate Ti-plasmid. The opines induce conjugation once the population of tumour-inciting bacteria has reached a particular density. The Ti-plasmid and its opine utilisation genes are, therefore, transferred, thus increasing the population of bacteria colonising the tumour that are able to utilise opines (reviewed in Greene and Zambryski, 1993).

Conjugation of the Ti-plasmid is tightly regulated and associated with the presence of opines and a high population density of Ti-plasmid conjugal donor cells (reviewed in Fuqua and Winans, 1996; Greene and Zambryski, 1993). *Agrobacterium tumefaciens* is thought to monitor and respond to population density with an *N*-acyl homoserine lactone. This family of signal molecules, collectively called autoinducers (AI's), are released by many gram-negative bacteria of diverse genera, and act as diffusible intercellular pheromones (Fuqua and Winans, 1996). Several AI's are known to activate target genes by way of cognate regulatory proteins. A particularly well studied example is that of a marine bioluminescent bacterium, *Vibrio fischeri*. This bacterium synthesises a freely cell-membrane-diffusible AI (3-oxo-*N*-(tetrahydro-2-oxo-3-furanyl)hexanamide, commonly referred to as [*N*-3-(oxo)hexanoyl]homoserine lactone), which interacts directly with the *lux* operon transcriptional activator, LuxR. Therefore, while living in the open ocean, *V. fischeri* cannot accumulate the AI to

concentrations high enough to induce the *lux* operon. Only after colonisation of the light organs of certain fish (such as *Monocentris japonicus*) and squid, and a subsequent increase in cell population, does the AI accumulate to a critical concentration. When the AI concentration exceeds this threshold level (10 nM is sufficient), its receptor, the transcriptional activator LuxR, induces transcription of the *lux* operon, and the bacteria become bioluminescent. The autoinduction system, therefore, allows *V. fischeri* to discriminate between the free-living state (low cell density) and the host-associated state (high cell density), and thus induce the luminescence system only when host associated (reviewed in Fuqua *et al.*, 1994; Greene and Zambryski, 1993). In the presence of opines, *Agrobacterium tumefaciens* uses a very similar system to monitor and respond to the population density of bacteria harbouring the Ti-plasmid, before induction of conjugal transfer (reviewed in Fuqua and Winans, 1996; Greene and Zambryski, 1993). Opines are imported into the bacterial cell where they interact with an opine catabolism repressor, such as the octopine-type OccR, which in turn de-represses transcription of opine utilisation, *traI* and *traR* genes located on the Ti-plasmid. The *traI* gene is involved in the synthesis of the diffusible *Agrobacterium* autoinducer (AAI) [*N*-3-(oxo)octanoyl]homoserine lactone, which interacts with the AAI receptor/sensor, TraR. When a critical local concentration of the AAI is exceeded, TraR activates transcription of the conjugal transfer genes. This pattern of gene expression occurs in the absence of recipient cells, suggesting that in contrast to other pheromone-regulated systems, Ti-plasmid conjugation is not responsive to signals released from recipient cells (Fuqua and Winans, 1996).

1.2 *A. TUMEFACIENS*: PLANT GENETIC ENGINEER

Agrobacterium is the only genus of bacteria known to use the remarkable ability of interkingdom genetic exchange as a normal part of its behavioural repertoire (Winans, 1992). It is this property that has been harnessed by plant genetic engineers. The T-DNA is delimited by 23-25 bp imperfect direct repeats bordering its left and right ends, termed the left border and right border, respectively. In contrast to other mobile DNA elements, the T-DNA itself does not encode the products that mediate its transfer, hence its integration into the plant genome remains stable. As none of the genes located in the T-DNA is required for transfer to the plant cell, the 23-25 bp borders are the only *cis*-elements necessary to direct T-DNA processing (Hille *et al.*, 1983). Any DNA placed between these borders is transferred to the plant cell, provided the borders remain intact (Hille *et al.*, 1983), and the necessary processing factors are provided either *in cis* or *in trans* (Hoekema *et al.*, 1983).

The genes encoding phytohormone and opine synthesis may be removed from the T-DNA, thereby disarming it and preventing tumourigenesis, and replaced with genes of interest destined for transfer to the host plant. Hoekema *et al.* (1983) showed that T-DNA transfer still proceeds if just the T-DNA and its borders are present on a plasmid (the binary vector), as long as another plasmid, the *vir* plasmid (usually a disarmed Ti-plasmid) is also present to provide *in trans* the factors required for T-DNA transfer. This binary system allows the manipulation of genes within the T-DNA to be performed on smaller, more manageable plasmids (6-20 kb), rather than in a 200 kb disarmed Ti-plasmid. Furthermore, the binary vector is usually designed to be easily manipulated in *Escherichia coli*, and to replicate in both *E. coli* and *A. tumefaciens* (reviewed in Hajdukiewicz *et al.*, 1994).

The binary plasmid system is the method of choice for plant transformation using *A. tumefaciens*, yet there are two main limitations to using *A. tumefaciens*-mediated transformation. First, the plant to be transformed has to be susceptible to *A. tumefaciens* infection. A study of 1150 plants revealed that 60% of the gymnosperms and dicots tested were hosts to *A. tumefaciens*, whereas the few monocots that developed crown gall were restricted to the Liliaceae and Araliaceae families (De Cleene and De Ley, 1976). The second limitation is that the susceptible host must be totipotent, and thereby be capable of regenerating a complete plant from a single transformed cell. To overcome these restrictions, some plants, such as *Arabidopsis thaliana*, may be transformed by applying *A. tumefaciens* cultures to whole portions of growing plants, such as seeds (Feldmann, 1991). As the seed imbibes water, the bacteria enter and migrate to the meristem of the embryo before

the swelling tissues close off access to the meristem. As the plants grow, bacteria are thought to migrate to the developing inflorescences, and transform the tissue so that some of the seed produced is transgenic. The populations of seed are then screened for the presence of the transgene.

1.3 *A. TUMEFACIENS*-MEDIATED PLANT TRANSFORMATION

The transformation of plant cells by *Agrobacterium tumefaciens* is a complex process comprising several steps. Initially, the bacterium detects wounded plant material, migrates towards it, then attaches to the wound site. Production of the Ti-plasmid-encoded virulence factors required *in trans* to process the T-DNA (the *vir* regulon products), is also induced. The T-DNA is then generated and directed to the recipient plant cell nucleus where it is integrated into the plant genome.

1.3.1 Ti-plasmid Structure

The most studied Ti-plasmids are the octopine and nopaline-types (reviewed in Hooykaas and Schilperoort, 1992; Winans, 1992). The octopine-type Ti-plasmid has two independently transferred T-DNA segments: the left T-DNA (T_L-DNA) encoding the phytohormone and octopine synthase genes; and the right T-DNA (T_R-DNA) encoding the production of other opines such as agropine, mannopine and fructopine (Fig. 1A, p. 10). The nopaline-type Ti-plasmid, however, has a single T-DNA (Fig. 1A) encoding both the phytohormone and nopaline synthesis genes.

On all Ti-plasmids, the virulence region is located outside the T-DNA. It contains the *vir* genes required for T-DNA synthesis, transfer and possibly integration (reviewed in Kado, 1991), and is organised as a large regulon, 40 kb and 28.6 kb for the octopine and nopaline-type Ti-plasmids, respectively (Hooykaas and Schilperoort, 1992; Rogowsky *et al.*, 1990). The genes are clustered into various numbers of operons depending upon the particular Ti-plasmid (Fig. 1B, p. 10). Basically, six operons, termed *virA*, *virB*, *virC*, *virD*, *virE*, and *virG*, are intrinsically involved in T-DNA processing and transfer (reviewed in Kado, 1991). Mutagenesis experiments showed that *virA*, *virB*, *virD*, and *virG* are essential for plant transformation, whereas *virC* and *virE* are not absolutely essential for transformation of some plant species (Stachel and Nester, 1986; Hirooka and Kado, 1986).

The operons of the *vir* regulon have different functions and contain different numbers of genes (reviewed in Winans, 1992). The *virA* and *virG* operons each contain one gene, and are involved in detection of plant wounds and induction of the rest of the *vir* operons. *virD* has five genes and is involved in the synthesis of T-DNA and its

Figure 1A-B. Comparison of the octopine and nopaline-type Ti-plasmids.

A. The arrangement of T-DNA and other features of the octopine and nopaline-type Ti-plasmids.

RB =right border; LB =left border; T_L-DNA =left T-DNA; T_R-DNA =right T-DNA; *vir* =virulence regulon; *oriV* =origin of replication.

B. The arrangement of genes within the *vir* regulon of octopine and nopaline-type Ti-plasmids (derived from Bevan and Chilton, 1982; Gelvin *et al.*, 1982; Holsters *et al.*, 1980; Hooykaas and Beijersbergen, 1994; Willmitzer *et al.*, 1982). Individual operons are described in the text.

A.

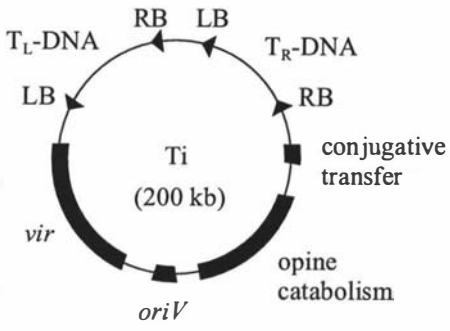

Octopine-type Ti-plasmid

eg: pTiA6; pTiAB6;
pTi15955; pTiAch5.

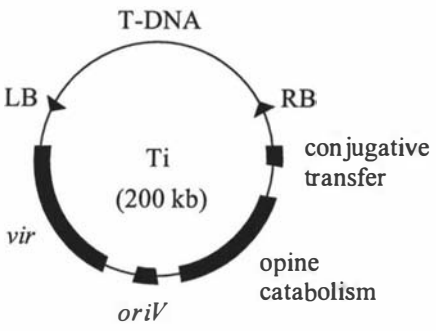

Nopaline-type Ti-plasmid

eg: pTiT37; pTiC58.

B.

Octopine-type *vir* region (44.3 kb)

Nopaline-type *vir* region (28.6 kb)

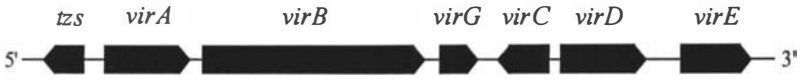

transfer to the plant nucleus. The *virC* locus comprises two genes and is thought to enhance synthesis of the T-DNA strand, whereas the two gene-products of the *virE* locus are involved in protection and transfer of the T-DNA strand. The 11 genes of the *virB* operon are also thought to be involved in the transfer of T-DNA to the plant cell.

Octopine and nopaline-type Ti-plasmids have a few accessory *vir* genes specific to those plasmids (Fig. 1B, p. 10). The *virF* operon is found in octopine-type Ti-plasmids, and contains a single gene involved in host determination. It was found that insertion and expression of the *virF* locus in *Nicotiana glauca*, which is not normally a host species for nopaline-type Ti-plasmids, rendered the plant susceptible to transformation by *Agrobacterium tumefaciens* nopaline-type Ti-plasmid strains (Regensburg-Tuïnk and Hooykaas, 1993). *pinF* (*virH*), also found in octopine-type Ti-plasmids, comprises two genes that possibly detoxify certain plant compounds that may adversely affect *A. tumefaciens*, thus influencing host determination (reviewed in Hooykaas and Schilperoort, 1992). The *tzs* locus in the nopaline-type Ti-plasmid has a single gene that is involved in cytokinin production and is thought to result in enhanced tumourigenicity on certain plants (Hooykaas and Schilperoort, 1992; Winans, 1992).

1.3.2 Induction of *vir* Genes

Like most plant pathogenic bacteria, other than some *Xanthomonas* species, *A. tumefaciens* is not equipped to penetrate plant surfaces and, therefore, enters the host through wounds (Kado, 1991). Correspondingly, transcription of the *vir* regulon and subsequent T-DNA transfer is tightly regulated, and not induced until chemical signals indicating the proximity of a plant wound are detected (Stachel *et al.*, 1985; Stachel and Zambryski, 1986; Zupan and Zambryski, 1995). Plant wounding generates characteristic environmental cues (such as the presence of particular monosaccharides, phenolics, and altered pH) which are detected by *A. tumefaciens*. Upon wounding of the plant cell and disruption of the cell wall structure, free monosaccharides (such as D-galacturonic and D-glucuronic acids) and oligosaccharides are generated by both mechanical means, and the enzymatic activity of cell wall glycosidases. These plant cell wall fragments elicit the production of phytoalexins and secondary metabolites (McNeil *et al.*, 1984), including phenolic compounds (such as acetosyringone) which are precursers to lignin production in healing woody plant cells (Kado, 1991). Furthermore, the environment in most plant wounds is acidic (pH 5.0-5.5) due to the acidity of most plant vacuoles (Winans, 1992). These plant wound signals serve as chemoattractants to the highly sensitive chemotaxis system possessed

by *A. tumefaciens* (reviewed in Vande Broek and Vanderleyden, 1995). The bacteria migrate to the wound site and adhere to the plant surface as individual cells. Then in response to plant signals, attached bacteria elaborate cellulose fibrils that entrap other bacteria, thus forming aggregates which bind very tightly to the plant cell surface. Four chromosomally located genetic loci, *chvA*, *chvB*, *pscA* (*exoC*), and *att*, have been identified as playing a role in the initial attachment of *A. tumefaciens* to plant cells (reviewed in Vande Broek and Vanderleyden, 1995).

Of the genes in the *vir* regulon, only the *virA* and *virG* gene products are transcribed during normal vegetative growth (Stachel and Zambryski, 1986). Together they form a two-component regulatory system comprising a sensor protein (VirA) and a DNA-binding response regulator/activator (VirG), which coordinately induce transcription of the *vir* regulon (reviewed by Hooykaas and Schilperoort, 1992; Winans, 1992). They are part of a two-component regulatory control family comprising a protein kinase (such as VirA) and its substrate, the response regulator (such as VirG). The kinase (usually a transmembrane environmental sensor) autophosphorylates a specific histidine residue, and transfers this phosphoryl moiety to a specific aspartate residue in a receiver domain of the cognate response regulator (usually an intracellular transcriptional regulator) (Chang and Winans, 1992). In the case of VirA and VirG, environmental stimuli (such as pH and the presence of monosaccharides and plant phenolics) lead to autophosphorylation of the VirA kinase domain at histidine 474, and the phosphate is transferred to aspartate residue 52 in the receiver domain of VirG, resulting in chemotaxis and induction of *vir* genes (Fig. 2 (step 1), p. 14).

VirA contains at least four domains, comprising an amino-terminal periplasmic domain and three cytoplasmic domains (the linker and histidine kinase domains, and the carboxyl terminal receiver domain), plus two transmembrane regions. It is thought that the activity of the histidine kinase domain, where autophosphorylation occurs, is modulated by the other domains in response to appropriate environmental stimuli (Chang and Winans, 1992). The periplasmic domain senses monosaccharides, through interaction with the chromosome-encoded ChvE periplasmic glucose-binding protein (Ankenbauer and Nester, 1990), and is involved in a response to low phenolic concentrations (Chang and Winans, 1992). It has also been shown to act as a pH sensor (Chen and Winans, 1991), but more recent data indicate that this is not so (Chang and Winans, 1992). The cytoplasmic linker domain, however, is required for sensing pH and phenolic compounds (Chang and Winans, 1992). The receiver domain

Figure 2. Overview of the molecular processes involved in *Agrobacterium tumefaciens*-mediated plant transformation.

The individual steps in this figure are referred to, and expanded upon, in the text.

Ti=tumour-inducing plasmid.

vir=virulence regulon.

Ⓟ=phosphoryl moiety.

D1=VirD1, D2=VirD2, and D4=VirD4.

C1=VirC1.

E1=VirE1, and E2=VirE2.

NLS=nuclear localisation signal.

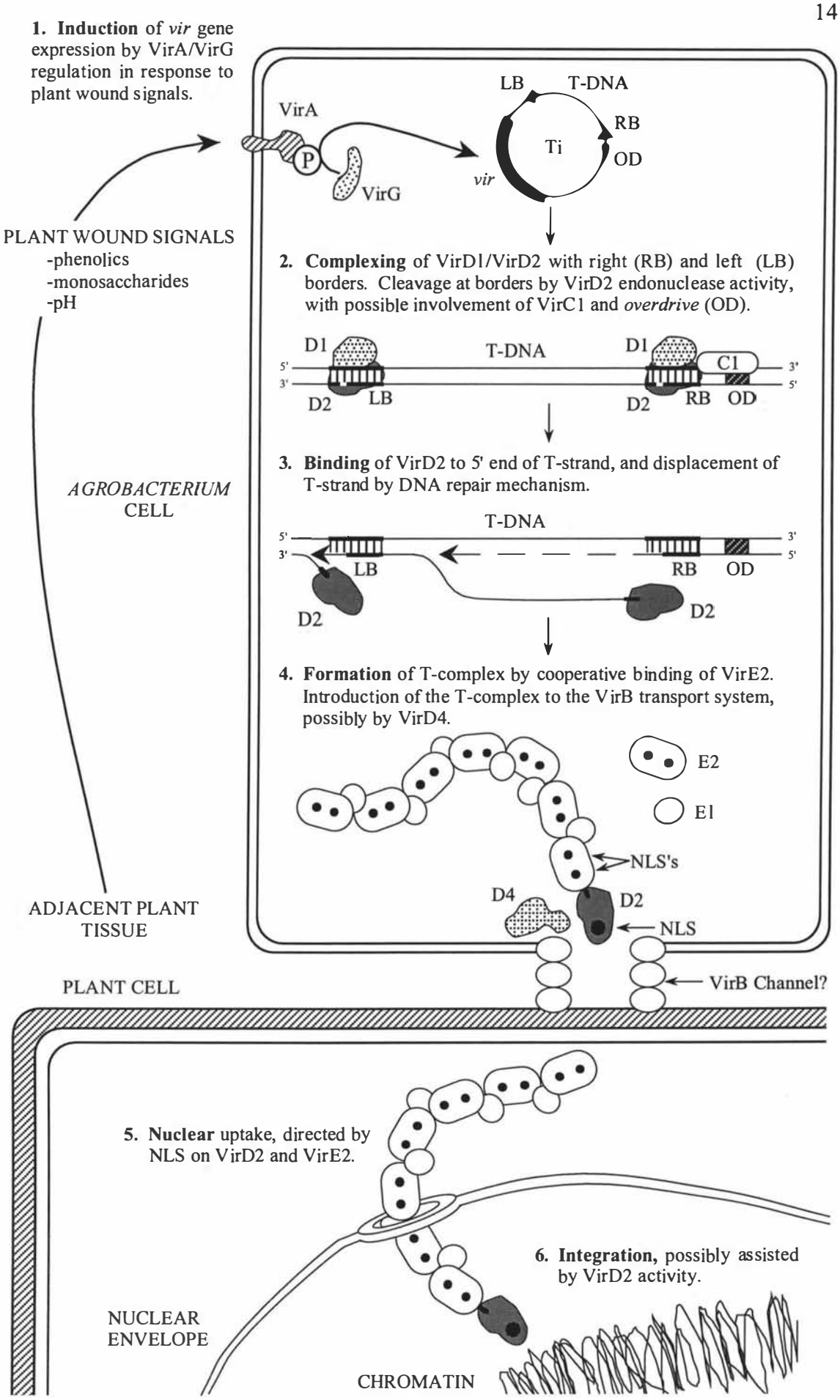
1. Induction of vir gene expression by VirA/VirG regulation in response to plant wound signals.
VirA
P
VirG
LB
T-DNA
RB
Ti
OD
vir
PLANT WOUND SIGNALS
-phenolics
-monosaccharides
-pH
2. Complexing of VirD1/VirD2 with right (RB) and left (LB) borders. Cleavage at borders by VirD2 endonuclease activity, with possible involvement of VirC1 and overdrive (OD).
D1
T-DNA
D1
C1
5'
3'
3'
5'
D2
LB
D2
RB
OD
3. Binding of VirD2 to 5' end of T-strand, and displacement of T-strand by DNA repair mechanism.
T-DNA
5'
3'
3'
5'
LB
RB
OD
D2
D2
AGROBACTERIUM CELL
4. Formation of T-complex by cooperative binding of VirE2. Introduction of the T-complex to the VirB transport system, possibly by VirD4.
E2
E1
NLS's
D4
D2
NLS
VirB Channel?
ADJACENT PLANT TISSUE
PLANT CELL
5. Nuclear uptake, directed by NLS on VirD2 and VirE2.
6. Integration, possibly assisted by VirD2 activity.
NUCLEAR ENVELOPE
CHROMATIN

is homologous to that of response regulator proteins, such as VirG, and it negatively modulates the ability of VirA to phosphorylate VirG, possibly by competing with the receiver domain of VirG for access to the kinase active site (Chang and Winans, 1992).

The periplasmic domain of VirA is necessary for both chemotaxis and tumourigenesis (Shaw, 1993). Furthermore, the periplasmic domain is required for induction of *vir* genes at low acetosyringone concentrations (5×10^{-6} M) but is unnecessary for induction of *vir* genes at high acetosyringone concentrations (1×10^{-4} M) (Chang and Winans, 1992). Based upon these observations, Shaw (1993) described an hypothesis to explain how the VirA-VirG system mediates two responses, a chemotactic and a virulence response, to the same ligand (acetosyringone). At low concentrations ($<10^{-7}$ M), acetosyringone may be bound to a high-affinity phenolic binding protein (PBP) which interacts with the periplasmic domain of VirA to stimulate a low level of phosphorylation. The resulting low levels of phosphorylated-VirG mediate chemotaxis. At higher concentrations ($>10^{-5}$ M), acetosyringone may also be bound by a lower affinity PBP which interacts with the transmembrane and cytoplasmic domains of VirA to trigger a much higher level of phosphorylation. This produces sufficient phosphorylated-VirG for the induction of *vir* genes.

VirG itself is a sequence-specific binding protein that regulates transcription of *vir* gene products. It contains two domains, an amino terminal receiver domain that is the target of the VirA kinase, and a carboxyl terminal domain that recognises and binds to specific DNA sequences (Chang and Winans, 1992). These sequences are *vir* boxes, a family of similar 12-14 bp *cis*-acting regulatory sequences located upstream of each *vir* promoter (Pazour and Das, 1990; reviewed in Winans, 1992). Phosphorylation, however, is not essential for the sequence-specific binding of VirG (Roitsch *et al.*, 1990). Furthermore, the protein has been shown to induce *vir* activity when present in large enough quantities generated by experimental systems containing extra copies of the *virG* gene (Rogowsky *et al.*, 1987). Competition experiments, however, do suggest that phosphorylation regulates VirG function by increasing its affinity for the *vir* box binding site (Roitsch *et al.*, 1990), thus inducing transcription of the *vir* genes in the presence of fewer virG molecules.

The *virG* gene is transcribed from two promoters, P1 and P2, resulting in transcripts that differ in length at the 5′ end by 50 nucleotides (Pazour and Das, 1990; Stachel and Zambryski, 1986). The longer transcript is derived from the upstream promoter P1, which is induced by phenolic compounds in a VirA-VirG dependent manner

(Mantis and Winans, 1992). The shorter transcript is derived from promoter P2, which is active at a base level in free-living bacteria, but is induced primarily by low pH (pH 5.0). Interestingly, promoter P2 does not resemble those of the other *vir* promoters, but is very similar at its -10 region to the consensus sequence of *Escherichia coli* heat shock promoters (Mantis and Winans, 1992). As the pool size of VirG can limit the efficiency of *vir* gene induction, Mantis and Winans (1992) hypothesised a two-step induction of *virG*. The first step involves the induction of *virG* by means independent of any *vir* proteins, that is, the induction of P2 in response to environmental stimuli. These can be thought of as 'pump-priming' stimuli that raise the concentration of VirG protein to a level sufficient such that it can, in conjunction with VirA, further induce its own transcription by binding to P1. This second step is a positive autoregulatory loop which could have the effect of strongly committing bacteria to plant infection.

Thus, in response to environmental stimuli indicative of wounded plant cells, VirA is autophosphorylated. The levels of the VirG protein also increase to a concentration whereby it can interact efficiently with VirA, and the phosphorylated-VirG then induces transcription of all the *vir* genes, including *virA* and *virG*. It is interesting to note that the *virG* gene of the nopaline-type Ti-plasmid, pTiC58, does not have an upstream *vir* box (Steck *et al.*, 1988), which could explain why the level of VirG is not induced beyond a basal level compared to the high concentrations induced from its counterpart locus in octopine-type Ti-plasmids (Rogowsky *et al.*, 1987).

It is also interesting to note that, although induced by phosphorylated-VirG, the *virC* and *virD* operons are negatively regulated by a repressor protein encoded by the *ros* chromosomal gene (Close *et al.*, 1987). Mutations in *ros*, moreover, cause constitutive expression of the *virC* and *virD* operons (Close *et al.*, 1985). The 15.5 kD Ros repressor binds to a 40 bp sequence, called the *ros* box, upstream of the divergent *virC* and *virD* promoter (D'Souza-Ault *et al.*, 1993). As the *ros* box overlaps the *vir* box, VirG and the Ros repressor compete for their respective binding sites, thus modulating transcription of *virC* and *virD*, and thereby modulating the amounts of T-DNA formed during the infection process (D'Souza-Ault *et al.*, 1993).

1.3.3 T-DNA Generation

Following induction of the *vir* regulon, T-DNA production begins with the generation of the T-strand, a single-stranded copy of the T-DNA region (Stachel *et al.*, 1986). This requires recognition and complexing, by *virD* gene products, of the left and right 23-25 bp imperfect direct repeats flanking the T-DNA (Filichkin and Gelvin, 1993; Yanofsky *et al.*, 1986) (Fig. 2 (step 2), p. 14). The VirD1/VirD2 complex mediates single-stranded endonucleolytic cleavage of the bottom strand of the border sequences. Primer extension analysis mapped the cleavage sites of octopine-type Ti-plasmid borders to be between the fourth and fifth bases (Albright *et al.*, 1987), whereas similar analysis mapped the nick site of nopaline-type Ti-plasmid borders to be between the third and fourth bases (Dürrenberger *et al.*, 1989). However, size fractionation of VirD2-cleaved synthetic oligonucleotides of both octopine and nopaline-type borders revealed the nick sites to be between the third and fourth bases (Pansegrau *et al.*, 1993a). The nick sites in the borders of octopine and nopaline-type Ti-plasmids are highly homologous to the origins of replication nick sites in other bacterial plasmids (such as IncPα and IncPβ plasmids) (Pansegrau *et al.*, 1994a), and suggest that the nick positions mapped by Dürrenberger *et al.* (1989) and Pansegrau *et al.* (1993a) are correct.

In addition to its role as an endonuclease (reviewed in Zambryski, 1992), VirD2 binds covalently to the 5′-termini of the bottom strand at each cleavage site (Fig. 2 (step 3), p. 14) (Dürrenberger *et al.*, 1989; Herrera-Estrella *et al.*, 1990). The nature of VirD2/DNA binding suggested involvement of tyrosine as the partner in the chemical bond (Dürrenberger *et al.*, 1989). Site-directed mutagenesis subsequently revealed that tyrosine 29 of VirD2 is essential for both endonuclease activity (Vogel and Das, 1992) and formation of a phosphodiester bond with the 5′-terminal nucleotide (Pansegrau *et al.*, 1993a). VirD2-mediated cleavage at the nick site of the borders is thought to consist of an attack on the DNA backbone by a transesterification reaction. This reaction is initiated by nucleophilic attack on the phosphodiester moiety at the nick site by the hydroxyl group of VirD2 tyrosine 29 (Pansegrau *et al.*, 1993b; Pansegrau *et al.*, 1994b).

Both VirD1 and VirD2 are required for the cleavage reaction *in vivo* (Jayaswal *et al.*, 1987) and *in vitro* (Scheiffele *et al.*, 1995). The effect of purified VirD1 on supercoiled plasmids prompted a suggestion that VirD1 is a DNA-relaxing enzyme (Ghai and Das, 1989). Scheiffele *et al.* (1995), however, detected no such topoisomerase activity in purified VirD1. They also determined that the VirD1/VirD2 cleavage reaction acts only upon negatively supercoiled double-stranded DNA, and

requires Mg^{2+} ions. Any hypothetical topoisomerase I activity of VirD1 would, therefore, be counterproductive, as the cleavage reaction requires negative superhelical DNA, not relaxed circular or linear DNA (Scheiffele *et al.*, 1995). Relaxation of double-stranded border sequences would inhibit local melting of the DNA and, therefore, prevent access of VirD2 to its target site (Pansegrau *et al.*, 1993b). VirD1, however, does have an affinity for the border sequence (Howard *et al.*, unpublished results cited in Zambryski, 1992), and it has been suggested that it recognises and binds to the T-DNA border, thus promoting VirD2 binding (Scheiffele *et al.*, 1995). It has also been suggested that the *virC* operon is associated with the complexing of VirD1/VirD2 with the right border, as VirC1 interacts with *overdrive* (a T-DNA transmission enhancer element adjacent to the right border of octopine-type Ti-plasmids) and VirD2 to enhance T-strand formation (Toro *et al.*, 1989) (Fig. 2 (step 2), p. 14).

Having first been nicked at both borders, and with the VirD2 protein covalently attached to the 5′-termini, subsequent T-strand generation is thought to result from displacement of the bottom strand of the T-DNA between the nicks, from the right border to the left, by a DNA repair mechanism (Fig. 2 (step 3), p. 14). The nick sites may act as starting points for DNA synthesis in the 5′ to 3′ direction, thus releasing the T-strands by displacement (reviewed in Hooykaas and Schilperoort, 1992; Zambryski, 1992).

The displaced T-strand is coated along its entire length with VirE2. This protein binds tightly and cooperatively to any single-stranded DNA in a non sequence-specific fashion (reviewed in Zambryski, 1992), and its stability is thought to be enhanced by interaction with the VirE1 protein (McBride and Knauf, 1988). The T-strand with the VirD2 covalently attached at the 5′-terminus and coated with VirE2, is referred to as the T-complex (Fig. 2 (step 4), p. 14). Attachment of VirD2 protects the T-complex from exonucleolytic degradation *in vitro* (Dürrenberger *et al.*, 1989), and VirE2 renders single-stranded DNA completely resistant to 3′ and 5′ exonucleases, as well as to endonucleases, *in vitro* (reviewed in Zambryski, 1992). *A. tumefaciens* cells with mutations in *virE2*, accumulate T-strands to the same extent as wild-type cells, yet T-strands accumulate to a considerably lower extent in the cytoplasm of tobacco protoplasts infected with *virE2* mutants than when infected with wild-type *A. tumefaciens* (Yusibov *et al.*, 1994). This suggests that VirE2 acts to protect the T-strand from exonucleolytic degradation *in planta* (Yusibov *et al.*, 1994).

There has been much debate as to whether the T-strand is the actual T-DNA copy, as double-stranded linear molecules, and even double-stranded circular molecules, have been isolated from acetosyringone-induced *A. tumefaciens* (reviewed in Kado, 1991). Evidence for the single-stranded T-DNA copy has been provided by Yusibov *et al.* (1994) who used a PCR-based protocol that detected single-stranded T-DNA in the cytoplasm of tobacco protoplasts within 30 min of bacterial cocultivation. In the same time frame, there was a concomitant decrease in the amount of T-strands present in the infecting *A. tumefaciens*, indicating export of T-strands to the plant protoplasts. The T-DNA detected in the cytoplasm was not double-stranded, as the PCR product could not be generated when the plant cytoplasmic fraction was first treated with S1 nuclease that possessed no detectable double-stranded DNase activity.

A second study, in which a sensitive extrachromosomal recombination assay was used, also strongly supports the hypothesis that the T-DNA copy transferred to the plant nucleus is single-stranded (Tinland *et al.*, 1994). A T-DNA was designed in which a *gus* (β-glucuronidase) gene was divided into two overlapping segments, hence *in planta* recombination was required to yield a full length active gene. Extrachromosomal recombination that takes place early after entry into the nucleus can discriminate between single-stranded and double-stranded DNA molecules. If the transfer intermediate is double-stranded, recombination should produce an intact *gus* gene, regardless of whether the segments in the T-DNA are of the same or opposite polarity. If the transfer intermediate is single-stranded, then a complete *gus* gene can be obtained through recombination much more efficiently when the segments are of opposite polarity as they can self-anneal. Prior to recombination, single-stranded intermediates with *gus* segments in the same polarity first have to become double-stranded. In infected protoplasts, Gus activity from T-DNA containing *gus* segments of opposite polarity was an order of magnitude greater than Gus activity from T-DNA containing *gus* segments of the same polarity. This infers that transferred T-DNA copies enter the plant nucleus in single-stranded form.

1.3.4 T-complex Transfer

The T-complex is transferred through the bacterial inner and outer membranes, as well as the bacterial cell wall, although the mechanisms have yet to be elucidated (reviewed in Zupan and Zambryski, 1995). It must then cross the plant cell wall and membrane, pass through the nuclear envelope and integrate into the plant genome. Current T-DNA transfer research is focusing on the relationship between the *virB* operon and transfer of the T-complex (Fig. 2 (step 4), p. 14). Analysis of the DNA sequence of *virB* and its 11 open reading frames has shown it to be related to other bacterial gene

clusters whose products form a membrane-associated complex involved in pilus formation, protein secretion, or DNA uptake (Kado, 1994; Lessl and Lanka, 1994).

The current T-complex transfer model, as described in Zambryski (1992) and Zupan and Zambryski (1995), is that *virB* proteins form a transmembrane channel, and the VirD4 protein mediates interactions between the T-complex and the putative transmembrane channel (Fig. 2 (step 4), p. 14). Energy for translocation of the T-complex could be provided by VirB4 and VirB11, both of which localise to the inner membrane and exhibit ATPase and protein kinase activities. Amino acid sequence similarities reveal that VirB11 may be a member of a class of ATPases that function specifically in complexes which translocate macromolecules and macromolecular complexes across the bacterial inner and outer membranes. Furthermore, the similarities with the pertussis toxin export operon of *Bordetella pertussis* indicate that the transport systems for T-DNA and conjugation may have evolved from a protein export system. The system may only recognise the protein component of the DNA/protein complexes, hence the T-strand, essentially coated with VirE2 and VirD2, would be carried along 'piggy-back' fashion with the protein (Zupan and Zambryski, 1995).

1.3.5 Nuclear Localisation

Before integration into the plant genome, the T-complex must first be imported into the plant nucleus (Fig. 2 (step 5), p. 14). As summarised in Sanderfoot *et al.* (1996), the transport of proteins across the nuclear membrane is an energy-dependent process mediated by proteins associated with nuclear pore complexes. Although nuclear pores have an effective size-exclusion limit of approximately 60 kD, proteins smaller than this do not appear to diffuse efficiently across the nuclear membrane. Karyophilic proteins contain nuclear localisation signals (NLS's), short basic regions of approximately 10-20 amino acids that interact with components of the nuclear pore complex for transport into the nucleus.

Amino acid sequence analysis of VirD2 revealed the presence of a monopartite NLS (consisting of a single cluster of positively charged amino acids) in the N-terminal region, and a bipartite NLS (consisting of two interdependent basic domains) in the C-terminal region (Wang *et al.*, 1990; Tinland *et al.*, 1992). The N-terminal NLS is capable of directing a β-galactosidase fusion protein to the nuclei of tobacco (Herrera-Estrella *et al.*, 1990) and yeast (Tinland *et al.*, 1992), as is the C-terminal bipartite NLS (Tinland *et al.*, 1992). The biological significance of these NLS's was revealed by Shurvinton *et al.* (1992), who showed that removal of the N-terminal NLS did not

affect tumourigenesis, whereas removal of the C-terminal bipartite NLS plus an adjacent uncharacterised third amino acid sequence (the omega sequence) decreased tumourigenicity by 96-99%. Although these C-terminal deletions had a marked affect on tumourigenicity, the production of T-strands was not altered (Shurvinton *et al.*, 1992). This is because the endonuclease and covalent binding domain is in the N-terminal half of VirD2, and such deletions in the C-terminal region only affect T-DNA transfer, not border nicking and subsequent T-strand production.

The T-complex headed by a covalently bound VirD2 protein is a very large structure. A typical 20 kb T-strand would bind about 600 molecules of VirE2 (approximately 60 kD each), and the subsequent T-complex would have a combined molecular mass of 50×10^3 kD and a predicted length of 3600 nm (Citovsky *et al.*, 1992; McBride and Knauf, 1988). This prompted research to investigate whether the 50×10^3 kD T-complex is piloted to the plant nucleus solely by the 49.7 kD VirD2 protein and its NLS's. Amino acid sequence analysis of both nopaline and octopine-type VirE2 proteins revealed two bipartite NLS's, of which both were required to direct a β-glucuronidase fusion protein to tobacco nuclei (Citovsky *et al.*, 1992; 1994). Since a single VirE2 NLS is not sufficient to fully direct the fusion protein to the nucleus, the activity of each VirE2 NLS is considered to be intrinsically weaker than that of each VirD2 NLS (Citovsky *et al.*, 1992).

Citovsky *et al.* (1992; 1994) proposed a model to explain the transport of large T-complexes into the plant nucleus. The T-strand with a VirD2 molecule covalently attached to its 5′ end is a folded and collapsed structure. Cooperative binding of VirE2 unfolds the single-stranded DNA to form a long and very thin (<2 nm) T-complex. Since any DNA sequence located between the borders can traverse the plant nuclear envelope, it is assumed that the T-strand is, therefore, passively transported 'piggy-back' fashion into the nucleus through its association with proteins bearing specific NLS's. As the NLS activity of VirD2 is intrinsically stronger than that of VirE2, it is proposed that VirD2 acts initially to target the T-complex to the nuclear pore in a polar fashion, thus facilitating uptake of the T-strand in a 5′-3′ direction (Fig. 2 (step 5), p. 14). VirE2 provides NLS's along the entire length of the T-complex. This may increase probability of T-complex interaction with the nuclear transport machinery, and ensure that the nuclear import of the long and unfolded complex is not interrupted, possibly by keeping both the cytoplasmic and nucleoplasmic sides of the nuclear pore open simultaneously.

1.3.6 Integration into Plant Nuclear DNA

Integration of the T-strand into the plant genome is the final step of the T-DNA transfer process (Fig. 2 (step 6), p. 14). The current model compares integration with illegitimate recombination (Gheyson *et al.*, 1991), and suggests that the VirD2-bound 5′ end of the T-strand joins a nick in the plant DNA. The plant DNA may further unwind to form a gap and the 3′ end of the T-strand may pair with an adjacent region of plant DNA. Plant repair and recombination enzymes then covalently join the 3′ end to the plant DNA, resulting in the introduction of the T-strand into one strand of plant DNA. Due to the torsional strain, a nick would be introduced into the opposite plant DNA strand, and gap repair and DNA synthesis using the T-strand as template would result in the final integration product.

This model has been extended by Pansegrau *et al.* (1993a), who provided evidence supporting the involvement of VirD2. Sequencing of junctions between integrated T-DNA and plant DNA reveals that a considerable proportion of integration events are precise with respect to the right (5′) end of the T-DNA. This precision suggests that VirD2, covalently bound to the 5′ terminus of the T-DNA in the bacterium, is directly involved in the illegitimate recombination process in the plant cell nucleus. It has been shown that single-stranded DNA covalently attached to VirD2 can be joined to a preformed 3′ end by a cleaving and joining reaction catalysed by VirD2 (Pansegrau *et al.*, 1993a). It is suggested that VirD2 recognises free 3′ termini (ie, nicks and gaps) in the plant DNA then joins the right end of the T-DNA to the plant genome. VirD2 has also been shown to have different specificities for cleavage with respect to double-stranded and single-stranded DNA, which has implications for its role in T-strand integration into the plant genome. *In vitro*, purified VirD2 cleaves double-stranded DNA only at specific border sequences, and requires VirD1 to do so (Jayaswal *et al.*, 1987; Scheiffele *et al.*, 1995), yet VirD2 alone can cleave and join a range of single-stranded substrate sequences *in vitro* with no need for accessory proteins (Pansegrau *et al.*, 1993a). The different activities of VirD2 support its role in T-strand integration as firstly: precise cleavage of double-stranded DNA (in association with VirD1) is necessary for T-strand production; and secondly: the relaxed specificity of the cleavage-joining reaction with single-stranded DNA by VirD2 alone in the plant nucleus, would be important for integration of the T-strand.

1.4 THE *OVERDRIVE* T-DNA TRANSMISSION ENHANCER

1.4.1 Discovery of *Overdrive*

The first indication that sequences outside the T-DNA and adjacent to the right border influence T-DNA transmission, as measured by tumourigenesis, was provided by Peralta and Ream (1985). Using a mutant of the octopine-type Ti-plasmid, pTiA6NC, from which the entire T_R-DNA and the right border of the T_L-DNA had been deleted, native fragments of differing sizes containing the T_L-DNA right border were reinserted near its original position. As the T_L-DNA contains all the genes required for tumour maintenance, restoration of the right border results in tumourigenicity. A portion of the Ti-plasmid that enhances oncogenicity was detected in a 1035 bp region to the right of right border, outside the T-DNA. Insertion of this fragment containing the right border and the 1035 bp region restored tumour induction fully, whereas a fragment containing only the right border and a further 4 bp resulted in much reduced oncogenicity.

More precise deletions in this region determined the T-DNA transmission enhancing sequence to be within 40 bp of the right border, yet removal of a further 15 bp towards the right border resulted in attenuated virulence (Peralta *et al.*, 1986). Analysis of this region revealed a conserved 24 bp sequence to the right of the right borders of both the T_L- and T_R-DNA of the octopine-type pTiA6NC. Comparison of the T_L-DNA 24 bp conserved sequence with regions adjacent to the right borders of a nopaline-type Ti-plasmid and an Ri-plasmid revealed little homology, apart from a highly conserved 8 bp motif (Fig. 3, p. 24). The left border regions of these plasmids were found not to contain any of these sequences. An oligonucleotide of the T_L-DNA 24 bp conserved sequence flanking the octopine-type T_L-DNA right border was synthesised and called *overdrive* (Peralta *et al.*,1986).

Throughout the rest of this Thesis, the *overdrive* oligonucleotide is referred to as the synthetic 24 bp octopine *overdrive* element, whereas the T_L-DNA conserved sequence, (from which the oligonucleotide is derived) in context with its flanking native Ti-plasmid region is referred to as the 24 bp octopine *overdrive* sequence. Furthermore, the highly conserved 8 bp motif is referred to as the *overdrive* consensus core.

1.4.2 *Overdrive* is an Enhancer Element

To test the influence of the synthetic 24 bp octopine *overdrive* element on tumour induction, Peralta *et al.* (1986) used the pTiA6NC deletion mutant of Peralta and Ream (1985). Tumourigenesis was promoted at the same low level (about 6% of full

pTiA6NC T_L: 5′ TTTGAGCTCGTGTGAA**TAAGTCGCTGTGTATGTTTGTTTG**ATTGTTTCTGT 3′

T_R: 5′ ATTCATTTTTATTGTC**TAAaTttCTGTaTtTGTTTGTTTG**ATTGTTTCTGT 3′

pTiT37 5′ GGCGTGAAAAGGTTTA**TccGTtcgTccaTtTGTaTGTgca**TGCCAACCACA 3′

pRiA4 T_L 5′ ----------ATATATGTTCCTGTC**ATGTTTGTTca**ATTGTTCAATT 3′

Figure 3. Comparison of *overdrive*-like sequences in right border regions of the octopine-type pTiA6NC T_L- and T_R-DNA, the nopaline-type pTiT37, and the *Agrobacterium rhizogenes* pRiA6 T_L-DNA.

Comparison, by Peralta *et al.* (1986), of the sequences adjacent to the right borders (underlined) of the pTiA6NC T_L- and T_R-DNA revealed a conserved sequence termed the 24 bp octopine-type *overdrive* sequence (**Bold**). Further comparison with the right border region of pTiT37, and the pRiA4 T_L-DNA revealed a highly conserved 8 bp sequence (**Bold underlined**), termed the *overdrive* consensus core (Peralta *et al.*, 1986). Bases within the putative *overdrive* regions that are not homologous with those of the 24 bp octopine-type *overdrive* sequence of the pTiA6NC T_L-DNA, are marked appropriately (**bold lowercase**).

virulence on carrot slices) after insertion of only the native right or left border sequences of pTiA6NC T_L-DNA, or a synthetic nopaline-type right border. Addition of the synthetic 24 bp octopine *overdrive* element fully restored tumourigenicity, regardless of its orientation with respect to the border sequences, indicating that this synthetic *overdrive* element behaves as an enhancer. Further, the results also suggested that border sequences themselves are intrinsically equal, with regard to T-DNA transmission, and that sequences flanking the right borders strongly influence the efficiency of T-DNA transmission.

At the same time, in a similar set of experiments to Peralta *et al.* (1986), Van Haaren *et al.* (1987a) isolated a T-DNA transmission enhancer-like element in a region to the right of the T_L-DNA right border of the an octopine-type Ti-plasmid, pTiAch5. Using a mutant of pTiAch5 from which the entire T_R-DNA and the T_L-DNA right border had been deleted, they (like Peralta *et al.* (1986)) also determined that native octopine-type left and right borders alone promoted tumourigenesis at an equally low level. Furthermore, co-insertion of the 626 bp enhancer-containing fragment with either the left or the right border produced wild-type virulence levels. Later sequence analysis of this fragment revealed the presence of the 24 bp octopine *overdrive* sequence (Van Haaren *et al.*, 1987b).

Extending these results within the same analysis system, Van Haaren *et al.* (1988) tested more T-DNA borders. They determined that alone, native and synthetic T_L-DNA right borders, native T_L- and T_R-DNA left borders, and a synthetic nopaline-type pTiT37 right border, were equally poor tumour inducers. Co-insertion of a 622 bp fragment containing the 24 bp octopine *overdrive* sequence restored virulence fully, thus mirroring the results of Peralta *et al.* (1986). Furthermore, right border regions of the other octopine and nopaline-type Ti-plasmids, and an Ri-plasmid that had been determined by Peralta *et al.* (1986) to have an *overdrive* consensus core, were also tested. Insertion of the native right border and flanking region containing a putative *overdrive* consensus core of either the pTiAch5 T_R-DNA, pTiT37 (nopaline-type), or the *A. rhizogenes* pRiA4 T_L-DNA, resulted in full tumourigenesis. This indicates the putative *overdrive* sequences identified only by sequence analysis do influence T-DNA transmission, as the border sequences alone result in attenuated virulence.

As determined by tumourigenesis assays, manipulation of fragments containing the 24 bp octopine *overdrive* sequence indicated that *overdrive* behaves as a true enhancer element, as it is effective when positioned both upstream or downstream of the border sequence (Ji *et al.*, 1989; Van Haaren *et al.*, 1987b), regardless of its orientation with

respect to the border sequences (Ji *et al.*, 1989; Peralta *et al.*, 1986; Van Haaren *et al.*, 1987b; Shurvinton and Ream, 1991). The 24 bp octopine *overdrive* sequence, normally found up to 15 bp away from the border repeat (Peralta *et al.*, 1986), also enhances oncogenicity from a distance. A 189 bp Ti-plasmid fragment containing the 24 bp octopine *overdrive* sequence was shown to be fully effective in enhancing tumour induction when placed up to 2059 bp to the right of the right border, and slightly less effective at 4381 and 6714 bp to the right of the right border (Van Haaren *et al.*, 1987b). Similarly, Ji *et al.* (1989) determined that tumourigenesis was unaffected when the synthetic *overdrive* element was separated from the right border by 553 bp, yet distances greater that 3000 bp diminished tumourigenesis. Although *overdrive* enhances oncogenicity, the element itself is not capable of inducing T-DNA transfer in the absence of a border repeat (Shaw *et al.*, 1984; Van Haaren *et al.*, 1987a; 1987b; 1988).

1.4.3 Characterising *Overdrive*

All previous experiments analysing *overdrive* activity had involved addition or removal of Ti-plasmid fragments containing the whole native *overdrive* region (Peralta and Ream, 1985; Peralta *et al.*, 1986; Van Haaren *et al.*, 1987a; 1987b; 1988), or addition and removal of the synthetic 24 bp octopine *overdrive* element (Ji *et al.*, 1989; Peralta *et al.*, 1986).

To determine which sequences in the *overdrive* region are required for enhancing T-DNA transmission, Shurvinton and Ream (1991) used a sensitive and quantitative potato tumourigenesis assay. They expanded upon the work of Peralta *et al.* (1986), and used the pTiA6NC deletion mutant, in which they performed progressively larger deletions through the native 24 bp octopine *overdrive* sequence towards the T_L-DNA right border (Fig. 4, p. 27). Removal of sequences to the right of the right (3′) end of the 24 bp octopine *overdrive* sequence did not affect virulence compared with the wild-type *overdrive* region (Fig. 4 (steps 1-2)), indicating that sequences from the right border through to the 3′ end of the *overdrive* sequence contain all the elements required for full *overdrive* activity. Deletion towards the right border of a further 15 bp containing half the 24 bp octopine *overdrive* sequence, including the 8 bp *overdrive* consensus core, abolished *overdrive* activity (Fig. 4 (step 3)), thus reducing virulence to that of pTiA6NC with the *overdrive* region removed (Fig. 4 (step 4)). This infers that the right half of the 24 bp octopine *overdrive* sequence contains

	Sequence from right border to *overdrive*	Virulence
	RB *overdrive*	
1)	5′ TTTGAGCTCG*TGTGA***ATAAGTCGCTGTGTATGTTTGTTTG**ATTGTTTCTGT 3′	100%
2)	5′ TTTGAGCTCG*TGTGA***ATAAGTCGCTGTGTATGTTTGTTTG**---------- 3′	100%
3)	5′ TTTGAGCTCG*TGTGA***ATAAGTCGCT**---------- 3′	1-3-4-3%
4)	5′ TTTGAGCTCG---------- 3′	3-5-4-3%
5)	5′ TTTGAGCTC**TATGTTTGTTTG**---------- 3′	30%
6)	5′ TTTGAGCTCG------**TAAGTCGCTGTGTATGTTTGTTTG**---------- 3′	26-35%
7)	5′ TTTGAGCT----------CG*TGTGA***ATAAGTCGCTGTGTATGTTTGTTTGA** 3′	100%

Figure 4. Characterising the octopine-type *overdrive.*

Shurvinton and Ream (1991) determined the effect on virulence (in a potato tumourigenesis assay) of progressively larger restriction deletions through the octopine-type *overdrive* towards the right border and T-DNA of pTiA6NC (steps 1-4), as well as determining the virulence of a synthetic right (3′) half of the 24 bp octopine *overdrive* sequence (step 5) or the entire synthetic 24 bp octopine *overdrive* element (step 6) when added to an *overdrive* region-deleted pTiA6NC. Furthermore, the virulence of a displaced larger *overdrive* element (24 bp *overdrive* sequence plus the 5′ TGTGA 3′ sequence) was also determined (step 7).

The 24 bp octopine-type *overdrive* sequence is marked (**bold**), as are the *overdrive* consensus core (**bold**), the 3′ end of right border (RB; underlined), and the 5′ TGTGA 3′ sequence (*italics underlined*). Where native *overdrive* region sequences have been deleted and replaced with pUC18 sequences is marked (------).

sequences essential for *overdrive* activity, whereas the left (5′) half alone is unable to exhibit *overdrive* activity. To test this further, a 12 bp oligonucleotide (5′-TA**TGTTTGTT**TG-3′) of the right half of the 24 bp octopine *overdrive* sequence, including the 8 bp *overdrive* consensus core (**bold**), was inserted adjacent to the right border (Fig. 4 (step 5), p. 27). This truncated form of *overdrive* stimulated T-DNA transmission as effectively as the synthetic 24 bp octopine *overdrive* element studied by Peralta *et al.* (1986) (Fig. 4 (step 6)), thus highlighting the importance of the region containing the 8 bp *overdrive* consensus core. Although previous tumourigenesis assays had shown the synthetic 24 bp octopine *overdrive* element to be as effective as the full native octopine-type *overdrive* region (Peralta *et al.*, 1986), the sensitive potato tumourigenesis assay revealed the synthetic 24 bp octopine *overdrive* element to be, in fact, only 25-35% as virulent as the full native octopine-type *overdrive* (Shurvinton and Ream, 1991) (Fig. 4 (step 6)). This indicates that other DNA elements between the right border and the 24 bp *overdrive* sequence are required for full *overdrive* function. Analysis of this region revealed the presence of the sequence 5′-TGTGA-3′ in similar positions in the pTiA6 T_L-DNA, the pTiAB3 T_A-region and the pRiA4 T_R-DNA, but not in the nopaline-type pTiT37 right border region (Shurvinton and Ream, 1991). This sequence abuts the 5′ end of the pTiA6NC 24 bp octopine *overdrive* sequence. Displacement of the conjoined 5′-TGTGA-3′ and 24 bp octopine *overdrive* sequences as a single entity, by insertion of various sized DNA fragments between this entity and the right border, still resulted in maximum virulence (Fig. 4 (step 7), p. 27). The absence of this sequence was the sole characteristic common to the *overdrive* regions in all strains that exhibited partial *overdrive* activity, conversely all strains that exhibited full *overdrive* activity contained this sequence (Shurvinton and Ream, 1991). Whether addition of this sequence raises the activity of the synthetic 24 bp octopine *overdrive* element to that of the native *overdrive* has yet to be tested.

1.4.4 Role of *Overdrive*

The proposed role of *overdrive* is to enhance the interaction between the right border and the appropriate *vir* proteins involved in T-DNA generation (Peralta *et al.*, 1986). Furthermore, as *overdrive* is part of the DNA flanking the right border, it must function during the early steps of T-DNA processing, as it would be separated from the T-strand during transfer (Toro *et al.*, 1988).

The exact mechanism of *overdrive* activity is not known, although Van Haaren *et al.* (1987b) first demonstrated a link between *overdrive* and its effect on both T-strand production and subsequent tumourigenesis. They showed that removal of a 189 bp

Ti-plasmid fragment containing a 24 bp octopine *overdrive* sequence severely attenuates T-strand production and virulence. Furthermore, stepwise increases in the distance between the right border and the 189 bp *overdrive* fragment leads to corresponding stepwise decreases in both T-strand levels and tumourigenesis. Other groups have also shown that the presence of an octopine *overdrive* increases T-strand production (Ji *et al.*, 1989; Toro *et al.*, 1988; Veluthambi *et al.*, 1988), as does a nopaline *overdrive* (Culianez-Macia and Hepburn, 1988). However, the octopine-type *overdrive* region itself, without a right border, is unable to induce T-strand production (Van Haaren *et al.*, 1987b). The increase in T-strand production may be due to interaction with cleavage at the right border. It has been shown that while *overdrive* is not essential for nicking at the right border (Pansegrau *et al.*, 1993a; Scheiffele *et al.*, 1995; Srinivasan *et al.*, 1989; Toro *et al.*, 1988; Veluthambi *et al.*, 1988), its presence does enhance nicking (Toro *et al.*, 1988). Other groups, however, have reported no enhancement (Culianez-Macia and Hepburn, 1988; Srinivasan *et al.*, 1989; Van Haaren *et al.*, 1987b), but of these, only Srinivasan *et al.* (1989) set out to directly measure differences in border nicking and used methods similar to Toro *et al.* (1988).

The *overdrive* has also been found to function as a quantitative factor enhancing T-strand generation when *vir* gene products are at limiting concentrations. In acetosyringone-induced *A. tumefaciens* strains, *overdrive* enhances T-strand production to wild-type levels, yet strains without *overdrive* may produce T-strands at wild-type levels upon introduction of additional copies of *virG*, *virC*, *virD*, and *virE* operons on a multicopy cosmid (Ji *et al.*, 1989; Veluthambi *et al.*, 1988).

1.4.5 *Overdrive* and the *virC* Operon

There is a close relationship between *overdrive* and the *virC* operon. Mutations which abolish products of both *virC* genes attenuate virulence about 100-fold, to that of an octopine-type *overdrive*-deleted strain (Ji *et al.*, 1989). Furthermore, a strain containing mutations in both *virC* and *overdrive* is as equally deficient in tumourigenesis as a strain containing either mutation alone (Ji *et al.*, 1989). The *overdrive* and the *virC* operon also have similar effects on T-strand production and nicking at the right border. *A. tumefaciens* strains containing mutations throughout the *virC* locus produce T-strands at low levels, whereas mobilisation of plasmids containing the wild-type *virC* locus, to complement these mutations, restores T-strand production to wild-type levels (Toro *et al.*, 1988). As with *overdrive*, *virC* gene-products are not essential for nicking at the right border (Pansegrau *et al.*, 1993a; Scheiffele *et al.*, 1995; Stachel *et al.*, 1987; Veluthambi *et al.*, 1987), but nicking is

enhanced by the presence of both VirC1 and VirC2 (Toro *et al.*, 1988). Scheiffele *et al.* (1995) also demonstrated that in the absence of *virC* gene-products, *overdrive* does not enhance nicking at the right border *in vitro*.

Like *overdrive*, the VirC1 protein has also been found to function as a quantitative factor in enhancement of T-strand generation when *vir* gene products are at limiting concentrations. In strains of *E. coli* in which expression of VirD1 and VirD2 is controlled by the native *A. tumefaciens virD* promoter, the VirC1 protein stimulates T-strand production. However, strains in which VirD1 and VirD2 are controlled by the highly active *tac* promoter do not require VirC1 for efficient T-strand production (De Vos and Zambryski, 1989). The VirC1 protein, therefore, enhances the efficiency of T-strand production when VirD1 and VirD2 are limiting.

The nature of the link between *overdrive* and the *virC* operon was determined by Toro *et al.* (1988), who revealed that VirC1 binds specifically to the synthetic 24 bp octopine *overdrive* element, without the involvement of other proteins. Furthermore, DNase I footprinting assays on a 285 bp octopine-type Ti-plasmid fragment showed that VirC1 protects a region containing the native 24 bp octopine *overdrive* sequence (Toro *et al.*, 1989). Although VirC1 binds to the synthetic 24 bp octopine *overdrive* element, it does not bind to a synthetic right border sequence (Toro *et al.*, 1989). Interestingly, the VirD2 protein was found to interact with both right border and *overdrive* sequences (Toro *et al.*, 1988). As the binding of VirD2 to *overdrive* was determined only in the presence of other acetosyringone-induced *vir* products, it was not possible to ascertain whether VirD2 binds directly to *overdrive* or through an interaction with other proteins, such as VirC1. The VirC2 protein, however, does not bind to either the *overdrive* or the right border sequences, yet it is required for full T-strand production (Toro *et al.*, 1988). The mechanism of *overdrive* activity, therefore, may be enhancement of T-strand production (possibly by improved cleavage at the right border) by binding of VirC1 which interacts with VirD2, possibly through VirC2, thus bringing the VirD2 endonuclease to the adjacent border sequence (Toro *et al.*, 1989) (Fig. 2 (step 2). p. 14).

The putative contacts between proteins bound at *overdrive* and the border repeat are not subject to exacting spatial restrictions as increasing the spacing between *overdrive* and the right border by 1.0 and 1.6 helical turns (Shurvinton and Ream, 1991) or 2 kb (Van Haaren *et al.*, 1987b) does not reduce efficiency of T-DNA transmission.

1.4.6 Is There a Nopaline-type *Overdrive*?

Using the octopine-type pTiA6NC T_L-DNA 24 bp *overdrive* sequence as a template, a search for similar sequences has been made in regions flanking the right borders of the octopine-type pTiA6NC T_R-DNA, pTiAB3 T_A-DNA, and pTi15955 T_R-DNA, the nopaline-type pTiT37, and the *Agrobacterium rhizogenes* pRiA6 T_L- and T_R-DNA (Peralta *et al.*, 1986; Shurvinton and Ream, 1991). A highly conserved 8 bp sequence, the *overdrive* consensus core, was detected, and is flanked by sequences with various degrees of homology to the 24 bp octopine *overdrive* sequence (Fig. 5, p. 32). The region adjacent to the right border of the nopaline-type Ti-plasmid pTiT37 contains a sequence with 75% homology (6 out of 8 bp) to the *overdrive* consensus core (Peralta *et al.*, 1986). This is the only putative consensus core thus far detected that is not 100% homologous to the *overdrive* consensus core. Furthermore, the sequences flanking this putative *overdrive* core have very little homology with the 24 bp octopine *overdrive* sequence (5 out of 16 bp outside the putative *overdrive* core), or any of the other analysed right border regions, except that of the pTiA6NC T_R-DNA (9 out of 10 bp through the putative *overdrive* core) (Peralta *et al.*, 1986) (Fig. 5, p. 32). Moreover, the putative *overdrive* cores of other Ti-plasmids are within 29 bp of the 3′ end of the right border, whereas the putative nopaline-type *overdrive* is 76 bp away from the right border (Peralta *et al.*, 1986). As the putative nopaline-type *overdrive* core only has 75% homology with that of the *overdrive* consensus core, and the flanking region shares little homology with the 24 bp octopine *overdrive* sequence (Fig. 5), there has been much debate as to whether this constitutes an *overdrive* enhancer (Kado, 1991; Wang *et al.*, 1987; Winans, 1992; Zambryski, 1992).

Wang *et al.* (1984) analysed the influence of sequences flanking a nopaline Ti-plasmid right border on tumour induction on tobacco leaves, in an environment of nopaline-type *vir* products. Using a nopaline Ti-plasmid, pTiC58, from which the right border and flanking region had been deleted, a synthesised 25 bp nopaline-type right border was inserted into the right border position. This resulted in wild-type tumour induction, as did insertion of a 3.2 kb fragment containing the native right border and flanking sequences. This indicated that the right border sequence alone was all that was necessary to attain efficient T-DNA transmission and that flanking sequences had no influence on tumourigenesis, a contrast to the octopine-type *overdrive* and *vir* environment studied by Peralta *et al.* (1986). Further investigation, using a more sensitive and quantifiable potato tumourigenesis assay system, revealed a moderate (55%) decrease in virulence when flanking sequences were removed from the nopaline-type right border (Wang *et al.*, 1987). Using a similar potato tumourigenesis assay, however, Shurvinton and Ream (1991) detected a 96% decrease in virulence

pTiA6NC T_L: 5′ TTTGAGCTCG*TGTGA*A**TAAGTCGCTGTGTATGTTTGTTTG**ATTGTTTCTGT 3′

T_R: 5′ ATTCATTTTTATTGTC**TAAaTttCTGTaTtTGTTTGTTTG**ATTGTTTCTGT 3′

pTiAB3 T_A: 5′ TTCGGGTTCG*TGTGA*A**TAAaTCGCTGTGTATGTTTGTTTG**ATTGTTTCTGT 3′

pTi15955 T_R: 5′ ATTCATTTTTATTGTC**TAAaTttCTGTaTtTGTTTGTTTG**TTCGGTTGTAA 3′

pTiT37 5′ GGCGTGAAAAGGTTTA**TccGTtcgTccaTtTGTaTGTgca**TGCCAACCACA 3′

pRiA4 T_R: 5′ -----GGTAGATAAATT*TGTGA***GgaG GTATGTTTGTTTa**GGAC------- 3′

T_L: 5′ --------------ATATATGTTCCTGTC**ATGTTTGTTca**ATTGTTCAATT 3′

Figure 5. Comparison of *overdrive*-like sequences in right border regions of a range of Ti- and Ri-plasmids.

Comparison, by Shurvinton and Ream (1991) and Peralta *et al.* (1986), of the sequences adjacent to the right borders (underlined) of a range of Ti- and Ri-plasmids showing the conserved sequence termed the 24 bp octopine-type *overdrive* sequence (**Bold**) and the highly conserved *overdrive* consensus core (**Bold underlined**). Where bases are not homologous to the 24 bp octopine-type *overdrive* sequence of the pTiA6NC T_L-DNA, they are marked appropriately (**bold lowercase**). The 5′-TGTGA-3′ sequence that may be involved in *overdrive* activity (Shurvinton and Ream, 1991) is marked (*italics double-underlined*).

when removing *overdrive* from the octopine-type right border in the octopine-type *vir* system of Peralta *et al.* (1986). Wang *et al.* (1987), proposed that unlike the octopine *overdrive* of Peralta *et al.* (1986), sequences flanking the nopaline-type right border only moderately enhance T-DNA transmission. Furthermore, as with Peralta *et al.*, (1986), Wang *et al.* (1987) could not detect any sequences near the nopaline-type right border with better than 75% homology (6 out of 8 bp) with the 8 bp *overdrive* consensus core. Wang *et al.* (1987) concluded, therefore, that since such 6 bp homologies occur throughout the T-region, they are unlikely to play a significant role in T-DNA transfer.

Many other researchers, however, provided evidence that sequences flanking the right border of nopaline Ti-plasmids have a large effect on T-DNA transmission. Van Haaren *et al.* (1988) repeated the experiments of Wang *et al.* (1984), but in an environment of octopine-type *vir* products. Tumourigenesis assays were performed upon a range of plants using a mutant of the octopine-type pTiAch5 from which the entire T_R-DNA and the T_L-DNA right border had been deleted. Insertion of the 3.2 kb fragment of the nopaline-type pTiT37 containing the native right border and flanking sequences fully restored virulence, whereas insertion of a synthetic nopaline-type right border sequence resulted in poor tumour induction: in direct contrast to the results of Wang *et al.* (1984; 1987).

Jen and Chilton (1986a), however, constructed binary mini-T plasmids from the nopaline-type Ti-plasmid pTiT37. These 35-45 kb plasmids did not contain the *vir* operon, but incorporated only the tumour induction genes and differing amounts of flanking DNA such that the plasmids had either left, right or both borders. The *vir* products were provided *in trans* by the octopine-type helper plasmid, pAL4404. The oncogenicity assays were conducted, therefore, with nopaline-type border regions in an environment of octopine-type *vir* products. Mini-T plasmids containing both borders or only the right border region were equally virulent and significantly more virulent than plasmids containing only the left border region (+ vs ++++). This indicates the presence of a native enhancing region associated with the nopaline-type right border. All the right border regions assayed contain the putative 8 bp *overdrive* consensus core. A more detailed investigation using the same system, assayed the effects of individually inserting the left or right border regions into a mini-T plasmid that contained only the oncogenes (Jen and Chilton, 1986b). Regardless of border orientation with respect to the oncogenes, the mini-T plasmids containing the right border and flanking region alone were highly virulent (++++), whereas those containing the left border region alone were weakly virulent (+). Again, this indicates

the nopaline-type right border region is intrinsically more active than the left border region in T-DNA transmission, most likely due to sequences near the right border (Jen and Chilton, 1986b).

All these experiments provide strong evidence of the potential nopaline-type *overdrive* greatly affecting T-DNA transmission in an octopine-type *vir* operon environment. Van Haaren *et al.* (1988) hypothesised that the differences between their results and those of Wang *et al.* (1984; 1987) were due to possible differences in the octopine and nopaline-type *vir* products and how they might interact with T-strand processing. They also concluded that in the nopaline-type Ti system, the sequence context of the right border repeats influences tumourigenicity almost undetectably, in contrast to the octopine-type Ti system.

Culianez-Macia and Hepburn (1988), however, provided evidence of the influence of the nopaline-type *overdrive* in a nopaline-type *vir* environment. A binary system comprising a disarmed nopaline-type pTiC58 helper plasmid and a large (62 kb) binary plasmid, was used. The binary plasmid contained the nopaline-type pTiT37 left border region and, inserted 2 kb away as a 103 bp fragment, the putative nopaline-type *overdrive*. Rather than performing tumourigenesis assays on plants, Culianez-Macia and Hepburn (1988) measured T-strand production within acetosyringone-induced bacteria. Reversing the orientation of the left border region with regard to the *overdrive* did not affect T-strand production, whereas deletion of the *overdrive* abolished detectable T-strand production, as determined by Southern analysis. The nopaline-type left border is capable, therefore, of producing single-stranded DNA with high efficiency, but its ability to do so is totally dependent on the presence of the putative nopaline-type *overdrive* region (Culianez-Macia and Hepburn, 1988). The putative nopaline-type *overdrive* was also shown to behave as an enhancer as it is effective regardless of its orientation with respect to the border repeat.

These experiments indicate that there is a nopaline-type *overdrive* element which influences T-DNA transfer and T-strand production in octopine and nopaline-type *vir* operon environments.

1.5 *OVERDRIVE* AND MULTIPLE T-DNA COPIES IN TRANSGENIC PLANTS

A major problem in transgenic plants is the presence of multiple copies of the introduced gene (transgene), gene-tag or enhancer/promoter trap in a high proportion of transformants. Identification and analysis of a tagged gene, or trapped enhancer/promoter of interest is complicated by the presence of the extra copies of those tags or traps. Also, transgene expression appears to be reduced or suppressed by the presence of extra copies of the introduced gene. This phenomenon, termed homology-dependent gene silencing, is associated with multiple copies of homologous DNA sequences regardless of whether they are at the same site (*cis*-inactivation) or spread throughout the plant genome (*trans*-inactivation) (reviewed in Matzke and Matzke, 1995). As the presence of multiple transgene copies has been associated with transgene silencing, Finnegan and McElroy (1994) suggested that gene silencing could be avoided by selecting or screening for transgenic plants containing a single intact copy of the transgene, or by developing a transformation method to ensure single-copy transgene integration. This would also facilitate the analysis of gene-tags and enhancer/promoter traps.

Direct gene transfer methods, such as biolistics, generally result in multiple transgene copy numbers, and complex insertional arrangements (Finegan and McElroy, 1994). In fact, biolistic transformation of tobacco has yielded transgenic plant populations where the average *gusA* gene copy number was 20.2 copies per plant, with a maximum of 77 copies per plant (Allen *et al.*, 1996). It may be that these large copy numbers result from the amount of DNA employed in the transformation protocols and that DNA concentration is a factor in transgene copy number. In *Agrobacterium tumefaciens*-mediated transformation systems, a correlation has already been established between removal of both the octopine and putative nopaline-type *overdrive*, and decreased T-strand production (Culianez-Macia and Hepburn, 1988; Toro *et al.*, 1988; Van Haaren *et al.*, 1987b; Veluthambi *et al.*, 1988). The decrease in T-strand production may result in a decreased incidence of multiple insertion events, although a relationship between *overdrive* removal and T-DNA copy number in transgenic plants has yet to be demonstrated. One objective of this Thesis will be to investigate whether *overdrive* does influence T-DNA copy number in transgenic *Nicotiana tabacum*.

1.6 AIMS

To date, no work has been performed to determine precisely which sequences comprise the nopaline-type *Agrobacterium tumefaciens overdrive* enhancer, or confirm if they involve the regions with homology to the *overdrive* consensus core detected by Peralta *et al.* (1986). Furthermore, there has been no investigation into deletions in the *overdrive* region and their influence on T-DNA copy number. The aim of this Thesis was to determine whether deletions centred upon the putative nopaline-type *overdrive* core influence T-DNA transmission to plant cells, thereby identifying sequences involved in nopaline-type *overdrive* activity, and confirming the concept of the *overdrive* consensus core hypothesised by Peralta *et al.* (1986). Another objective was to determine whether these deletions also influence T-DNA copy number in transgenic *Nicotiana tabacum*, and in so doing, a transformation method may be developed that generates a high proportion of plants containing a single T-DNA insert.

CHAPTER 2 MATERIALS AND METHODS

2.1 BACTERIAL PROCEDURES

2.1.1 Growth of Bacteria

Agrobacterium tumefaciens cultures were grown with vigorous shaking (300 rpm) at 26°C in TY broth (Section A1.5, p. 164) or YEB broth (Section A1.6, p. 164). Both maintenance of *A. tumefaciens*, and single colony isolations, were performed on solid AB (Section A1.1, p. 163), TY or YEB. Media were supplemented with antibiotics (Section A3.1, p. 167), as required, at the following concentrations (μg ml^{-1}): Ap, 100; Cb, 100; Km, 100; Rf, 20; Sm, 25; and Sp, 250.

Escherichia coli cultures were grown with vigorous shaking (300 rpm) at 37°C in LB broth (Section A1.2, p. 163). *E. coli* cultures were maintained and single-colony isolated on solid LB (Section A1.2). Media were supplemented with antibiotics, as required, at the following concentrations (μg ml^{-1}): Ap, 100; Cb, 50; and Km, 50.

Bacterial cultures maintained on solidified media were stored at 4°C and sub-cultured approximately every four to six weeks. Every three months the stored cultures on solid media were replaced by fresh inoculations from frozen long-term storage cultures.

In order to store bacteria for the long term, they were preserved as frozen glycerol stocks. The cells of overnight (37°C) *E. coli* LB broth cultures, or 20 h (26°C) *A. tumefaciens* TY broth cultures, were harvested by centrifugation at 4000 ***g*** for 10 min and resuspended in 100 μl of LB broth. Of this, 20 μl were added to a pre-sterilised NUNC cryotube containing 1.0 ml of LB broth supplemented with glycerol to a final concentration of 15% (v/v). These glycerol stocks were stored at -80°C.

2.1.2 Bacterial Strains and Plasmids

The bacterial strains and plasmids used in this study are listed in Table 1 (p. 38).

2.1.3 Transformation of *A. tumefaciens*: Tri-parental Mating

To transform *A. tumefaciens*, a method based upon that of Ditta *et al.* (1980), was employed, whereby the plasmid of interest was conjugated from the host *E. coli* strain to the recipient *A. tumefaciens* strain by tri-parental mating. The mobilisation functions required for the plasmid transfer were provided by an *E. coli* strain containing the helper plasmid pRK2013. All bacterial strains were cultured under the appropriate antibiotic selection (Table 1, p. 38; Section 2.1.1, p. 37).

Table 1. Bacterial strains and plasmids used in this study.

Strain/Plasmid	Genotype or Relevant Characteristics	Source or Reference
BACTERIAL STRAINS		
Escherichia coli		
DH5α™	F⁻ *ϕ80dlacZΔM15 supE44 gyrA96 deoR recA1 endA1 relA1 Δ(lacZYA-argF)U169 hsdR17* (r_k^-, m_k^+) λ^- *thi-1*	*Focus* (1986) 8:9
DH10B™	F⁻ *ϕ80dlacZΔM15 mcrA araD139 Δ(ara, leu)7697 Δ(mrr-hsdRMS-mcrBC) ΔlacX74 deoR recA1 endA1 galU galK* λ^- *rpsL nupG*	Lorow and Jessee (1990)
HB101	F⁻ *Δ(gpt-proA)62 leu supE44 ara14 galK2 lacY1 Δ(mcrC-mrr) rpsL20* (Sm^r) *xyl5 mtl1 recA13*	Boyer and Roulland-Dussoix (1986)
Agrobacterium tumefaciens		
A1021	Sm^r, Km^r; C58 chromosomal background; an oncogenic octopine-type strain with an insertional mutation in *virC1* gene (pTiB6-*virC1*::Tn5).	Garfinkel and Nester (1980)
GV3101	Rf^r, Gm^r, Km^r; C58 chromosomal background; harbours a disarmed derivative of the nopaline-type Ti-plasmid pTiC58, which provides nopaline-type *vir* function in a binary system for *A. tumefaciens*-mediated plant transformation.	Koncz and Schell (1986)
LBA4404	*thi*$^+$, Sm^r; Ach5 chromosomal background; harbours both a large cryptic plasmid and pAL4404, a disarmed derivative of the octopine-type Ti-plasmid, pTiAch5, which provides *vir* gene-products in a binary system for *A. tumefaciens*-mediated plant transformation.	Ooms *et al.* (1982); Hoekema *et al.* (1983)
MOG1010	Rf^r, Sp^r; C58 chromosomal background; harbours a disarmed derivative of the octopine-type Ti-plasmid, pTiB6, which provides *vir* function in a binary system for *A. tumefaciens*-mediated plant transformation.	Mozo and Hooykaas (1992); Hooykaas *et al.* (1980)
MOG1010-C	Rf^r, Sp^r, Cb^r; a *virC2* mutant derivative of MOG1010 (TiB6-*virC2*::Tn3HoHo1).	Mozo and Hooykaas (1992)

Table 1 continued.

Strain/Plasmid	Genotype or Relevant Characteristics	Source or Reference
PLASMIDS		
Plasmids that replicate in *E. coli*		
pUC18	Ap^r; multiple cloning site; high copy number.	Yanisch-Perron *et al.* (1985)
pMTL22P	Ap^r; multiple cloning site; high copy number.	Chambers *et al.* (1988)
pMTL25P	Ap^r; multiple cloning site; high copy number.	Chambers *et al.* (1988)
pANDY1 pANDY2 pANDY3 pANDY4	Ap^r, Km^r; vectors in which the P_{35S}-*nptII-ocs3'* fusion from pSLJ491 underwent a series of subclonings to incorporate extra enzyme-sites, and to facilitate ligation into plant transformation vectors.	This study; Section 3.2.2 This study; Section 3.2.3 This study; Section 3.2.4 This study; Section 3.2.4
pJIT166	Ap^r; source of *gusA* probe for Southern analysis.	Guerineau *et al.* (1988)
Plasmids that replicate in both *A. tumefaciens* and *E. coli*		
pRK2013	Km^r; Mob$^+$, Tra$^+$; mobilisation helper plasmid for triparental mating.	Ditta *et al.* (1980)
pSLJ491	Ap^r; low copy number plant transformation vector; source of the P_{35S}-*nptII-ocs3'* fusion for the pANDY series of vectors.	Jones *et al.* (1992)
pBIN19/GTG	Ap^r/Cb^r, Km^r; a promoter-tagging vector with a promoterless *gusA* gene; border regions derived from the nopaline-type Ti-plasmid, pTiT37.	Kerr (1996)
pANDY6	Ap^r/Cb^r, Km^r; derived from pBIN19/GTG by removing the P_{nos}-*nptII* fusion; has no plant-selectable marker.	This study; Section 3.1.3
pANDY7	Ap^r/Cb^r, Km^r; derived from pBIN19/GTG by removing the *ocs3'* terminator sequence of the promoterless *gusA* gene.	This study; Section 3.1.3
pANDYOD$^-$2 pANDYOD$^-$3	Ap^r/Cb^r, and Km^r; derived from pANDY6 by performing various exonuclease BAL 31 deletions in the putative nopaline-type *overdrive* region.	This study; Section 3.1.5 This study; Section 3.1.5
pANDY8 pANDY9 pANDY10	Ap^r/Cb^r, and Km^r; derived from pANDY6, pANDYOD$^-$2 and pANDYOD$^-$3, respectively, by insertion of the modified P_{35S}-*nptII* plant-selectable marker from pANDY4; used to test the influence deletions in the putative nopaline-type *overdrive* region have upon plant transformation and T-DNA copy number.	This study; Section 3.3.2 This study; Section 3.3.2 This study; Section 3.3.2

Cells of the recipient *A. tumefaciens* strain were grown overnight in a 10 ml TY broth (Section A1.5, p. 164), and harvested by centrifugation at 4000 ***g*** for 10 min at 4°C. The supernatant was discarded, and the cells resuspended thoroughly in 10 ml of TY medium. Likewise, two overnight 10 ml LB (Section A1.2, p. 163) broths, one containing the *E. coli* strain harbouring the plasmid to be transferred, the other containing *E.coli* strain HB101 harbouring the helper plasmid pRK2013, were harvested and resuspended in 10 ml of fresh LB medium. A 40 µl aliquot of the resuspended *A. tumefaciens* broth was combined with 25 µl each of the resuspended *E. coli* broths. The resulting mixture was placed on antibiotic-free solid TY medium, and allowed to dry for 30 min before sealing and incubating overnight at 26°C. The resulting bacterial mass was resuspended in 1 ml of sterile MilliQ water, and diluted a further 1×10^5 fold in sterile MilliQ water. *E. coli* cells are less robust than *A. tumefaciens* cells when exposed to this level of osmotic stress, thus reducing the number of viable *E.coli* cells in the *A. tumefaciens* cultures. *A. tumefaciens* cells transformed with the plasmid of interest were selected by spreading a 100 µl aliquot of diluted cells on solid AB minimal medium (Section A1.1, p. 163) containing antibiotics pertinent to the *Agrobacterium* strain and the plasmid of interest (Table 1, p. 38; Section 2.1.1, p. 37). After incubation for four days at 26°C, 10-15 individual colonies were pooled and subjected to two further cycles of selection on the same minimal medium. Single cell purified transformants were evaluated for the presence of the appropriate plasmid using diagnostic restriction endonuclease digests (Section 2.2.13, p. 49) of DNA isolated by alkaline lysis (Section 2.2.1, p. 43).

2.1.4 Transformation of *A. tumefaciens*: Electroporation

Electrocompetent *A. tumefaciens* cells (Section 2.1.5, p. 41) were thawed on ice and divided into 20 µl aliquots, to which 20 ng of desalted plasmid DNA (Section 2.4.6, p. 61) were added prior to electroporation. The cells and DNA were placed in an ice-cold GIBCO BRL Cell-Porator® 0.15 cm gap microelectroporation cuvette (Life Technologies, Inc.). As recommended by Singh *et al.* (1993), the Cell-Porator® was set to a capacitance of 330 µF and a cell medium impedance of Low Ω, and to give a pulse length of 6 ms, the Voltage Booster was set to 4 kΩ. To obtain the required field strength of 12.5 kV cm^{-1} over the 0.15 cm gap in the microcuvette, a pulse of 1.875 kV was required. This was generated by releasing the pulse when the Cell-Porator® voltage controller reached approximately 290 V. Immediately after the pulse, the cells were removed from the cuvette and dispersed in 1 ml of YM medium (Section A1.7, p. 164) in a 1.5 ml microfuge tube. The cells were then allowed to recover and express the resistance genes by shaking the microfuge tube at 300 rpm for 2 h at 28°C. After recovery, the cells were pelleted by centrifugation for 30 s in a microcentrifuge, and 900 µl of the supernatant were discarded. The cells were resuspended in the remaining liquid and spread on solid TY (Section A1.5, p. 164) or YM medium containing the appropriate antibiotics (Table 1, p. 38; Section 2.1.1,

p. 37). The plates were grown at 28°C for 48-72 h, or until the colonies were approximately 1-2 mm in diameter. Colonies were then single cell purified on solid TY medium containing the appropriate antibiotics. Single cell purified transformants were evaluated for the presence of the appropriate plasmid using diagnostic restriction endonuclease digests (Section 2.2.13, p. 49) of DNA isolated by alkaline lysis (Section 2.2.1, p. 43).

2.1.5 Preparation of Electrocompetent *A. tumefaciens* Cells

Preparation of electrocompetent *A. tumefaciens* cells was derived from methods by Mattanovich *et al.* (1989), and Mozo and Hooykaas (1992). A 250 ml YEB broth (Section A1.6, p. 164), supplemented with 0.5% (w/v) glucose and the appropriate antibiotics (Table 1, p. 38; Section 2.1.1, p. 37), was inoculated with 2.5 ml from an overnight 10 ml YEB broth culture of the required *A. tumefaciens* strain. The 250 ml broth was grown at 28°C with vigorous shaking (300 rpm) to an OD_{600} of 0.5-0.8, and then chilled on ice for 15 min. The cells were then harvested by centrifugation at 4000 ***g*** for 10 min at 4°C. The supernatant was discarded, and the cells washed by three cycles of resuspension and centrifugation in 10 ml of ice-cold sterilised 1 mM HEPES (pH 7.0). After a further wash cycle in 10 ml of ice-cold filter-sterilised (Millipore 0.45 μm membrane filter) 10% (v/v) glycerol, the supernatant was removed and the cells resuspended in 1.5 ml of ice-cold filter sterilised 10% (v/v) glycerol (cell density approximately $2.0\text{-}8.0\times10^{10}$ cells ml^{-1}). The electrocompetent cells were then divided into 50 μl aliquots and used immediately (Section 2.1.4, p. 40), or frozen in a -80°C methanol bath and stored at -80°C.

2.1.6 Transformation of *E.coli*: $CaCl_2$ Method

A 300 μl aliquot of stored cells made transformation-competent with $CaCl_2$ (Section 2.1.7, p. 41) was thawed on ice prior to the addition of 50-100 ng of plasmid DNA that had been desalted (Section 2.4.6, p. 61). After incubation on ice for 30 min, the cells were heat-shocked for 2 min at 42°C. They were then mixed with a 700 μl aliquot of LB (Section A1.2, p. 163) and allowed to recover with shaking at 37°C for a minimum of 45 min. Aliquots of the cell suspension were spread on solid LB supplemented with the appropriate antibiotics (Table 1, p. 38; Section 2.1.1, p. 37) pertinent to the *E. coli* strain and plasmid, and where necessary, X-gal and IPTG (Section 2.2.20, p. 52). The plates were incubated overnight at 37°C. Single cell purified transformants were evaluated for the presence of the appropriate plasmid using diagnostic restriction endonuclease digests (Section 2.2.13, p. 49) of DNA isolated by the STET method (Section 2.2.2, p. 44).

2.1.7 Preparation of Competent *E. coli* Cells with $CaCl_2$

A 40 ml LB broth (Section A1.2, p. 163), supplemented with the appropriate antibiotics (Section 2.1.1, p. 37), was inoculated with 0.4 ml from an overnight 10 ml

LB broth culture of the required *E. coli* strain. The 40 ml broth was grown with vigorous shaking (300 rpm) at 37°C to an OD_{600} of 0.5-0.8, then chilled on ice for 15 min. The cells were transferred to a prechilled screw-top NALGENE™ Oak Ridge centrifuge tube and harvested by centrifugation at 2500 ***g*** for 5 min at 4°C. The supernatant was discarded and the pellet resuspended very gently in a 10 ml aliquot of prechilled sterile 60 mM calcium chloride ($CaCl_2$). A further 10 ml volume of 60 mM $CaCl_2$ was added and the cell suspension incubated on ice for 30 min. The cells were again harvested by centrifugation at 2500 ***g*** for 5 min at 4°C. After discarding the supernatant, the pellet was resuspended very gently in a 4 ml aliquot of prechilled 60 mM $CaCl_2$ supplemented with 15% (v/v) glycerol. After storage at 4°C overnight, the cells were divided into 300 µl aliquots and either used immediately (Section 2.1.6, p. 41), or snap-frozen in liquid nitrogen and stored at -80°C.

2.1.8 Transformation of *E. coli*: Electroporation

E. coli was transformed by electroporation if the concentration of plasmid DNA was low, or the vector size was large (>10 kb). Stored electrocompetent *E. coli* cells (Section 2.1.9, p. 43) were thawed on ice and divided into 20 µl aliquots in prechilled microfuge tubes. After the addition of 20 ng of plasmid DNA that had been desalted (Section 2.4.6, p. 61), the cells were transferred to an ice-cold GIBCO BRL Cell-Porator® 0.15 cm gap microelectroporation cuvette (Life Technologies, Inc.). The Cell Porator® and Voltage Booster (Life Technologies, Inc.) were set to those values described in Section 2.1.4, p. 40).

For efficient electroporation of *E. coli* strain DH10B™ (Table 1, p. 38), a field strength of 17.66 kV cm^{-1} was required (GIBCO BRL Cell-Porator® Voltage Booster (Life Technologies, Inc.) instruction manual). This was generated over the 0.15 cm gap of the microcuvette by releasing a pulse of 2.65 kV, which occurred when the Cell-Porator™ voltage controller reached 410 V. Efficient transformation of the *E. coli* strain DH5α™ (Table 1, p. 38) required a field strength of 17.24 kV cm^{-1} (GIBCO BRL Cell-Porator® Voltage Booster (Life Technologies, Inc.) instruction manual), which was generated by releasing the pulse when the voltage controller reached 400 V.

Immediately after the pulse was released, the electroporated cells were transferred to a 2 ml microfuge tube containing 1 ml of room temperature SOC (Section A1.4, p. 163) and allowed to recover with vigorous shaking (300 rpm) at 37°C for at least 45 min. A 100 µl aliquot of the cell suspension was spread on solid LB supplemented with the appropriate antibiotics (Table 1, p. 38; Section 2.1.1, p. 37) pertinent to the *E. coli* strain and plasmid, and where necessary, X-gal and IPTG (Section 2.2.20, p. 52). The plates were incubated overnight at 37°C. The remaining cell suspension was centrifuged for 30 s in a microfuge and the supernatant discarded except for

approximately 100 µl. The pellet was then resuspended and spread on solid LB and incubated as described above. Single cell purified transformants were evaluated for the presence of the appropriate plasmid using diagnostic restriction endonuclease digests (Section 2.2.13, p. 49) of DNA isolated by the STET method (Section 2.2.2, p. 44).

2.1.9 Preparation of Electrocompetent *E. coli* Cells

The preparation of *E. coli* electrocompetent cells was derived from a protocol described in the GIBCO BRL Cell-Porator® Voltage Booster (Life Technologies, Inc.) instruction manual. A 250 ml SOB broth (Section A1.3, p. 163) (without magnesium), supplemented with the appropriate antibiotics (Table 1, p. 38; Section 2.1.1, p. 37), was inoculated with a 2.5 ml from an overnight 10 ml SOB (without magnesium) broth culture of the required *E. coli* strain. The 250 ml broth was grown at 37°C with vigorous shaking (300 rpm) to an OD_{600} of 0.5-0.8, and then chilled on ice for 15 min. After harvesting the cells by centrifugation at 2600 ***g*** for 10 min at 4°C, the supernatant was discarded and the pellet washed by resuspension in 100 ml ice-cold filter-sterilised (Millipore 0.45 µm filter membrane) 10% (v/v) glycerol, then centrifuged again and the supernatant discarded. This wash cycle was repeated and the resulting pellet resuspended in 1 ml ice-cold sterile 10% (v/v) glycerol. The cell suspension was divided into 50 µl aliquots and either used immediately or frozen in a -80°C methanol bath and stored at -80°C.

2.2 DNA PROCEDURES

2.2.1 Plasmid Isolation from *A. tumefaciens*: Alkaline Lysis

Small amounts of plasmid DNA were isolated from *A. tumefaciens* using a method derived from those of Birnboim and Doly (1979) and Ish-Horowicz and Burke (1981). A 10 ml TY (Section A1.5, p. 164) broth culture, containing appropriate antibiotics (Table 1, p. 38; Section 2.1.1, p. 37) was grown for 20 h at 28°C. Cells of a 1.5 ml aliquot were pelleted by centrifugation for 30 s at 12000 rpm in a microcentrifuge, the supernatant was drained, and the cells thoroughly resuspended by vortexing in 100 µl of a freshly prepared Cell Resuspension Buffer (Section A4.5, p. 169). The resuspended cells were then allowed to stand on ice for 25 min. Following the addition of 2 vol of ice-cold freshly prepared Cell Lysis Solution (Section A4.6, p. 169), the mixture was thoroughly combined by gentle inversion, and left to incubate on ice for 5 min. Next, 0.5 vol of ice-cold 3 M sodium acetate ($CH_3COOHNa$, pH 4.8) was added and the solution mixed by gentle inversion, prior to incubation on ice for 45 min. The resulting precipitate was pelleted by centrifugation at 4°C for 10 min at 12000 rpm in a microcentrifuge, and the supernatant transferred to a fresh 1.5 ml microfuge tube. To precipitate the nucleic acids, 2.5 vol of cold (-20°C) absolute ethanol were added and the solution mixed by inversion. The DNA was pelleted by centrifugation at 4°C for 15 min at 12000 rpm in a microcentrifuge, and the

supernatant discarded. The pellet was dried briefly in a Speedvac® and resuspended in 100 µl of sterile MilliQ water. After a further cycle of DNA precipitation by adding 0.1 vol of 3 M sodium acetate (pH 4.8), 2.5 vol of cold (-20°C) absolute ethanol, mixing, centrifuging at 4°C for 15 min in a microcentrifuge, and discarding the supernatant, the pellet was overlaid with 80% (v/v) ethanol, which was then gently decanted. The DNA was dried briefly in a Speedvac®, resuspended in 40 µl of sterile MilliQ water, then stored at -20°C.

2.2.2 Plasmid Isolation from *E. coli*: STET Method

Small amounts of plasmid DNA were isolated using the following protocol adapted from the rapid boiling lysis method of Holmes and Quigley (1981). The cells of a 10 ml overnight LB (Section A1.1, p. 163) broth culture, supplemented with the appropriate antibiotics (Table 1, p. 38; Section 2.1.1, p. 37), were harvested by centrifugation at 3000 ***g*** for 10 min at 4°C. The supernatant was discarded and the cells thoroughly resuspended by vortexing in 100 µl of LB medium prior to the addition of 700 µl of STET Buffer (Section A4.7, p. 169). The solution was mixed gently and transferred to a 1.5 ml microfuge tube containing 20 µl of a freshly prepared lysozyme solution (10 mg ml^{-1} in sterile MilliQ water). After incubation at room temperature for 10 min, the tube was placed in a boiling water bath for 2 min. The bacterial lysate was then centrifuged for 10 min at 12000 rpm in a microcentrifuge, and the resulting gelatinous pellet removed with a sterile toothpick. RNA was degraded by adding 50 µg DNase-free RNase-A (Section A4.4, p. 169) and incubating the tube at 37°C for 10 min. The solution was deproteinated with the addition of an equal volume of a equilibrated phenol (Section A4.8, p. 170): chloroform: iso-amyl alcohol solution (25:24:1 v/v, respectively). The aqueous and non-aqueous phases were mixed thoroughly by vortexing the tube for 15 s, and the phases separated by centrifugation at 12000 rpm in a microcentrifuge for 5 min. The aqueous supernatant was transferred to a fresh microfuge tube, and the phenol/chloroform extraction repeated. To precipitate the nucleic acids, the aqueous supernatant was transferred to a fresh microfuge tube, and an equal volume of isopropanol added. The DNA was pelleted by centrifugation at 4°C for 15 min at 12000 rpm in a microcentrifuge, and the supernatant discarded. The pellet was dried briefly in a Speedvac®, then resuspended in 100 µl of a 0.1 M NaCl solution. To this was added 2.5 vol of cold (-20°C) absolute ethanol and the nucleic acids were pelleted by centrifugation at 4°C for 15 min at 12000 rpm in a microcentrifuge. The pellet was overlaid with 80% (v/v) ethanol, which was then decanted gently, prior to drying the pellet briefly in a Speedvac®. The DNA was resuspended in 40 µl of sterile MilliQ water and stored at -20°C.

2.2.3 Plasmid Isolation from *E. coli*: Large Scale Alkaline Lysis

In order to prepare larger quantities of plasmid DNA (0.5 mg), a Wizard™ MaxiPrep

(Promega) kit was used that based its extraction upon the alkaline lysis methods of Birnboim and Doly (1979), and Ish-Horowicz and Burke (1981). A 10 ml LB (Section A1.2, p. 163) broth culture supplemented with the appropriate antibiotics (Table 1, p. 38; Section 2.1.1, p. 37) was grown for 8 h, and used to inoculate a 200 ml LB broth containing the appropriate antibiotics. This broth culture was grown overnight at 37°C, and the cells harvested by centrifugation at 4000 ***g*** for 10 min at 4°C. The DNA was then extracted from the cells according to the manufacturers instructions, and stored in 1 ml aliquots at -20°C.

2.2.4 Precipitation of DNA

To precipitate DNA, the solution in which it was suspended was made 0.3 M with respect to sodium acetate ($CH_3COOHNa$, pH 4.8), and the nucleic acids were precipitated with 2.5 vol cold (-20°C) absolute ethanol. The DNA's were pelleted by centrifugation for 10 min in a microfuge, and the salts removed by overlaying the pellet with 80% (v/v) ethanol and discarding the supernatant. After drying in a Speedvac® for 5 min, the DNA's were resuspended an appropriate volume of sterile MilliQ water or reaction buffer.

2.2.5 DNA Quantification by Spectrophotometry

To quantify DNA using this technique, as described by Sambrook *et al.* (1989), the sample was placed in a 1 cm light path quartz cuvette and the absorbence determined by scanning between 200 and 300 nm on a Cary 1E UV-Visible Spectrophotometer (Varian). The concentration of nucleotide solutions was calculated assuming that for double stranded DNA, an A_{260} of 1.0 corresponds to approximately 50 μg ml^{-1}. Relatively pure DNA solutions have an A_{260}/A_{280} ratio of 1.8, a value that decreases with the presence of contaminants such as proteins and phenol.

2.2.6 DNA Quantification by Serial Dilution on Agarose Gels

This method was a visual comparison of serially diluted DNA samples against those of a standard sample on an agarose gel containing ethidium bromide. The method generated more consistent quantification than spectrophotometry (Section 2.2.5, above) when DNA samples had been extracted in the presence of CTAB (Section 2.4.1, p. 58). The DNA sample underwent an initial dilution, usually 1000-fold, such that its concentration was approximately 10-50 mg ml^{-1}. Of this diluted sample, 1 μl was made to 10 μl with GLB (Section A4.13, p. 171), and 5 μl of this was loaded on to a 0.8% (w/v) agarose gel containing ethidium bromide (0.5 μg ml^{-1}) (Section 2.2.9, p. 46). The remaining 5 μl were made to 10 μl with GLB, of which 5 μl were loaded beside the first sample on the minigel. This series of two-fold dilutions was repeated until a total of eight samples were loaded on the gel. A series of eight two-fold dilutions was made in the same way from a 10 mg ml^{-1} phage λ genomic DNA stock (Promega), and loaded onto the same minigel. The samples underwent electrophoresis

until the bromophenol blue dye had migrated approximately 2 cm, then the DNA was visualised and photographed as described (Section 2.4.1, p. 46). DNA concentration was estimated by comparing the number of dilutions required to no longer visualise the sample, with that of the standard.

2.2.7 DNA Quantification by Fluorometry

To quantify DNA contaminated with compounds affecting spectrophotometry (such as CTAB), a fluorometric method was employed based upon that of Rago *et al.* (1990). The DNA sample to be quantified was diluted initially in sterile MilliQ water to a final concentration of 10-50 $\mu g\ ml^{-1}$. A 20 µl aliquot of the prediluted sample or DNA standard was made to 100 µl with TNE (Section A4.9, p. 170). To this was added a 100 µl aliquot of Hoechst 33258 (Sigma Chemical Company) dye (20 $\mu g\ ml^{-1}$) in TNE that had been prepared by diluting a dye stock (1 $mg\ ml^{-1}$ Hoechst 33258 in MilliQ water) 1 in 50 in TNE. Fluorescence was determined in a Perkin Elmer LS 50 B Luminescence Spectrometer and plate reader (Perkin-Elmer, Ltd) by exciting the samples in a microtitre plate at 350 nm, and measuring the emission at 460 nm. The DNA sample was then quantified by comparing its emission with those of a standard curve derived from the fluorescence of standards containing 5, 10, 15, 20, 25, 30, 40, and 50 $\mu g\ ml^{-1}$ phage λ DNA (Promega), respectively. Results from all samples and standards were derived from a minimum of three replicates.

2.2.8 Determining DNA Fragment Size

The sizes of DNA fragments were determined from their mobility relative to that of known standards run on the same agarose gel (Section 2.2.9, below). This data was entered into a computer programme, DNAFIT (National Institutes of Health, Bethesda, Maryland 20892) employing a four-parameter logistic model to describe the relationship between electrophoretic mobility and the $\log_{10}$ molecular size (Oerter *et al.*, 1990). The standards were generated by combining a *Hin*dIII digest with a *Hin*dIII/*Eco*RI digest of phage λ DNA (Section A4.10, p. 170).

2.2.9 Agarose Gel Electrophoresis of DNA

In order to analyse DNA fragments, they were resolved electrophoretically through a horizontal TAE agarose gel. Electrophoresis of plasmid DNA was generally performed in a mini-gel (90×70 mm gel bed) apparatus or a Bio-Rad Wide Mini-Sub™ Cell (150×100 mm gel bed), whereas most plant genomic DNA underwent electrophoresis in a Bio Rad DNA Sub Cell™ (150×150 mm gel bed) or a Pharmacia Gel Apparatus (200×200 mm gel bed) (Pharmacia LKB Biotechnology). Agarose concentrations varied from 0.4% to 1.5% (w/v), although 0.8% (w/v) gels were used for general analysis. To make an agarose gel, an appropriate quantity of GIBCO BRL ultraPURE™ electrophoresis grade agarose (Life Technologies, Inc.) was added to a

volume of TAE electrophoresis buffer (Section A4.11, p. 170) and melted in a microwave. Ethidium bromide was added to the gel only, to a final concentration of 0.5 $\mu g\ ml^{-1}$, then the gel was poured and allowed to set. DNA samples were loaded with either a 0.1 vol of SUDS (Section A4.12, p. 170) or an equal volume of GLB (Section A4.13, p. 171). To resolve plasmid DNA fragments, the electrophoretic field strength was initially 5 $V\ cm^{-1}$, until the DNA had migrated into the gel. It was then increased to 7-10 $V\ cm^{-1}$ till the end of electrophoresis. Digested plant genomic DNA, however, was loaded, initially resolved electrophoretically at 3 $V\ cm^{-1}$ till the DNA had migrated into the gel, then resolved at 1.5 $V\ cm^{-1}$ for 16-20 h. Progress of the electrophoresis was monitored by migration of bromophenol blue dye and also the DNA fragments themselves, as visualised with a hand-held long wave (366 nm) UV lamp. After electrophoresis, the DNA fragments were visualised on a short wave (340 nm) UV transilluminator, and photographed on Polaroid type 667 film.

2.2.10 DNA Recovery from Agarose Gels: DEAE-Cellulose Method

This procedure, derived from that of Sambrook *et al.* (1989), is useful for recovering DNA fragments greater than 10 kb from agarose gels. Having been separated from other DNA fragments by electrophoresis through an agarose gel, a slit was made just ahead of the leading edge of the DNA band of interest. A piece of Servacel® DEAE ion exchange paper (Serva) that had been trimmed to the size of the band to be recovered, was inserted into the slit. Another portion of DEAE-paper was placed above the band of interest to prevent cross contamination by migration of other DNA bands during the recovery process. Electrophoresis was then resumed until the entire band had migrated onto the DEAE-paper. The paper containing the DNA band was removed from the gel, rinsed vigorously in the surrounding electrophoresis buffer to remove any agarose, and placed in a microfuge tube containing 100 µl DEAE-Elution Buffer (Section A4.14, p. 171). The membrane was crushed gently prior to two DNA elution incubations. The first was at 68°C for 30 min, after which the supernatant was transferred to a microfuge tube and replaced with 75 µl DEAE-elution buffer for a further elution at 68°C for 30 min. The two elution volumes were combined and centrifuged at 12000 rpm for 15 min in a microcentrifuge to pellet any contaminating DEAE-paper. The supernatant was transferred to a fresh microfuge tube and made 10 mM with respect to $MgCl_2$. To precipitate the nucleic acids eluted from the DEAE-membrane, 2.5 vol of cold (-20°C) absolute ethanol were added and the solution mixed by gentle inversion. The DNA was pelleted by centrifugation at 4°C for 15 min at 12000 rpm in a microcentrifuge, and the supernatant discarded. To remove salts, the pellet was overlaid with 80% (v/v) ethanol, which was decanted gently. The DNA was either air-dried, or dried briefly in a Speedvac®, and resuspended in 10 µl of sterile MilliQ water. Prior to storage at -20°C, the recovered fragments were quantified (Section 2.2.5, p. 45), then visualised on an agarose gel (Section 2.2.9, p. 46) to check for size and contamination from other DNA bands.

2.2.11 DNA Recovery from Agarose: Silica Powder Method

In this method, the plug of agarose containing the DNA band was excised from the gel and the DNA adsorbed onto silica powder using a method derived from that of Vogelstein and Gillespie (1979). Using either a GENECLEAN® (BIO 101, Inc.), or a GIBCO BRL GlassMAX™ Isolation Matrix System (Life Technologies, Inc.) kit, the agarose plug was excised with a minimum amount of excess agarose, weighed, and placed in a microfuge tube. To this was added 6 M NaI at a ratio of 3 ml per 1 g agarose. The mixture was incubated at 55°C for 2 min or until the agarose had melted to release the DNA. An appropriate volume of well mixed silica powder slurry was added according to manufacturer's instructions, and after a minimum of 15 min, the silica:DNA complex was pelleted by centrifugation for 30 s at 12000 rpm in a microcentrifuge. The pellet was washed by three cycles of resuspending in a supplied wash buffer, pelleting the silica:DNA complex by centrifugation, and discarding the supernatant. The DNA was eluted from the silica powder by two cycles of resuspending the mixture in 10 µl of sterile MilliQ water, incubating it at 55°C for 2 min, pelleting the silica by centrifugation, and collecting the supernatant. The combined supernatants were centrifuged for 5 min to pellet any silica powder remaining, and the supernatant removed carefully. Prior to storage at -20°C, the recovered fragments were quantified (Section 2.2.5, p. 45), then visualised on an agarose gel (Section 2.2.9, p. 46) to check for size and contamination from other DNA bands. This quick method was not suitable for fragments larger than 10 kb, as they tended to shear.

2.2.12 DNA Recovery from Agarose: Spin-Column Method

To recover DNA fragments less than 400 bp in size, a protocol was developed in the laboratory that combined the initial steps of a GENECLEAN®/GlassMAX ™ method with the DNA purification procedure of a Wizard™ MiniPrep System or PCR Prep kit (Promega). A plug of agarose containing the DNA band of interest was excised and melted in the presence of NaI, as described in Section 2.2.11 (above). The mixture was then added to 1 ml of thoroughly resuspended Wizard™ MiniPreps DNA Purification Resin (Promega), and combined well. The resin was loaded into a Wizard™ Minicolumn (Promega) and washed with three 2 ml volumes of 80% (v/v) isopropanol. The last of the isopropanol was removed by placing the column in a microfuge tube and centrifuging it at 1600 rpm for 45 s. To elute the DNA from the resin, a 50 µl aliquot of 70°C sterile MilliQ water was applied to the column and incubated for 1 min. The DNA was collected by centrifugation at 1600 rpm for 30 s. This elution procedure was repeated, and the aliquots combined. Prior to storage at -20°C, the recovered fragments were quantified (Section 2.2.5, p. 45), then visualised on an agarose gel (Section 2.2.9, p. 46) to check for size and contamination from other DNA bands.

2.2.13 Restriction Digestion of Plasmid DNA

All plasmid DNA's were digested by a restriction endonuclease in the buffer recommended by the enzyme manufacturer. The enzyme was added to final concentration of approximately 5 U μg^{-1} of DNA prior to digestion for approximately 1.5 h at the temperature pertinent to the particular enzyme. To reduce the incidence of 'star' activity, whereby endonucleases cleave sequences similar but not identical to their defined cleavage sites, the total glycerol concentration of the digest reaction was kept below 5% (v/v), and the enzyme concentration never exceeded 100 U μg^{-1} of DNA. When DNA that contained RNA was digested, the RNA was degraded by the addition of 10 µg of DNase-free RNase-A (Section A4.4, p. 169) during the last 10 min of the digestion reaction. The reactions were terminated either by inactivation of the enzyme by heat, usually at 65°C for 20 min, or by the addition of 0.1 vol SUDS (Section A4.12, p. 170). Upon completion of diagnostic digests of plasmids, they were resolved by electrophoresis (Section 2.2.9, p. 46) to reveal their characteristic fragment patterns.

2.2.14 Partial *Eco*RI Digestion of *Hin*dIII-linearised Plasmid DNA

To delete a *Hin*dIII/*Eco*RI digested fragment from a plasmid containing a single *Hin*dIII and many *Eco*RI restriction sites, it was necessary to perform a complete *Hin*dIII digestion followed by a partial *Eco*RI digestion. The resulting series of *Hin*dIII/partially *Eco*RI digested fragments could then be separated by electrophoresis through an agarose gel and the species of the desired size be recovered. A series of digests was performed to optimise the enzyme concentration required to obtain the maximum yield of the desired partial-digestion product. To do this, a 50 µl reaction mixture containing 10 µg of DNA and restriction enzyme buffer B (Boehringer Mannheim, GmbH) was digested to completion by the addition of 50 U *Hin*dIII. After incubation at 37°C for 30 min, the reaction mixture was divided into a 10 µl aliquot and eight 5 µl aliquots. A 1 µl aliquot containing 20 U *Eco*RI (Boehringer Mannheim, GmbH) was added to the 10 µl aliquot, the solutions were mixed, and a 5 µl aliquot removed and added to one of the 5 µl reaction mixture aliquots. After mixing, a 5 µl aliquot was removed and added to another 5 µl reaction mixture aliquot. This two-fold enzyme dilution step was repeated with the remaining reaction mixtures. After digestion at 37°C for 20 min, the reactions were terminated by the addition of 0.1 vol SUDS (Section A4.12, p. 170).

2.2.15 Exonuclease BAL 31 Deletions in pANDY6

The exonuclease BAL 31 was used to degrade 3′ and 5′ termini of duplex DNA in a controlled manner. To determine the units of BAL 31 required to remove the desired number of base-pairs from a certain concentration of DNA termini over a certain period of time, the following equation (Sambrook *et al.*, 1989) was used (see following page).

$$\frac{dMt}{dt} = \frac{-2V_{max}M_n}{[K_M + (S)_0]}$$

Where: $\frac{dMt}{dt}$ is the removal of nucleotides (Dalton min^{-1} DNA $molecule^{-1}$)

V_{max} is the enzyme's maximal rate (moles nucleotides removed l^{-1} min^{-1}) and was set at 1.5×10^{-4}.

M_n is the average molecular mass of sodium mononucleotide (330 Dalton)

K_M is the enzyme's Michaelis constant (moles double-stranded DNA termini l^{-1}) and was set at 4.9×10^{-9}.

$(S)_0$ is the concentration of double-stranded termini at t=0 min (mol l^{-1}).

A time course of BAL 31 digests was performed to determine the optimal reaction period required to obtain the desired degree of DNA degradation. Prior to degradation by BAL 31, pANDY6 DNA (Section 3.1.3, p. 68) prepared by the STET method (Section 2.2.2, p. 44), was *Sph*I-linearised by digesting to completion five 40 µl reaction mixtures, each containing 30 µg of the target DNA, 20 U *Sph*I and restriction endonuclease buffer B (Boehringer Mannheim GmbH). The reactions were terminated by heating to 65°C for 20 min. To suit the requirements of BAL 31, the reaction buffer was modified to a final molarity of 20 mM Tris, 12 mM $MgCl_2$, 0.6 M NaCl, 12 mM $CaCl_2$, and 1 mM EDTA. The precalculated units of BAL 31 (New England Biolabs, Inc.) were then added to a final reaction volume of 50 µl, and the reaction incubated at 30°C for 1-5 min. The reactions were terminated in sequence at 1 min intervals over 5 min by the addition of EGTA to a final concentration of 20 mM. The DNA's were precipitated with absolute ethanol and washed as described (Section 2.2.4, p. 45). After drying in a Speedvac® for 5 min, the DNA's were resuspended in 10 µl sterile MilliQ water.

2.2.16 End-filling 5′ Overhangs

DNA fragments with 5′ overhangs were converted to blunt-ended fragments using a DNA polymerase. The enzyme used was a modified T7 DNA polymerase with no 3′-5′ exonuclease activity: Sequenase™ Version 2.0 (USB™ United States Biochemical Corporation/Amersham International, plc; Tabor and Richardson, 1989). To create blunt-ended DNA fragments, 1 µl (13 U) of Sequenase™ Version 2.0 was added to a 30 µl reaction mixture containing 3-5 µg DNA, 33 µM each of dATP, dTTP, dCTP, and dGTP, 10 mM DTT, and 4 µl Sequenase™ buffer (supplied). The reaction was incubated at room temperature for 5 min, the at 37°C for 5 min, and terminated by heating to 75°C for 10 min.

2.2.17 Recessing 3′ Overhangs

The 3′ overhangs on DNA fragments were recessed to form blunt ends using 3′-5′ exonuclease activity of T4 DNA Polymerase. Three units of T4 DNA Polymerase (New England Biolabs, Inc.) were added to a 20 µl reaction mix containing 1-5 µg of digest DNA, 2 µl of the supplied 10× T4 DNA Polymerase buffer, 20 µg BSA, and 33 µM each of dATP, dTTP, dCTP, and dGTP. After incubation at 37°C for 40 min, the reaction was terminated by heating to 75°C for 10 min.

2.2.18 CAP-Treatment of Vector DNA

To inhibit self-ligation of compatible ends, the 5′ phosphate groups of vector DNA fragments were removed by calf intestinal alkaline phosphatase (CAP). Typically, CAP (Boehringer Mannheim GmbH) was added during the last 20 min of the restriction endonuclease digestion to a final concentration of 0.6 U μg^{-1} of DNA. The reaction was terminated by heating to 65°C for 10 min in the presence of 20 mM EDTA and 0.5% (w/v) SDS. If the restriction endonuclease digestion yielded a blunt-ended fragment or one with a 3′ overhang (such as *Sac*I), then to be effective the CAP treatment had to be more rigorous. The DNA fragments were supplemented with CAP to a final concentration of 5 U μg^{-1} of DNA, incubated at 37°C for 15 min, then at 56°C for another 15 min. A further aliquot of CAP was added, and the incubations repeated. The reaction was terminated as described above.

2.2.19 DNA Ligation

To ligate fragments with compatible cohesive ends, 2 U of GIBCO BRL T4 DNA Ligase (Life Technologies, Inc.) were added to a 20 µl total reaction volume that contained 4 µl of GIBCO BRL 5× T4 DNA Ligase buffer (Life Technologies, Inc.), and the appropriate concentrations of the vector and insert. For optimal ligation conditions, the molar ratio of CAP-treated vector (Section 2.2.18, above) to insert was 1:2, and that the DNA concentration yielded 0.1-1.0 µM in 5' termini. Ligation mixes were incubated overnight at 16°C, or 4 h at 24°C. To check the ligation progress, a 2 µl aliquot of the ligation reaction was examined electrophoresis on an agarose gel (Section 2.2.9, p. 46). Prior to using the completed ligation reaction to transform bacteria (Section 2.1.3-2.1.8, pp. 37-42), it was purified by Sepharose CL-6B spin-column chromatography as described (Section 2.4.6, p. 61).

The ligation of blunt-ended fragments was less efficient than that of fragments with compatible cohesive ends. To accommodate for this, the molar ratio of CAP-treated vector (Section 2.2.18, p. 51) to insert was adjusted to 3:1, and the ATP concentration in the reaction buffer reduced, as recommended by Boehringer Mannheim GmbH. To ligate the fragments, 2 U of GIBCO BRL T4 DNA Ligase (Life Technologies, Inc.) were added to a total reaction volume of 20 µl that contained 4 µl of 5× Blunt End Buffer (Section A4.16, p. 171) and the appropriate concentrations of the vector and

insert. Ligation mixes were incubated overnight at 16°C and progress of the ligation reaction checked and the DNA purified as described above.

2.2.20 Screening Recombinant Plasmids: β-Galactosidase Method

The β-galactosidase histochemical screen identifies colonies harbouring recombinant plasmids, as the insert disrupts α-complementation of the β-galactosidase protein, resulting in white or pale blue in the presence of X-gal. To perform this screen, the vector and bacterial strain must be compatible for α-complementation of the *lacZ* gene product. To prepare solid media for β-galactosidase histochemical screening, the chromogenic substrate for β-galactosidase, X-gal (Sigma Chemical Company), was dissolved in DMF to a final concentration of 20 mg ml^{-1}. A 20 μl aliquot was taken from this stock, mixed with 30 μl sterile MilliQ water, and spread on a solid bacterial medium plate. If the plasmid contained the *lac* operon repressor gene, *lacI*, addition of IPTG was also necessary in order to induce expression of the *lacZ* gene. In this case, an IPTG stock was prepared by dissolving IPTG in MilliQ water to a final concentration of 25 mg ml^{-1}. The stock was filter sterilised (Millipore 0.45 μm membrane filter) and 20 μl spread onto a solid bacterial medium containing X-gal.

2.2.21 Screening Recombinant Plasmids: Rapid Colony Lysis

In the absence of β-galactosidase histochemical screening (Section 2.2.20, p. 52), colony lysis was used as a rapid procedure to identify *E. coli* cells containing recombinant plasmids with DNA inserts. Single-cell purified colonies colony were subjected to an alkaline lysis procedure, and the plasmids resolved by agarose gel electrophoresis. The migration rates of the plasmids were compared with those of plasmids released from control colonies containing the vector only. To perform this rapid lysis, derived from the Promega handbook (1990) (pp. 96-98), the colonies of interest were picked directly off the bacterial medium and resuspended in a microfuge tube containing 50 μl 10 mM EDTA. A 50 μl aliquot of fresh 2× Cracking Buffer (Section A4.17, p. 171) was added to each tube prior to vortexing well and incubating at 70°C for 5 min. After cooling to room temperature, 1.5 μl 4 M KCl and 0.5 μl 0.4% (w/v) bromophenol blue solution were added, and the reaction mix incubated on ice for 5 min. Cell debris was then pelleted by centrifuging in a microfuge for 5 min, and the supernatant analysed by agarose gel electrophoresis (Section 2.2.9, p. 46).

2.2.22 DNA Sequence Analysis: Sequencing Reactions

Double-stranded DNA was sequenced with a Sequenase™ Version 2.0 DNA Sequencing Kit (USB™ United States Biochemical Corporation/Amersham International, plc) that was developed from the chain-termination method (Sanger, *et al.*, 1977) using a modified Sequenase™ T7 DNA polymerase (Tabor and Richardson, 1989). Approximately 3-5 μg of plasmid DNA template, prepared by the STET

method (Section 2.2.2, p. 44), were alkaline denatured as described in the kit protocol. Primer annealing, and all subsequent sequencing reaction steps, including the addition of 1000 Ci mmol^{-1} [α-^{35}S]-dATP (ICN Biomedicals, Inc.), were performed according to the manufacturer's instructions. The resulting 10 µl termination reactions were analysed immediately (Section 2.2.23, below), or stored at -20°C for a maximum of one week. Sequence close to the primer annealing site was determined by performing the sequencing reactions in the presence of manganese, according to the manufacturer's instructions.

2.2.23 DNA Sequence Analysis: Sequencing Gels

The termination reactions were analysed by electrophoresis through a vertical 0.4 mm thick 6% polyacrylamide denaturing gel containing 8.3 M urea in TBE buffer. The gel was made by adding, in a final volume of 100 ml, 50 g urea, 10 ml 10× TBE stock solution (Section A4.18, p. 171), 15 ml 40% acrylamide solution (Section A4.19, p. 171), and MilliQ water. After mixing for at least one hour to dissolve the urea, the solution was filtered through Whatman® No. 1 filter paper, prior to the addition of 2 ml fresh 10% (w/v) ammonium peroxodisulphate solution and 20 µl TEMED. One of a pair of GIBCO BRL Model S2 glass sequencing plates (Life Technologies, Inc.) was treated with two coats of 2% (v/v) dimethylsilane in chloroform. The two plates were separated by 0.4 mm thick spacers (Life Technologies, Ltd), the sides and base sealed with Sleek™ medical tape (Smith and Nephew, Ltd), and the gel mix poured in gently, so as to prevent formation of air-bubbles. The flat side of two 14 cm GIBCO BRL vinyl doublefine sharkstooth combs (Life Technologies, Ltd) was inserted between the plates and into the gel to a depth of 3-5 mm. The apparatus was wrapped with cling film and allowed to polymerise for at least one hour, after which the combs and basal sealing tape were removed, and the plates installed into the GIBCO BRL Model S2 Sequencing Gel Electrophoresis System (Life Technologies, Inc.). The TBE running buffer (Section A4.18, p. 171) was poured into the top and bottom chambers, and the combs inserted teeth downward until the teeth made contact with the gel surface. Prior to loading the termination reactions (Section 2.2.22, p. 52), the gel was prerun for 15 min at 65 W and the wells were flushed to remove accumulated urea. The termination reactions were denatured immediately prior to loading by heated at 80°C for 2 min and rapidly cooling on ice. In order to determine more than 150 bp of sequence, one third of each termination reaction (loaded in the order G A T C) was subjected to electrophoresis at 65 W for 3.0 h. A further aliquot of each termination reaction was then loaded and electrophoresis continued for 1 h 40 min. The gel apparatus was dismantled and the gel fixed in a solution of 5% (v/v) acetic acid: 5% (v/v) methanol for 20 min. After transfer to a sheet of Whatman® 3MM Chr chromatography paper, the gel was dried in a vacuum gel-drier for 1.5 h at 80°C, then placed in a Hypercassette™ (Amersham International, plc) with NIF RX Fuji Medical X-ray Film (Fuji Photo Film Co., Ltd) from one to seven days.

2.3 PLANT PROCEDURES

2.3.1 Growth of *Arabidopsis thaliana*

All *A. thaliana* tissue cultures and *in vitro*-grown plants were maintained at an ambient temperature of 25°C under a 16 h light/8 h dark regime. Illumination was provided by cool white fluorescent 58 W tubes (OSRAM) emitting 400 $\mu E\ m^{-2}\ s^{-1}$ at plant level. A layer of yellow acetate was placed over the plant material to filter out UV-A, thus preventing photo-oxidation of EDTA(Fe) to formaldehyde which is known to detrimentally affect some tissue cultured material (Hangarter and Stasinopoulos, 1991). Although beneficial for *Arabidopsis* culture, it was not required for *Nicotiana tabacum* (Section 2.3.5, p. 55). Plants transferred to soil were grown in a PH2 category containment planthouse which had an ambient temperature of 22°C and natural light as the only light source. The *A. thaliana* ecotype found to be most suitable for transformation experiments was Norwegian No-0, gifted by Mr Paul Sanders, Department of Biology, U.C.L.A., Los Angeles, California, U.S.A.

2.3.2 *A. thaliana*: Bulk Seed Production

A bulk seed store of the *A. thaliana* ecotype No-0 was created by sterilising and germinating approximately 50 seeds as described below (Section 2.3.3). After 5 days, the seedlings were transplanted to soil in the containment planthouse at a ratio of 3 seedlings to each 120×140 mm polythene soil bag. A clear plastic bag was placed over each soil bag to maintain humidity as the seedlings hardened-off. This cover was removed after one week, and the seedlings left to grow, flower, and produce seed (approximately 8 to 10 weeks). When the majority of the siliques had matured and begun to dry, the inflorescences were harvested and placed in a large paper bag. This was transferred to a 28°C incubator for three days to dry the plant material prior to releasing the seed from the siliques by rubbing them on a 1×1 mm wire screen mesh. The seed that passed through the mesh was purified by two further rounds of sieving with the same mesh. The seed was then stored at 4°C in an air-tight container.

2.3.3 *A. thaliana*: Seed Sterilisation and Germination

This seed sterilisation protocol was modified from that of Valvekens *et al.* (1988). Approximately 200 *A. thaliana* seeds, previously vernalised at 4°C for at least seven days, were placed in a 1.5 ml microfuge tube with 1.5 ml of 70% (v/v) ethanol. After mixing by rapid inversion for two minutes, the seeds were pelleted by centrifugation at 6000 rpm for 30 s in a microcentrifuge, and the supernatant removed. A 1.5 ml aliquot of seed sterilisation solution, consisting of 5% (v/v) commercial bleach (sodium hypochlorite, 5% available chlorine) and 0.5% (w/v) SDS, was then added and the seeds were agitated constantly for 20 min. Prior to rinsing, the seeds were pelleted by centrifugation at 6000 rpm for 30 s, and the sterilising solution removed. The seeds were then rinsed seven times with sterile MilliQ water by vigorous resuspension of the seeds, followed by centrifugation at 6000 rpm for 30 s, then

removal of the water. The seeds were plated onto GM medium (Section A2.1, p. 165) in 100×60 mm clear plastic tissue culture pots (ALMED). To facilitate rapid transfer of germinated seedlings to other containers, it was important to plate the sterilised seeds as individuals, rather than clumps. The sterilised seeds were resuspended in approximately 0.5 ml of sterile MilliQ water and drawn up into a sterile glass pasteur pipette. By dotting the pipette tip on the surface of the germination medium, it was possible to plate individual seeds rapidly. The plated seeds were then left to dry in the laminar flow cabinet for 20 min before being sealed and left to germinate in the culture conditions described above (Section 2.3.1, p. 54).

2.3.4 *A. thaliana*: Producing Root Explants

Arabidopsis thaliana seeds of the bulked-up ecotype were sterilised as described above, and plated onto GM medium (Section A2.1, p. 165) in 100×60 mm clear plastic tissue culture pots (ALMED). After five days, the germinated seedlings were transplanted to fresh solid GM-containing pots at a rate of four per container. The use of a medium containing high concentrations of agar (18 g l^{-1}) was based upon media prepared by Chaudhury and Signer (1989) to encourage root growth primarily on the surface of the medium. This facilitated the harvest of quality root explants for subsequent transformation experiments (Section 2.3.8, p. 56). The seedlings were left to grow for at least three weeks, but the optimum root explant harvesting window was between 25 and 40 days. As soon as the plants developed an inflorescence their efficiency as root explants for transformation decreased markedly.

2.3.5 Growth of *Nicotiana tabacum*

All tobacco (*Nicotiana tabacum*) seedlings, plants, and tissue cultures were grown at an ambient temperature of 26°C in continuous light provided by cool white fluorescent 58 W tubes (OSRAM) emitting 400 μE m^{-2} s^{-1}. The cultivar used in all tobacco transformation experiments was *Nicotiana tabacum* cv. 'Wisconsin-38' (often referred to as *N. tabacum* W38), a gift from T. J. Higgins, CSIRO, Canberra, Australia.

2.3.6 *N. tabacum*: Producing Leaf Disc Explants

N. tabacum seeds were sterilised as described above (Section 2.3.3, p. 54), and plated onto solid ½MS medium (Section A2.6, p. 166) in 100×60 mm plastic tissue culture pots (ALMED). After germination, seedlings were transplanted, using aseptic technique, to GM-containing (Section A2.1, p. 165) pots at a rate of three seedlings per container. The plants required two months of growth before leaves could be harvested for leaf disc explants. When the plant had grown too large for its container, the top three nodes plus the apical meristem were transferred to GM-containing (Section A2.1) pots. In this way, the plants could be maintained indefinitely.

2.3.7 Plant Transformation

All plant tissue culture was performed in a sterile laminar-flow cabinet, and general sterile technique adhered to. The tissue culture tools were sterilised by autoclaving in water for 15 min at 121°C prior to each day's work. Prior to disposal, all plant tissues that had been exposed to *A. tumefaciens* were autoclaved at 121°C for 15 min.

Until the stage of shoot maturation, plant tissue was cultured in 90×25 mm tissue culture dishes (Labserv®). The resulting shoots were placed in 100×60 mm plastic tissue culture pots (ALMED) for root-initiation. To maximise experimental uniformity, all *A. tumefaciens* strains grown for cocultivation with plant material were inoculated into broths directly from long-term storage (-80°C).

2.3.8 Plant Transformation: *Arabidopsis thaliana*

In order to generate transgenic *A. thaliana* plants, a method was developed based upon those of Valvekens *et al.* (1988), Márton and Browse (1991), and Clarke *et al.* (1992). A 10 ml YEB (Section A1.6, p. 164) broth containing the appropriate antibiotic selection was inoculated with *Agrobacterium tumefaciens.* When transforming plant material with the pANDY8-10 series harboured by *A. tumefaciens* strain LBA4404 (Section 3.5, p. 97), the antibiotic selection was streptomycin and kanamycin (Section A3.1, p. 167) at a final concentration of 25 μg ml^{-1} and 100 μg ml^{-1}, respectively. After 18-36 h growth, the cells were pelleted by centrifugation at 4000 ***g*** for 10 min, and the supernatant discarded. The pellet was then resuspended in 10 ml liquid ARM I medium (Section A2.3, p. 165), and the resulting suspension diluted to an OD_{600} of 0.1. Roots from 4-6 week old *A. thaliana* plants, grown as described (Section 2.3.4, p. 55), were excised and precultured on solid ARM I medium (Section A2.3) for three days prior to *A. tumefaciens* inoculation. They were then chopped into approximately 0.5 cm lengths, immersed in a 5 ml aliquot of the resuspended *A. tumefaciens* broth, agitated gently for 5 min, then blotted on sterile Whatman® No. 1 filter paper to remove excess inoculum. The roots were then spread on solid ARM I medium supplemented with 200 mM acetosyringone (Section A3.4, p. 168), as recommended by Sheikholeslam and Weeks (1987), and left to cocultivate for 48 h.

The bacterial mass was removed by three rounds of swirling the cocultivated roots in liquid ARM I medium supplemented with timentin (Section A3.1, p. 167) to a final concentration of 200 μg ml^{-1}, and discarding the supernatant. Excess moisture was removed by blotting the roots briefly on sterile filter paper, and they were then spread on ARM I medium supplemented with timentin. After 48 h, the roots were transferred to solid ARM II shoot-initiating medium (Section A2.4, p. 165) containing kanamycin (50 μg ml^{-1}) for selection of transgenic shoots and timentin (100 μg ml^{-1}). The plant material was maintained on this medium and subcultured every 10 days while the transgenic shoots developed into plantlets. When sufficiently mature, the plantlets

were transferred to ARM III root-initiating medium (Section A2.5, p. 166) supplemented with kanamycin and timentin as described above. As roots often failed to develop, the plantlets were transferred to the containment planthouse (Section 2.3.1, p. 54), planted in soil and covered with a clear plastic bag to maintain humidity. After a week, the bag was removed gradually over a period of three days. During this time, most plants developed a root system and commenced flowering.

2.3.9 Plant Transformation: *Nicotiana tabacum*

Transgenic tobacco plants were produced using a method based upon that of Horsch *et al.* (1985). A TY (Section A1.5, p. 164) broth containing the appropriate antiobiotic selection was inoculated with *A. tumefaciens*. When transforming plant material with the pANDY8-10 series harboured by *A. tumefaciens* strain LBA4404 (Section 3.5, p. 97), the antibiotic selection was streptomycin and kanamycin (Section A3.1, p. 167) at a final concentration of 25 $\mu g\ ml^{-1}$ and 100 $\mu g\ ml^{-1}$, respectively. When the pANDY8-10 series was harboured by *A. tumefaciens* strain MOG1010 (Section 3.5), the antibiotic selection was rifampicin, spectinomycin, and kanamycin (Section A3.1) at a final concentration of 20 $\mu g\ ml^{-1}$, 250 $\mu g\ ml^{-1}$, and 100 $\mu g\ ml^{-1}$, respectively. After 18-36 h growth, the cells were pelleted by centrifugation at 4000 ***g*** for 10 min, and resuspended in 5 ml 10 mM $MgSO_4$. The resulting suspension was then diluted with 10 mM $MgSO_4$ to an OD_{600} of 2.0. Tobacco leaf discs, with a diameter of 7 mm, were cut from the leaves of plants grown as described (Section 2.3.6, p. 55) and stored on sterile Whatman® No. 1 filter paper soaked in 10 mM $MgSO_4$ till required. The leaf disc explants were then immersed in a 5 ml aliquot of the resuspended *A. tumefaciens* broth in a petri dish. After sealing the plate and agitating the broth/leaf disc mixture gently for 5 min, the discs were removed and blotted on sterile filter paper to remove excess inoculum. The leaf discs were then placed on a solid Nic I medium (Section A2.7, p. 166) and left to cocultivate for 72 h. After cocultivation, the leaf discs were transferred to a fresh solid Nic II medium (Section A2.8, p. 166) to initiate transgenic shoots. The discs and shoots were maintained on this medium with fortnightly subculturing. When sufficiently mature, the shoots were transferred to solid Nic III-containing tissue culture pots (Section A2.9, p. 166) to initiate roots, where they remained with fortnightly subculturing.

2.4 SOUTHERN ANALYSIS

2.4.1 Isolation of *N. tabacum* Genomic DNA

Large amounts of genomic DNA were isolated from plant material using a CTAB extraction method derived from that of Doyle and Doyle (1987; 1990). Liquid nitrogen was added to 0.5-1.0 g of fresh leaf tissue in a prechilled mortar. As the liquid nitrogen evaporated, the material was ground to a fine powder and scraped into a 30 ml screw-top NALGENE™ Oak Ridge centrifuge tube containing 7.5 ml of preheated (65°C) Genomic Extraction buffer (Section A4.32, p. 173). After mixing vigorously, the tube was incubated at 65°C for 30-45 min with periodic gentle swirling to redistribute the plant material throughout the extraction buffer. An equal volume of a chloroform: iso-amyl alcohol solution (24:1 v/v, respectively) was then added, and the organic and aqueous phases were mixed thoroughly by gently inverting the tube. To separate the phases, the tube was centrifuged at 12000 ***g*** for 5 min, and the aqueous supernatant transferred to a fresh 50 ml screw-top FALCON® BLUE MAX™ conical centrifuge tube. The nucleic acids were precipitated by the addition of a two thirds volume of isopropanol, and then pelleted by centrifugation at 5000 ***g*** for 10 s. The supernatant was discarded and the pellet dried briefly under vacuum. To remove RNA's from the DNA preparation, the pellet was first resuspended in 1 ml of TE buffer (Section A4.3, p. 169) containing DNase-free RNase-A (Section A4.4, p. 169) to a final concentration of 50 $\mu g\ ml^{-1}$, then incubated at 37°C for 30 min. To reduce the coprecipitation of plant polysaccharides during the final DNA precipitation step, the resuspended DNA's were diluted with 2 vol of sterile MilliQ water. Ammonium acetate (CH_3COONH_4, pH 7.7) was added to a final concentration of 2.5 M, and the nucleic acids precipitated with 2.5 vol of cold (-20°C) absolute ethanol, then pelleted by centrifugation at 5000 ***g*** for 2 min. After discarding the supernatant, the salts were removed by overlaying the pellet with 80% (v/v) ethanol, then removing the supernatant. The pellet was dried briefly under vacuum, resuspended by incubating at 37°C for 45 min in 300 µl of sterile MilliQ water, then stored at -20°C. Prior to storage, the DNA was quantified using either serial dilution (Section 2.2.6, p. 45) or fluorometry (Section 2.2.7, p. 46).

2.4.2 Restriction Digestion and Electrophoresis of Genomic DNA

N. tabacum genomic DNA was digested with *Hin*dIII or *Eco*RI in buffer B or H (Boehringer Mannheim GmbH), respectively. To dilute carbohydrates copurified with the DNA that may interfere with the action of the restriction endonucleases, the final digest reaction volume was made to 300 µl . Typically, 10-15 µg of DNA extracted as described (Section 2.4.1, above) was digested overnight at 37°C using 100 U of enzyme. The following morning, the reaction mix was supplemented with a further 100 U of enzyme, and the digestion continued for another 4-5 h. The reaction mix was made 2.5 M with respect to ammonium acetate (CH_3COONH_4, pH 7.7) and the DNA's precipitated with 2.5 vol of cold (-20°C) absolute ethanol. The DNA's were

pelleted by centrifugation for 15 min at 12000 rpm in a microfuge and the supernatant discarded. The pellet was desalted by washing with 80% (v/v) ethanol, dried in a Speedvac® for 5 min and resuspended in 10 µl of sterile MilliQ water. A 1 µl volume of SUDS (Section A4.12, p. 170) was added to the digested DNA, which was then loaded onto 0.8% (w/v) agarose gel in either a Bio Rad DNA Sub Cell™ or a Pharmacia Gel Apparatus (Pharmacia LKB Biotechnology) and resolved by electrophoresis as described (Section 2.2.9, p. 46). Electrophoresis was discontinued when the bromophenol dye was 2-5 cm from the base of the gel.

2.4.3 Southern Blotting: Conventional Alkaline Transfer

DNA fragments resolved by agarose gel electrophoresis (Section 2.4.2, above) were transferred from the gel to a nylon membrane under alkaline conditions using a method derived from that of Reed and Mann (1985). Following electrophoresis, the gel was trimmed to remove the wells, photographed (Section 2.5), then immersed in 0.25 M HCl and agitated gently for 30 min to depurinate the DNA. During the depurination step, three pieces of Whatman® 3MM Chr chromatography paper were cut to fit a plastic tray and extend into the wells at either end. These sheets were placed in the tray and wells, and soaked with 0.4 M NaOH. Air trapped between the 3MM sheets was removed by rolling a test tube across the paper, and then the wells were filled with 0.4 M NaOH. The gel, having been rinsed in MilliQ water, was inverted and placed gently upon the 3MM paper in the tray, so as to exclude air bubbles. The exposed 3MM paper surrounding the gel was covered with strips of Whatman® laboratory sealing film, as were the wells at either end. A piece of Hybond™-N^+ nucleic acid transfer membrane (Amersham International, plc), was trimmed to gel size, presoaked for 5 min in 0.4 M NaOH, and placed on the gel. On top of the membrane were placed two gel-sized pieces of 3MM paper, presoaked in 0.4 M NaOH, and then a further two pieces of dry gel-sized 3MM paper. Care was taken at every stage to exclude air bubbles. A 5 cm stack of paper towels was placed on top of the gel/membrane/3MM stack, and the entire apparatus capped by a glass plate and a 200 g weight. After capillary transfer for 18 to 24 h, the apparatus was dismantled and the membrane washed in 5× SSPE (Section A4.22, p. 172), then sealed in plastic and stored at 4°C till required.

2.4.4 Southern Blotting: Downward Alkaline Transfer

This more efficient method devised by Chomczynski (1992) superseded the Conventional Alkaline Transfer described above (Section 2.4.3). In addition to the protocol described by Chomczynski (1992), the gel underwent an initial Depurination step (Section 2.15.1) after trimming and photographing (Section 2.5). It was then placed in Transfer Solution (0.4 M NaOH; 1.5 M NaCl) and agitated gently for 30 min in order to denature the DNA. During the Depurination/Denaturation steps, four pieces of Whatman® 3MM Chr chromatography paper were trimmed to a size

slightly larger than that of the gel, and placed on a 5 cm stack of paper towels. A gel-sized piece of 3MM paper, presoaked in Transfer Solution, was placed on a glass or perspex plate. Upon this was placed a gel-sized sheet of Hybond™-N⁺ nucleic acid transfer membrane (Amersham International, plc), presoaked in Transfer Solution. The gel was placed carefully on the membrane to exclude any air bubbles, and the 3MM/membrane/gel assembly then transferred to the 3MM/paper towel stack. The gel was surrounded by strips of Whatman® laboratory sealing film to cover the exposed paper towels. Three pieces of gel-sized 3MM paper, presoaked in Transfer Solution, were placed on top of the gel. A wick was then made of three pieces of presoaked 3MM paper cut large enough to cover the gel and extend into an elevated dish containing Transfer Solution. Again, care was taken to exclude air bubbles. Strips of laboratory sealing film were laid upon the 3MM paper wick to prevent the evaporation of Transfer Buffer. After capillary transfer for 1-3 h, the apparatus was dismantled and the membrane washed in 5× SSPE (Section A4.22, p. 172) prior to being sealed in plastic and stored at 4°C till required.

2.4.5 Preparing [^{32}P]-Labelled Probe DNA

The probe DNA to be labelled were an *nptII* and a *gusA* gene. The nptII probe was a 536 bp *Nco*I-*Sph*I fragment that had been excised from a large scale preparation (Section 2.3.4, p. 44) of pANDY1 (Section A7.8, p. 183) by double-digestion with *Nco*I and *Sph*I in buffer M (Section 2.7.1, p. 49) (Boehringer Mannheim GmbH). The fragments were resolved by 0.8% (w/v) agarose gel electrophoresis (Section 2.2.9, p. 46), and the 536 bp fragment recovered from the gel (Section 2.2.12, p. 48). The *gusA* probe was a 1.9 kb *Nco*I-*Eco*RI fragment that had been excised from large scale prepared (Section 2.3.4) pJIT166 DNA (Section A6.13, p. 188) by digestion in buffer H (Boehringer Mannheim GmbH) and recovered from a 0.8% (w/v) agarose gel as detailed above.

To radioisotope-label probe DNA, a number of different kits were used, each based upon a random-priming method using either DNA-polymerase I (Klenow fragment), or T7 polymerase for nucleotide incorporation. The kits, Prime-It™ II (Stratagene Cloning Systems), Ready-To-Go™ (Pharmacia P-L Biochemicals Inc.), and Hi-Prime (Boehringer Mannheim GmbH), all required 25 ng probe DNA and 5 µl 3000 Ci mmol^{-1} [α-^{32}P]-dCTP (ICN Biomedicals, Inc.) per labelling reaction. Each reaction was performed according to manufacturer's instructions.

The efficiency of incorporation of radioisotope-labelled nucleotides into the probe DNA was monitored by thin-layer chromatography of DNA on Cellulose F_{245}-coated aluminium strips (Merck). From the terminated the labelling reaction (above), a 2 µl aliquot was pipetted on to the cellulose strip approximately 1 cm from the base, and allowed to dry. The strip was placed vertically in a beaker containing 0.5 cm of

Nucleotide TLC Phosphate Buffer (Section A4.20, p. 172) until the solvent front had migrated 10 cm above the sample. The strip was removed from the buffer, air-dried, then exposed to NIF RX Fuji Medical X-ray film (Fuji Photo Film Co., Ltd) for 5 min. The film was developed and the intensity of the unincorporated nucleotides, migrating just behind the solvent front, was visually compared with that of the slow moving labelled probe DNA. Prior to hybridisation, the radio-labelled probe was purified as described in Section 2.4.6 (below).

2.4.6 Purifying [^{32}P]-Labelled Probe DNA

Unincorporated nucleotides were separated from probe DNA using Sepharose CL-6B spin-column chromatography. Spin columns were constructed by piercing the base of a 750 µl PCR tube (Eppendorf) with a fine needle, then filling the tube with TE-equilibrated Sepharose CL-6B (Section A4.21, p. 172). The PCR tube was placed in a 2.0 ml microfuge tube, and centrifuged at 3000 rpm for 2 min in a microfuge to remove the void volume. The PCR tube was transferred to a fresh 2.0 µl microfuge tube and the sample, to a maximum volume of 100 µl, was loaded onto the column. The column was again centrifuged at 3000 rpm for 2 min in a microfuge. The solution in the 2 ml microfuge tube contained the radio-labelled probe DNA, whereas the column retained the unincorporated nucleotides, reaction dyes and salts. This method was also used to purify or desalt plasmid DNA or ligation reactions prior to further manipulation or transformation into bacteria.

2.4.7 Hybridisation: SSPE Method

This protocol was derived from that detailed in the handbook accompanying Hybond™-N$^+$ nucleic acid transfer membrane (Amersham International, plc), but was superseded by the simpler and faster SDS method (Section 2.4.8, below). A 25 ml aliquot of filtered (Millipore 0.45 µm membrane filter) SSPE Hybridisation Solution (Section A4.24, p. 172) was heated to 65°C in a Hybaid™ Hybridisation Oven (Hybaid Ltd). Fragmented Herring Testes DNA (Section A4.25, p. 172) was denatured by boiling for 5 min and added immediately to the heated SSPE Hybridisation Solution to a final concentration of 0.2 mg ml^{-1}. The nylon membrane containing the transferred DNA (Section 2.4.3 or 2.4.4, p. 60) was placed carefully (so as to exclude air bubbles) on Hybaid™ nylon mesh (Hybaid Ltd) in a shallow container of 2× SSPE (Section A4.22, p. 172). The mesh and membrane were rolled up together, placed in a preheated (65°C) Hybaid™ screw-top glass tube with the 2× SSPE and unrolled. The 2× SSPE was decanted and replaced with preheated SSPE Hybridisation/Herring Testes DNA solution. After prehybridisation for at least 2 h, the solution was removed and discarded, except for a 15 ml aliquot. The purified ^{32}P-labelled probe (Section 2.4.5, p. 61), having been denatured by boiling for 5 min, was mixed immediately with the remaining 15 ml hybridisation solution. The entire solution was then poured back into the tube and hybridisation commenced. After 16-

20 h at 65°C, the hybridisation solution was decanted and the membrane underwent a series of washes. The first was for 15 min in 100 ml preheated (65°C) 2× SSPE Wash (Section A4.26, p. 173), which was then discarded. This wash was repeated, then followed by 20 min in 100 ml preheated (65°C) 1× SSPE Wash (Section A4.27, p. 173), and finally a 15 min wash in 100 ml preheated (65°C) 0.1× SSPE Wash (Section A4.28, p. 173). The membrane was unrolled, separated from the mesh, and sealed in plastic. It was then exposed to NIF RX Fuji, or Kodak XAR-5, X-ray film in a Hypercassette™ (Amersham International, plc) with a Hyperscreen™ (Amersham International, plc) intensifying screen for two to seven days at -80°C. Up to six membranes were hybridised in the same tube at one time, and care was taken to ensure that among the blots there was at least one negative control (untransformed *N. tabacum* genomic DNA digested as with the other samples), and one positive control for each probe used (plasmid DNA).

2.4.8 Hybridisation: SDS Method

A quick and simple procedure, this method was developed from that of Church and Gilbert (1984). The membrane was rolled up on Hybaid™ nylon mesh as described above (Section 2.4.7, p. 62), and placed into a preheated (65°C) Hybaid™ screw-top glass tube. The 2× SSPE was replaced with 25 ml preheated SDS Hybridisation Solution (Section A4.30, p. 173). The membrane was left to prehybridise for 10 min, although it was usually longer as the purified ^{32}P-labelled probe (Section 2.4.5, p. 61) was prepared during this period. Having denatured the probe by boiling for 5 min, the hybridisation solution was discarded, except for a 15 ml aliquot into which the probe was mixed. This aliquot was returned to the glass tube and the contents hybridised with the membrane for 16-20 h at 65°C. After hybridisation, the membrane was washed as described (Section 2.4.7, above), except the first wash was replaced by a 15 min wash in 100 ml of preheated SDS Wash Solution (Section A4.31, p. 173). The membrane was then sealed and exposed to X-ray film as described (Section 2.4.7, p. 62). Up to six membranes were hybridised in the same tube at one time, and care was taken to ensure that among the blots there was at least one negative control (untransformed *N. tabacum* genomic DNA digested as with the other samples), and one positive control for each probe used (plasmid DNA).

2.4.9 Stripping Blots

Radioisotope-labelled probe DNA that had hybridised to the Southern blots was removed by pouring boiling 0.5% SDS (w/v) on to the membranes, and allowing the solution to cool to room temperature. The blot was then rinsed in 2× SSPE, sealed, and exposed to X-ray film as described (Section 2.4.7, p. 62) overnight, to determine if ^{32}P-labelled probe remained. If so, the stripping procedure was repeated.

CHAPTER 3 RESULTS

PART I VECTOR CONSTRUCTION

3.1 DELETING THE PUTATIVE *OVERDRIVE* CORE

3.1.1 Overview

A series of binary vectors was created that contained various deletions centred upon the putative nopaline-type *overdrive* core. This series was derived from a binary promoter-tagging vector, pBIN19/GTG (Section A6.1, p. 176), that was constructed by D. H. Kerr (1996) and contained left and right border regions derived from pBIN19 (Bevan, 1984), which were in turn derived from the nopaline-type Ti-plasmid, pTiT37. To make deletions in the putative nopaline-type *overdrive* region, pBIN19/GTG was linearised at the *Sph*I site adjacent to the putative *overdrive* core, then digested with exonuclease BAL 31. To facilitate this procedure, the other *Sph*I site present in pBIN19/GTG, located in the chaemeric P_{nos}-*nptII* plant-selectable marker (Section A6.1), was removed. This required excision of the selectable marker as a 1.6 kb fragment by a partial *Eco*RI digestion of *Hin*dIII-linearised pBIN19/GTG, thus creating pANDY6 (Section A6.2, p. 177). A summary of this procedure is detailed in Figure 6 (p. 64).

3.1.2 Optimising Partial *Eco*RI Digestion of pBIN19/GTG

Partial *Eco*RI digestion of *Hin*dIII-linearised pBIN19/GTG yielded a range of vector fragments (Fig. 7, p. 65). Therefore, it was necessary to optimise production of partially *Eco*RI-digested fragments to maximise the yield of the 15.5 kb fragments, one of which was a vector fragment from which only the P_{nos}-*nptII* fusion had been removed (Fig. 7). A reaction mixture, containing pBIN19/GTG plasmid DNA prepared by the STET-method (Section 2.2.2, p. 44), was predigested to completion with *Hin*dIII and divided into 5 µl aliquots containing various step-wise *Eco*RI dilutions, as described (Section 2.2.14, p. 49). The fragments from each reaction mixture were separated by electrophoresis through a 0.4% (w/v) agarose gel (Section 2.2.9, p. 46) at 4°C (Fig. 8, p. 67). The optimal *Eco*RI concentration required to obtain the desired spectrum of partially digested fragments was determined to be 0.0078 U μl^{-1} of reaction mix at 37°C for 20 min (Fig. 8, lane 10, p. 67). A 10-times optimal *Eco*RI concentration stock (0.078 U μl^{-1}) was made in restriction endonuclease dilution buffer (Section A4.15, p. 171) and used in all subsequent *Hin*dIII/partial *Eco*RI digestion reactions.

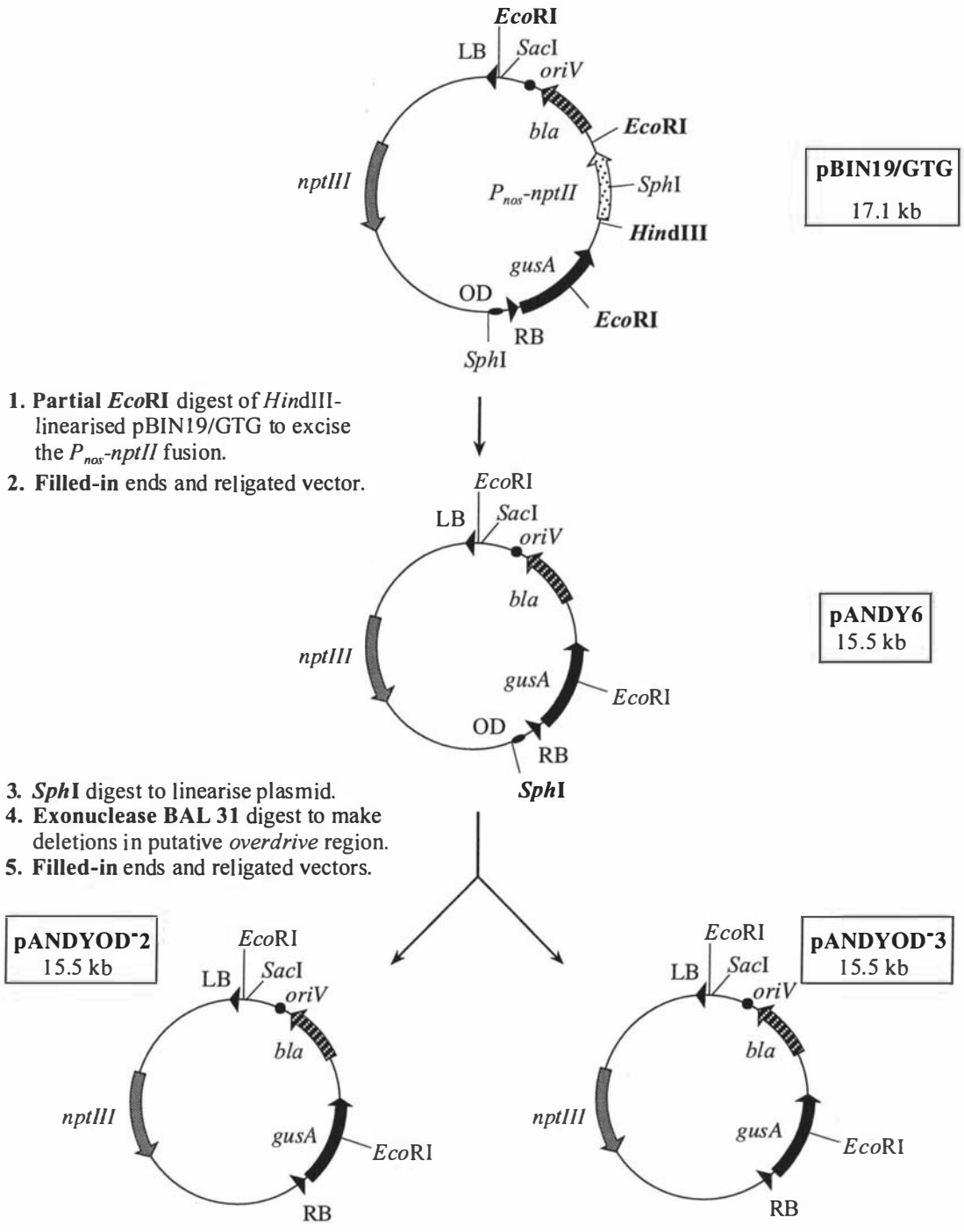

Figure 6. Summary of construction of pANDY6, pANDYOD-2, and pANDYOD-3.

RB=right border; LB=left border; OD=putative nopaline-type *overdrive* core; *oriV*=origin of replication; *bla*=β-lactamase gene; P_{nos}-*nptII*=neomycin phosphotransferase gene driven by *nos* promoter and terminated by *ocs3'* sequence; *gusA*=β-glucuronidase gene; *nptIII*=neomycin phosphotransferase gene.

Figure 7. Fragments generated by a partial *Eco*RI digestion of *Hin*dIII-linearised pBIN19/GTG.

Partial *Eco*RI digestion of *Hin*dIII-linearised pBIN19/GTG generated a range of fragments, each comprising differing deletions of *Eco*RI fragments. The species of interest was the 15.5 kb fragment (**bold**) from which the *Hin*dIII/*Eco*RI portion containing the P_{nos}-*nptII* fusion had been deleted. This species co-migrated with another 15.5 kb fragment, one from which the *Eco*RI/*Hin*dIII *gusA* termination sequence had been removed. This diagram shows only fragments greater than 11.2 kb in size.

H =*Hin*dIII, and E =*Eco*RI restriction sites.

RB =right border; LB =left border; OD =putative nopaline-type *overdrive* core; *oriV* =origin of replication; *bla* =β-lactamase gene; P_{nos}-*nptII* =neomycin phosphotransferase gene driven by *nos* promoter and terminated by *ocs3'* sequence; *gusA* =β-glucuronidase gene; *nptIII* =neomycin phosphotransferase gene.

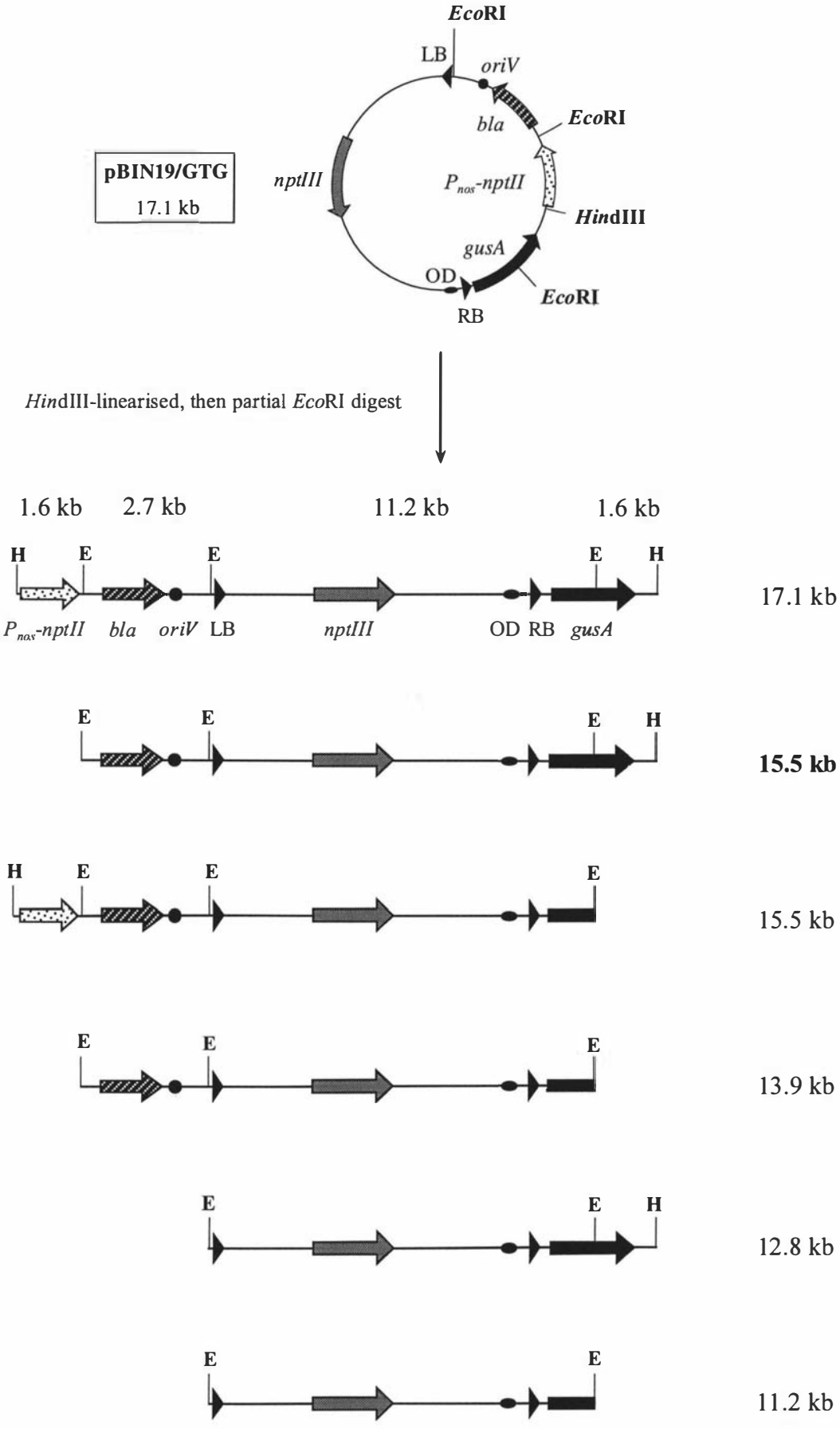
EcoRI
LB
oriV
bla
EcoRI
pBIN19/GTG
17.1 kb
nptII
P nos-nptII
HindIII
gusA
OD
EcoRI
RB
HindIII-linearised, then partial EcoRI digest
1.6 kb
2.7 kb
11.2 kb
1.6 kb
H
E
E
E
H
P nos-nptII
bla
oriV
LB
nptIII
OD
RB
gusA
17.1 kb
15.5 kb
15.5 kb
13.9 kb
12.8 kb
11.2 kb

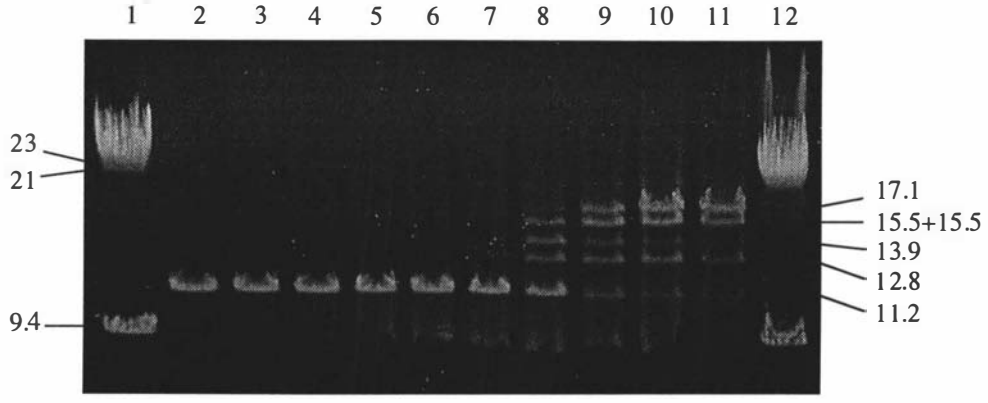

Figure 8. Establishing the optimal *Eco*RI concentration for production of partially *Eco*RI-digested fragments of *Hin*dIII-linearised pBIN19/GTG.

Digestion of 1 μg *Hin*dIII-linearised pBIN19/GTG for 20 min with *Eco*RI. *Eco*RI concentration in the reaction volume was (U μl^{-1}): 2.0 (lane 2); 1.0 (lane 3); 0.5 (lane 4); 0.25 (lane 5); 0.125 (lane 6); 0.0625 (lane 7); 0.0313 (lane 8); 0.0156 (lane 9); 0.0078 (lane 10); 0.0039 (lane 11). The numbers on the left of the figure refer to the size (kb) of fragments generated by *Hin*dIII plus *Hin*dIII/*Eco*RI digested phage λ DNA (lanes 1 and 12) (Section A4.10, p. 170). Numbers on the right of the figure indicate the size (kb) of fragments generated by partial *Eco*RI digests of *Hin*dIII-linearised pBIN19/GTG.

3.1.3 Removal of P_{nos}-*nptII* fusion to create pANDY6

The plasmid pANDY6 (Section A6.2, p. 177) was created by scaling up to 50 µl, the optimised digestion reaction described above (Section 3.1.2, p. 63). The fragments were separated by electrophoresis (Section 2.2.9, p. 46) through a 0.4% agarose gel at 4°C. The 15.5 kb fragments were recovered from the gel by elution onto DEAE-cellulose membrane (Section 2.2.10, p. 47), end-filled (Section 2.2.16, p. 50), ethanol-precipitated (Section 2.2.4, p. 45), then self-ligated (Section 2.2.19, p. 51). The ligation reaction was transformed into *Escherichia coli* strain DH5α™ cells made competent with $CaCl_2$, which were spread on solid LB medium supplemented with kanamycin and ampicillin (Section 2.12.4, p. 41). Since the 15.5 kb *Hin*dIII/*Eco*RI fragment comprised two similarly sized species (Fig. 7, p. 65), the transformants harboured either pANDY6 or pANDY7 (Fig. 9A, p. 69). The use of diagnostic *Eco*RI digests (Section 2.2.13, p. 49) of DNA (prepared by the STET-method (Section 2.2.2, p. 44)) from single-cell purified colonies, distinguished between the two species (Fig. 9B, p. 69), thus identifying pANDY6 (Section A6.2, p. 177).

3.1.4 Optimising BAL 31 Reaction Conditions

The putative nopaline-type *overdrive* core in pANDY6 was located outside the T-DNA, 76 bp downstream (3′) from the right border, and immediately adjacent to the unique *Sph*I site (Section A6.2, p. 177). To create deletion mutations in the *overdrive* region of pANDY6, the plasmid was linearised at the unique *Sph*I site, then digested with exonuclease BAL 31, as summarised in Figure 6 (steps 3-5)(p. 64). Using the equation described (Section 2.2.15, p. 49), the units of BAL 31 required in a 50 µl reaction volume to remove approximately 70 bp of duplex DNA per termini per minute from 30 µg of *Sph*I-linearised 15.5 kb pANDY6 DNA, was calculated to be 0.1 U. To test this, five reaction mixes were prepared, the DNA linearised with *Sph*I, BAL 31-degraded for 1-5 min, the reaction terminated, and the DNA precipitated, and resuspended as described (Section 2.2.15).

Efficacy of the BAL 31 digestion was monitored by the effect of the BAL 31 digestion upon the size of the diagnostic 700 bp *Sph*I/*Eco*RV fragment, as determined by migration of the fragment in a 0.8% (w/v) agarose gel (Section 2.2.9, p. 46; Fig. 10A, p. 71). From each resuspended BAL 31 reactions (above), a 2 µl aliquot was digested with 5 U *Eco*RV in restriction endonuclease buffer B (Boehringer Mannheim GmbH) (Section 2.2.13, p. 49). Digestion with 0.1 U BAL 31 for 1 to 5 min did not appear to influence the size of the diagnostic fragment (Fig. 10B, p. 71), and it was concluded that the enzyme had failed to work at the calculated concentration.

Figure 9A-B. Identification of pANDY6.

A. Recovery and ligation of the co-migrating 15.5 kb fragments generated by a partial *Eco*RI digestion of *Hin*dIII-linearised pBIN19/GTG created two plasmids, pANDY6 and ANDY7. Plasmid pANDY6 was derived from the self-ligated fragment from which the *Hin*dIII/*Eco*RI fragment containing the P_{nos}-*nptII* fusion had been deleted. Plasmid pANDY7, however, was derived from the self-ligated fragment from which the *Eco*RI/*Hin*dIII fragment containing the *ocs*3′ termination sequence of *gusA* had been deleted. Adjacent to each plasmid is a table containing the size of fragments generated by an *Eco*RI digest of that vector.

E =*Eco*RI and H =*Hin*dIII restriction sites.
(E+H) =filled-in junction of *Eco*RI and *Hin*dIII sites.
RB =right border; LB =left border; OD =putative nopaline-type *overdrive* core; *oriV* =origin of replication; *bla* =β-lactamase gene; P_{nos}-*nptII* =neomycin phosphotransferase gene driven by *nos* promoter and terminated by *ocs*3′ sequence; *gusA* =β-glucuronidase gene; *nptIII* =neomycin phosphotransferase gene.

B. An *Eco*RI diagnostic digest of 1 μg of pANDY6 (lane 1), pBIN19/GTG (lane 2), and pANDY7 (lane 3). Numbers on the right of the figure refer to the size (kb) of fragments generated by *Hin*dIII plus *Hin*dIII/*Eco*RI digested phage λ DNA (Section A4.10, p. 170) (lane 4).

A.

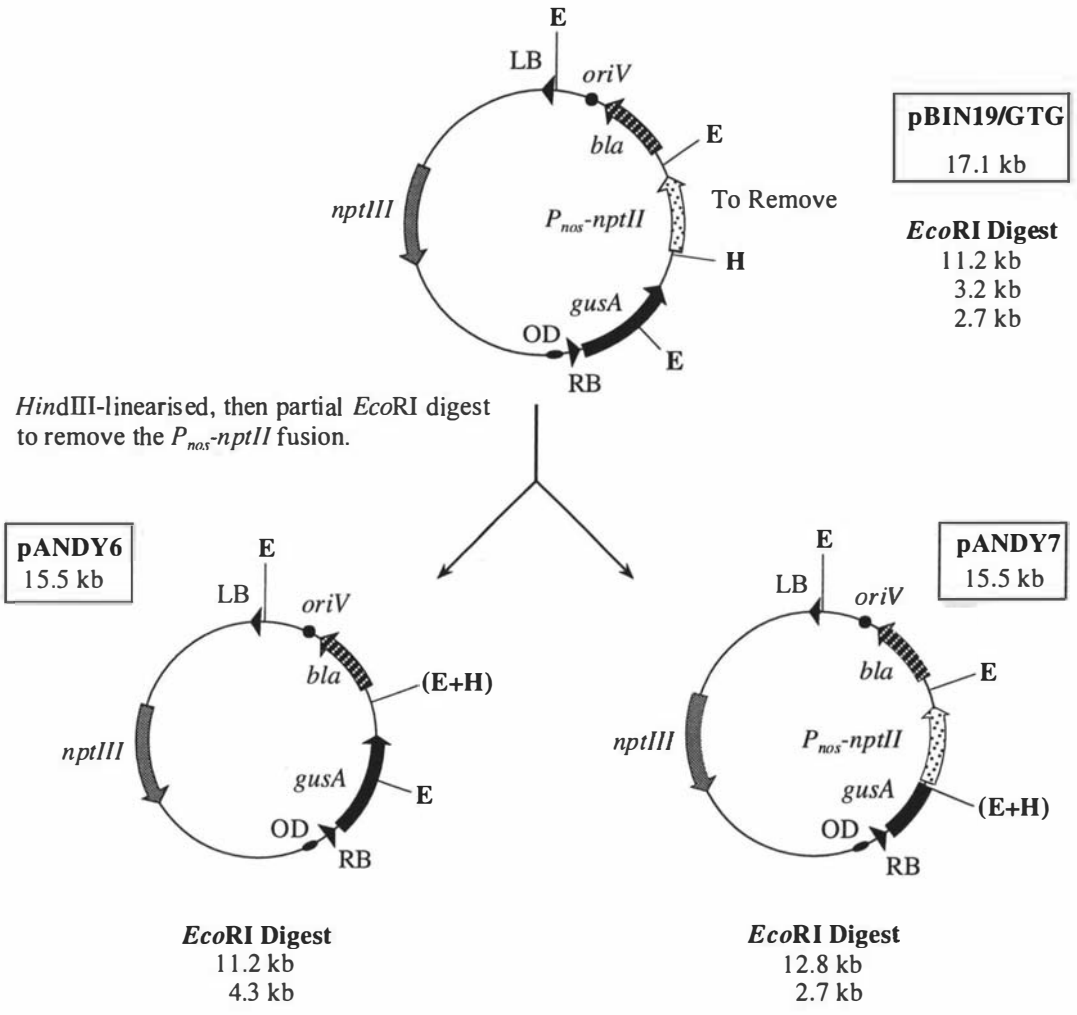
E
LB
oriV
bla
E
To Remove
nptIII
P nos-nptII
H
gusA
OD
E
RB
pBIN19/GTG
17.1 kb
EcoRI Digest
11.2 kb
3.2 kb
2.7 kb
HindIII-linearised, then partial EcoRI digest
to remove the P nos-nptII fusion.
pANDY6
15.5 kb
E
LB
oriV
bla
(E+H)
nptIII
gusA
E
OD
RB
EcoRI Digest
11.2 kb
4.3 kb
E
LB
oriV
pANDY7
15.5 kb
bla
E
nptIII
P nos-nptII
gusA
(E+H)
OD
RB
EcoRI Digest
12.8 kb
2.7 kb

B.

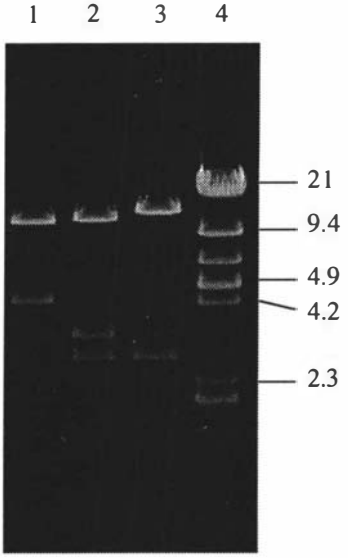
1
2
3
4
21
9.4
4.9
4.2
2.3

Figure 10A-C. Optimising BAL 31 reaction conditions.

A. An *Eco*RV/*Sph*I digestion of pANDY6 yielded a 700 bp fragment containing the putative nopaline-type *overdrive* core (OD), right border (RB) and a portion of the 5′ end of *gusA*. Efficacy of BAL 31 activity on *Sph*I digested pANDY6 was determined by its effect on the size of the 700 bp diagnostic *Eco*RV/*Sph*I fragment.

RB =right border; OD =putative nopaline-type *overdrive* core; *gusA* =β-glucuronidase gene.

B. Efficacy of 0.1 U BAL 31 on 30 μg *Sph*I digested pANDY6 in a 50 μl reaction volume after digestion for 1 min (lane 3), 2 min (lane 4), 3 min (lane 5), 4 min (lane 6), and 5 min (lane 7), as determined by an *Eco*RV digestion of a 2 μl aliquot from each reaction volume. Lanes 2 and 8 contained 1 μg pANDY6 digested with *Eco*RV and *Sph*I. Numbers to the left of the figure indicate the size (bp) of fragments generated by *Hin*dIII plus *Hin*dIII/*Eco*RI digested phage λ DNA (Section A4.10, p. 170) (lane 1). The arrow on the right of the figure indicates the diagnostic 700 bp *Eco*RV/*Sph*I fragment. Numbers beneath the figure refer to the duration (min) of the BAL 31 digestion.

C. Efficacy of 5 U BAL 31 on 30 μg *Sph*I digested pANDY6 in a 50 μl reaction volume after digestion for 5 min (lane 3), 10 min (lane 4), 15 min (lane 5), 20 min (lane 6), and 25 min (lane 7), as determined by an *Eco*RV digestion of a 2 μl aliquot from each reaction volume. Lanes 2 and 8 contained 1 μg pANDY6 digested with *Eco*RV and *Sph*I. Numbers to the left of the figure indicate the size (bp) of fragments generated by *Hin*dIII plus *Hin*dIII/*Eco*RI digested phage λ DNA (Section A4.10) (lane 1). The arrow on the right of the figure indicates the diagnostic 700 bp *Eco*RV/*Sph*I fragment. Numbers beneath the figure refer to the duration (min) of the BAL 31 digestion.

A.

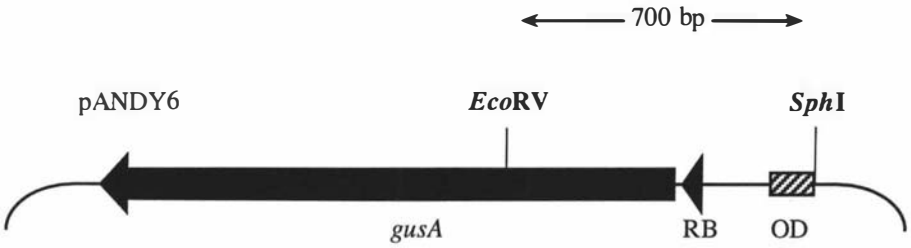
700 bp
pANDY6
*Eco*RV
*Sph*I
gusA
RB
OD

B.

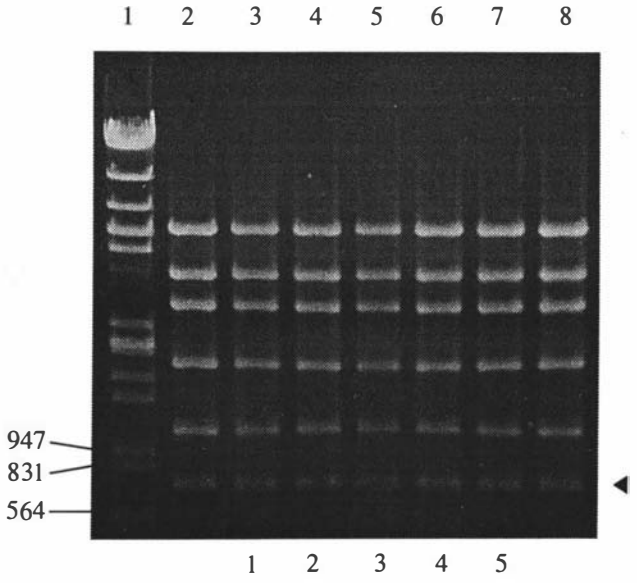
1 2 3 4 5 6 7 8
947
831
564
1 2 3 4 5

C.

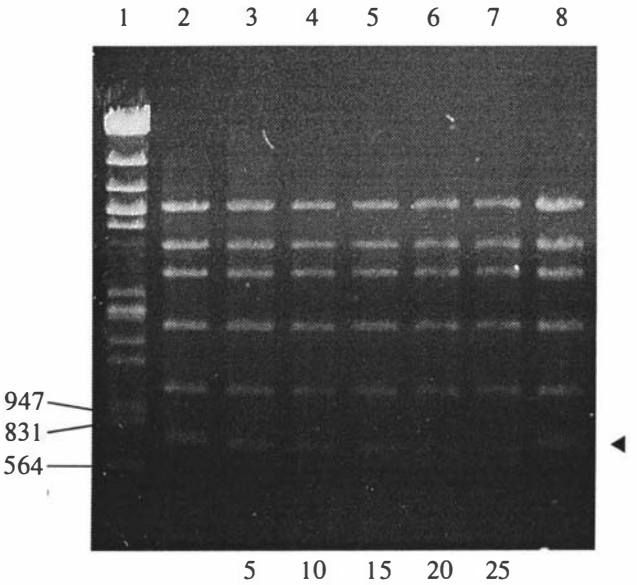
1 2 3 4 5 6 7 8
947
831
564
5 10 15 20 25

The procedure was repeated using 5 U of BAL 31 over a time course of 5 to 25 min with reactions terminated at 5 min intervals. An *Eco*RV digestion of an aliquot of each reaction demonstrated the influence the duration of the BAL 31 digestion had on the size of the diagnostic 700 bp *Sph*I/*Eco*RV fragment (Fig. 10C, p. 71). After a 25 min digestion, the diagnostic fragment was no longer a discrete band, indicating that the species within the aliquot varied markedly in size. As a few base pairs only were required to be removed to delete portions of the putative nopaline-type *overdrive* (Section A6.3, p. 178), the 5 min reaction mix (Fig. 10C), which exhibited minimal reduction in size, was further analysed (Section 3.1.5, below).

3.1.5 Identifying Clones with Putative Deletions in *Overdrive*

Before DNA from the 5 min BAL 31 reaction mix (Section 3.1.5, above) could be self-ligated efficiently, it had to be end-filled (Section 2.2.16, p. 50), as digestion with BAL 31 yields a population of fragments with a mixture of blunt and 5′ overhang ends. The DNA was precipitated (Section 2.2.4, p. 45), and ligated (without CAP-treatment) as blunt-ended fragments (Section 2.2.19, p. 51). The ligation reaction was transformed into *E. coli* strain DH5α™ cells made competent with $CaCl_2$, which were subsequently spread on solid LB medium supplemented with kanamycin and ampicillin (Section 2.1.6, p. 41). Of the resulting colonies, 12 were selected from which DNA was extracted using the STET-method (Section 2.2.2, p. 44), and digested with *Eco*RV and *Sph*I in restriction endonuclease buffer B (Boehringer Mannheim GmbH) (Section 2.2.13, p. 49; Fig. 11, p. 74). This identified plasmids in which the *Sph*I site was inactive, either as a result of filling-in at the *Sph*I site, or deletion of DNA containing the *Sph*I site. Only those clones not cutting at the *Sph*I site (pANDYOD^{-}1, pANDYOD^{-}2, pANDYOD^{-}3, and pANDYOD^{-}6) were selected for sequencing (Fig. 11).

3.1.6 Sequencing Deletions in the Putative *overdrive* Region

The selected clones (Section 3.1.5, above) were sequenced across the *overdrive* region to determine what deletions had occurred. DNA from the selected clones was prepared by the STET-method (Section 2.2.2, p. 44) and sequenced as described (Section 2.2.22, p. 52). The sequencing reactions were primed by a right border 26mer primer (5′-GCCGGATCCCCGGGATCAGATTGTCG-3′) (courtesy of D. H. Kerr) that annealed within the T-DNA region, 142 bp upstream of the putative nopaline-type *overdrive* core. The clones exhibited a range of deletions in the *overdrive* region

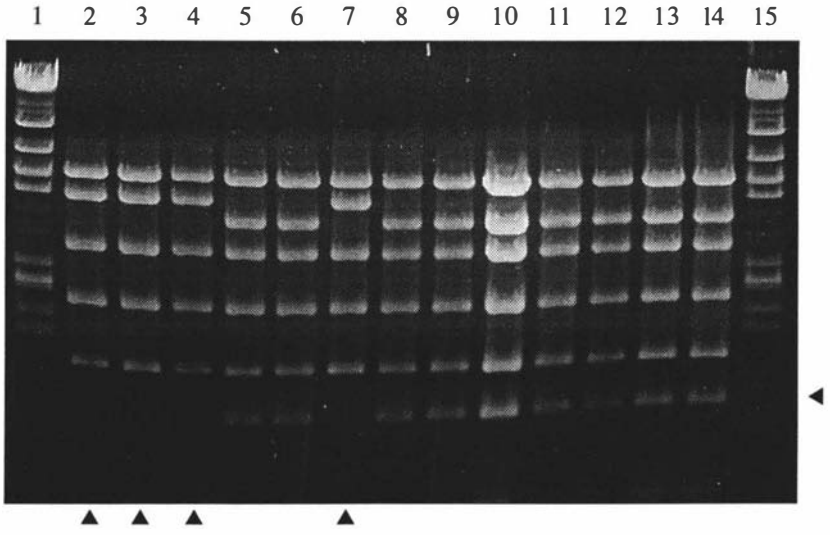

Figure 11. Identification of clones with deletions in the putative nopaline-type *overdrive* core.

Clones with deletions around the *Sph*I site were identified by an *Eco*RV/*Sph*I digest of 1 μg of DNA extracted from colonies transformed with BAL 31 degraded pANDY6. Lanes 2-7 contained colonies pANDYOD⁻1 to pANDYOD⁻6, and lanes 9-14 contained colonies pANDYOD⁻7 to pANDYOD⁻12. Lane 8 contained an *Eco*RI/*Sph*I digest of 1 μg pANDY6. Lanes 1 and 15 contained fragments generated by *Hin*dIII plus *Hin*dIII/*Eco*RI digested phage λ DNA (Section A4.10, p. 170). The arrow on the right of the figure indicates the position of the 700 bp diagnostic *Eco*RI/*Sph*I fragment, whereas the arrows along the bottom of the figure indicate clones pANDYOD⁻1, pANDYOD⁻2, pANDYOD⁻3 and pANDYOD⁻6 that were not cut by *Sph*I.

(Fig. 12A, p. 76), of which the smallest was harboured by pANDYOD^{-}6. This 4 bp deletion appeared to result from the BAL 31 removal of the *Sph*I-generated 4 bp 3′ overhang (Fig. 12B, p. 76), hence pANDYOD^{-}6 retained the putative *overdrive* core. The pANDYOD^{-}2 clone lost a 15 bp fragment containing the 8 bp putative *overdrive* core plus 3 bp upstream and 4 bp downstream to the *Sph*I site, whereas pANDYOD^{-}1 contained a more extensive 23 bp deletion removing the putative *overdrive* core and sequence beyond the *Sph*I site (Fig. 12B, p. 76). The most extensive deletion occurred in pANDYOD^{-}3, from which a 36 bp region comprising most of the *overdrive* had been removed (Fig. 12B). Further BAL 31 deletions were performed as described (Section 3.1.4, p. 68), and a total of 13 clones were sequenced for deletions across the *overdrive*. Of these, not one exhibited deletions differing from those described in Figure 12 (p. 76).

pANDYOD^{-}2 and pANDYOD^{-}3 were the clones chosen for analysis of the influence of deletions in the putative nopaline-type *overdrive* region upon plant transformation frequency and T-DNA copy number *in planta*. This was because pANDYOD^{-}2 was the clone with the most precise deletion of the putative core of the *overdrive*, and pANDYOD^{-}3 was the clone with the most extensive deletion throughout the *overdrive* region which removed the region with some homology to the octopine-type *overdrive* (Fig. 12) (Section A6.3, p. 178).

The result of these modifications was the production of a series of plant transformation vectors (which were also promoter-trapping vectors) that contained various deletions in the putative nopaline-type *overdrive* region. Furthermore, any plant-selectable marker could be inserted into the T-DNA at either of the two unique restriction sites (*Sac*I and *Kpn*I) adjacent to the left border (Section A6.3, p. 178).

Figure 12A-B. Sequence data detailing various deletions centred upon the putative nopaline-type *overdrive* core of the pANDYOD$^-$ series.

A. Data detailing deletions made by BAL 31 digestion around the *overdrive* region of pANDY6 to create pANDYOD$^-$6, pANDYOD$^-$2, pANDYOD$^-$1 and pANDYOD$^-$3 were contained in autoradiographs 1 to 4, respectively. Letters above each autoradiograph refer to the order in which the sequencing termination reactions were loaded onto the gel, whereas letters to the left of each autoradiograph refer to the sequence surrounding the deletion as detailed in Fig. 12B (below). The highlighted letters (**bold underlined**) indicate the nucleotides on either side of a deleted region.

B. A spatial representation of the various deletions harboured by the pANDYOD$^-$ series, relative to each other and to pANDY6 from which they were derived. The sequence data corresponds to that detailed in Fig. 12A (above), as do the highlighted letters (**bold underlined**) which refer to those nucleotides immediately adjacent to a deletion. The numbers below the pANDY6 sequence refer to the distance (bp) 3′ downstream of the right border. The diagram shows the position and orientation of the 26mer primer with respect to the right border (RB) and the putative nopaline-type *overdrive* region (OD).

RB =right border; OD =putative nopaline-type *overdrive* core; *gusA* =β-glucuronidase gene; *ocs*3′ =transcription termination sequence of octopine synthase gene.

A.

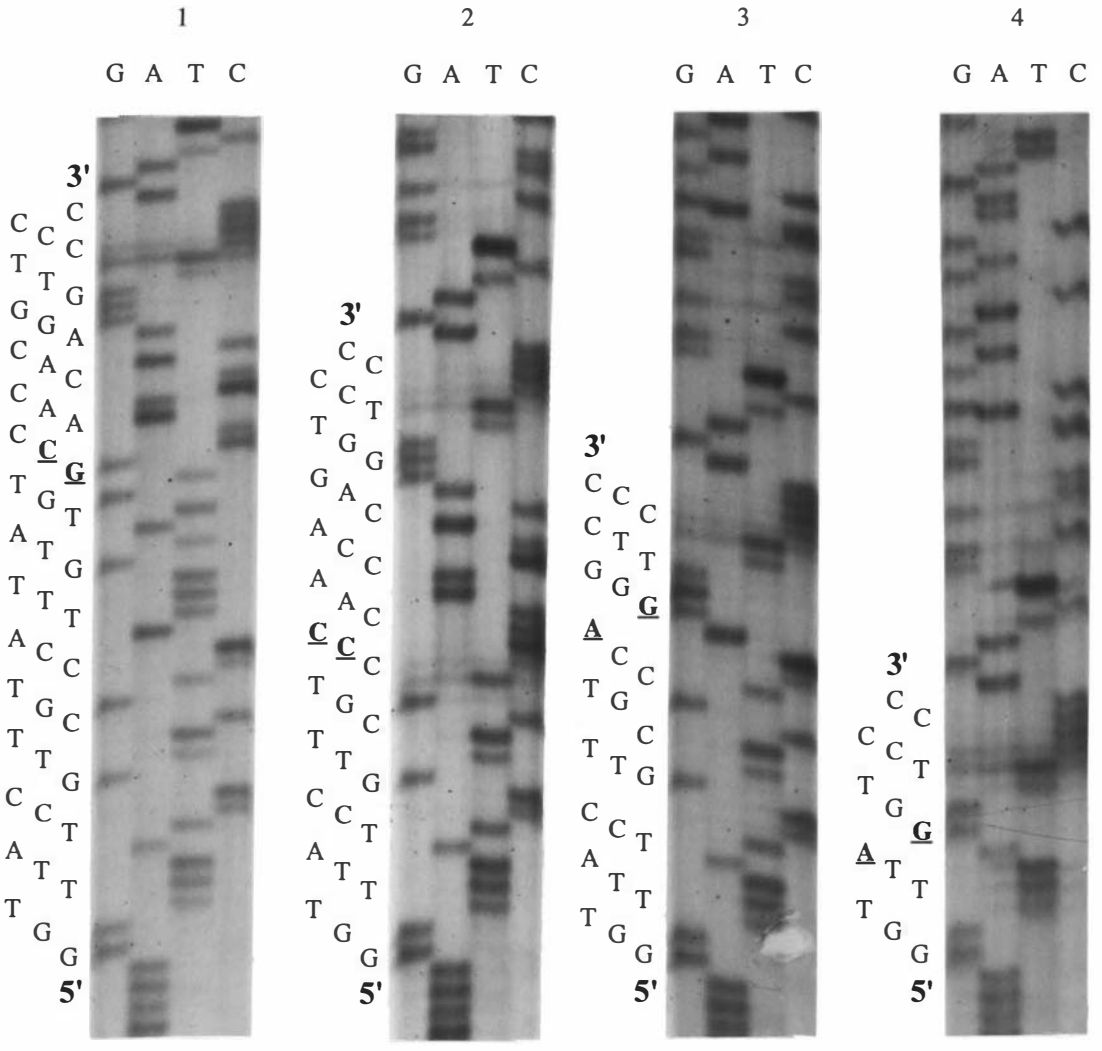

B.

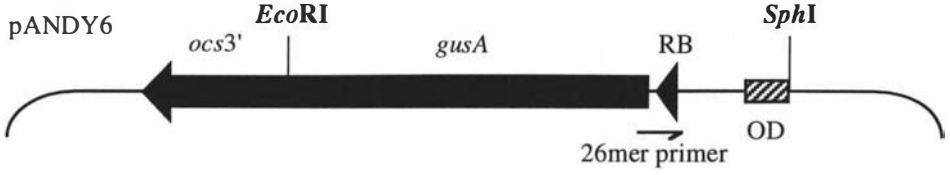

putative *overdrive* core — *Sph*I

pANDY6 5' CGTTTATCCGTTCGTCCATTTGTATGTGCATGCCAACCACAGGGTTCCCC 3'

60 70 80 90 100

pANDYOD⁻6 5' GGTTTATCCGTTCGTCCATTTGTATGT**G**.....**C**CAACCACAGGGTTCCCC 3'

pANDYOD⁻2 5' GGTTTATCCGTTCGTC**C**.....**C**CAACCACAGGGTTCCCC 3'

pANDYOD⁻1 5' GGTTTATCCGTTCGTCC**A**.....**G**GGTTCCCC 3'

pANDYOD⁻3 5' GGTTT**A**.....**G**GTTCCCC 3'

3.2 MODIFYING P_{35S}-*nptII* PLANT SELECTABLE MARKER

3.2.1 Overview

Before either pANDY6, pANDYOD$^-$2, or pANDYOD$^-$3 (Section 3.1, p. 63) could be used in plant transformation experiments, a plant selectable marker needed to be inserted into one of the two unique restriction sites (*Sac*I and *Kpn*I) adjacent to the left border (Section A6.2, p. 177; Section A6.3, p. 178). The chosen plant-selectable marker was cloned from the binary vector pSLJ491 (Section A6.4, p. 179), and comprised a divergent bi-directional plant-active promoter driving an *nptII* gene terminated by an *ocs*3′ sequence (Section A6.8, p. 183). The promoter consisted of a $P_{mas2'}$ promoter operating divergently from the strong constitutive P_{35S} promoter which controlled transcription of the *nptII* gene. Throughout this Thesis, this chaemeric fusion is referred to as P_{35S}-*nptII* fusion.

Prior to insertion into the vectors, the P_{35S}-*nptII* fusion needed to be modified. The main requirement was for the attachment of a pUC18 mcs (multiple cloning site) adjacent to the divergent $P_{mas2'}/P_{35S}$ promoters. This would increase the number of enzyme sites available for use in both Southern analysis of the transgenic plants produced, and plasmid rescue of plant genomic DNA flanking the right border (should it be required). The final modification was the positioning of this mcs-P_{35S}-*nptII* fusion in such a restriction enzyme context that it could be easily ligated into the unique *Sac*I site of pANDY6 and its pANDYOD$^-$ derivatives. A summary of these procedures is detailed in Figure 13 (p. 80).

3.2.2 Preparing P_{35S}-*nptII* Fusion for Attachment of an mcs

Prior to the attachment of a pUC18 mcs, the P_{35S}-*nptII* fusion needed to be excised from the low copy number binary vector, pSLJ491 (Section A6.4, p. 179), and inserted into the more manageable high copy cloning vector, pMTL22P (Section A6.5, p. 181), thus creating pANDY1 (Section A6.8, p. 183; Fig. 13 (steps 1-2), p.80). In so doing, the plant selectable marker was inserted into a vector from which large quantities of the fusion could easily be prepared for the next step in the modification process: attachment of a pUC18 mcs.

pSLJ491 DNA prepared by the Large Scale method (Section 2.2.3, p. 44), was digested with both *Hin*dIII and *Cla*I in buffer B (Boehringer Mannheim GmbH) (Section 2.2.13, p. 49). The 3017 bp fragment containing P_{35S}-*nptII* was separated from the 23.4 kb vector by electrophoresis through a 0.8% (w/v) agarose gel (Section 2.2.9, p. 46), recovered using GENECLEAN® (Section 2.2.11 , p. 48), and ligated (Section 2.2.19, p. 51) into a pMTL22P vector (Section A6.5, p. 180) of which STET-

Figure 13. Summary of modification of the P_{35S}-*nptII* fusion prior to its insertion into plant transformation vectors.

The individual steps in this figure are referred to, and expanded upon, in the text.

$P_{mas2'}$=2′ promoter of the mannopine synthase gene; P_{35S}=promoter of the Cauliflower Mosaic Virus 35S RNA subunit; *nptII*=neomycin phosphotransferase gene; *ocs*3′=transcription termination sequence of octopine synthase gene; *lacZ′*=portion of the β-galactosidase gene; *oriV*=origin of replication; *bla*=β-lactamase gene; P_{35S}-*nptII*=a P_{mas2}/P_{35S} dual promoter driving an *nptII* gene terminated by *ocs*3′; mcs=pUC18 multiple cloning site; mcs-P_{35S}-*nptII*=a multiple cloning site from pUC18 attached to a P_{mas2}/P_{35S} dual promoter driving an *nptII* gene terminated by *ocs*3′.

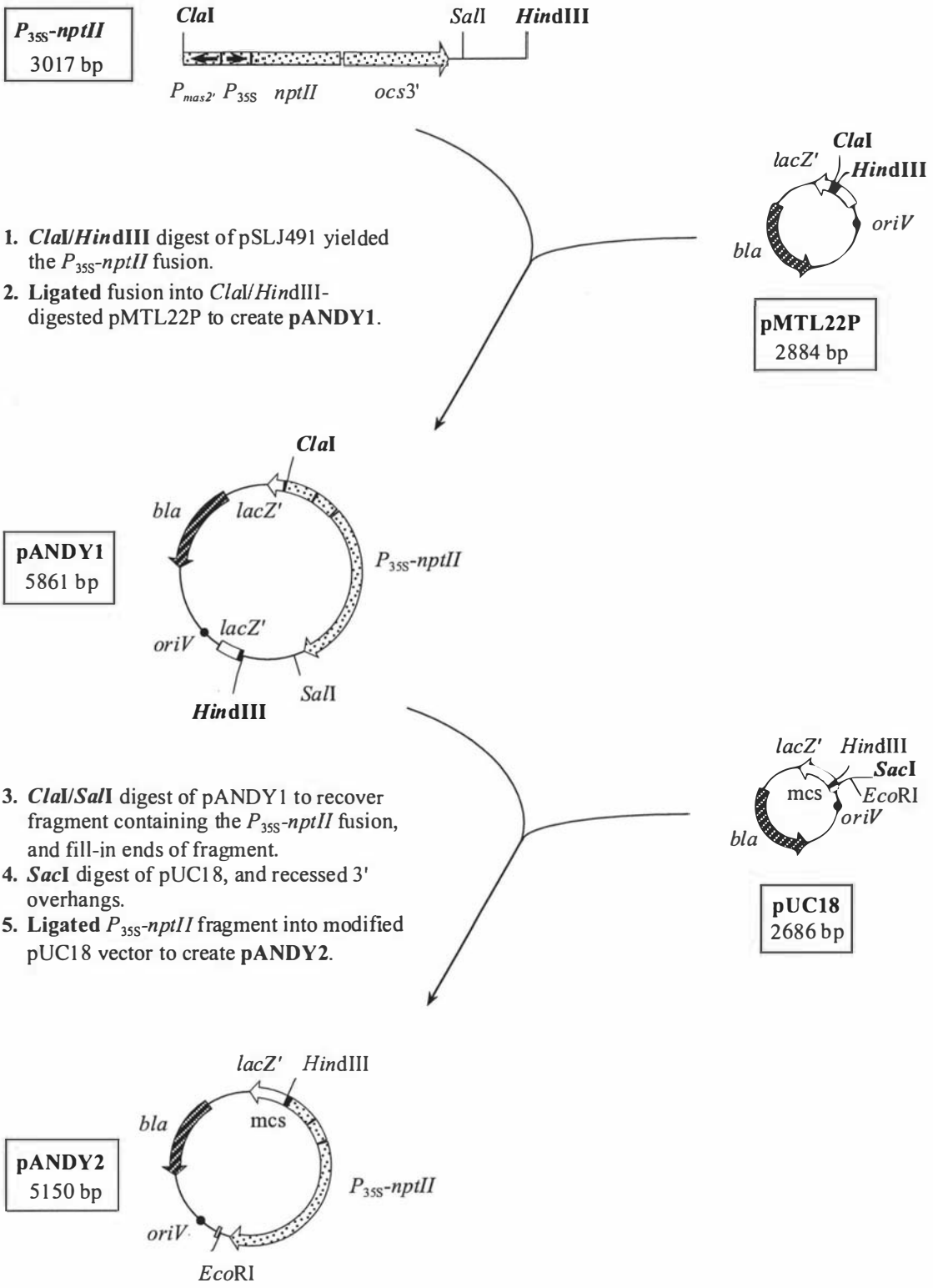
P35S-nptII
3017 bp
ClaI
SalI
HindIII
Pmas2' P35S nptII ocs3'
1. ClaI/HindIII digest of pSLJ491 yielded the P35S-nptII fusion.
2. Ligated fusion into ClaI/HindIII-digested pMTL22P to create pANDY1.
ClaI
lacZ'
HindIII
oriV
bla
pMTL22P
2884 bp
ClaI
bla
lacZ'
P35S-nptII
pANDY1
5861 bp
oriV
lacZ'
SalI
HindIII
3. ClaI/SalI digest of pANDY1 to recover fragment containing the P35S-nptII fusion, and fill-in ends of fragment.
4. SacI digest of pUC18, and recessed 3' overhangs.
5. Ligated P35S-nptII fragment into modified pUC18 vector to create pANDY2.
lacZ'
HindIII
SacI
mcs
EcoRI
oriV
bla
pUC18
2686 bp
lacZ'
HindIII
bla
mcs
P35S-nptII
pANDY2
5150 bp
oriV
EcoRI

Figure 13 (continued).

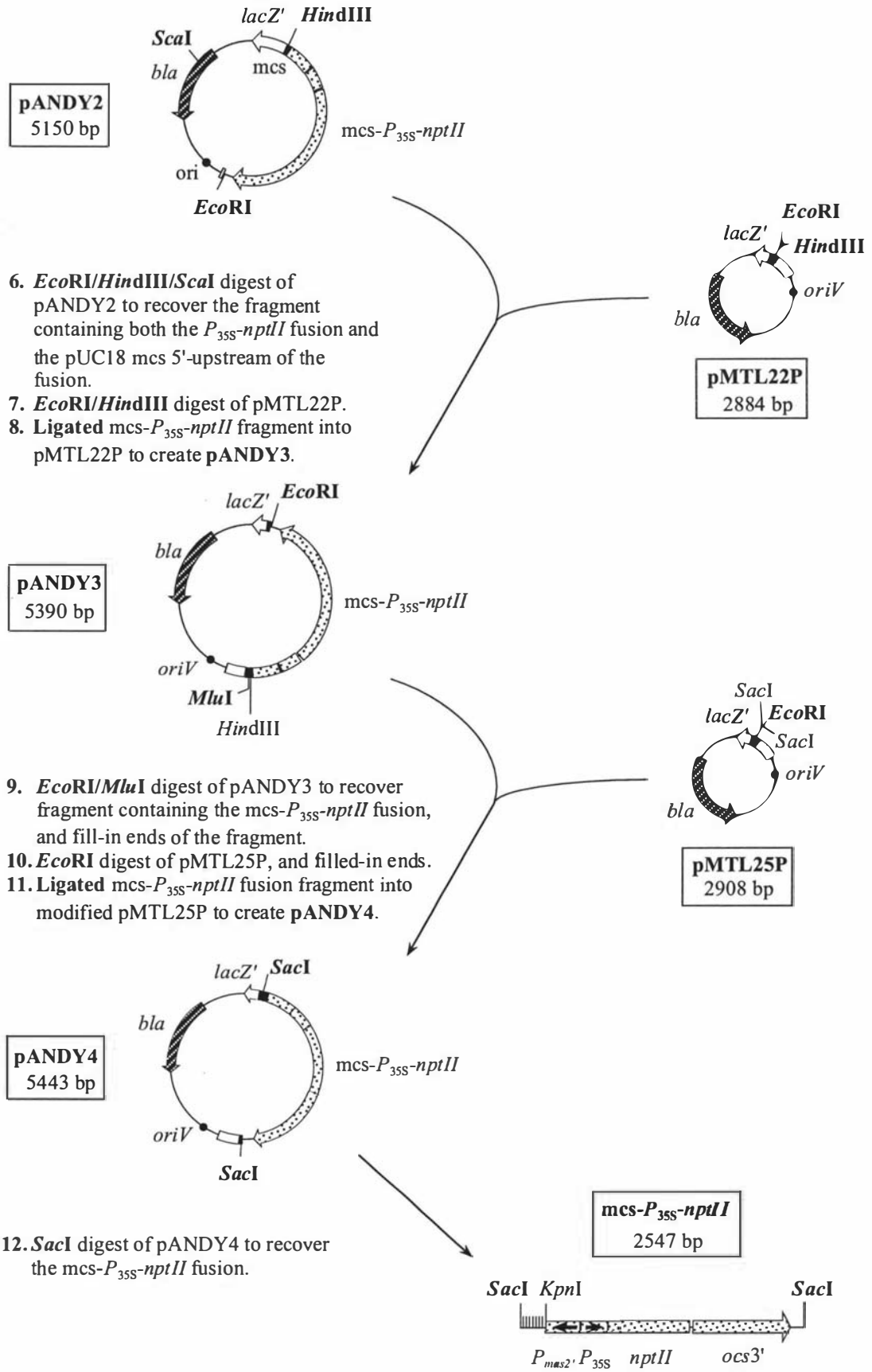

prepared DNA (Section 2.2.2, p. 44) had been previously digested with both *Hin*dIII and *Cla*I. The ligation reaction was transformed into *E. coli* strain DH5α™ cells made competent with $CaCl_2$, from which aliquots were spread on solid LB medium supplemented with ampicillin, IPTG and X-gal (Section 2.1.6, p. 41). Colonies harbouring recombinant plasmids containing the insert were identified using the β-galactosidase histochemical screen (Section 2.2.20, p. 52), then single cell purified. The resulting plasmid, pANDY1 (Section A6.8, p. 183), was identified by *Hin*dIII, *Cla*I, *Sal*I, and *Sph*I diagnostic digests of plasmid DNA prepared by the STET-method (Section 2.2.2, p. 44) (Data not presented).

3.2.3 Attaching pUC18 mcs to P_{35S}-*nptII* Fusion

To attach the pUC18 mcs to the promoters of the P_{35S}-*nptII* fusion, the fusion was excised from pANDY1 as a *Cla*I/*Sal*I fragment, which was end-filled and ligated into a *Sac*I-digested, 3′ overhang-recessed pUC18 vector (Fig. 13 (steps 3-5), p. 80). The P_{35S}-*nptII* fusion was excised as a 2465 bp *Cla*I/*Sal*I fragment rather than as a *Cla*I/*Hin*dIII fragment, thus reducing the amount of non-essential DNA downstream of the *ocs*3′ termination sequence by 552 bp (Section A6.8, p. 183). pANDY1 DNA prepared by the STET-method (Section 2.2.2, p. 44) was digested with both *Cla*I and *Sal*I in H buffer (Boehringer Mannheim GmbH) (Section 2.2.13, p. 49), and the fragments separated by electrophoresis through a 0.8% (w/v) agarose gel (Section 2.2.9, p. 46). The 2465 bp fragment containing the P_{35S}-*nptII* fusion was recovered using GENECLEAN® (Section 2.2.11, p. 48), and end-filled (Section 2.2.16, p. 50). It was then ligated (Section 2.2.19, p. 51) into a pUC18 vector (Section A6.7, p. 182) of which STET-prepared DNA (Section 2.2.2, p. 44) had been previously *Sac*I-digested in buffer A (Boehringer Mannheim GmbH) (Section 2.2.13, p. 49), 3′ overhang-recessed (Section 2.2.17, p. 51) and CAP-treated (Section 2.2.18, p. 51) (Fig. 13 (steps 3-5), p. 80). The ligation reaction was transformed into *E. coli* strain DH5α™ cells made competent with $CaCl_2$, from which aliquots were spread on solid LB medium supplemented with ampicillin, IPTG and X-gal (Section 2.1.6, p. 41).

The β-galactosidase histochemical screen (Section 2.2.20, p. 52) detected only pUC18 vectors whose termini had not been recessed, which thus re-ligated and appeared as blue colonies. To distinguish between re-ligated pUC18 vectors that had been recessed, and those harbouring the inserted P_{35S}-*nptII* fusion, a Rapid Colony Lysis was performed (Section 2.2.21, p. 52). DNA from those colonies putatively containing an insert was extracted using the STET-method (Section 2.2.2, p. 44), then digested with *Sal*I or *Pst*I (Section 2.2.13, p. 49) to determine the orientation of the insert with respect to the pUC18 mcs (Fig. 14A-C, p. 84). Construction of pANDY2

Figure 14A-C. Determining orientation of the P_{35S}-*nptII* insert with regard to the pUC18 mcs during construction of pANDY2.

A. The pUC18 vector was digested with *Sac*I, blunt-ended by recessing the 3′ overhang, then CAP-treated. The *Cla*I/*Sal*I P_{35S}-*nptII* fragment from pANDY1 was filled-in (filler nucleotides in **bold**) and ligated into the pUC18 vector. Insertion and ligation of the fragment was predicted to restore the *Sal*I site (5′-GTCGAC-3′), thus providing an excellent diagnostic enzyme site for determining the orientation of the P_{35S}-*nptII* fusion within pUC18.

Numbers below restriction enzyme sites refer to their position (bp) in the plasmid.

H=*Hin*dIII; S=*Sph*I; X=*Xba*I; B=*Bam*HI; Sm=*Sma*I; K=*Kpn*I; E=*Eco*RI.
mcs=pUC18 multiple cloning site; $P_{mas2'}$=2′ promoter of the mannopine synthase gene; P_{35S}=promoter of the Cauliflower Mosaic Virus 35S RNA subunit; *nptII*=neomycin phosphotransferase gene; *ocs*3′=transcription termination sequence of octopine synthase gene.

B. A *Pst*I diagnostic digest of 1 µg DNA of pUC18 (lane 2); a plasmid with the P_{35S}-*nptII* fusion inserted in the incorrect orientation (lane 3); and a plasmid with the fusion inserted in the correct orientation (pANDY2) (lane 4).

Numbers to the left of the figure refer to the size (kb) of fragments generated by *Hin*dIII plus *Hin*dIII/*Eco*RI digested phage λ DNA (Section A4.10, p. 170) (lane 1).

C. A *Sal*I diagnostic digest of 1 µg DNA of pUC18 (lane 2); a plasmid with the P_{35S}-*nptII* fusion inserted in the incorrect orientation (lane 3); and a plasmid with the fusion inserted in the correct orientation (pANDY2) (lane 4).

Numbers to the left of the figure refer to the size (kb) of fragments generated by *Hin*dIII plus *Hin*dIII/*Eco*RI digested phage λ DNA (Section A4.10, p. 170) (lane 1). Although the plasmid in lane 3 was identified as pANDY2 by a *Pst*I digest, it did not generate the expected fragments when digested with *Sal*I.

A.

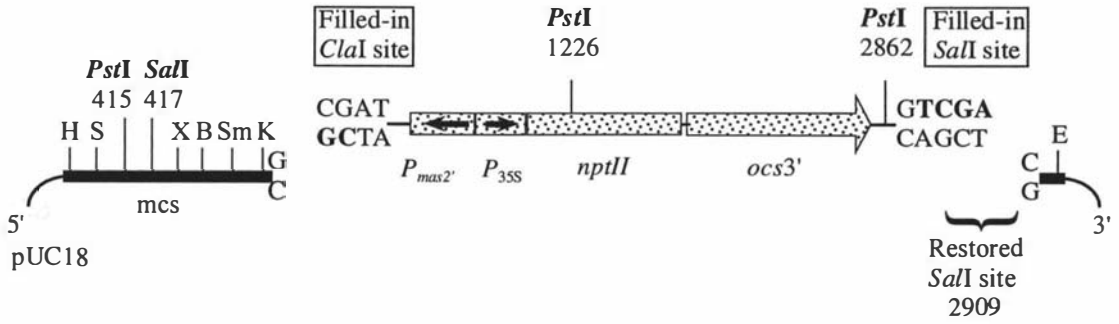

Correct Orientation (pANDY2)
Expected *Pst*I fragments: 2703, 1636, 811 bp
Expected *Sal*I fragments: 2658, 2492 bp

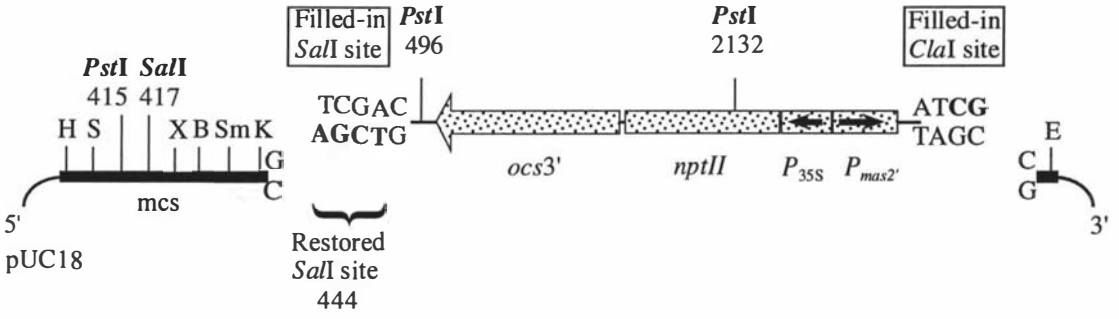

Incorrect Orientation
Expected *Pst*I fragments: 3434, 1636, 81 bp
Expected *Sal*I fragments: 5122, 28 bp

B.

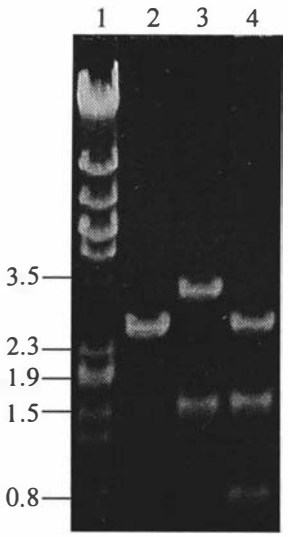

C.

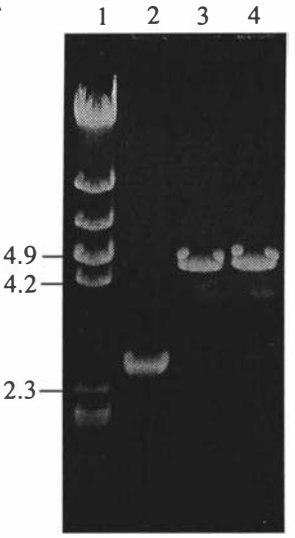

by insertion and ligation of the correctly orientated blunt-ended *Cla*I/*Sal*I P_{35S}-*nptII* fragment into the blunt-ended *Sac*I-digested pUC18 vector, should have restored the *Sal*I enzyme site (Figure 14A). Hence, digestion with this enzyme would have determined the orientation of the insert with respect to the pUC18 mcs, depending upon the fragments generated (Figure 14A, p. 84). However, none of the clones with the required orientation (determined by a *Pst*I digest (Fig. 14B, p. 84)) exhibited this diagnostic feature (Figure 14C, p. 84). Sequencing over the region of the selected clone at the completion of the modification of the mcs-P_{35S}-*nptII* (Section 3.2.5, p. 87), however, revealed that the T4 polymerase had deleted an extra base-pair when recessing the *Sac*I-generated 3′ overhang in pUC18, thus preventing regeneration of the *Sal*I site in pANDY2.

3.2.4 Preparing mcs-P_{35S}-*nptII* for Insertion into pANDY6, pANDYOD⁻ Vector Series

Prior to inserting the mcs-P_{35S}-*nptII* fusion into the unique *Sac*I site of pANDY6 and the pANDYOD⁻ derivatives, the fusion was positioned such that it was flanked by *Sac*I sites. The aim was to ligate the modified fusion from pANDY2, *via* an intermediate cloning step which created pANDY3 (Section A6.10, p. 185), and then into the unique *Eco*RI site of pMTL25P, which is flanked immediately on either side by a *Sac*I site (Section A6.6, p. 181). A summary of this procedure is detailed in Figure 13 (steps 6-11) (p. 81).

The mcs-P_{35S}-*nptII* fusion could be excised as a 2515 bp *Hin*dIII/*Eco*RI fragment from pANDY2 (Section A6.9, p. 184). As this fragment and the vector fragment differed in size by only 120 bp, it was difficult to separate them by agarose gel electrophoresis. Therefore, pANDY2 DNA prepared by the STET-method (Section 2.2.2, p. 44), was triple-digested with *Hin*dIII, *Eco*RI, and *Sca*I in buffer B (Boehringer Mannheim GmbH) (Section 2.2.13, p. 49). The *Sca*I enzyme bisected the *Hin*dIII/*Eco*RI vector fragment to yield a 906 bp and a 1729 bp fragment (Section A6.9) (Fig. 13 (step 11), p. 81). This permitted clear resolution, by electrophoresis through a 0.8% (w/v) agarose gel (Section 2.2.9, p. 46), of the fragment containing mcs-P_{35S}-*nptII* fusion, which was then recovered using GENECLEAN® (Section 2.2.11, p. 48).

Rather than immediately filling-in the termini of the fragment and ligating it into an *Eco*RI-digested and blunt-ended pMTL25P vector, the *Hin*dIII/*Eco*RI mcs-P_{35S}-*nptII* fusion was ligated (Section 2.2.19, p. 51) into a *Hin*dIII/*Eco*RI-digested (Section 2.2.13, p. 49) pMTL22P vector (Section A6.5, p. 180) to create pANDY3 (Fig. 13 (steps 6-8), p. 81; Section A6.10, p. 185). *E. coli* strain DH5α™ cells made

competent with $CaCl_2$ were transformed with the ligation mix (Section 2.1.6, p. 41), and colonies containing pANDY3 were selected by β-galactosidase screening for white colonies (Section 2.2.20, p. 52) on solid LB medium supplemented with ampicillin, IPTG and X-gal. After extracting DNA using the STET-method (Section 2.2.2, p. 44), pANDY3 (Section A6.10, p. 185) was identified by a diagnostic *Eco*RI/*Mlu*I digest in buffer H (Boehringer Mannheim GmbH) (Section 2.2.13, p. 49).

This intermediate cloning step was performed to preserve the unique *Hin*dIII site located in the mcs attached to the fusion promoter, as end-filling the *Eco*RI/*Hin*dIII fragment containing the fusion prior to its insertion into a vector would destroy the *Hin*dIII site. By constructing pANDY3, the mcs-P_{35S}-*nptII* fusion could be excised as an *Eco*RI/*Mlu*I fragment, thus protecting the *Hin*dIII site immediately adjacent to the *Mlu*I site when end-filling the termini prior to insertion into pMTL25P to create pANDY4 (Fig. 13 (step 9-11), p. 81; Section A6.11, p. 186). This *Hin*dIII site was used extensively in the completed series of plant transformation vectors (Section 3.4, p. 92) for Southern analysis of plants when determining T-DNA copy number (Section 3.8, p. 114).

To place the mcs-P_{35S}-*nptII* fusion such that it was flanked by *Sac*I sites, it was excised from STET-prepared (Section 2.2.2, p. 44) pANDY3 DNA by an *Eco*RI/*Mlu*I digest (Section 2.2.13, p. 49). DNA in the reaction mixture was precipitated (Section 2.2.4, p. 45), end-filled (Section 2.2.16, p. 50), and the fragment containing the mcs-P_{35S}-*nptII* fusion separated from the vector by electrophoresis through a 0.8% (w/v) agarose gel (Section 2.2.9, p. 46), and then recovered using GENECLEAN® (Section 2.2.11, p. 48). STET-prepared DNA (Section 2.2.2) of the recipient vector, pMTL25P (Section A6.6, p. 181), was *Eco*RI digested (Section 2.2.13, p. 49), end-filled (Section 2.2.16, p. 50), and CAP-treated (Section 2.2.18, p. 51). The end-filled *Eco*RI/*Mlu*I mcs-P_{35S}-*nptII* fragment was ligated (Section 2.2.19, p. 51) into the blunt-ended pMTL25P vector (Fig. 13 (steps 9-11), p. 81), the ligated DNA transferred to *E. coli* strain DH10B cells by electroporation, and aliquots of the cells were spread on solid LB medium supplemented with carbenicillin, IPTG and X-gal (Section 2.1.8, p. 42). Colonies containing vectors that had not been end-filled were identified by the β-galactosidase histochemical assay (Section 2.2.20, p. 52), in which they became blue. White colonies, therefore, were single cell purified and analysed for the presence of inserts using Rapid Colony Lysis (Section 2.2.21, p. 52). DNA from colonies harbouring the pMTL25P vector and a putative insert was extracted using the STET-method (Section 2.2.2, p. 44). Diagnostic digests of this DNA, using *Sac*I and *Eco*RI, identified those colonies containing pANDY4 (Section A6.11, p. 186;

Fig. 15B, p. 89). These digests revealed that the filled-in *Eco*RI site of pMTL25P was restored as predicted when ligated to the filled-in *Mlu*I site of the insert (Figure 15A-B, p. 89). The *Eco*RI site was an important addition to the mcs attached to the P_{35S}-*nptII* fusion, as it was used extensively in Southern analysis of plants when determining T-DNA copy number (Section 3.8, p. 114).

The result of this series of cloning steps was the modification of the P_{35S}-*nptII* fusion from pSLJ491 by the addition of a pUC18 mcs to the promoters of the fusion, and the placement of the modified fusion such that it could be excised as a *Sac*I fragment (Fig. 13 (step 12), p. 81). This *Sac*I fragment may then be ligated into the unique *Sac*I site located in the left border region of the T-DNA of the plant transformation vector, pANDY6 (Section A6.2, p. 177), and the pANDYOD$^-$ derivatives containing deletions in the putative nopaline-type *overdrive* region (Section A6.3, p. 178).

3.2.5 Sequencing Junctions of mcs-P_{35S}-*nptII* in pANDY4

Prior to inserting the mcs-P_{35S}-*nptII* fusion from pANDY4 into pANDY6 and the pANDYOD$^-$ derivatives, the fusion was sequenced across either end. This was to detect any corruptions that may have occurred during the cloning steps, particularly in the attached pUC18 mcs. To determine the nucleotide sequence across the pUC18 mcs region, the sequencing reactions (Section 2.2.22 p. 52) were primed with the -40 Universal sequencing primer (5′-GTTTTCCCAGTCACGAC-3′) (Figure 16A, p. 91). This revealed that the pUC18 mcs sequence was intact, and that the end-filling and 3′ overhang recessing reactions had also proceeded as predicted, thus restoring the *Eco*RI site (Figure 16B, p. 91). The 3′ terminator region of the mcs-P_{35S}-*nptII* fusion was sequenced (Section 2.2.22) using the -44 Reverse sequencing primer (5′-GCGGATAACAATTTCACAGGA-3′) (Figure 16A), which demonstrated that recessing the *Sac*I-generated 3′ overhang when constructing pANDY2 (Section 3.2.3, p. 82) removed an extra base-pair, a G-C pair (Figure 16C, p. 91). Furthermore, filling-in the *Eco*RI termini of pMTL25P (Section 3.3.3, p. 85) added an extra base-pair, a T-A pair (Figure 16C). Neither of these abberations had any effect on the final outcome of this series of cloning steps. However, removal of the C-G nucleotide pair prevented restoration of the filled-in *Sal*I site at the terminus of the P_{35S}-*nptII* fragment when inserted into pUC18 to create pANDY2. This enzyme would have been a useful diagnostic enzyme for determining the orientation of the P_{35S}-*nptII* fusion with regard to the pUC18 mcs (Figure 14, p. 84).

Figure 15A-B. Restoration of the *Eco*RI site during the construction of pANDY4.

A. The pMTL25P vector was digested with *Eco*RI and end-filled (filler nucleotides in **bold**) and CAP-treated. The *Mlu*I/*Eco*RI mcs-P_{35S}-*nptII* fragment from pANDY3 was also end-filled (filler nucleotides in **bold**), then ligated into the pMTL25P vector to create pANDY4. Insertion of the fragment recreated the filled-in pMTL25P *Eco*RI site (5′-GAATTC-3′) when ligated to the filled-in *Mlu*I site upstream of the pUC18 mcs. The highlighted (**bold**) *Sac*I sites indicate the enzymes to be used to excise the mcs-P_{35S}-*nptII* from pANDY4 prior to insertion into the pANDY6 and pANDYOD$^-$ vector series. The table below the diagram details the expected fragment sizes generated by an *Eco*RI and a *Sac*I digest of pANDY4.

mcs =pUC18 multiple cloning site; $P_{mas2'}$=2′ promoter of the mannopine synthase gene; P_{35S}=promoter of the Cauliflower Mosaic Virus 35S RNA subunit; *nptII*=neomycin phosphotransferase gene; *ocs*3′ =transcription termination sequence of octopine synthase gene.

B. A *Sac*I digest (lane 1) and an *Eco*RI digest (lane 2) of 1 μg of pANDY4 generated the expected fragments described in Figure 15A (above). Lane 3 contained 1 μg uncut pANDY4. Numbers to the left of the figure refer to the size (bp) of fragments generated by *Hin*dIII plus *Hin*dIII/*Eco*RI digested phage λ DNA (Section A4.10, p. 170) (lane 4).

A.

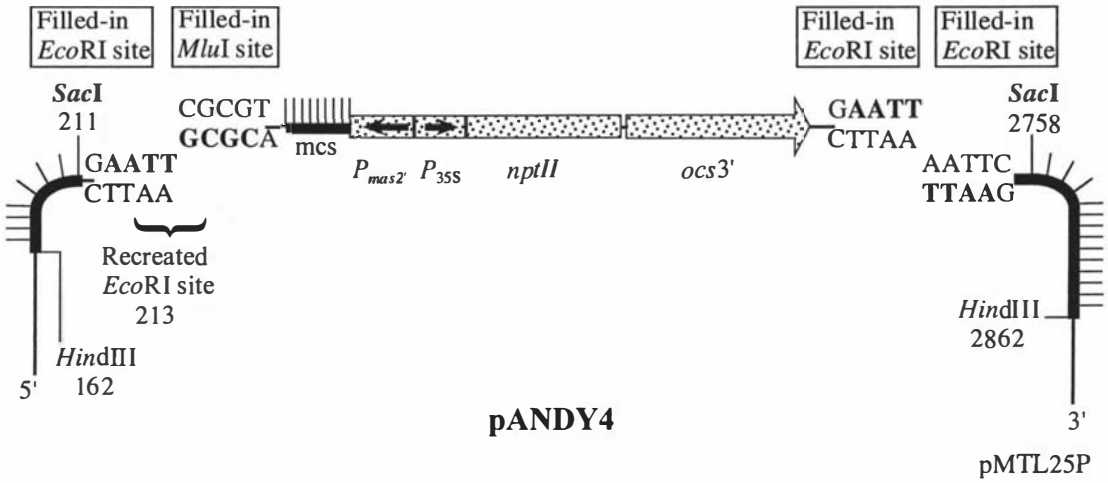

Expected Fragments

*Eco*RI digest: 5443 bp
*Sac*I digest: 2898, 2547 bp

B.

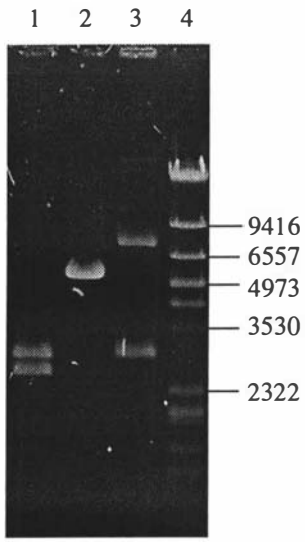

Figure 16A-C. Nucleotide sequence of the junctions of the mcs-P_{35S}-*nptII* fusion with pMTL25P in pANDY4.

A. A diagram showing the position and orientation of both the -44 Reverse (Rev) and -40 Universal (Uni) sequencing primers with regard to the mcs-P_{35S}-*nptII* fusion in pANDY4. Vertical lines adjacent to the primers represent enzyme sites in the pMTL25P multiple cloning region. The highlighted enzymes (**bold**) refer to those from the pUC18 mcs in pANDY2, whereas the marked (*) *Sac*I sites represent the boundaries of the *Sac*I digested mcs-P_{35S}-*nptII* fragment to be inserted into the pANDY6 and pANDYOD$^-$ plant transformation vectors.

bla=β-lactamase gene; $P_{mas2'}$=2′ promoter of the mannopine synthase gene; P_{35S}=promoter of the Cauliflower Mosaic Virus 35S RNA subunit; *nptII*=neomycin phosphotransferase gene; *ocs*3′=transcription termination sequence of octopine synthase gene.

B. Sequence data of the region upstream of the mcs-P_{35S}-*nptII* fusion in pANDY4 generated using the Universal sequencing primer (Uni) was derived from the sequencing gel shown in Section A5.1 (p. 174). It demonstrated the integrity of the pUC18 mcs (enzymes in **bold**) upstream of the bi-directional $P_{mas2'}$/P_{35S} promoter of the mcs-P_{35S}-*nptII* fusion. When constructing pANDY4 (Section 3.2.4, p. 85), the filled-in *Mlu*I site (**bold** underline) of the mcs-P_{35S}-*nptII* fragment was ligated to the filled-in *Eco*RI site of pMTL25P, thus restoring that *Eco*RI site (5′-GAATTC-3′). When constructing pANDY2 (Section 3.2.3, p. 82), the filled-in *Cla*I site (**bold** underline) of the mcs-P_{35S}-*nptII* fusion was ligated to the recessed *Sac*I site of the pUC18 mcs. The sequence of this junction reveals no extra or deleted nucleotides. The *Sac*I site used to excise mcs-P_{35S}-*nptII* fusion from pANDY4 is indicated (*).

C. Sequence data of the region downstream of the mcs-P_{35S}-*nptII* fusion generated using the Reverse sequencing primer (Rev) was derived from the sequencing gel shown in Section A5.2 (p. 175). It demonstrated the integrity of the *Sac*I site (*) with which the mcs-P_{35S}-*nptII* fusion was to be excised from pANDY4. The sequence also revealed that when constructing pANDY4 (Section 3.2.4, p. 85), an extra base pair (**T•**) was incorporated when filling-in the *Eco*RI site (**bold** underline) of pMTL25P prior to ligation to the filled-in *Eco*RI site of the mcs-P_{35S}-*nptII* fragment from pANDY3. Furthermore, when constructing pANDY2 (Section 3.2.3, p. 82), an extra base pair was deleted (**-G**) from the pUC18 *Sac*I site when it was recessed. This meant that when ligated to the filled-in *Sal*I site (**bold** underline) of the mcs-P_{35S}-*nptII* fusion to create pANDY2, the *Sal*I site (5′-GTCGAC-3′) was not restored.

A.

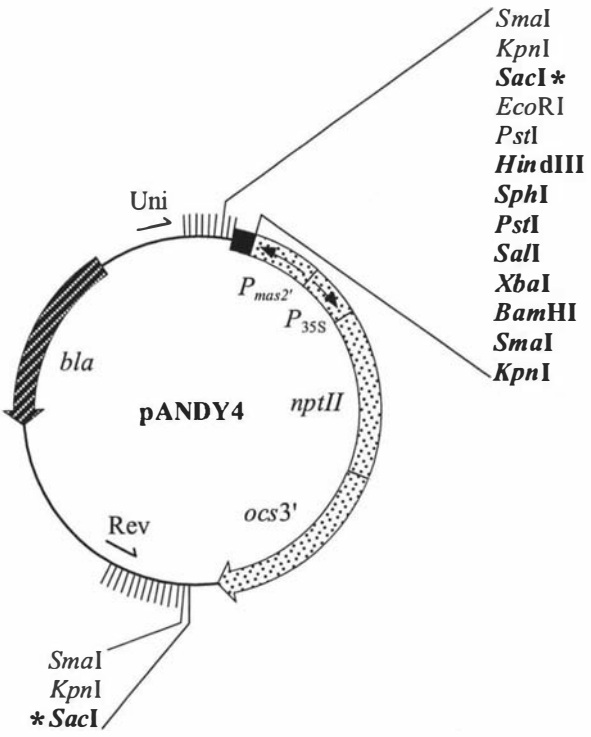
SmaI
KpnI
SacI*
EcoRI
PstI
HindIII
SphI
PstI
SalI
XbaI
BamHI
SmaI
KpnI
Uni
Pmas2'
P35S
bla
pANDY4
nptII
ocs3'
Rev
SmaI
KpnI
*SacI

B.

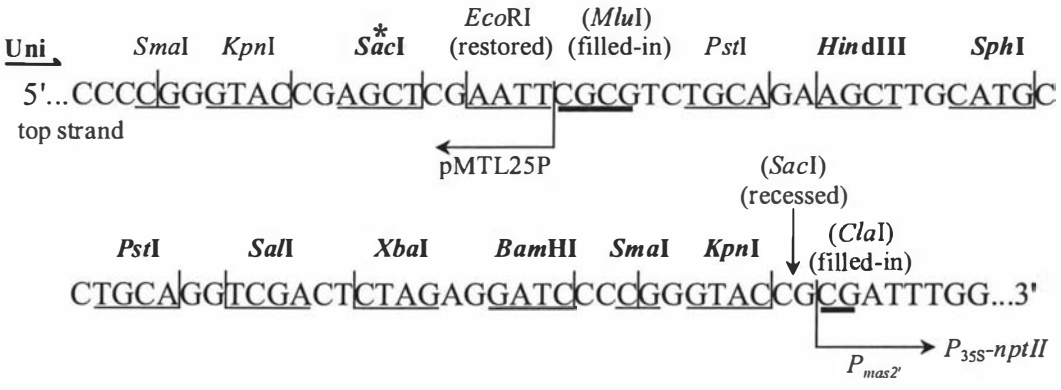
Uni
SmaI
KpnI
*SacI
EcoRI
(restored)
(MluI)
(filled-in)
PstI
HindIII
SphI
5'...CCCCGGGTACCGAGCTCGAATTCGCGTCTGCAGAAGCTTGCATGC
top strand
pMTL25P
(SacI)
(recessed)
PstI
SalI
XbaI
BamHI
SmaI
KpnI
(ClaI)
(filled-in)
CTGCAGGTCGACTCTAGAGGATCCCCGGGTACCGCGATTTGG...3'
P35S-nptII
Pmas2'

C.

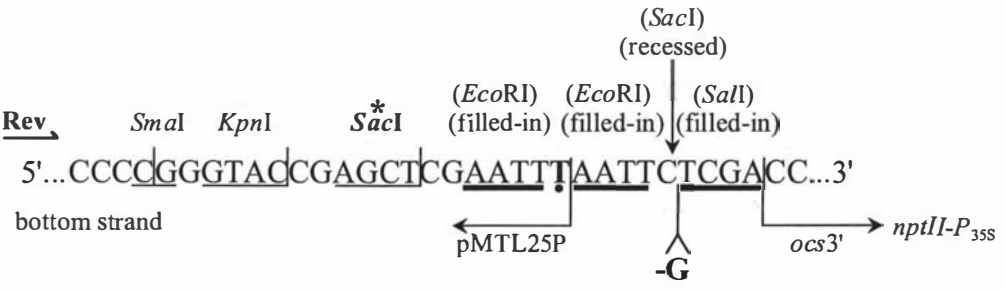
(SacI)
(recessed)
Rev
SmaI
KpnI
*SacI
(EcoRI)
(filled-in)
(EcoRI)
(filled-in)
(SalI)
(filled-in)
5'...CCCCGGGTACCGAGCTCGAATTTAATTCTCGACC...3'
bottom strand
pMTL25P
-G
ocs3'
nptII-P35S

3.3 COMPLETION OF pANDY VECTOR SERIES

3.3.1 Overview

The modified mcs-P_{35S}-*nptII* plant-selectable marker (Section 3.2, p. 78) was ligated into the unique *Sac*I site of the plant transformation vector pANDY6 and its *overdrive* deletion derivatives, pANDYOD$^-$2 and pANDYOD$^-$3, to create pANDY8, pANDY9, and pANDY10 (Section A.7.12, p. 187), respectively, as summarised in Figure 17 (p. 93).

3.3.2 Construction of pANDY8, pANDY9, and pANDY10

STET-prepared DNA (Section 2.2.2, p. 44) of pANDY4 (Section A6.11, p. 186) was digested by *Sac*I in buffer A (Boehringer Mannheim GmbH) (Section 2.2.13, p. 49), and the fragment containing the mcs-P_{35S}-*nptII* fusion separated from the vector by electrophoresis through a 0.8% (w/v) agarose gel (Section 2.2.9, p. 46). This 2547 bp fragment was recovered using GENECLEAN® (Section 2.2.11, p. 48), and ligated (Section 2.2.19, p. 51) into each of previously STET-prepared, *Sac*I-digested, CAP-treated (Section 2.2.18, p. 51) pANDY6 (Section A6.2, p. 177), pANDYOD$^-$2 and pANDYOD$^-$3 (Section A6.3, p. 178) vectors. After transformation of each of the ligation reactions into *E. coli* strain DH10B cells by electroporation, aliquots were spread on solid LB medium supplemented with kanamycin and carbenicillin (Section 2.1.8, p. 42). Colonies harbouring a plant transformation vector with the modified plant selectable marker in the required orientation were identified using *Eco*RI diagnostic digests (Fig. 18, p. 96) of STET-prepared (Section 2.2.2) DNA. Thus, pANDY8 (pANDY6 plus plant-selectable marker), pANDY9 (pANDYOD$^-$2 plus plant-selectable marker), and pANDY10 (pANDYOD$^-$3 plus plant-selectable marker), were identified (Section A6.12, p. 187). An *Sph*I digest or an *Eco*RI/*Sph*I double-digest distinguished pANDY8 from those vectors with deletions in the putative *overdrive* region, such as pANDY9 and pANDY10 (Data not presented). However, since there is no diagnostic digest available to distinguish between pANDY9 and pANDY10, only sequence data of the putative *overdrive* region may conclusively identify pANDY9 or pANDY10.

3.3.3 Sequencing Junctions of mcs-P_{35S}-*nptII* in pANDY8 to pANDY10

The regions adjacent to the promoter and the terminator of the mcs-P_{35S}-*nptII* fusion were sequenced to detect corruptions that may have occurred (particularly in the mcs of the fusion) during construction of pANDY8, pANDY9, and pANDY10. The -40 Universal primer (5′-GTTTTCCCAGTCACGAC-3′) was used for sequence determination (Section 2.2.22, p. 52) of the region downstream of the *ocs*3′ portion of the mcs-P_{35S}-*nptII* fusion (Section A6.12, p. 187), whereas the sequence upstream of the

Figure 17. Summary of construction of pANDY8, pANDY9, and pANDY10.

The individual steps in this figure are referred to, and expanded upon, in the text.

RB =right border; LB =left border; OD =putative nopaline-type *overdrive* core; *oriV* =origin of replication; *bla* =β-lactamase gene; *gusA* =β-glucuronidase gene; *oriV* =origin of replication; *nptIII* =neomycin phosphotransferase gene; $P_{mas2'}$ =2′ promoter of the mannopine synthase gene; P_{35S} =promoter of the Cauliflower Mosaic Virus 35S RNA subunit; *nptII* =neomycin phosphotransferase gene; *ocs*3′ =transcription termination sequence of octopine synthase gene; mcs-P_{35S}-*nptII* =a multiple cloning site from pUC18 attached to a P_{mas2}/P_{35S} dual promoter driving an *nptII* gene terminated by *ocs*3′.

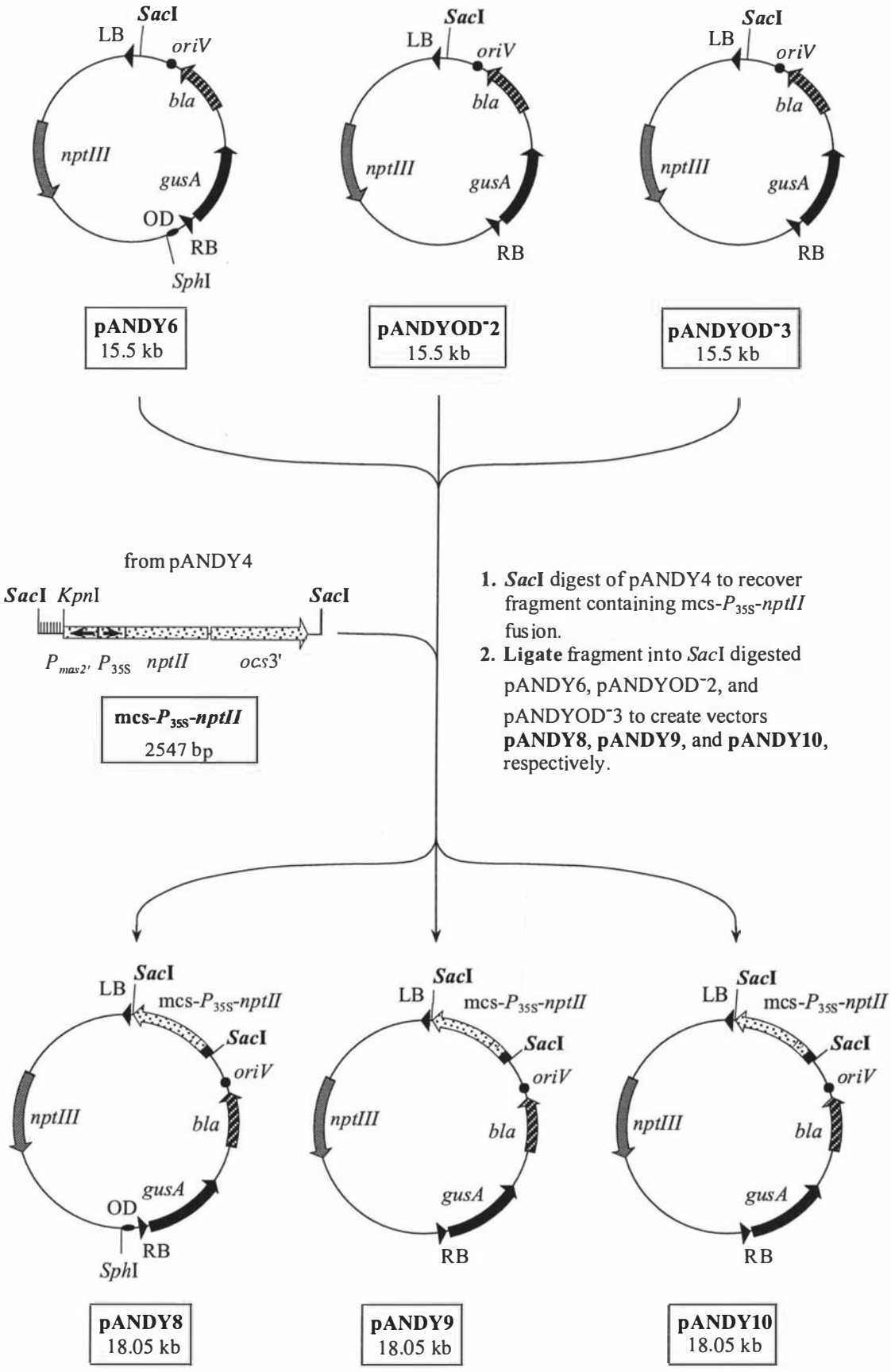
SacI
LB
oriV
bla
nptIII
gusA
OD
RB
SphI
pANDY6
15.5 kb
pANDYOD⁻2
15.5 kb
pANDYOD⁻3
15.5 kb
from pANDY4
SacI KpnI
SacI
Pmas2' P35S nptII ocs3'
mcs-P35S-nptII
2547 bp
1. SacI digest of pANDY4 to recover fragment containing mcs-P35S-nptII fusion.
2. Ligate fragment into SacI digested pANDY6, pANDYOD⁻2, and pANDYOD⁻3 to create vectors pANDY8, pANDY9, and pANDY10, respectively.
pANDY8
18.05 kb
pANDY9
18.05 kb
pANDY10
18.05 kb

Figure 18A-D. Identification of plasmids pANDY8, pANDY9, and pANDY10.

A. The diagram shows vectors in which the mcs-P_{35S}-*nptII* fusion was inserted into the *Sac*I site of pANDY6, pANDYOD^{-}2, and pANDYOD^{-}3 in the required orientation (pANDY8, pANDY9, and pANDY10), and in the reverse orientation. Below each vector map is a table detailing the sizes (kb) of expected fragments generated when digested by *Eco*RI.

RB =right border; LB =left border; mcs-P_{35S}-*nptII* =a multiple cloning site from pUC18 attached to a $P_{mas2'}/P_{35S}$ dual promoter driving an *nptII* gene terminated by *ocs*3′ sequence; *oriV* =origin of replication; *bla* =β-lactamase gene; *gusA* =β-glucuronidase gene; *nptIII* =neomycin phosphotransferase gene.

B. An *Eco*RI diagnostic digest of 1 μg of reverse orientation mcs-P_{35S}-*nptII* plasmid (lane 1), and pANDY8 (lane 2). Numbers to the right of the figure refer to sizes (kb) of fragments generated by *Hin*dIII plus *Hin*dIII/*Eco*RI digested phage λ DNA (Section A4.10, p. 170) (lane 3).

C. An *Eco*RI diagnostic digest of 1 μg of reverse orientation mcs-P_{35S}-*nptII* plasmid (lane 2), and pANDY9 (lane 3). Numbers to the left of the figure refer to the size (kb) of fragments generated by *Hin*dIII plus *Hin*dIII/*Eco*RI digested phage λ DNA (Section A4.10, p. 170) (lane 1).

D. An *Eco*RI diagnostic digest of 1 μg of pANDY10 (lane 2). Numbers to the left of the figure refer to the size (kb) of fragments generated by *Hin*dIII plus *Hin*dIII/*Eco*RI digested phage λ DNA (Section A4.10, p. 170) (lane 1).

A.

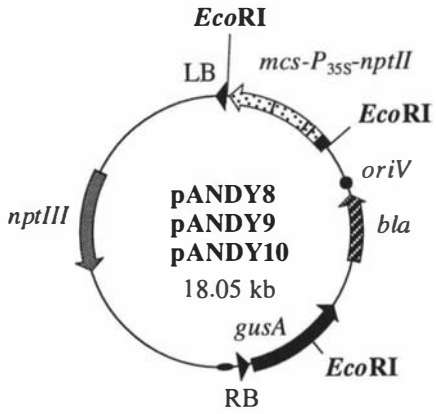

Required orientation

***Eco*RI digest**
11.2
4.3
2.55

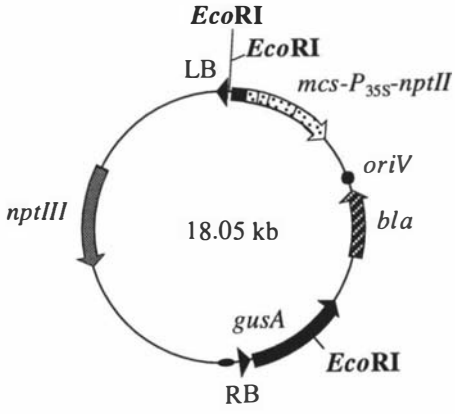

Reverse orientation

***Eco*RI digest**
11.2
6.85

B.

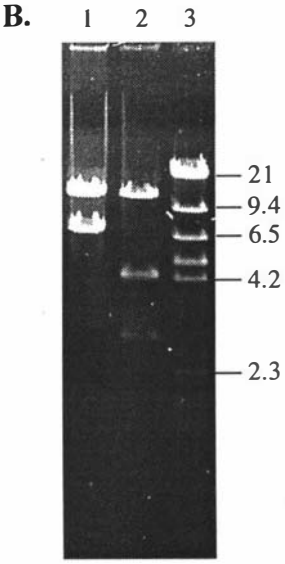

C.

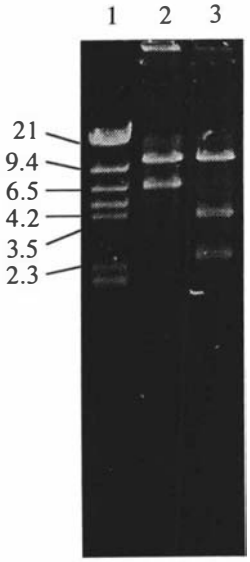

D.

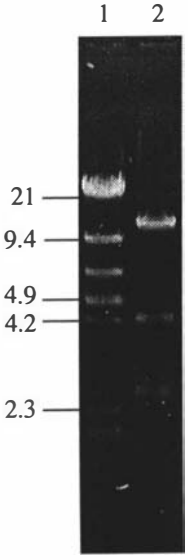

P_{35S}, across the mcs and towards the plant transformation vector was ascertained using a 25mer PCR primer, 2.1 (5′-GGCGGTACCGAAATGGATAATAGCC-3′; courtesy of Dr D. W. R. White), of which 17 bp annealed to a portion of the *mas2′* promoter (Section A6.12, p. 187). To elucidate sequence close to the primers, sequencing reactions were performed in the presence of manganese (Section 2.2.22, p. 52). The nucleotide sequences of the restriction sites at either end of the mcs-P_{35S}-*nptII* fusion in pANDY8, pANDY9, and pANDY10 indicated that no further corruptions had occurred when transferring the fusion from pANDY4 (Data not presented).

3.3.4 Transferring pANDY8-10 Series to *A. tumefaciens*

Prior to transformation of *Nicotiana tabacum*, the plasmids pANDY8, pANDY9, and pANDY10, were transferred to *Agrobacterium tumefaciens* strain LBA4404, which harbours pAL4404, a disarmed mutant of the octopine-type Ti-plasmid, pTiAch5 (Hoekema *et al.*, 1983; Ooms *et al.*, 1982). Previous data indicated that the effects of the nopaline-type *overdrive* are less noticeable in a nopaline-type *vir* environment (Wang *et al.*, 1987) than in an octopine-type *vir* environment (Van Haaren *et al.*, 1988), possibly due to differences in the activity of the *vir* products (Bakkeren *et al.*, 1989; Van Haaren *et al.*, 1988). An octopine-type *vir* environment may, therefore, provide a more sensitive assay for determining the impact of deletions in the putative nopaline-type *overdrive* core. To test this, the pANDY8-10 series was assayed in both an octopine and a nopaline-type *vir* gene-product environment as provided by LBA4404 and GV3101, respectively..

Vectors pANDY8 and pANDY9 were transferred by tri-parental mating as described (Section 2.1.3, p. 37), and transformed LBA4404 cells were selected on solid AB medium supplemented with kanamycin and carbenicillin. Electroporation was used to transfer pANDY9 to LBA4404 (Section 2.1.4, p. 40), and transformed cells were selected on solid TY medium supplemented with kanamycin and carbenicillin. To determine the integrity of the transferred plasmids, DNA was extracted (Section 2.2.1, p. 44) from single-cell purified colonies, then double-digested with *Eco*RI and *Sph*I (Section 2.2.13, p. 49) in buffer M (Boehringer Mannheim GmbH). Those colonies containing plasmids with the correct digest profile (Fig. 19A-D, p. 99) were stored as glycerol stocks at -80°C (Section 2.1.1, p. 37), which were used as the sole source of inoculum in all subsequent plant transformation experiments. The vectors were also transferred by electroporation (Section 2.1.4) to the disarmed octopine-type *A. tumefaciens* strains, MOG1010, its *virC2* mutant derivative, MOG1010-C, an oncogenic octopine-type *virC1* mutant (A1021), and GV3101, a wild-type disarmed nopaline-type strain.

Figure 19A-D. Identification of *A. tumefaciens* strain LBA4404 colonies harbouring either pANDY8, pANDY9, or pANDY10.

A. The diagram shows the restriction sites for *Eco*RI and *Sph*I in pANDY8, pANDY9, and pANDY10. Below each vector map is a table detailing the sizes (kb) of expected fragments generated by an *Eco*RI/*Sph*I digest.

RB =right border; LB =left border; OD =putative nopaline-type *overdrive* core; mcs-P_{35S}-*nptII* =a multiple cloning site from pUC18 attached to a P_{mas2}/P_{35S} dual promoter driving an *nptII* gene terminated by *ocs3'* sequence; *oriV* =origin of replication; *bla*=β-lactamase gene; *gusA* =β-glucuronidase gene; *nptIII* =neomycin phosphotransferase gene.

B. An *Eco*RI/*Sph*I diagnostic digest of 1 μg pANDY8 extracted from *E. coli* strain DH5α™ (lane 2), and 0.5 μg pANDY8 extracted from LBA4404 (lane 3). Numbers to the left of the figure refer to sizes (kb) of fragments generated by *Hin*dIII plus *Hin*dIII/*Eco*RI digested phage λ DNA (Section A4.10, p. 170) (lane 1).

C. An *Eco*RI/*Sph*I diagnostic digest of 0.5 μg pANDY9 extracted from LBA4404 (lane 1), and 1 μg pANDY9 extracted from DH5α™ (lane 2). Numbers to the right of the figure refer to sizes (kb) of fragments generated by *Hin*dIII plus *Hin*dIII/*Eco*RI digested phage λ DNA (Section A4.10, p. 170) (lane 3).

D. An *Eco*RI/*Sph*I diagnostic digest of 1 μg pANDY10 extracted from DH5α™ (lane 2), and 0.5 μg pANDY10 extracted from LBA4404 (lane 3). Numbers to the left of the figure refer to sizes (kb) of fragments generated by *Hin*dIII plus *Hin*dIII/*Eco*RI digested phage λ DNA (Section A4.10, p. 170) (lane 1).

A.

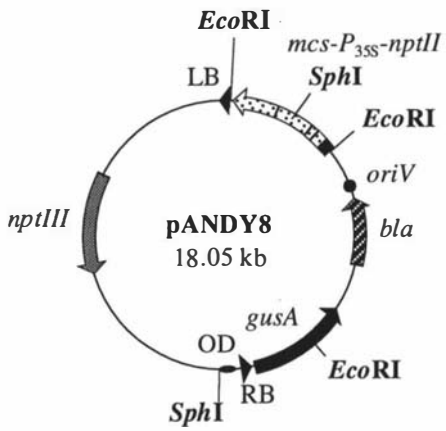

Required orientation

*Eco*RI/*Sph*I digest
9.2
4.3
2.0
1.35
1.2

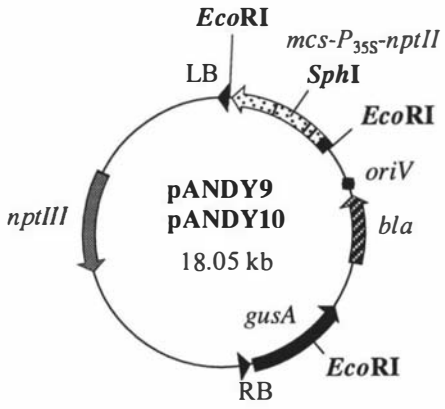

Required orientation

*Eco*RI/*Sph*I digest
11.2
4.3
1.35
1.2

B.

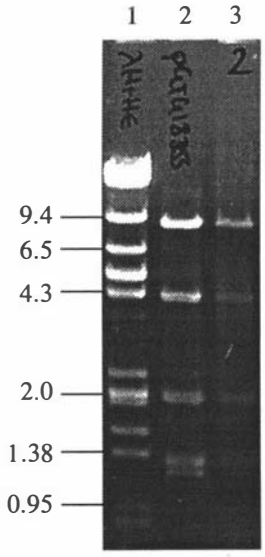

C.

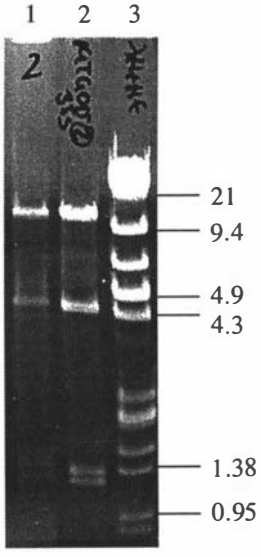

D.

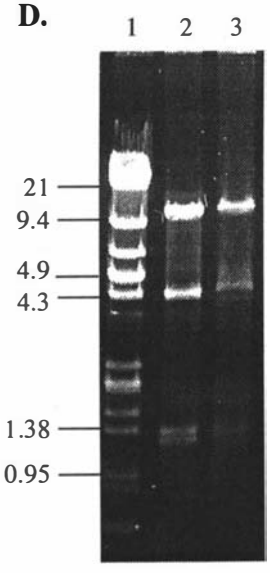

3.6 SUMMARY OF VECTOR MODIFICATIONS

The outcome of these modifications was the construction of a series of plant transformation vectors, and their transfer into *A. tumefaciens*. These vectors contained differing deletions in the putative nopaline-type *overdrive* region so that the influence of such deletions on plant transformation frequency and T-DNA copy number could be determined. The introduction of the mcs-P_{35S}-*nptII* fusion provided a strong constitutive plant-selectable marker, as well as an increased range of restriction sites available for use in Southern analysis of transgenic plant developed from these vectors. Furthermore, the plasmids may also have been used as promoter-tagging vectors and they contained features that made them amenable to plasmid rescue of plant genomic DNA flanking the right border. These included a reduction (20.5%) from 7.8 kb in pBIN19/GTG to 6.2 kb in pANDY6 (and its derivatives) in the amount of T-DNA required to be rescued with plant genomic DNA. This was due to resiting the bacterial selectable marker and pBR322 *oriV* located in the T-DNA, to a position immediately adjacent to the promoterless *gusA*, when constructing pANDY6 (Section 3.1.2, p. 68). The addition of the mcs-P_{35S}-*nptII* fusion also increased the range of restriction enzymes available for plasmid rescue. The original promoter-tagging vector, pBIN19/GTG only had the enzymes *Sac*I and *Kpn*I available for plasmid rescue (Section A6.1, p. 176), whereas pANDY8, pANDY9 and pANDY10 had *Sac*I, *Kpn*I, *Sph*I, *Xba*I, and *Hin*dIII (Section A6.12, p. 187).

3.7 *OVERDRIVE* AND PLANT TRANSFORMATION

3.7.1 *N. tabacum* Transformation Experimental Design

A *Nicotiana tabacum* leaf disc transformation protocol (Section 2.3.9, p. 57) was quantified to determine what influence, if any, deletions in the putative nopaline-type *overdrive* had upon transformation frequency. The parameters assayed were based upon observations made during the course of transgenic *N. tabacum* production, where it was observed that leaf discs produced discrete calli, of which a subset of calli produced chlorophyll, and of these, a further subset became organogenic and developed shoots. Therefore, the transformation parameters measured were: the total number of discrete calli produced per leaf disc; the number of these calli per leaf disc that produced chlorophyll; and the number of green calli per leaf disc that became organogenic and produced viable, putatively transgenic shoots. Shoot viability was determined by ability to produce roots in a kanamycin-containing selective Nic III-medium (Section 2.3.9, p. 57). Transformation frequency was, therefore, determined by the number of organogenic calli.

The vectors, pANDY8, pANDY9, and pANDY10, harboured by *A. tumefaciens* strain LBA4404 (Section 3.3.4, p. 97), were used to transform 30 freshly cut *N. tabacum* leaf discs each, as described (Section 2.3.9, p. 57). To reduce variation between treatments caused by differences in leaf material, the leaf discs were randomly divided into three groups, one for each vector treatment. Immediately after removing excess inoculum, each set of 30 leaf discs exposed to a particular vector was randomly divided into three replicates of 10 individually numbered leaf discs. Due to the highly variable number of calli, and subsequent green and organogenic calli produced on any one leaf disc, the parameters measured per leaf disc were collated within each replicate, and expressed as a total per 10 leaf discs. Parameter measurement began after completion of the cocultivation period, when the discs were placed on a selective medium (Nic II) (Section 2.3.9, p. 57), and each leaf disc was scored for the parameters every three days over a 60 day period.

3.7.2 *Overdrive* and Callus Production in *N. tabacum*: a Time-Course

For all three vector treatments, the average number of calli/10 leaf discs (derived from the three replicates within each treatment) was plotted against time on the same graph (Fig. 20, p. 102). Generally, calli appeared between 6 and 9 days after cocultivation, then rapidly increased in number within the first 20 days, after which production of new callus slowed, and in all three treatments had ceased 39 days after cocultivation.

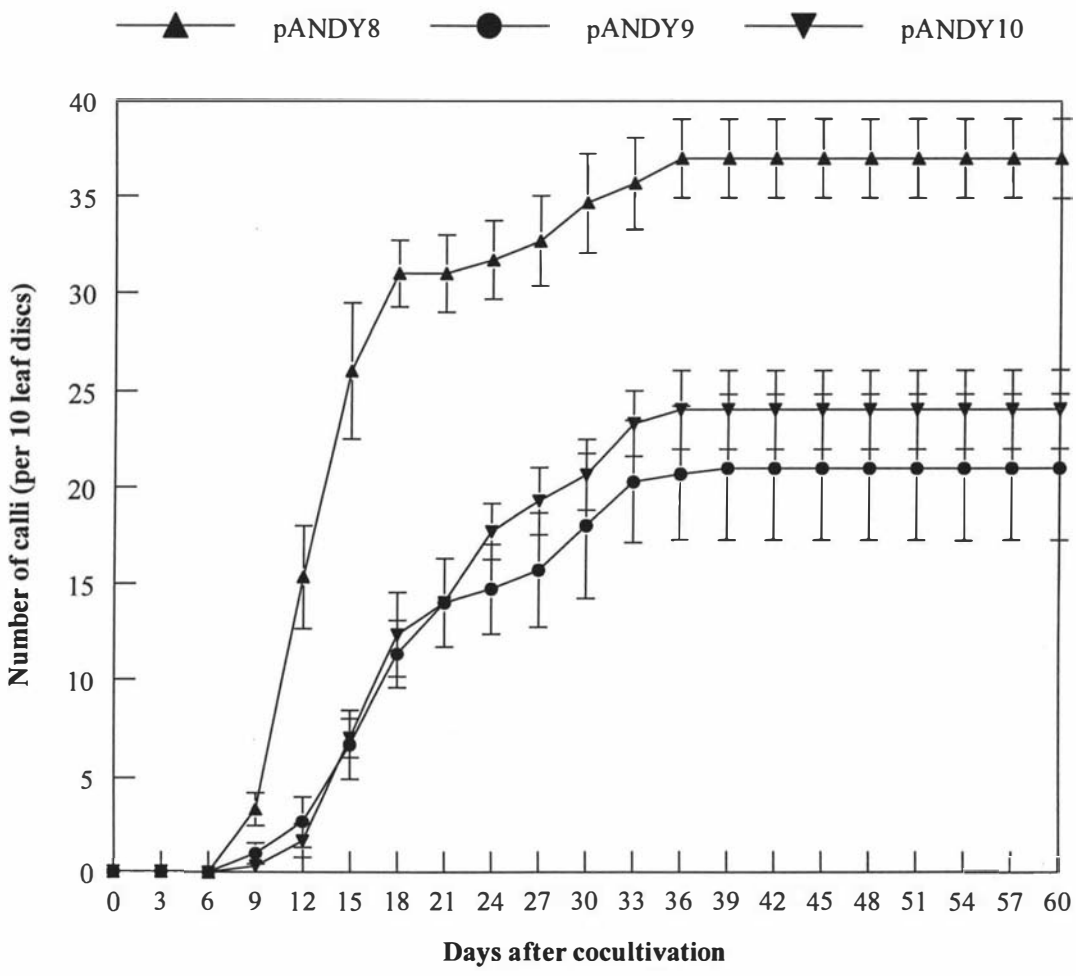

Error bars represent ±SEM of values calculated from three measurements.

Figure 20. Deletions in the putative nopaline-type *overdrive* region of plant transformation vectors, and their influence upon mean cumulative callus production (calli per 10 leaf discs) plotted against time (days after cocultivation).

Data presented in Figure 20 (p. 102) revealed that, when harboured by the octopine-type *A. tumefaciens* strain LBA4404, deletions in the putative nopaline-type *overdrive* region of the plant transformation vectors, influenced cumulative callus production significantly. *Nicotiana tabacum* leaf discs exposed to pANDY8 (intact putative nopaline-type *overdrive* region) produced callus rapidly between days 6 and 18 after cocultivation (26.0 calli/10 leaf discs), then slowed, finally ceasing by day 36, having produced a final average of 37.0 calli/10 leaf discs. However, leaf discs exposed to either pANDY9 (15 bp deletion of the putative nopaline-type *overdrive* core) or pANDY10 (36 bp deletion of the putative nopaline-type *overdrive* core) developed calli less rapidly, producing only 11.33 and 12.33 calli/10 leafs discs, respectively, by day 18, before slowing and ceasing by day 39, having produced an average of 21 and 24 calli/10 leaf discs, respectively. Hence, deletions in the putative nopaline-type *overdrive* region reduced final callus production by 40%. Furthermore, the 15 bp deletion of the putative nopaline-type *overdrive* core (pANDY9) and the 36 bp deletion (pANDY10) were equally influential upon callus production, as their effects were statistically indistinguishable (Fig. 20, p. 102).

3.7.3 The *overdrive* and Production of Callus, Green Callus, and Organogenic Callus in *N. tabacum*

Upon completion of the 60 day time course, the effects of deletions in the putative nopaline-type *overdrive* on total production of calli, green calli, and organogenic calli, were compiled and are presented in Figure 21 (p. 105). Deletions in the putative nopaline-type *overdrive* region led to a 40% decrease in both the total calli produced (per 10 leaf discs) (37.0 for pANDY8, to 11.33 and 12.33 for pANDY9 and pANDY10, respectively), and the total number of calli that greened (29.7 for pANDY8, to 18.0 and 19.0 for pANDY9 and pANDY10, respectively). The deletions, however, led to a 47% decrease in transformation frequency, as determined by the number of organogenic calli (per 10 leaf discs) (13.3 for pANDY8 to 7.3 and 7.0 for pANDY9 and pANDY10, respectively). As with the time-course of callus production in *N. tabacum* (Section 3.7.2, above), the influence of the plant transformation vectors with deletions in the putative nopaline-type *overdrive* were statistically indistinguishable, indicating that the 15 bp deletion of the putative nopaline-type *overdrive* core (pANDY9) was as influential upon callus production and transformation frequency as the 36 bp deletion (pANDY10).

Presented in Figure 22 (p. 105), is the proportion of calli that became green (%), and the proportion of green calli that became organogenic and produced shoots (%). Although deletions in the putative nopaline-type *overdrive* region reduced callus

Figure 21. Deletions in the putative nopaline-type *overdrive*, and their influence upon the production of callus, green callus, and organogenic callus (transformation frequency), after a 60 day cultivation period on a selective medium.

Figure 22. Deletions in the putative nopaline-type *overdrive*, and their influence upon the proportion (%) of *N. tabacum* calli that became green, and the proportion (%) of green calli that became organogenic, after a 60 day cultivation period on a selective medium.

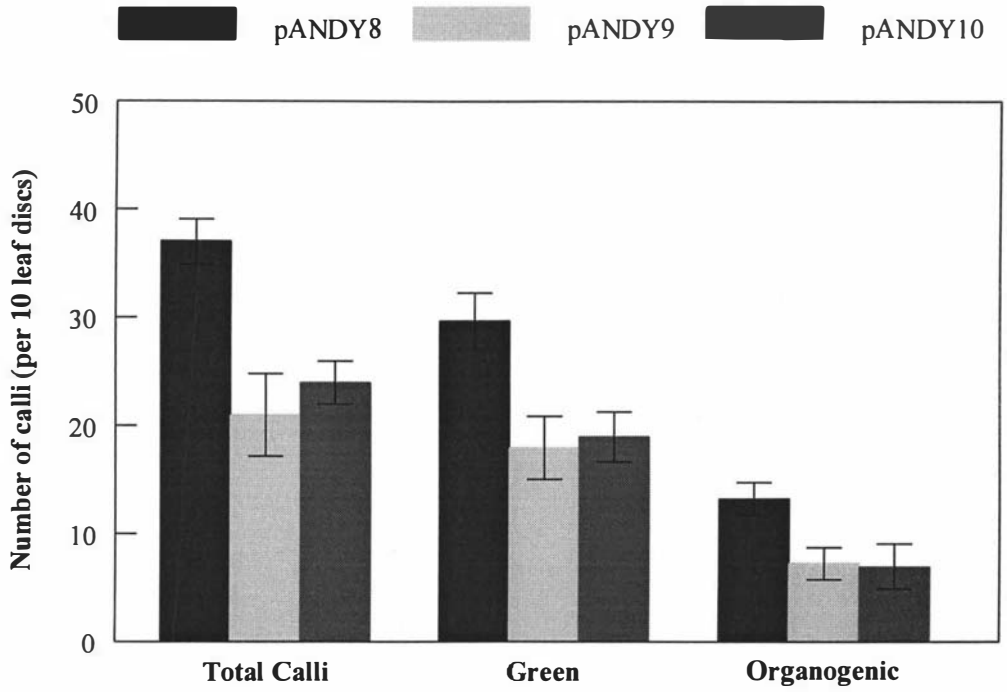

Error bars represent ±SEM of values calculated from three measurements

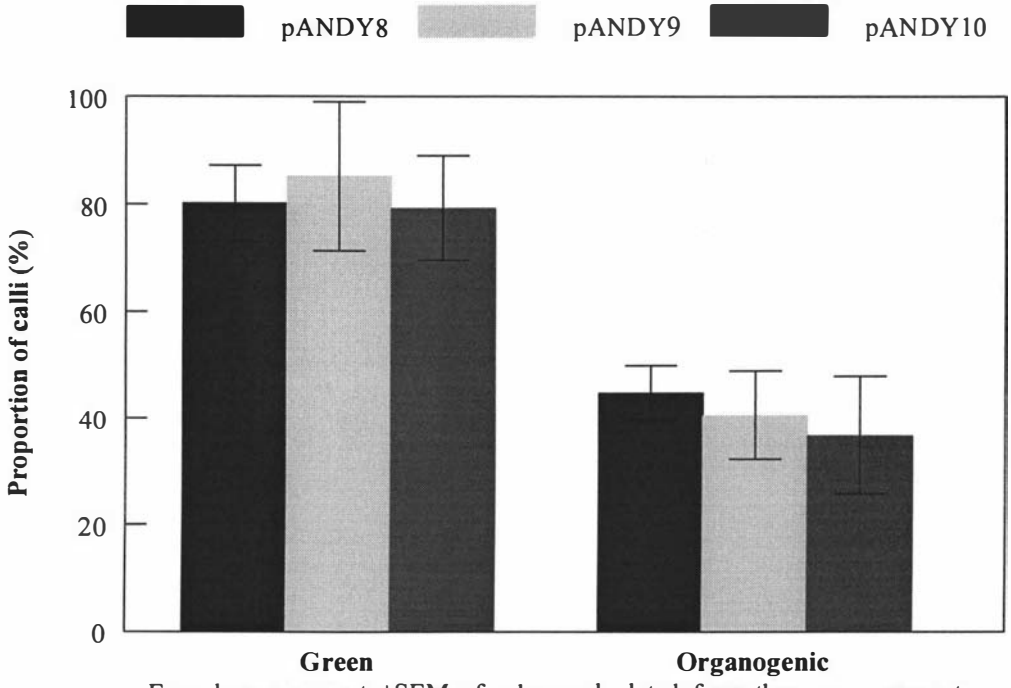

Error bars represent ±SEM of values calculated from three measurements

production, hence transformation frequency (Fig. 21, p. 105), there was, however, no effect on either the proportion of calli that greened (approximately 80% in each vector treatment) or the proportion of green calli that became organogenic (approximately 40% in each vector treatment) (Fig. 22, p. 105). This indicates that, unlike callus production, the process of regeneration and shoot production in *N. tabacum* on a selective medium was unaffected by deletions in the putative *overdrive* region.

3.7.4 *Overdrive* and Other Strains of *A. tumefaciens*

To determine if the observed differences in the transformation frequency generated by the pANDY8-10 vector series were not due to some intrinsic interaction between *N. tabacum* and the *A. tumefaciens* strain, LBA4404, the vector series was transferred to MOG1010 (Section 3.3.4, p. 97), an octopine-type *A. tumefaciens* strain of different chromosomal background to that of LBA4404 (Table 1, p. 38). The vectors, harboured by LBA4404 and MOG1010, were used to transform 30 *N. tabacum* leaf discs each, as described (Section 2.3.9, p. 57). To reduce variation between treatments caused by differences in leaf material, the leaf discs were randomly divided into six groups, one for each vector in LBA4404 and MOG1010. The relationship between deletions in the putative nopaline-type *overdrive* and transformation frequency of *N. tabacum* was very similar in both LBA4404 (Fig. 23A-C, p. 108) and MOG1010 (Fig. 24A-C, p. 110). In LBA4404, removal of the putative nopaline-type *overdrive* core resulted in a 47% reduction in transformation frequency (13.3 organogenic calli per 10 leaf discs reduced to 7.3 and 7.0 for pANDY8, pANDY9, and pANDY10, respectively) (Fig. 24D, p. 110a), and in MOG1010, removal of the putative core resulted in a 40% transformation frequency reduction (14.7 organogenic calli per 10 leaf discs reduced to 8.7 and 9.0 for pANDY8, pANDY9, and pANDY10, respectively).

3.7.5 *Overdrive* and *vir* Environment

To determine whether the relationship between deletions in the putative nopaline-type *overdrive* and plant transformation frequency was influenced by the *vir* gene-product environment, the plasmid series was transferred to GV3101 (Section 3.3.4, p. 97), a disarmed nopaline-type *A. tumefaciens* strain. The strains LBA4404 and GV3101 harbouring the vector series pANDY8-10 were used to transform 30 *N. tabacum* leaf discs each, as described (Secton 2.3.9 p. 57). To reduce variation between treatments caused by differences in leaf materal, the leaf discs were randomly divided into replicates of 10 leaf discs, and there were three replicates for each vector in LBA4404 and GV3101. In the octopine-type *vir* environment (LBA4404), there was a 48% decrease in transformation frequency (21.7, 11.3, and 10.3 organogenic calli per 10

Figure 23A-C. Deletions in the putative nopaline-type *overdrive* region of the plant transformation vectors (pANDY8-10), and their influence upon callus production in *N. tabacum*, when harboured by LBA4404.

A. Callus production in *N. tabacum* leaf discs that had been inoculated with *A. tumefaciens* strain LBA4404 harbouring pANDY8, and cultivated on a selective medium for 21 days.

B. Callus production in *N. tabacum* leaf discs that had been inoculated with *A. tumefaciens* strain LBA4404 harbouring pANDY9, and cultivated on a selective medium for 21 days.

C. Callus production in *N. tabacum* leaf discs that had been inoculated with *A. tumefaciens* strain LBA4404 harbouring pANDY10, and cultivated on a selective medium for 21 days.

A.

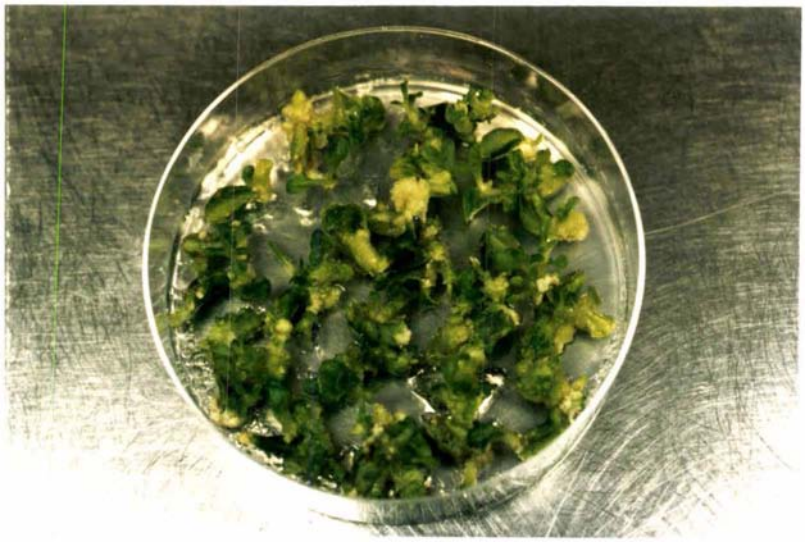

B.

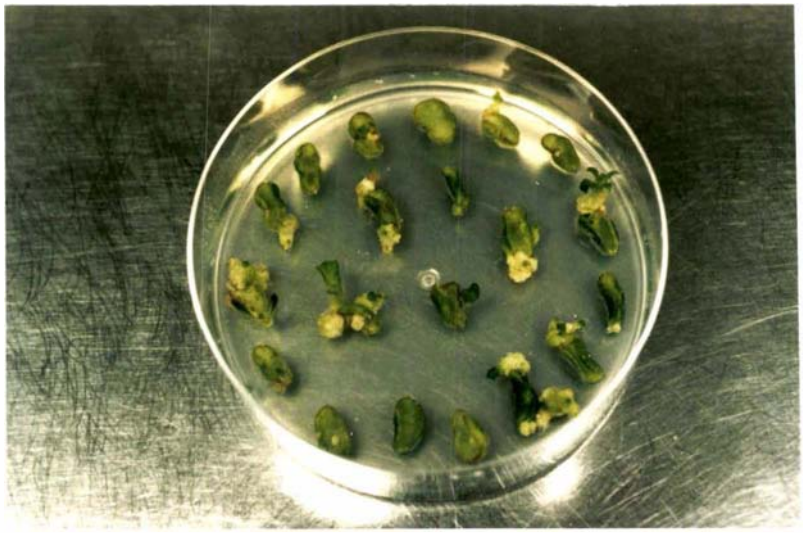

C.

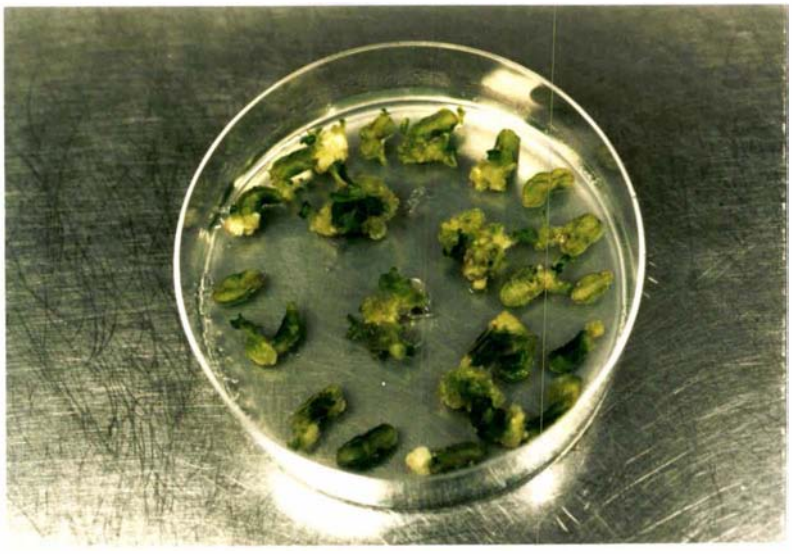

Figure 24A-C. Deletions in the putative nopaline-type *overdrive* region of the plant transformation vectors (pANDY8-10), and their influence upon callus production in *N. tabacum*, when harboured by MOG1010.

A. Callus production in *N. tabacum* leaf discs that had been inoculated with *A. tumefaciens* strain MOG1010 harbouring pANDY8, and cultivated on a selective medium for 21 days.

B. Callus production in *N. tabacum* leaf discs that had been inoculated with *A. tumefaciens* strain MOG1010 harbouring pANDY9, and cultivated on a selective medium for 21 days.

C. Callus production in *N. tabacum* leaf discs that had been inoculated with *A. tumefaciens* strain MOG1010 harbouring pANDY10, and cultivated on a selective medium for 21 days.

A.

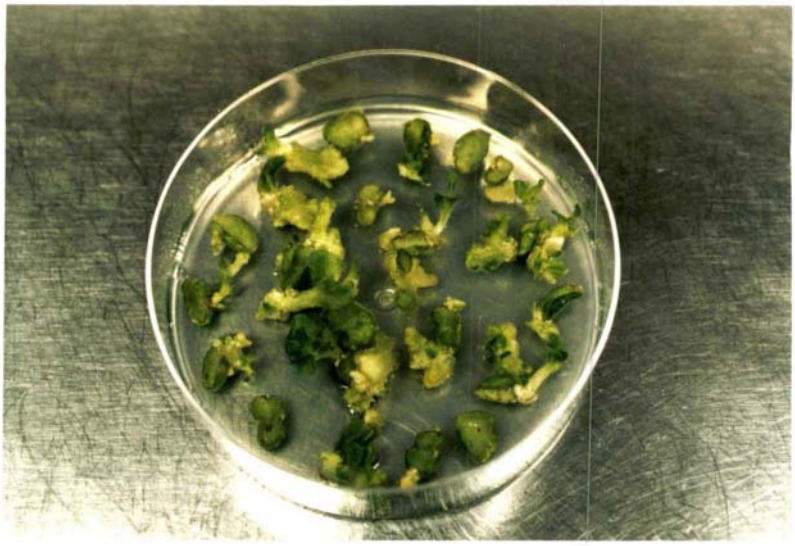

B.

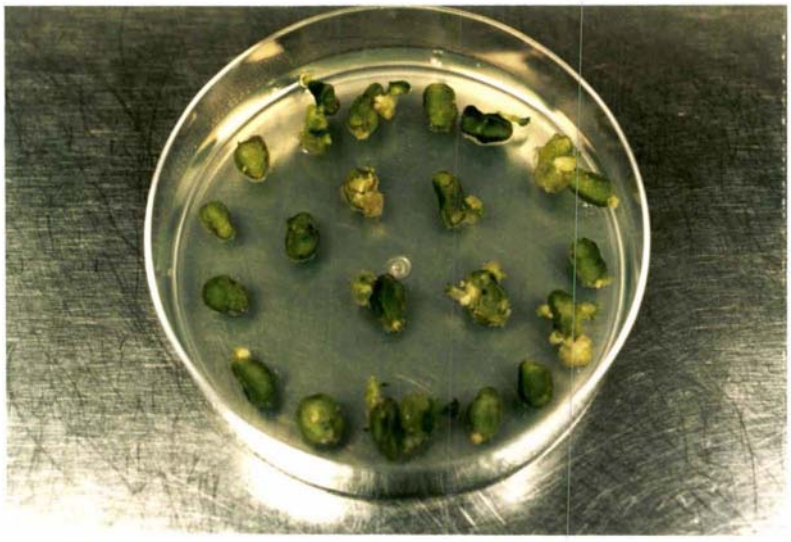

C.

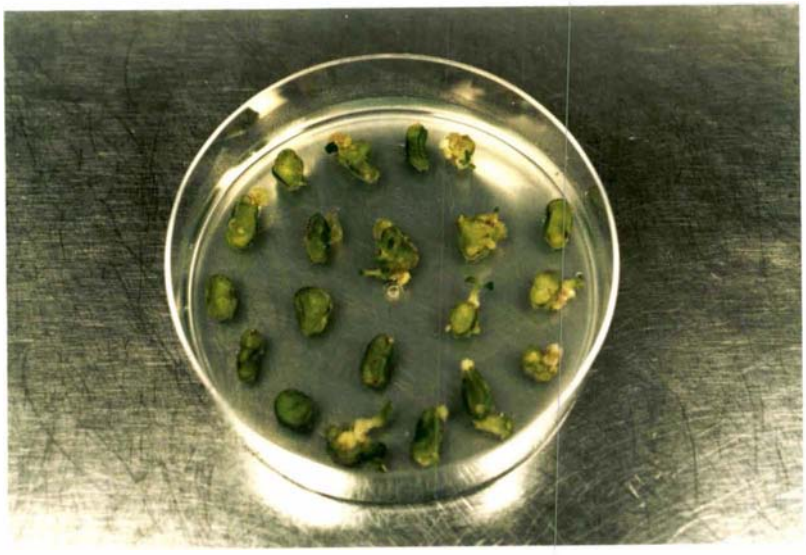

Figure 24D-F. Deletions in the putative nopaline-type *overdrive* region of the plant transformation vectors (pANDY8-10), and their influence upon callus production in *N. tabacum*, when harboured by LBA4404, MOG1010, GV3101, and MOG1010-C.

D. Influence of deletions in the putative nopaline-type *overdrive* upon *N. tabacum* transformation frequency (organogenic calli per 10 leaf discs) in octopine-type *A. tumefaciens* strains LBA4404 and MOG1010. Transformation frequency was determined after 60 days cocultivation on a selective medium.

Error bars represent ±SEM of values calculated from three measurements.

E. Influence of deletions in the putative nopaline-type *overdrive* upon *N. tabacum* transformation frequency (organogenic calli per 10 leaf discs) in an octopine-type *A. tumefaciens* strain (LBA4404) and a nopaline-type strain (GV3101). Transformation frequency was determined after 60 days cocultivation on a selective medium.

Error bars represent ±SEM of values calculated from three measurements.

F. Influence of deletions in the putative nopaline-type *overdrive* upon *N. tabacum* transformation frequency (organogenic calli per 10 leaf discs) in octopine-type *A. tumefaciens* strains with a wild-type *vir* regulon (MOG1010) and a *virC2* mutation (MOG1010-C). Transformation frequency was determined after 60 days cocultivation on a selective medium.

Error bars represent ±SEM of values calculated from either three measurements (MOG1010) or six measurements (MOG1010-C).

D.

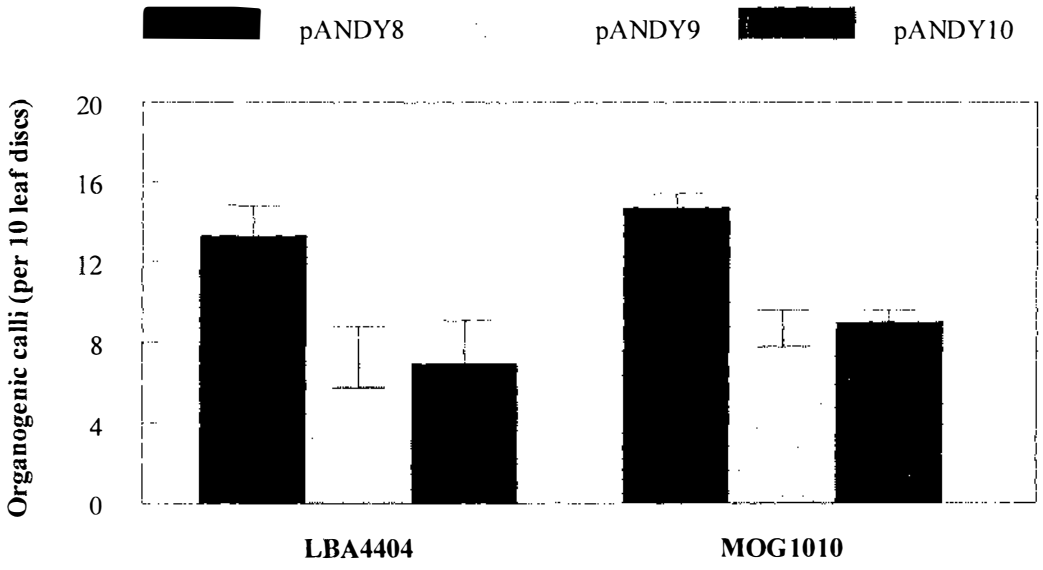
pANDY8
pANDY9
pANDY10
Organogenic calli (per 10 leaf discs)
20
16
12
8
4
0
LBA4404
MOG1010

E.

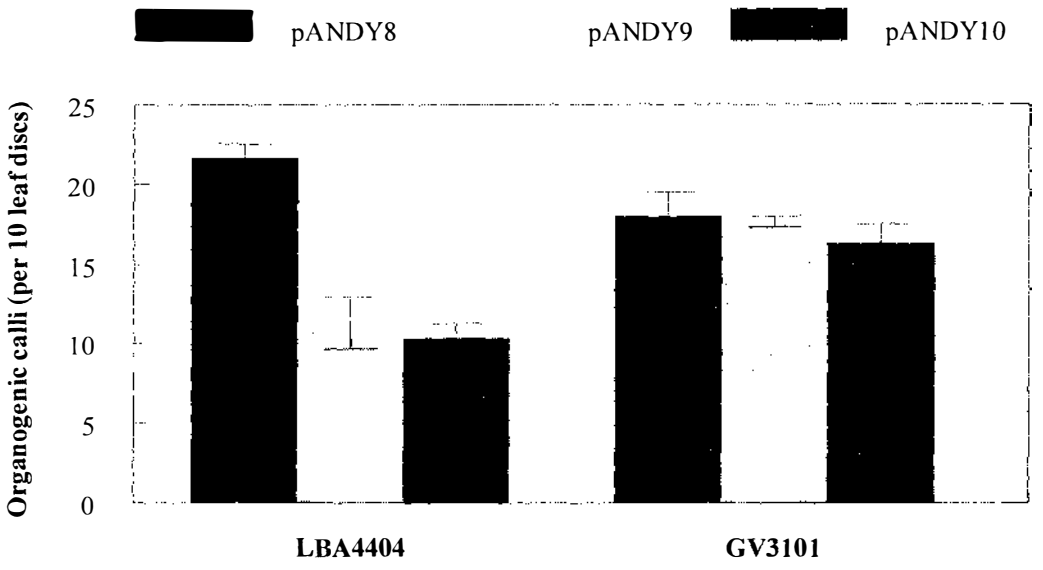
pANDY8
pANDY9
pANDY10
Organogenic calli (per 10 leaf discs)
25
20
15
10
5
0
LBA4404
GV3101

F.

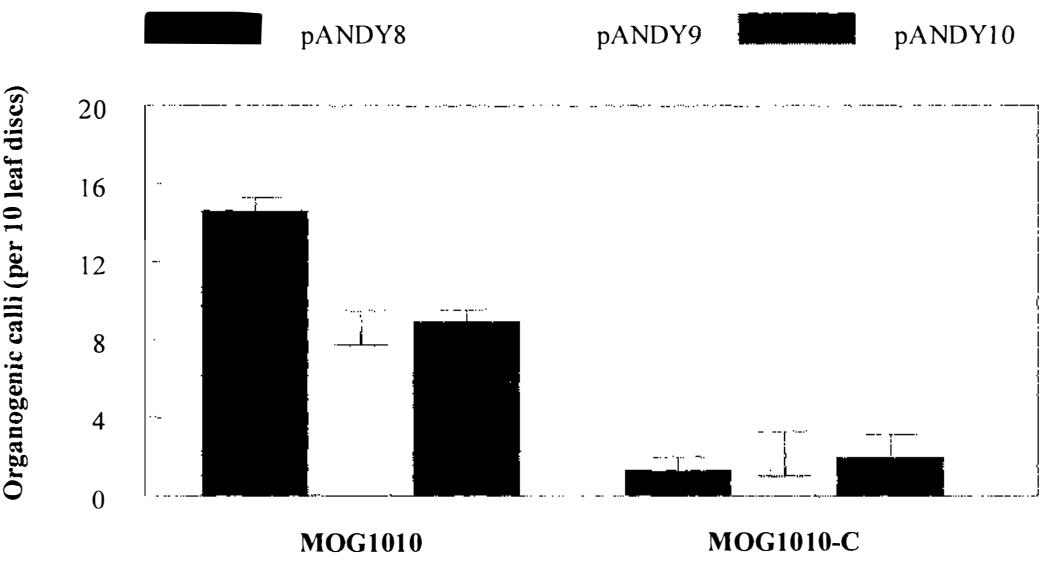
pANDY8
pANDY9
pANDY10
Organogenic calli (per 10 leaf discs)
20
16
12
8
4
0
MOG1010
MOG1010-C

leaf discs for pANDY8, pANDY9, and pANDY10, respectively) upon removal of the putative nopaline-type *overdrive* core (Fig. 24E, p. 110a). In the nopaline-type *vir* environment (GV3101), however, deletions in the putative nopaline-type *overdrive* core had no statistically significant influence upon transformation frequency (18.0, 18.7, and 16.3 organogenic calli per 10 leaf discs for pANDY8, pANDY9 and pANDY10, respectively) (Fig. 24E, p. 110a).

3.7.6 *Overdrive* and the *virC* Operon

As described (Section 1.4.5, p. 29), there is an intimate interaction between the *virC* operon and *overdrive*. To help determine whether the putative nopaline-type *overdrive* behaved as an *overdrive* with respect to the *virC* operon, the plasmid series pANDY8-10 was transferred to an octopine-type *A. tumefaciens virC1* mutant strain (A1021) and an octopine-type *virC2* mutant strain (MOG1010-C) (Section 3.3.4, p. 97). The vectors harboured by A1021 and MOG1010-C were then used to transform 60 *N. tabacum* leaf discs each as described (Section 2.3.9, p. 57). The 60 leaf discs for each plasmid were randomly divided into six replicates, each containing ten discs. The octopine-type strain MOG1010 provided a wild-type *vir* operon control and each of the pANDY8-10 series harboured by MOG1010 were used to transform 30 *N. tabacum* leaf discs as described (Section 2.3.9). The 30 leaf discs for each plasmid were randomly divided into three replicates of ten leaf discs. In the wild-type *vir* regulon strain, MOG1010, deletions in the putative nopaline-type *overdrive* resulted in a 40% reduction in plant transformation frequency (14.7, 8.7, and 9.0 organogenic calli per 10 leaf discs for pANDY8, pANDY9, and pANDY10, respectively) (Fig. 24F, p. 110a). In the MOG1010 *virC2* mutant strain (MOG1010-C), however, deletions in the putative nopaline-type *overdrive* core had no detectable influence upon transformation frequency (Fig. 24F). Furthermore, the transformation frequency was reduced significantly in MOG1010-C, an average of 87.5% less than the intact putative *overdrive* (pANDY8) in MOG1010. In contrast, not a single organogenic callus (or any calli) was produced by the pANDY8-10 series when harboured by the *virC1* mutant strain A1021, hence it appeared to be an avirulent strain (data not presented).

3.7.7 *Overdrive* and *Arabidopsis thaliana*

To determine if the relationship between deletions in the putative nopaline-type *overdrive* region and plant transformation was not restricted to *N. tabacum*, the transformation experiments were performed with an unrelated plant species, *Arabidopsis thaliana*. The vectors pANDY8, pANDY9, and pANDY10, harboured by *A. tumefaciens* strain LBA4404, were used to transform *A. thaliana* root material, as described (Section 2.3.8, p. 56). When using the *A. thaliana* transformation, it was

difficult to quantify transformation parameters (such as callus production), on a per unit of explant basis, as the explant source was a mass of chopped root material (Section 2.3.8). This, in turn, made it difficult to quantify the influence of deletions in the putative nopaline-type *overdrive* region on transformation frequency, hence visual observations only were made.

Deletions in the putative nopaline-type *overdrive* did influence callus production in *Arabidopsis thaliana*, as can be seen in Figure 25A-C (p. 113). Root explants exposed to pANDY8 (intact putative nopaline-type *overdrive* region) produced noticeably more organogenic calli after three weeks on a selective medium (Fig. 25A, p. 113), than root explants exposed to either pANDY9 (15 bp deletion of the putative nopaline-type *overdrive* core) (Fig. 25B, p. 113), or pANDY10 (36 bp deletion of the putative nopaline-type *overdrive* core) (Fig. 25C, p. 113). Although difficult to quantify, it appears that both deletions in the putative nopaline-type *overdrive* region (pANDY9 and pANDY10) had similar effects on callus production (Fig. 25B-C).

Figure 25A-C. Deletions in the putative nopaline-type ***overdrive*** region of the plant transformation vectors (pANDY8-10), and their influence upon callus production in ***Arabidopsis thaliana***, when harboured by LBA4404.

A. Callus production in *A. thaliana* root explants that had been inoculated with *A. tumefaciens* strain LBA4404 harbouring pANDY8, and cultivated on a selective medium for three weeks.

B. Callus production in *A. thaliana* root explants that had been inoculated with *A. tumefaciens* strain LBA4404 harbouring pANDY9, and cultivated on a selective medium for three weeks.

C. Callus production in *A. thaliana* root explants that had been inoculated with *A. tumefaciens* strain LBA4404 harbouring pANDY10, and cultivated on a selective medium for three weeks.

A.

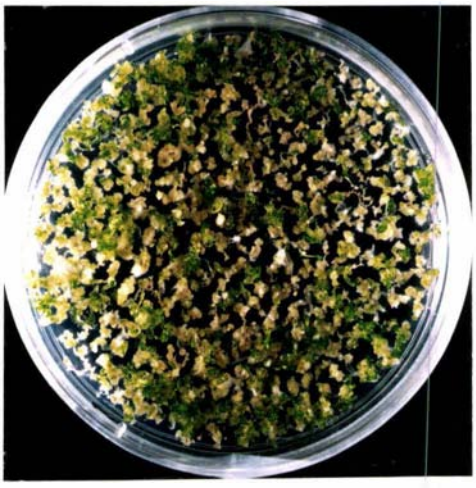

B.

C.

3.8 DETERMINING T-DNA COPY NUMBER IN *N. TABACUM*

Populations of *N. tabacum* plants transformed with either pANDY8, pANDY9, or pANDY10, were analysed to determine if deletions in the putative nopaline-type *overdrive* influenced the incidence of multiple T-DNA insertion events. T-DNA copy number was determined by Southern analysis of *N. tabacum* genomic DNA that had been digested to completion with restriction enzymes. [^{32}P]-radiolabelled probes were chosen to hybridise to regions near either the right or left borders of the integrated T-DNA.

3.8.1 Determining T-DNA Copy Number

The aim of this study was to determine the number of T-DNA insertion events that had occurred in the genome of each plant, rather than characterise the architecture of individual T-DNA. The *nptII* gene adjacent to the left border of the pANDY8-10 vector series T-DNA, was chosen for T-DNA copy number analysis on the basis that this gene was the plant selectable marker, and selection of transgenic plants on a medium containing kanamycin would ensure the presence of at least one intact copy of this gene. With this in mind, the T-DNA copy number of individual *N. tabacum* plants was determined by Southern analysis of *Hin*dIII-digested genomic DNA, as outlined (Fig. 26A-C, p. 115). When the DNA was digested with *Hin*dIII (Section 2.4.2, p. 58) and Southern blotted (Section 2.4.3, p. 59; or 2.4.4, p. 59) (Fig. 27, p. 117), T-DNA copy number was revealed by hybridisation (Section 2.4.7, p. 61; or 2.4.8, p. 62) with a [^{32}P]-radiolabelled 536 bp *nptII* probe (Section 2.4.5, p. 60) (Fig. 28, p. 118) that annealed to a portion of *nptII* near the left border (Fig. 26A). As *Hin*dIII cut once within the T-DNA, the number of bands in a lane was interpreted to indicate the number of T-DNA left border/plant DNA junctions, hence T-DNA insertions within an individual plant genome (Section A7, Tables 2 to 4, pp. 189-194).

In order to corroborate this data, a number of plants were selected at random for further analysis of the integrated T-DNA. Some Southern blots of *Hin*dIII digested genomic DNA that had been hybridised with the [^{32}P]-labelled *nptII* probe (described above), were stripped (Section 2.4.9, p. 62) and hybridised (see above) with a [^{32}P]-labelled 1.9 kb *gusA* gene (Section 2.4.5, p. 60) that hybridised to *gusA* adjacent to the right border of the T-DNA. In some cases *Eco*RI digested genomic DNA (see below) that had been probed with [^{32}P]-labelled *nptII* were stripped and reprobed with [^{32}P]-labelled *gusA*. With the exception of 11 plants, comprising 21.6% of the random sample evaluated (n=51), T-DNA copy number determined using the *gusA* right border probe yielded identical copy number results (Section A7, Tables 3 to 5, pp. 195-197). Given that rearrangements in T-DNA during transfer and integration are well

Figure 26A-C. Determining T-DNA copy number with *Hin*dIII digested plant genomic DNA.

A. A diagram of the 9 kb T-DNA region of pANDY8, pANDY9 and pANDY10. The numbers above the figure indicate the position of restriction sites within the T-DNA relative to the Right Border.

RB =right border; LB =left border; *gusA* =β-glucuronidase gene; *ocs*3′ =transcription termination sequence of octopine synthase gene; *bla* =β-lactamase gene; *oriV* =origin of replication; mcs-P_{35S}-*nptII* =a multiple cloning site from pUC18 attached to a P_{mas2}/P_{35S} dual promoter driving an *nptII* gene terminated by *ocs*3′ sequence; E =*Eco*RI site; H =*Hin*dIII site.

B. The presence of a single T-DNA in the plant genome is detected by digestion of genomic DNA with *Hin*dIII, an enzyme that cuts throughout the genome and only once within the T-DNA. To determine T-DNA copy number, a Southern blot of this digest was hybridised with a [^{32}P]-radiolabelled *nptII* probe homologous to the *nptII* gene adjacent to the T-DNA left border/plant DNA junction. Autoradiography of the blot will reveal a single band, as shown in the representative autoradiograph on the right of the figure. T-DNA copy number determined using an *nptII* probe may be corroborated using a [^{32}P]-radiolabelled *gusA* probe homologous to the *gusA* gene adjacent to the T-DNA right border/ plant DNA junction, as shown in the representative autoradiograph on the right of the figure. The bold wavy lines represent plant genomic DNA flanking the T-DNA insert.

H =*Hin*dIII site.

C. The presence of two T-DNA inserts in the plant genome is detected by digestion of genomic DNA with *Hin*dIII. Autoradiography of a Southern blot hybridised with either a [^{32}P]-radiolabelled *nptII* probe will reveal two bands. Representative autoradiograph are shown on the right of the figure. T-DNA copy number determined using an *nptII* probe may be corroborated using a [^{32}P]-radiolabelled *gusA* probe homologous to the *gusA* gene adjacent to the T-DNA right border/ plant DNA junction, as shown in the representative autoradiograph on the right of the figure.The bold wavy lines represent plant genomic DNA flanking the T-DNA insert. Three T-DNA copies, or more, may be detected with this process.

H =*Hin*dIII site.

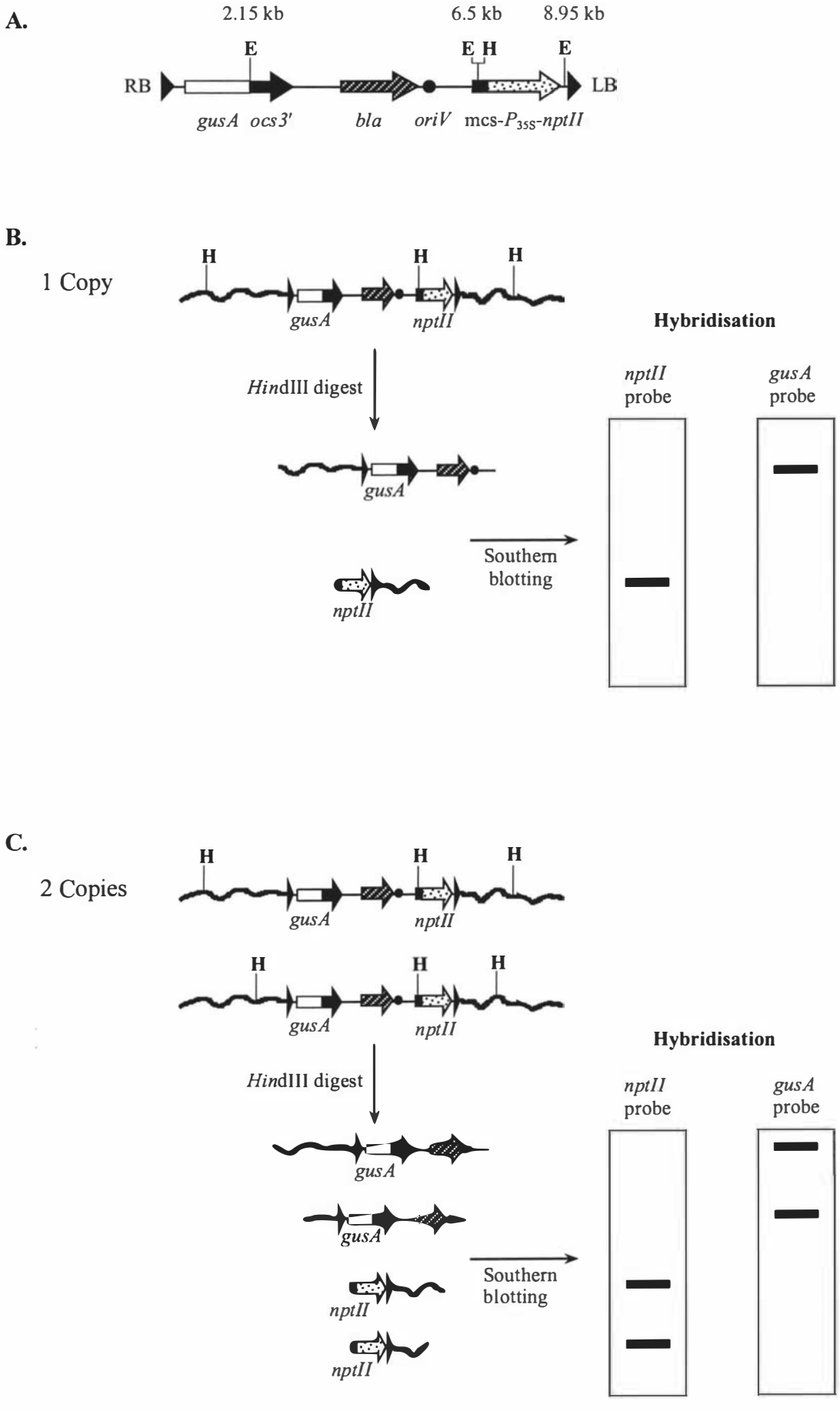
A.
2.15 kb
6.5 kb
8.95 kb
E
E H
E
RB
LB
gusA ocs3'
bla
oriV
mcs-P35S-nptII
B.
1 Copy
H
H
H
gusA
nptII
HindIII digest
gusA
nptII
Southern blotting
Hybridisation
nptII probe
gusA probe
C.
2 Copies
H
H
H
gusA
nptII
H
H
H
gusA
nptII
HindIII digest
gusA
gusA
nptII
nptII
Southern blotting
Hybridisation
nptII probe
gusA probe

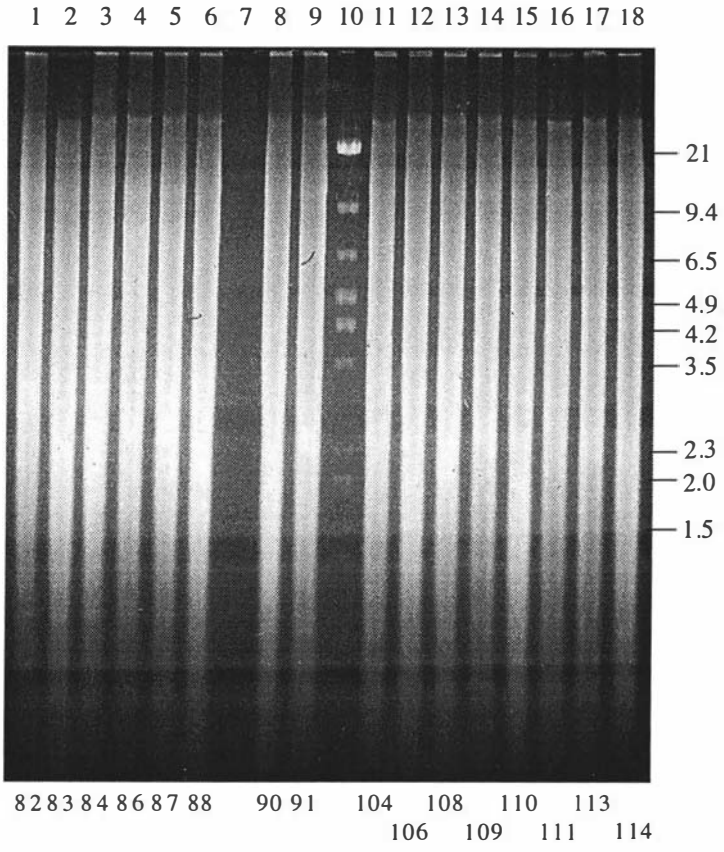

Figure 27. Representative *Hin*dIII digest of *N. tabacum* genomic DNA.

Genomic DNA extracted from *N. tabacum* plants transformed with one of the pANDY8-10 vector series, was digested with *Hin*dIII and resolved by electrophoresis through a 0.8% (w/v) agarose gel as described (Section 2.4.2, p. 59). Immediately after this photograph was taken, the DNA was transferred to nylon membrane as described (Section 2.4.3, p. 60). Numbers below the figure refer to the plant from which the DNA was extracted. Numbers on the right of the figure refer to the size (kb) of fragments generated by *Hin*dIII plus *Hin*dIII/*Eco*RI digested phage λ DNA (Section A4.10, p. 170) (lane 10).

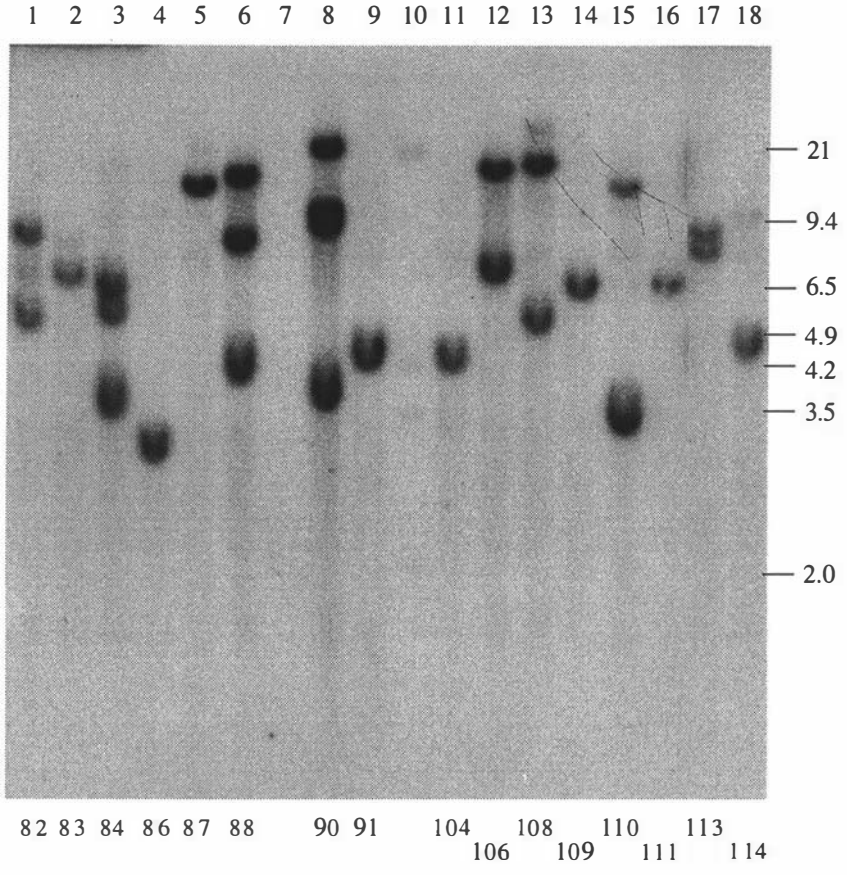

Figure 28. Representative autoradiograph of *Hin*dIII-digested *N. tabacum* genomic DNA hybridised with [^{32}P]-labelled *nptII* probe.

The Southern blot of the *Hin*dIII-digested *N. tabacum* genomic DNA shown in Figure 27 (p. 117) was hybridised with a [^{32}P]-labelled *nptII* probe as described (Section 2.4.8, p. 63). T-DNA copy number in each plant was determined by the number of bands which represent individual T-DNA left border/plant genomic DNA junctions. Numbers below the figure refer to the plant from which the DNA was extracted. Numbers on the right of the figure refer to the size (kb) of fragments generated by *Hin*dIII plus *Hin*dIII/*Eco*RI digested phage λ DNA (Section A4.10, p. 170) (lane 10).

documented (Deroles and Gardner, 1988b; Martineau *et al.*, 1994), evidence of occasional copy number discrepancies when using the *gusA* probe, compared to the *nptII* probe, was not unexpected. However, for the purpose of this study, the corroboration of copy number by the *gusA* probe demonstrated that detection of a left border T-DNA insertion using the *nptII* probe was regarded as a valid mechanism to determine T-DNA insertion events.

Incomplete digestion of genomic DNA is a major factor with the potential to distort accurate determination of T-DNA copies. Incomplete DNA digestion is primarily associated with DNA preparations which are heavily contaminated with proteins and carbohydrates known to inhibit restriction enzyme digestion (Fang *et al.*, 1993; Michaels *et al.*, 1994). The consequence of poor digestion using restriction enzymes is that T-DNA copy number is overestimated. To minimise the impact of poor digestion on the data set, a trial was conducted to determine which of a number of plant genomic DNA extraction methods procured the most reliably cutting DNA quickly. Furthermore, post-extraction purification steps, such as phenol/chloroform extraction or binding of DNA to glassmilk to remove potential contaminants, were also tested. The DNA preparations were extracted from the same plant (transformed with pANDY8), then Southern analysed by digestion with *Hin*dIII (Section 2.4.2, p. 58), blotting (Section 2.4.3, p. 59), and hybridisation (Section 2.4.7, p. 61) with a [^{32}P]-radiolabelled 536 bp *nptII* probe (Section 2.4.5, p. 60). As there were no differences in determination of T-DNA copy number when using the different extraction and post-extraction procedures (Data not presented), the CTAB method (Section 2.4.1, p. 58) was chosen since it allowed for rapid extraction of many samples in a given time period without compromising DNA quality.

As an internal control for complete digestion of genomic DNA, parallel digests of the analysed plants were made using *Eco*RI (Section 2.4.2, p. 58), which excised a 2.45 kb fragment containing the mcs-P_{35s}-*nptII* fusion from within the T-DNA (Fig. 29, p. 120). This fragment was detected by Southern blotting of the digests (Section 2.4.3, p. 59), and hybridisation (Section 2.4.7, p. 61) with a [^{32}P]-radioisotope labelled 536 bp *nptII* probe (Section 2.4.5, p. 60) (Fig. 30, 122). The presence of multiple bands in a lane indicated either incomplete digestion (often associated with unequal band hybridisation intensity), or corruption of *Eco*RI sites within the inserted T-DNA when more than one T-DNA was present (often associated with equal band hybridisation intensity). Single bands differing in size to that expected indicated a

Figure 29A-C. Determining completeness of genomic digestion using *Eco*RI.

A. A diagram of the 9 kb T-DNA region of pANDY8, pANDY9 and pANDY10. The numbers above the figure indicate the position of restriction sites within the T-DNA relative to the Right Border.

RB =right border; LB =left border; *gusA* =β-glucuronidase gene; *ocs*3′ =transcription termination sequence of octopine synthase gene; *bla* =β-lactamase gene; *oriV* =origin of replication; mcs-P_{35S}-*nptII* =a multiple cloning site from pUC18 attached to a $P_{mas2'}/P_{35S}$ dual promoter driving an *nptII* gene terminated by *ocs*3′ sequence; E =*Eco*RI site; H =*Hin*dIII site.

B. Digestion of *N. tabacum* genomic DNA containing the pANDY8-10 series T-DNA with *Eco*RI yields a 2.45 kb fragment containing the *nptII* gene. Autoradiography of a blot hybridised with [^{32}P]-labelled *nptII* probe, should reveal a single band of the correct size as shown should appear, as shown in the representative autoradiograph on the right of the figure. Multiple bands, particularly of different intensity, indicate partial digestion of the genomic DNA. Bands differing in size to that expected indicate corruptions in the T-DNA that have affected the size of the fragments, or the fidelity of the *Eco*RI site. T-DNA copy number may also be determined using a [^{32}P]-radiolabelled *gusA* probe homologous to the *gusA* gene adjacent to the T-DNA right border/ plant DNA junction, as shown in the representative autoradiograph on the right of the figure. The bold wavy lines represent plant genomic DNA flanking the T-DNA insert.

E =*Eco*RI site.

C. When two T-DNA inserts are present in the plant genome, hybridising Southern blots of *Eco*RI-digested genomic DNA with the *nptII* probe should still reveal a single 2.45 kb band upon autoradiography (as shown in representative autoradiograph on the right of the figure). As mentioned above, bands differing in size to that expected indicates possible corruption of the T-DNA. Multiple bands of equal intensity indicate that one or both T-DNA inserts are corrupt, whereas bands of unequal intensity represent possible partial genomic DNA digestion. T-DNA copy number may also be determined using a [^{32}P]-radiolabelled *gusA* probe homologous to the *gusA* gene adjacent to the T-DNA right border/ plant DNA junction, as shown in the representative autoradiograph on the right of the figure. Three or more T-DNA copies may be detected in this manner.

E =*Eco*RI site.

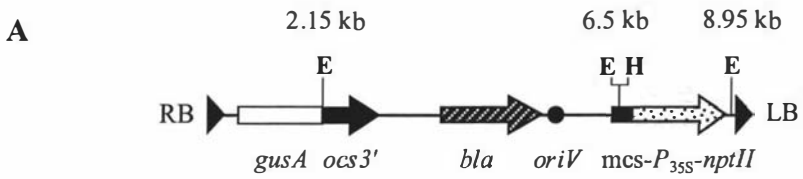
A
2.15 kb
6.5 kb
8.95 kb
E
E H
E
RB
LB
gusA ocs3'
bla
oriV
mcs-P35S-nptII

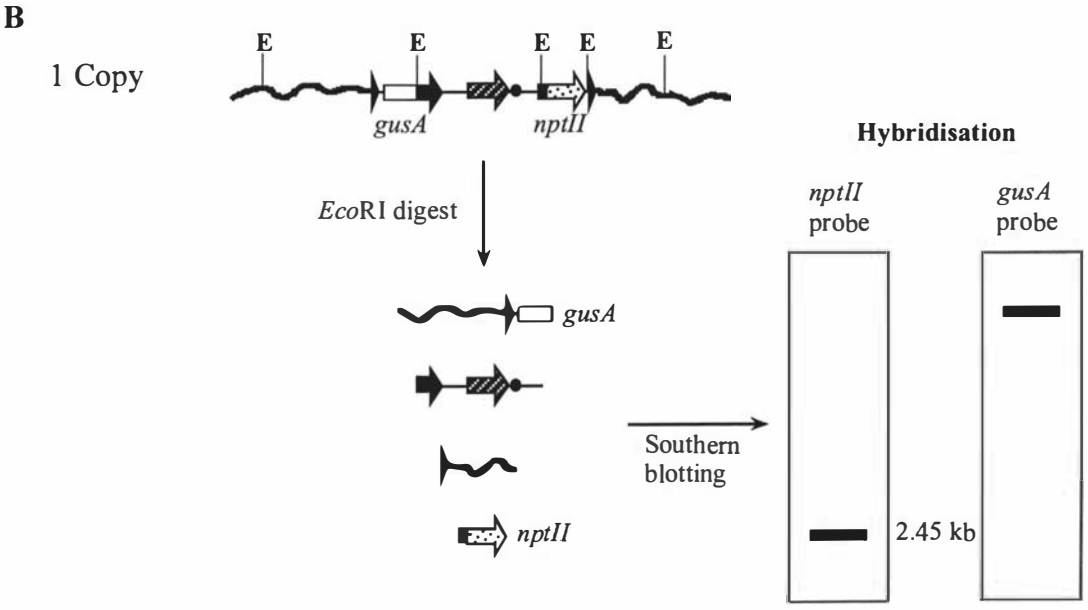
B
1 Copy
E E E E E
gusA
nptII
Hybridisation
EcoRI digest
nptII probe
gusA probe
gusA
nptII
Southern blotting
2.45 kb

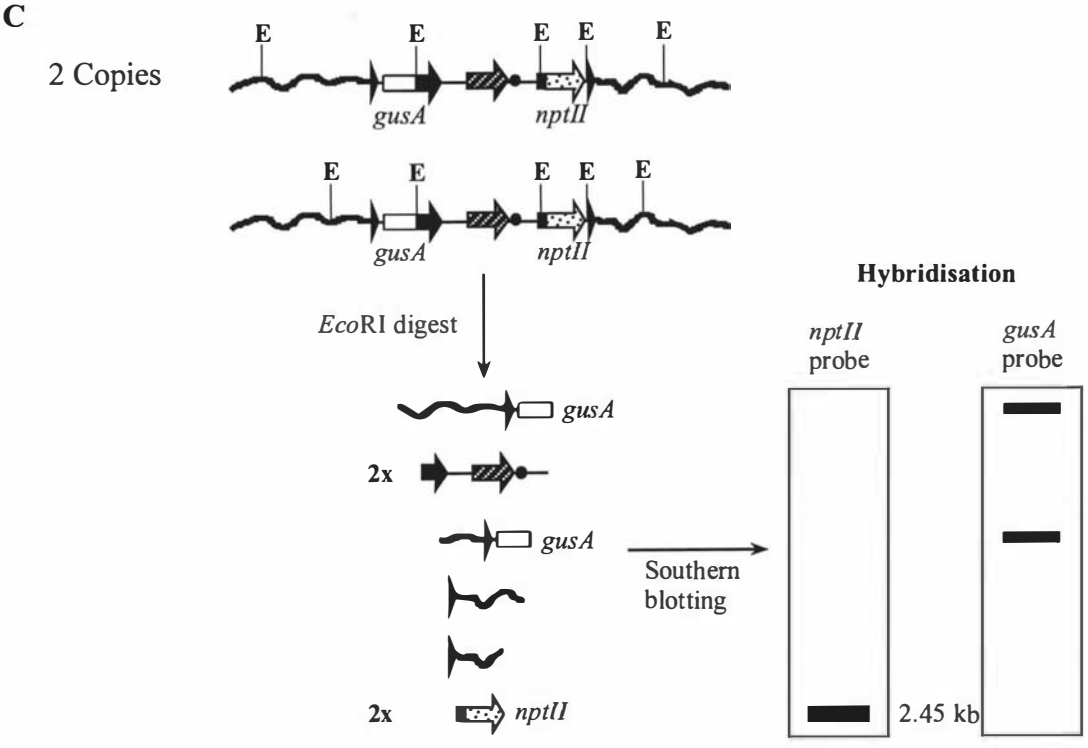
C
2 Copies
E E E E E
gusA
nptII
Hybridisation
EcoRI digest
nptII probe
gusA probe
2x
gusA
nptII
Southern blotting
2.45 kb

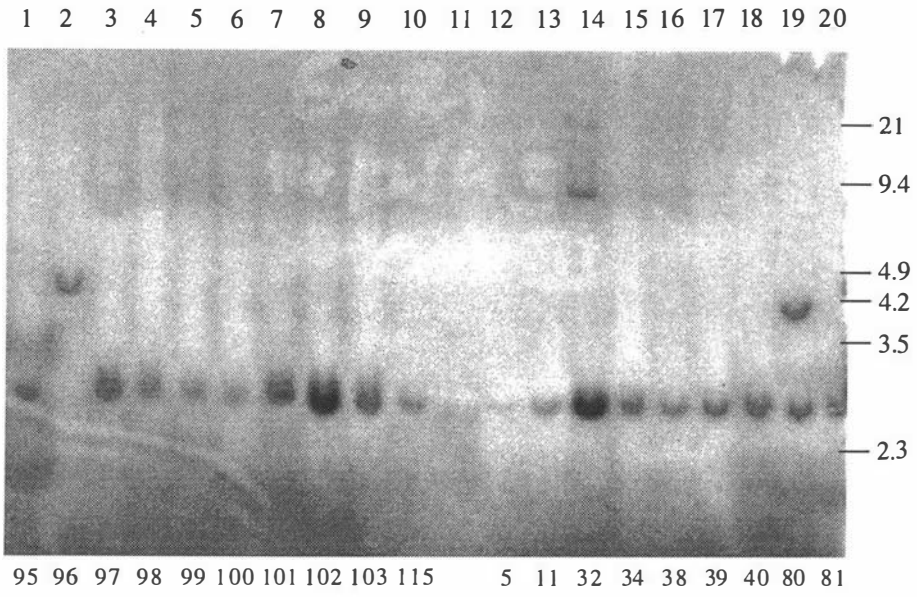

Figure 30. Representative autoradiograph of *Eco*RI-digested *N. tabacum* genomic DNA hybridised with [^{32}P]-labelled *nptII* probe.

A Southern blot of the *Eco*RI-digested *N. tabacum* genomic DNA was hybridised with a [^{32}P]-labelled *nptII* probe as described (Section 2.4.8, p. 63). The single band in each lane represents complete digestion of uncorrupted *Eco*RI sites. Numbers below the figure refer to the plant from which the DNA was extracted. Numbers on the left of the figure refer to the size of the *Eco*RI fragment containing the *nptII* gene as excised from the T-DNA. Numbers on the right of the figure refer to the size (kb) of fragments generated by *Hin*dIII plus *Hin*dIII/*Eco*RI digested phage λ DNA (Section A4.10, p. 170) (lane 11).

corruption of the T-DNA insert. Such abnormalities were observed in 32 of 143 plants tested (22.4%), and of these, 14 (9.8%) were suspected partial digests (Section A7, Tables 2 to 4, pp. 189-194).

3.8.2 T-DNA Copy Number

Deletions in the *overdrive* region halved the incidence of multiple T-DNA insertion events, as determined by Southern analysis using *nptII* left border probes (Fig. 31, p. 124). Of the population of *N. tabacum* plants generated by transformation with pANDY8, 34.7% contained two or more inserts, whereas of the population of plants generated by pANDY9 and pANDY10, only 12.2% and 14.3%, respectively, contained multiple inserts. A χ^2 test comparing the proportion of plants containing multiple inserts with those containing single inserts, within each population generated by each of the three vectors, proved to be significant ($P<0.01$). This demonstrated that deletions of the *overdrive* core influences the ratio of multiple to single T-DNA insertion events, significantly.

3.8.3 Spread of T-DNA Copy Number

Deletions in the *overdrive* region also affected the range of T-DNA copy numbers present in *N. tabacum*, as determined by Southern analysis with *nptII* left border probes. Of the 12.2% and 14.3% of plants generated by pANDY9 and pANDY10, respectively, that contained multiple T-DNA inserts, not one had more than two T-DNA copies (Fig. 32, p. 125). Of the population of plants generated from pANDY8, however, 16.7% contained two T-DNA copies, 12.5% three copies, and 5.6% four or more copies (Fig. 32). This relationship could not be assessed using the χ^2 test, as the *overdrive* core-deleted vectors had zero values for three and four or more T-DNA, which undermines the power of this analysis (Helen Dick, Statistician, personal communication).

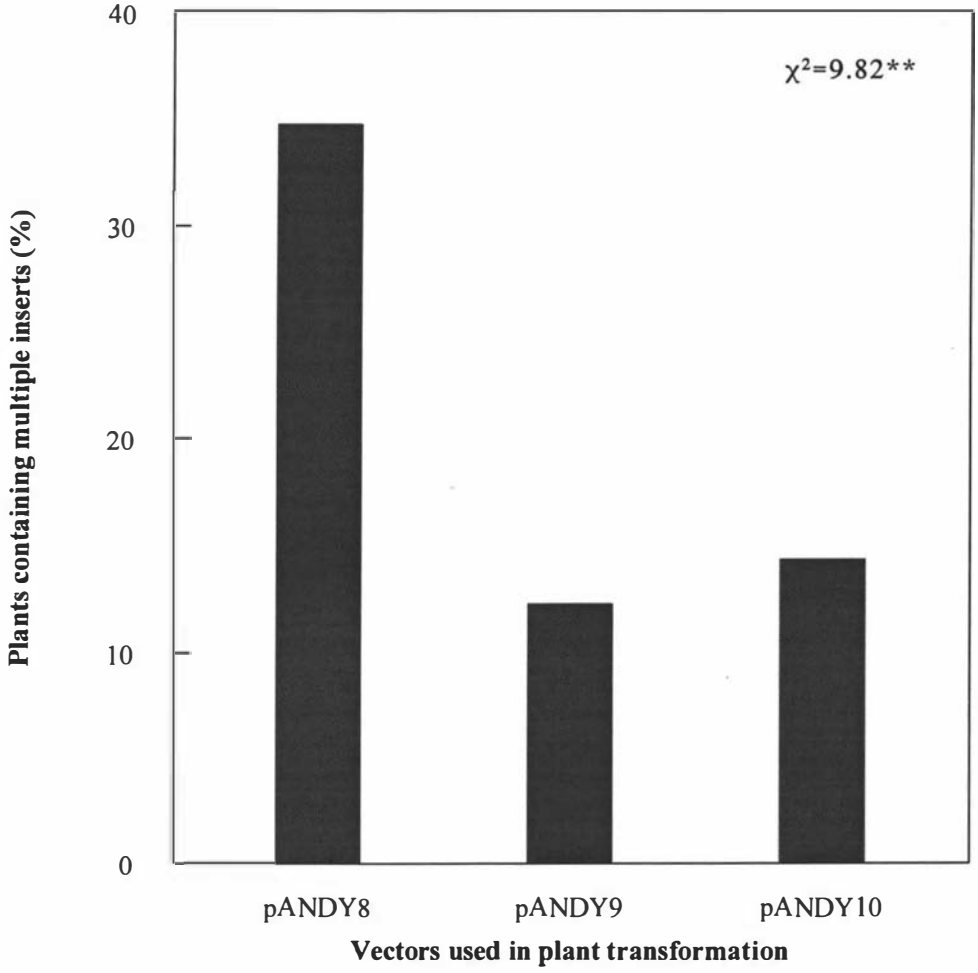

Figure 31. The effect of deletions in the *overdrive* region upon the incidence of multiple T-DNA insertion events in transgenic *N. tabacum.*

The T-DNA copy number in transgenic *N. tabacum* was determined by Southern analysis of *Hin*dIII digested genomic DNA hybridised with an *nptII*-containing [^{32}P]-radioisotope-labelled 536 bp *Nco*I/*Sph*I fragment of pANDY1 (Section A7.8, p. 183). The proportion of plants containing multiple T-DNA inserts was determined for each population of transgenic *N. tabacum* plants generated by transformation with either pANDY8, pANDY9, or pANDY10. A χ^2 test (df=2) performed on the data demonstrated that significantly fewer plants ($P<0.01$) generated from transformation with either pANDY9 or pANDY10 contained multiple T-DNA inserts (12.2% (n=49) and 14.3% (n=28), respectively) compared with those generated from pANDY8 (34.7% (n=72)).

df=degrees of freedom; ** =significant at the 1% level ($P<0.01$)

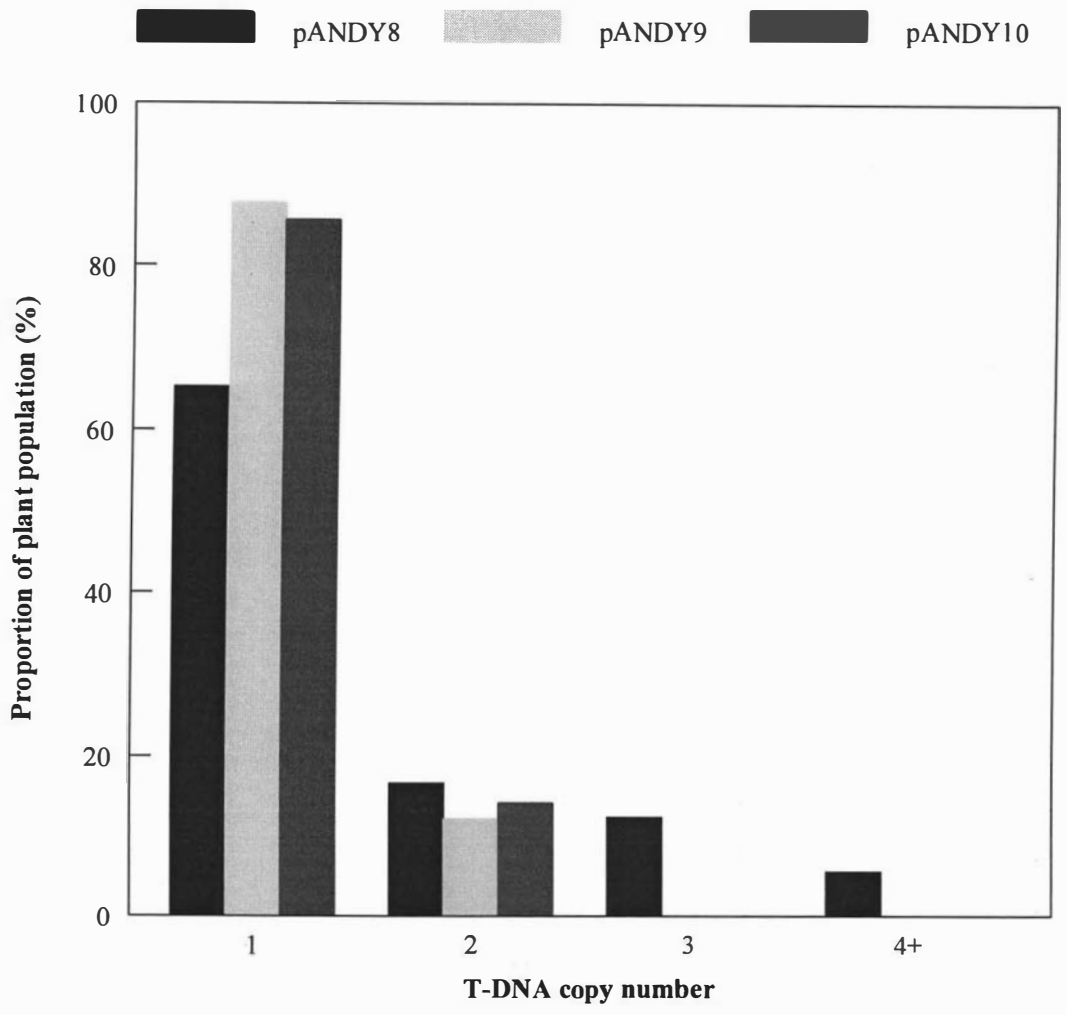

Figure 32. The effect of deletions in the *overdrive* region upon the range of T-DNA copy number in transgenic *N. tabacum.*

The data described in Figure 31 (p. 124) were further analysed to reveal the range of T-DNA copy numbers present in each population of plants generated by transformation with either pANDY8, pANDY9, or pANDY10. Of those plants generated by pANDY8 (n=72), 16.7% contained two T-DNA copies, 12.5% contained three copies and 5.6% contained four or more copies. Of those plants generated by pANDY9 (n=49) and pANDY10 (n=28), however, not one of the 12.2% and 14.3%, respectively, that contained multiple T-DNA inserts, contained more that two T-DNA copies.

CHAPTER 4 DISCUSSION

The *overdrive* consensus core proposed initially by Peralta *et al.* (1986), was identified by analysing conserved sequences adjacent to the right borders of an octopine, a nopaline-type Ti-plasmid, and an Ri-plasmid. Since then, however, *overdrive* consensus cores have been found adjacent to seven right borders in a total of five plasmids (Peralta *et al.*, 1986; Shurvinton and Ream, 1991) (Fig. 5, p. 32). Only one consensus core, that of the octopine-type pTiA6NC T_L-DNA *overdrive*, has thus far been analysed to determine if this sequence has a role in *overdrive*-activity. This core does have a role, as deletion of 15 bp containing the consensus core flanked by 5 bp (5′) upstream and 2 bp (3′) downstream, abolishes *overdrive* activity (Peralta *et al.*, 1986; Shurvinton and Ream, 1991) (Fig. 4 (step 3), p. 27).

In this Thesis, a second core region, that of the putative nopaline-type pTiT37 *overdrive*, was analysed. A series of binary vectors containing various deletions of this nopaline-type *overdrive* consensus core region was constructed. These plasmids were then used to test the influence of the putative nopaline-type *overdrive* core and its flanking sequences on both the frequency of transformation of *Nicotiana tabacum* and *Arabidopsis thaliana*, and the incidence of multiple T-DNA insertion events in *N. tabacum.*

4.1 ANALYSING THE PUTATIVE NOPALINE-TYPE *OVERDRIVE*

As detailed in the Introduction (Section 1.4.6, p. 31), tumourigenesis assays have provided much evidence of an *overdrive*-like T-DNA transmission enhancer near the right border of nopaline-type Ti-plasmids. Little clue has been provided, however, as to which sequences comprise the nopaline-type *overdrive*, as it has little homology with the octopine-type or other *overdrive* sequences (Fig. 5 (pTiT37), p. 32). Analyses of sequences near the nopaline-type right border have identified a region with 75% homology to the 8 bp *overdrive* consensus core (Peralta *et al.*, 1986; Wang *et al.*, 1987), but this is the only putative consensus core detected thus far that is not 100% homologous to that of the octopine-type *overdrive* core (Fig. 5). Furthermore, this putative nopaline-type core is located 76 bp away from the 3′ end of the right border, whereas the cores detected thus far in other plasmids (such as octopine-type and Ri-plasmids), are a maximum of 29 bp distant from the right border. There has been much debate as to the significance of this putative core sequence, yet this core is present in all the nopaline-type Ti-plasmid fragments exhibiting *overdrive*-like activity studied thus far. The smallest of these studied fragments is a 103 bp portion of the right border region (Culianez-Macia and Hepburn, 1988).

4.1.1 Identification of Regions Necessary for Function of the Putative Nopaline-type *Overdrive*

This study identified discrete sequences that may be involved in putative nopaline-type *overdrive* activity. The search for nopaline-type *overdrive* sequences was centred upon the only region of known homology to other *overdrive* regions, the putative consensus core. Deletions were made in the region of the putative consensus core in order to establish whether this sequence did indeed act, as had been proposed, as a T-DNA transmission enhancer (as determined by transformation frequency) (Culianez-Macia and Hepburn, 1988; Peralta *et al.*, 1986; Van Haaren *et al.*, 1988).

Of deletions made in the putative nopaline-type *overdrive* consensus core (Section 3.2.3, p. 73), two were selected for study in this Thesis. The first (in pANDY9; Section A6.12, p. 187) removed the putative consensus core plus an extra 3 bp (5′) upstream and 4 bp (3′) downstream. The second (in pANDY10; Section A6.12) encompassed the putative core and the entire region that would be the equivalent of the 24 bp octopine *overdrive* sequence, plus a further 10 bp. This second deletion was performed to determine to what degree the putative core alone influenced *overdrive*-like activity, as compared to the influence of the putative core plus its flanking sequences. Both the deletions of the putative core (pANDY9, pANDY10) decreased the rate at which calli appeared (Fig. 20, p. 102), and decreased the transformation frequency (as determined by the number of organogenic calli) by 47%, compared with that of the intact putative *overdrive* core (pANDY8) (Fig. 21, p. 105; Fig. 23, p. 108). The actual number of organogenic calli induced by the plasmids pANDY8, pANDY9 and pANDY10 varied between transformation experiments (compare the values for LBA4404, Fig. 24D and Fig. 24E, p. 110a). However, the proportional reduction in organogenic calli produced due to deletions in the putative *overdrive* core remained constant (47% and 48% for LBA4404, Fig. 24D and Fig. 24E, respectively). Both the deletions were equal with regard to their influence upon the rate at which calli appeared (Fig. 20), and upon the transformation frequency (Fig. 21). Since the larger deletion in the putative *overdrive* region did not have an incrementally larger effect on transformation frequency than the smaller deletion, the more precise deletion of the putative core was, therefore, considered to be as effective as the larger deletion in reducing transformation frequency. This suggests that either sequences required for full *overdrive*-like activity were located in the core, or that the smaller deletion disrupted the rest of the putative nopaline-type *overdrive* region such that it was unable to operate effectively. Interestingly, in the octopine-type *overdrive*, removal of a similar 15 bp region

containing the consensus core abolishes *overdrive* activity, reducing transformation frequency by 94-98% (Peralta *et al.*, 1986; Shurvinton and Ream, 1991).

The pattern of relative differences in the transformation frequency of *N. tabacum*, as generated by pANDY8, pANDY9 and pANDY10 (described above) was repeated when the plasmids were harboured by *Agrobacterium tumefaciens* strain MOG1010 (Fig. 24, p. 110). This strain contains a disarmed octopine-type helper plasmid, and its chromosomal background (C58) differs to that of LBA4404 (Ach5). Furthermore, the pattern was repeated (using LBA4404) in another plant species, *Arabidopsis thaliana* (Fig. 25, p. 113). This indicates that the relationship between deletions in the putative nopaline-type *overdrive* core and subsequent transformation frequency was not due solely to some interaction with either the bacterial strain or the plant species involved.

The putative core of the nopaline-type *overdrive* shares only 75% homology with that of the octopine-type consensus core. Wang *et al.* (1987) detected such homologies throughout the nopaline-type T-region and concluded that the putative nopaline-type *overdrive* adjacent to the right border was unlikely to play a significant role in T-DNA transfer. Subsequent studies, however, showed that a 103 bp fragment of the nopaline-type right border region containing this putative core behaved as an *overdrive* enhancer (Culianez-Macia and Hepburn, 1988). Furthermore, the studies in this Thesis revealed that discrete deletions of this putative core influenced transformation frequency indicating that this sequence does indeed play a role in T-DNA transfer.

4.1.2 The Putative Nopaline-type *Overdrive* does not Influence Processes after T-DNA Transfer

Although the deletions in the putative nopaline-type *overdrive* region decreased transformation frequency, they did not affect the physiological process of shoot development from callus. While both the total numbers of green calli, and the total numbers of organogenic calli decreased when deletions were made in the *overdrive* (Fig. 21, p. 105), the proportion of calli that became green and the proportion of green calli that became organogenic remained constant, regardless of whether or not an intact putative *overdrive* was present in the inciting vector (Fig. 22, p. 105). This indicates that process of shoot formation from transgenic calli was not influenced by deletions of the putative nopaline-type *overdrive.* Peralta *et al.* (1986) reported a similar phenomenon with the octopine-type *overdrive* where once tumours had appeared on carrot slices and *Nicotiana tabacum*, they grew normally, regardless of whether the inciting strain had *overdrive.* Although their data were purely

observational and not quantitative, Peralta *et al.* (1986) concluded that *overdrive* influences the efficiency of tumour induction, but not subsequent tumour growth.

4.1.3 Nopaline vs Octopine-type *vir* Environment

The nature of the *vir* regulon is an important determinant in the frequency of T-DNA transfer and has an influence upon the effect which deletions in the *overdrive* region have upon transformation frequency. In a nopaline-type *vir* environment, removal of 3.2 kb of nopaline-type Ti-plasmid sequence (including the putative *overdrive* region) flanking the right border reduced tumourigenesis by 57-78%, as determined by a quantitative potato tumourigenesis assay (Wang *et al.*, 1987). In an octopine-type *vir* environment, however, the substitution of the octopine-type right border and flanking sequences (including *overdrive*) with the nopaline-type right border resulted in a drastic reduction in tumourigenesis (++++ vs +), as determined by a non-quantitative tobacco assay (Van Haaren *et al.*, 1988). Similarly extensive deletions adjacent to the octopine-type right border resulted in a 96-98% reduction in transformation frequency in an octopine-type *vir* environment, as determined by a quantitative potato tumourigenesis assay (Shurvinton and Ream, 1991). These differences in transformation frequency are not due to an intrinsic difference in the activity of the octopine and nopaline-type right border sequences themselves as the borders have been shown to be equal with regard to transformation frequency when both compared within an octopine-type *vir* environment (Peralta *et al.*, 1986; Van Haaren *et al.*, 1988) and in a nopaline-type *vir* environment (Wang *et al.*, 1987).

The influence of different *vir* regulons on plant transformation frequency may be due to subtle differences between octopine and nopaline *vir* proteins themselves, as proposed by Van Haaren *et al.* (1988). The most plausible explanation, however, may reside in the relative accumulation of *vir* gene-products by octopine and nopaline strains, where nopaline strains have been shown to produce higher levels of *vir* proteins than octopine-type strains (Bakkeren *et al.*, 1989). As previously mentioned, increased concentrations of *vir* gene-products, including VirD1 and VirD2, override the requirement for the *overdrive* enhancer. The nopaline-type strain may, therefore, provide an environment where the *overdrive* element has a less enhancing effect and, upon its removal, transformation frequency falls back to an intrinsically higher level than that of an octopine-type strain. This apparent basal level of T-DNA transfer in nopaline-type *vir* environments has obvious bearing on the outcome and interpretation of results when experimentation is directed at assaying the impact of various sequences on *overdrive* activity. If attempts are being made to identify the contribution of small sequence alterations to the *overdrive* region, the octopine-type

vir environment, with a low intrinsic rate of T-DNA transfer in the absence of an *overdrive* element, may provide a more sensitive assay system. Evidence of this is provided in the Thesis where removal of 15 or 36 bp containing the putative nopaline-type *overdrive* had no detectable influence upon plant transformation frequency when using *A tumefaciens* strain GV3101, a nopaline-type *vir* regulon strain (Fig. 24E, p. 110a). However, the same deletions in an octopine-type *vir* environment (*A. tumefaciens* strain LBA4404) resulted in a 48% reduction in plant transformation frequency (Fig. 24E).

That deletions in the putative nopaline-type *overdrive* region had no detectable influence upon plant transformation frequency when performed in a nopaline-type *vir* environment contrasts with the study of Wang *et al.* (1987). In that study, a 57-78% reduction in tumourigenesis was detected when making deletions in the putative nopaline-type *overdrive* region in a nopaline-type *vir* environment. However, the deletions made were very extensive (3.2 kb) compared to those made in this Thesis (15 and 36 bp in pANDY9 and pANDY10, respectively). It could be that the lack of a detectable reduction in plant transformation frequency when using the pANDY8-10 plasmid series in a nopaline-type *vir* environment may indicate that the plant transformation assay is not sensitive enough to detect the influence of such small deletions in a nopaline-type *vir* environment. It may also be that sequences still remain in pANDY9 and pANDY10 which exhibit a partial *overdrive*-like activity that in a nopaline-type *vir* environment maintains plant transformation frequency yet in an octopine-type *vir* environment is not enough to retain maximal transformation frequency. This is discussed in Section 4.1.4 (below).

4.1.4 Was Putative Nopaline-type *Overdrive* Activity Abolished?

In this Thesis, a maximum of 36 bp was removed from the putative nopaline-type *overdrive* region (pANDY9, pANDY10; Section A6.12, p. 187), leaving intact all the native sequence between the right border and the putative *overdrive* consensus core. In an octopine-type *vir* environment (*A. tumefaciens strain* LBA4404), removal of the 36 bp sequence reduced transformation frequency by 47% (Fig. 21, p. 105). This value was repeatable as further experiments using LBA4404 revealed that while the actual number of organogenic calli varied, the proportional decrease in plant transformation frequency (the number of organogenic calli produced) upon removing the putative nopaline-type *overdrive* core remained constant at 47-48% (Fig. 24E, p. 110a). Halving the plant transformation frequency upon removal of the putative nopaline-type *overdrive* core contrasts with the activity of the octopine-type *overdrive* core which, when removed, effectively abolishes *overdrive* activity, reducing

transformation frequency by 96-98% in an octopine-type *vir* environment (Peralta *et al.*, 1986; Shurvinton and Ream, 1991). Since removal of 36 bp from the putative nopaline-type *overdrive* (as shown in this Thesis) did not decrease transformation frequency to the same degree as removal of the octopine-type *overdrive* core, it appears as if this sequence is not the sole determinant of *overdrive*-like activity associated with the nopaline-type right border region.

Further evidence that sequences may remain that exhibit partial nopaline-type *overdrive* activity, was provided by an *Agrobacterium tumefaciens* strain harbouring a mutation in *virC2*. As described previously (Section 1.4.5, p. 29), there is an intimate relationship between the *virC* operon and *overdrive* which affects their influence upon T-DNA border nicking and transformation frequency (Toro *et al.*, 1988; 1989). It has also been shown that mutations in either *virC2* or the octopine-type *overdrive* result in equally poor tumourigenesis (Ji *et al.*, 1989). The transformation frequency of *Nicotiana tabacum* by a disarmed *A. tumefaciens virC2* mutant strain (MOG1010-C) containing the pANDY8-10 series, was uniformly very poor. There was an average 87.5% reduction in plant transformation frequency when using MOG1010-C compared with that of pANDY8 in the wild-type *vir* operon strain MOG1010 (Fig. 24F, p. 110a). However, removal of the putative nopaline-type *overdrive* core in MOG1010 reduced plant transformation frequency by only 40% (Fig. 24F). As previously mentioned, studies have shown that removal of the octopine-type *overdrive* core reduces plant transformation frequency to that of either a *virC1* or *virC2* mutant strain (Ji *et al.*, 1989). In this Thesis, however, it was revealed that removal of a similar sequence from the putative nopaline-type *overdrive* region did not reduce plant transformation frequency to that of a *virC2* mutant strain (Fig. 24F). This suggests that there may be intrinsic differences in the activity and core components of the putative nopaline-type *overdrive* compared with the octopine-type *overdrive*. Furthermore, in a wild-type *vir* environment, the plasmids with deletions in the putative nopaline-type *overdrive* maintained a plant transformation frequency 7-fold greater than the pANDY8-10 vector series in a *virC2* environment (Fig. 24F). This indicates that sequences may remain in pANDY9 and pANDY10 with which VirC2 can interact, whether directly or through an intermediate factor.

To determine if further sequences do indeed remain that exhibit any nopaline-type *overdrive* activity, more extensive deletions would have to be made in the pANDY series of plasmids and tested against the current series. This would allow for the first time a direct quantitative comparison (within the same assay system) to be made

between small deletions in the putative nopaline-type *overdrive* region and removal of the entire sequence flanking the right border.

It is important to note, however, that detailed comparison of quantitative data presented in this Thesis with results from other studies is difficult, as it is complicated by the variety of assay methods presented in the literature. These methods utilize different host plant species, and, without exception, tumourigenesis or T-DNA production assays. In this Thesis, rather than using a tumourigenesis assay, a quantitative tobacco leaf disc transformation system was used in which T-DNA transfer frequency was determined by counting calli developing under antibiotic selection on a regeneration medium. This method measures callus and plant production resulting from both exposure to exogenous phytohormones and T-DNA-imparted resistance against a selective agent. Tumourigenesis assays, however, use virulent *Agrobacterium* strains and measure callus production resulting from alterations in endogenous phytohormone levels imparted by the introduced T-DNA. Quantitative tumourigenesis assays, therefore, count each callus as the product of T-DNA transfer, whereas the tobacco leaf disc transformation assay counts only calli that survive and develop on a selective regeneration medium to be the product of T-DNA transfer. It is important, however, in the transformation assay to count only the calli that develop normally under selection, as many of the initial calli that arise may not be transformed.

With few exceptions, assays of *overdrive* activity in the literature employ non-quantitative methods (such as +, ++, +++-type scoring) to determine differences in tumourigenicity. A direct comparison between results generated by quantitative and non-quantitative scoring of tumourigenesis assays is provided by Shurvinton and Ream (1991). They revealed that the synthetic 24 bp *overdrive* element, which previously had been shown to restore full tumourigenesis in non-quantitative tobacco tumourigenesis assays (Peralta *et al.*, 1986), restored only 25-35% of wild-type virulence when the same experiments were repeated in a quantitative potato tumourigenesis assay (Shurvinton and Ream, 1991). This indicates how non-quantitative assays can skew data. The only quantitative data in all the *overdrive* work reported, concerns the octopine-type *overdrive* in an octopine-type *vir* environment, using either a carrot disc tumourigenesis assay (94% decrease in virulence upon removal of *overdrive* (Peralta *et al.*, 1986)), or a potato disc tumourigenesis assay (96-98% decrease in virulence upon removal of *overdrive* (Shurvinton and Ream, 1991)), and the nopaline-type *overdrive* in a nopaline-type *vir* environment, also using a potato disc tumourigenesis assay (55-78% decrease in virulence upon removal of *overdrive*

(Wang *et al.*, 1987)). In as much as the absolute values of different quantitative assay systems using different plant species cannot be compared, relative differences in tumourigenesis may still provide a valid comparison. This was shown when removal of sequences flanking the octopine-type right border resulted in a 94% reduction in virulence in a carrot disc assay (Peralta *et al.*, 1986), and the same plasmids used with a potato disc assay resulted in a very similar 96-98% reduction in virulence (Shurvinton and Ream, 1991).

4.1.5 Importance of Sequences between the Right Border and the *Overdrive* Region

As mentioned previously, there is evidence that sequences may remain in the putative nopaline-type *overdrive* that exhibit partial *overdrive*-like activity. Thus far, only the octopine-type *overdrive* and the sequences between the consensus core and the right border have been studied in any detail. Although the consensus core has been shown to be necessary for activity of both the octopine and putative nopaline-type *overdrive* (see above), the question arises as to whether the core contains all the sequences sufficient for *overdrive* activity. In this regard, characterisation of the octopine-type *overdrive* by Shurvinton and Ream (1991), using a quantitative potato tumourigenesis assay, revealed several new findings (Section 1.4.3, p. 29). Of these, an oligonucleotide of the *overdrive* core itself, plus two base-pairs flanking either end, was found to be as effective in enhancing tumourigenesis as the synthetic 24 bp octopine *overdrive* element (Fig. 4 (steps 5 and 6), p. 27). This strongly suggests that all the sequences required for *overdrive* activity do reside in the consensus core region. However, both the core and the synthetic 24 bp octopine-type *overdrive* element each exhibited only 25-35% tumourigenesis of the wild-type octopine-type right border and *overdrive*. This indicates that the 14 bp between the octopine-type right border and the 24 bp *overdrive* sequence contain a region that alone is unable to enhance tumourigenicity (Fig. 4 (step 3), p. 27), yet may interact with the *overdrive* core to promote full tumourigenesis (Fig. 4 (step 2)).

Shurvinton and Ream (1991) noted that all their strains exhibiting full *overdrive* activity contained a 5′-TGTGA-3′ sequence immediately adjacent to the *overdrive* (Fig. 4 (steps 1, 2, and 7), p. 27), but whether addition of this sequence increases the virulence of the synthetic 24 bp octopine *overdrive* element has not been tested. Insertion of extra sequences between the right border and a larger *overdrive* region incorporating the 5′-TGTGA-3′ sequence did not affect tumourigenicity (Fig. 4 (step 7), whereas precise replacement of the 5′-TGTGA-3′ sequence with pUC18 sequence in conjunction with the synthetic 24 bp octopine *overdrive* element, decreased virulence

by 65-74% (Shurvinton and Ream, 1991) (Fig. 4 (step 6)). This indicates that the octopine-type *overdrive* may be a larger element than previously thought, and that the 5′-TGTGA-3′ sequence may be an important feature of that element. The octopine-type *overdrive* region tested by Van Haaren *et al.* (1988) also included the 5′-TGTGA-3′ sequence, but as the assays were non-quantitative, it is difficult to compare the activity of this larger *overdrive* region with that of other *overdrive* regions or synthetic *overdrive* elements studied in the literature. Interestingly, the putative *overdrive* adjacent to the right border of the T_R-DNA of an Ri-plasmid, pRiA4, appears to only comprise the 5′-TGTGA-3′ sequence and the consensus core (Fig. 5, p. 32), although the activity of this *overdrive* has yet to be characterised. Analysis of the DNase I footprinting assays performed by Toro *et al.* (1989) on a 285 bp octopine-type Ti-plasmid fragment containing the T_L right border, revealed that VirC1 protects a region encompassing both the 24 bp octopine-type *overdrive* and the 5′-TGTGA-3′ sequences (Fig. 33, p. 135). Although protected by VirC1, the 5′-TGTGA-3′ motif is, however, not necessary for binding VirC1, as Toro *et al.* (1988) used a synthetic 24 bp octopine-type *overdrive* element alone (in sequence-specific DNA affinity chromatography) to determine that VirC1 binds to *overdrive.* It is tempting to speculate, however, that the 5′-TGTGA-3′ sequence is required for maximum VirC1 binding, or that a different spectrum of proteins binds to the larger *overdrive* region, resulting in maximum *overdrive* activity.

Analysis of the putative nopaline-type pTiT37 *overdrive* region tested in this Thesis, reveals the presence (in the appropriate location) of a region with four out of five base-pair identity to the 5′-TGTGA-3′ sequence. In this 5′-CGTGA-3′ sequence, the first thymine is replaced by another pyrimidine (Fig. 5 (pTiT37, bp 3-7), p. 32), which may suggest that this nucleotide is not an essential component of the motif. Interestingly, the DNase I footprinting assays of Toro *et al.* (1989) revealed that VirC1 protection of the top strand of the octopine-type *overdrive* region does not include the first T of the 5′-TGTGA-3′ sequence (Fig. 33, p. 135). Due to the crudeness of this assay, however, inferences cannot be made regarding the relationship between VirC1 binding and this particular nucleotide. An assay which allows for precise analysis of protein-DNA interactions at the nucleotide level (such as Hydroxyl Radical Footprinting (Chalepakis and Beato, 1989; Dixon *et al.*, 1991)), may determine which bases in this extended *overdrive* region are intimately involved in the binding of VirC1. To test whether the octopine or nopaline-type *overdrive* sequences do in fact consist of two separate interdependent regions (comprised of a consensus *overdrive* core bordered 5′ by the smaller 5′-TGTGA-3′ motif), the effects on transformation frequency of both combining the 5′-TGTGA-3′ (or 5′-CGTGA-3′) motif and the *overdrive* core, and altering

Top strand 5′ TTTGAGCTCG***TGTGA***AT**AAGTCGCTGTGTAtgtttgttTG**ATTGTTTCTGTTGT 3′

Bottom strand 3′ AAACTCGAGC**ACACTTATTCAGCGACACATacaaacaaAC**TAACAAAGACAACA 5′

Figure 33. The top and bottom strand sequence of the T_L-DNA right border and *overdrive* region of the octopine-type Ti-plasmid pTiA6 that is protected by VirC1 in DNase I footprint analysis.

DNase I protection experiments were performed by Toro *et al.* (1989) upon a 285 bp fragment of pTiA6 (containing the T_L-DNA right border region), to determine which sequences were protected through the binding of VirC1 to the *overdrive*. Protected sequences are marked (double underlined), as are the right border (underlined), the 5′-TGTGA-3′ motif (***bold italics***), the 24 bp octopine-type *overdrive* sequence (**Bold**), and the *overdrive* consensus core (**bold lowercase**).

the type and amount of sequence between them, can be evaluated. Site-directed mutagenesis could determine more precisely, sequences important for *overdrive* activity within both the consensus core and the 5′-TGTGA-3′ or 5′-CGTGA-3′ motifs.

4.1.6 Importance of the *Overdrive* Consensus Core

Of all the previously identified *overdrive* core sequences, the putative nopaline-type core is the most different, as it is the only one not 100% homologous to the proposed consensus core (Fig. 5, p. 32). Like the octopine-type *overdrive* (Fig. 4 (step 2), p. 27), however, a 15 bp region containing the putative nopaline-type *overdrive* core, plus an extra 3 bp upstream and 4 bp downstream of the core, was shown to be essential for full nopaline-type *overdrive* activity (Fig. 20, p. 102; Fig. 21, p. 105; Fig. 23, p. 108). Therefore, not only is the *overdrive* consensus core a highly conserved sequence over a range of plasmids, but two quite different cores in two quite different *overdrive* regions have been shown to be essential for *overdrive* activity (Peralta *et al.*, 1986; Shurvinton and Ream, 1991; this Thesis).

Interestingly, no work has yet been performed to determine whether deletions of, or in, the consensus core of any *overdrive* region influence the binding activity of factors (such as the VirC1 protein) involved in *overdrive* activity. In fact, whether factors bind at all to the nopaline-type *overdrive* has yet to be determined, and this is the next logical step to confirm the role of this sequence as an *overdrive*-like enhancer.

4.1.7 Is the Putative Nopaline-Type *Overdrive* Core an *Overdrive* Core?

What features comprise the activity of an *overdrive* transformation enhancer element? As the most detailed analysis of *overdrive* has been performed with the octopine-type *overdrive*, this then becomes the model against which all other putative *overdrive* regions are tested. As previously mentioned in the Introduction (Section 1.4, p. 23), the octopine-type *overdrive* demonstrates the following characteristics:

Plant Transformation Frequency Enhancer: Removal of the *overdrive* core sequence reduces transformation frequency by 90-98% in tumourigenesis assays in an octopine-type *vir* environment (Peralta *et al.*, 1986; Van Haaren *et al.*, 1987a, 1987b, 1988; Ji *et al.*, 1989; Shurvinton and Ream, 1991). Addition of either fragments containing the *overdrive* region or the 24 bp *overdrive* sequence or the core itself enhances tumourigenicity (Peralta *et al.*, 1986; Van Haaren *et al.*, 1987a, 1987b, 1988; Ji *et al.*, 1989; Shurvinton and Ream, 1991);

Position-Independent Activity: The octopine-type *overdrive* element enhances tumourigenesis independent of it position relative to the right border when inserted as part of a larger Ti-plasmid fragment (Van Haaren *et al.*, 1987a, 1987b), even when inserted up to 2059 bp from the right border (Van Haaren *et al.*, 1988), or when inserted as a 24 bp synthetic *overdrive* (Peralta *et al.*, 1986) up to 553 bp from the right border (Ji *et al.*, 1989);

Orientation-Independent Activity: The octopine-type *overdrive* behaves as a true enhancer as it enhances tumourigenesis irrespective of its orientation relative to the right border (Peralta *et al.*, 1986; Van Haaren *et al.*, 1987b; Ji *et al.*, 1989; Shurvinton and Ream, 1991).

Enhancement of T-strand Production: The octopine-type *overdrive* enhancer is associated with increased T-strand production as removal of a fragment containing the *overdrive* region severely attenuates T-strand production (Van Haaren *et al.*, 1987b), whereas the addition of the 24 bp *overdrive* sequence increases T-strand production (Toro *et al.*, 1988; Veluthambi *et al.*, 1988; Ji *et al.*, 1989).

Interaction with the virC Operon: Mutations abolishing either gene-product of the *virC* operon attenuate virulence to that of an octopine-type *overdrive*-deleted strain (Ji *et al.*, 1989), and also reduce T-strand production (Toro *et al.*, 1988). It was discovered that the 24 bp octopine-type *overdrive* sequence binds VirC1 (Toro *et al.*, 1988), and DNase I footprinting of an octopine-type Ti-plasmid fragment containing *overdrive* revealed that VirC1 protects the 24 bp *overdrive* sequence including the *overdrive* core (Toro *et al.*, 1989).

The region of the nopaline-type Ti-plasmid which contains the putative *overdrive* core exhibits many of the properties associated with octopine-type *overdrive* activity. It exhibits:

Plant Transformation Frequency Enhancement: In an octopine-type *vir* environment, insertion of a 3.2 kb nopaline-type Ti-plasmid fragment (containing the putative nopaline-type *overdrive* core) enhances to wild-type levels the tumourigenicity of an octopine-type Ti-plasmid from which the octopine-type *overdrive* region has been deleted (Van Haaren *et al.*, 1988).

Position-Independent Activity: A 103 bp fragment containing the putative nopaline-type *overdrive* core enhanced T-strand production when inserted 2 kb away from the

T-DNA border region of a binary vector that contained only nopaline-type left and right border sequences (Culianez-Macia and Hepburn, 1988).

Orientation-Independent Activity: Reversing the orientation of the 103 bp fragment with respect to the border sequences did not affect T-strand production (Culianez-Macia and Hepburn, 1988).

Enhancement of T-strand Production: A 103 bp fragment of the nopaline-type right border region that contains the putative nopaline-type *overdrive* core enhances T-strand production as its removal abolished detectable T-strand production (Culianez-Macia and Hepburn, 1988).

Interaction with the virC Operon: As to whether the putative nopaline-type *overdrive* interacts with the *virC* operon has yet to be determined. No studies have been performed to ascertain whether VirC1, or in fact anything, binds to the putative nopaline-type *overdrive* region. In this Thesis, the pANDY8-10 series was assayed for plant transformation frequency in both a *virC1* and a *virC2* mutant *A. tumefaciens* strain. The *virC1* mutant strain (A1021) failed to produce any calli at all and appeared to be avirulent (data not presented), hence it was impossible to draw any conclusions pertaining to the relative plant transformation frequency of the plasmid series in a VirC1-free environment. In a VirC2-free environment, however, the plant transformation frequency was approximately 10-fold less than that of the wild-type *vir* environment (Fig. 24E, p. 110a). More importantly, in a VirC2-free environment, there were no differences between the plasmids with regard to plant transformation frequency (Fig. 24E). If there remained a difference in the plant transformation frequencies of the pANDY8-10 series in a *virC2* mutant strain, this would then imply that the mechanism by which the deletions reduced transformation frequency operated independently of VirC2 which contradicts one of the properties of the octopine-type *overdrive.*

The putative nopaline-type *overdrive*, therefore, exhibits at least four of the characteristic properties of the octopine-type *overdrive*, which provides strong evidence that nopaline-type Ti-plasmids do in fact have an *overdrive*-like enhancer adjacent to the right border. More importantly, within the 103 bp nopaline-type Ti-plasmid fragment which exhibits T-strand enhancement and position and orientation-independent characteristics, there is only one putative *overdrive* consensus core sequence. This putative core was the one upon which deletions were performed to create pANDY9 and pANDY10 (this Thesis). That deletion of the only putative

core in a region exhibiting *overdrive*-like properties reduced plant transformation frequency provides strong evidence that this putative core is in fact an *overdrive* core. To ascertain conclusively whether or not this putative core sequence is in fact part of a nopaline-type *overdrive* element would require some further experimentation. A Loss of Function/Gain of Function series of experiments performed by deleting and subsequently reinserting various sequences containing the putative *overdrive* core would determine which sequences are necessary for function of the nopaline-type *overdrive*, and which sequences are sufficient for full *overdrive* actvity. To determine if there is a relationship between *virC* and the nopaline-type *overdrive* at the molecular level a series of gel retardation assays would be performed to first determine whether anything binds to the putative nopaline-type *overdrive*, and then determine what deletions in the putative core influence the binding of those factors. A similar set of experiments with VirC1 as the binding factor would be very interesting, as would DNase I Footprinting or Hydroxyl Radical Footprinting to ascertain which sequences, if any, are protected by VirC1 or other bound factors.

4.1.8 Biological Significance of *Overdrive*

As previously mentioned in the Introduction (Section 1.4.4, p. 28), *overdrive* is thought to enhance interactions between the right border and the appropriate *vir* proteins, thus improving T-strand production by enhanced nicking at the right border. However, the presence of additional copies of *vir* genes overrides the effect of *overdrive* (Ji *et al.*, 1989; Veluthambi *et al.*, 1988). Furthermore, elevated expression of the *virD* operon eliminates enhancement of T-strand production by the *virC* operon, which is intimately involved with *overdrive* (De Vos and Zambryski, 1989) (Section 1.4.5, p. 29). This suggests that in the presence of raised *vir* protein levels, particularly VirD1 and VirD2, the enhancing effect of *overdrive* is not required for efficient T-strand production. Therefore, the role of *overdrive* may be to attain efficient T-strand production (hence tumourigenicity) in the presence of minimal *vir* protein levels, through interaction with *virC* gene-products. Thus, the presence of *overdrive* reduces the concentration of *vir* proteins required to mediate efficient synthesis of T-DNA, and in so doing, the physiological cost to the bacterium is reduced.

4.1.9 *Overdrive* in other DNA Transfer Systems

There is much evidence suggesting that the T-DNA generation/transfer system and bacterial conjugation are functionally related, and that they are derived from the same ancestral process (reviewed in Hooykaas and Beijersbergen, 1994; Lessl and Lanka, 1994; Pansegrau *et al.*, 1994a; Waters and Guiney, 1993; Zupan and Zambryski,

1995). As mentioned in the reviews above, the conjugative transfer system of the broad host range IncP promiscuous plasmids in particular, appears to be related to Ti-plasmid-induced plant transformation. A comprehensive analysis of IncPα plasmids (such as RP4) has revealed that the closest relationships at the nucleotide level are not with F or F-like plasmids (with which no extensive similarities were observed), but with plasmid functions of *Agrobacterium* spp. (Pansegrau *et al.*, 1994a). Whereas portions of Ti-plasmids are transferred to plants, IncP plasmids are stably transferred to a wide variety of Gram-negative and Gram-positive bacteria, as well as yeasts. These transformation systems are similar, not only in terms of the process of the production of a single-stranded DNA molecule, and mode of transfer to the recipient cell, but also in terms of the arrangement of operons involved in the process. In fact, it is the similarities in the amino acid sequence, gene organisation and physical properties of members of the IncPα *tra2* operon (which is involved in mating-pair formation, including pilus formation), that is providing clues as to the function of members of the Ti-plasmid *virB* operon.

The conjugative transfer process of the IncPα plasmids requires the production of a single-stranded copy of the plasmid which is directionally transferred to the recipient cell. Nicking is initiated by the binding of TraJ (the equivalent of VirD1) to a motif adjacent to the *oriT* (origin of transfer). The *oriT* is the equivalent of Ti-plasmid border sequences, with which it shares a highly conserved motif that forms the nick site. TraJ is thought to load the endonuclease TraI (the equivalent of VirD2) on to the nick site, and the entire complex, or relaxosome, is stabilised by TraH (the equivalent of VirD3). A nick is introduced at the nick site, and TraI covalently binds to the 5′ end of the strand in a manner very similar to that of VirD2. The strand is displaced and coated with a single-stranded DNA binding protein, TraC (the equivalent of VirE2). The DNA/TraI/TraC complex is then thought to be introduced by TraG (the equivalent of VirD4) to the Tra2 transfer apparatus (the equivalent of VirB complex) and subsequently transported to the recipient cell.

As there are such strong similarities between conjugative transfer of IncPα plasmids and T-DNA generation and transfer, there may be a functional analogue of *overdrive* adjacent to the *oriT* of IncPα plasmids. This hypothesis was first mooted by Waters *et al.* (1991). Approximately 100 bp distal from the *oriT* nick site, there is a region that has an intrinsic structural bend which, when removed, results in a 200-fold decrease in the mobilisation frequency of the IncPα plasmid, RP4 (Pansegrau *et al.*, 1990). Coincidently, this is similar to the 100-fold decrease in plant transformation frequency exhibited upon removal of *overdrive* in an octopine-type system (Peralta *et*

al., 1986; Shurvinton and Ream, 1991). Furthermore, this structural bend is the binding site of TraK, a protein that enhances nicking at *oriT* (Fürste *et al.*, 1989; Waters *et al.*, 1991). It does appear, therefore, that this bend region may be a functional analogue of *overdrive*, although it does not harbour any sequences that share homology with the *overdrive* consensus core, or either of the octopine or nopaline-type *overdrive* regions. Moreover, whereas *overdrive* has a consensus core that is intrinsically involved in *overdrive* activity, there does not appear to be a similar feature in the structural bend. Within the TraK binding site on the structural bend there is 49 bp sequence containing an inverted repeat sequence that is structurally conserved between quite different plasmids, RP4 (IncPα) and R751 (IncPβ) (Fürste *et al.*, 1989), yet the significance of this site is unclear as TraK does not form a complex with the RP4 49 bp sequence when the sequence is inserted in non-*oriT* context (Ziegelin *et al.*, 1992).

There is also a functional analogue of the *virC* operon: the leader operon. This operon, of which TraK is a member, is not only functionally similar to the *virC* operon, but it also shares some conserved amino acid sequences (reviewed in Pansegrau *et al.*, 1994a). In a role analogous to that of VirC1, TraK enhances nicking at *oriT* (Fürste *et al.*, 1989; Waters *et al.*, 1991). Nicking is enhanced possibly by introducing local topological changes to the DNA substrate upon binding of TraK to the bent region, where almost 200 bp of DNA become wrapped around a core of multimeric TraK subunits (Ziegelin *et al.*, 1992). The mechanism by which VirC1 enhances nicking at the right border, however, has yet to be determined. Unlike VirC1, which is not essential for plant transformation, TraK not only enhances nicking at *oriT*, but is also essential for conjugative transfer of IncPα plasmids (Fürste *et al.*, 1989; Lessl *et al.*, 1993). Further dissimilarities between VirC1 and TraK occur with respect to their DNA binding mechanisms. As TraK does not seem to bind to a precise nucleotide sequence site, it appears that, unlike VirC1, TraK belongs to a novel class of prokaryotic DNA-binding proteins that recognise the target DNA by structural features, such as bendability, rather than by the nucleotide sequence (Ziegelin *et al.*, 1992). However, the other gene-products specified by the *virC*-analogous leader operon, TraL and TraM, behave more similarly to *virC* proteins than does TraK. Like *virC* proteins, TraL and TraM are not essential for conjugative transfer, yet they both enhance conjugative transfer (Lessl *et al.*, 1993; Pansegrau *et al.*, 1994a). Like VirC1, with which it shares conserved DNA sequences, TraL may enhance conjugative transfer through interaction with DNA, as it contains a type A nucleotide binding site (Pansegrau *et al.*, 1994a). Furthermore, although its function is not well characterised, deletion of TraM results in a 300-fold decrease in conjugative transfer (Lessl *et al.*,

1993). This figure is similar to the 100-fold reduction in plant transformation frequency exhibited by *virC2* mutants (Ji *et al.*, 1989) or by deletions of the *overdrive* in an octopine-type system (Peralta *et al.*, 1986; Shurvinton and Ream, 1991). The mechanism by which TraL and TraM enhances conjugative transfer, and whether it be *via* enhanced nicking at the *oriT* nick site, has yet to be elucidated.

Although only preliminary studies of the structure and function of TraL and TraM have been made, it appears as if the leader operon is a functional analogue of *virC*, whereas the structural bend is the current candidate for an *overdrive*-like region. More detailed studies of the structure and mechanisms of *virC* gene products and those of the leader operon are required to confirm this hypothesis. If the hypothesis is confirmed, it provides interesting evidence of a mechanism conserved among DNA transfer processes that enhances cleavage at the appropriate nick site. To date, no research has been performed to determine if increased levels of the proteins intimately involved with nicking at *oriT* (TraJ and TraI) override the nicking-enhancement effect of the leader operon gene-products, or the structural bend. If nicking enhancement was shown to be overridden, it would further indicate functional similarities between IncP plasmid conjugative transfer and Ti-plasmid-induced plant transformation. Furthermore, it would provide evidence of a conserved mechanism whereby efficient nicking is attained with minimal production of nicking proteins.

4.2 INFLUENCE OF *OVERDRIVE* ON T-DNA COPY NUMBER

This study is the first to demonstrate a correlation between manipulation of sequences outside the T-DNA in a binary vector, and subsequent T-DNA insertion number in transformed plants. The deletions of the nopaline-type putative *overdrive* core and surrounding sequence influenced T-DNA copy number equally, and halved the incidence of plants containing multiple T-DNA inserts (Fig. 31, p. 124). Furthermore, both deletions influenced the range of T-DNA copy number in the different plant populations to a similar extent, and restricted copy number to either one or two inserts (Fig. 32, p. 125). Only plants in the population generated by the vector with the intact *overdrive* region (pANDY8) contained more than two T-DNA inserts. It is interesting to note that the deletions, which as well as having an equal influence on T-DNA copy number, also had an effect on transformation frequency (Fig. 21, p. 105). This suggests a link between frequency of T-DNA transfer and the number of T-DNA copies inserted into the host plant genome.

The decrease in T-DNA copy number following deletions in the nopaline-type *overdrive* may be a result of lower levels of T-strand production. As previously mentioned (Section 1.4.4, p. 28), there is a direct link between *overdrive* and T-strand production. The presence of an octopine-type *overdrive* in an octopine-type *vir* environment increases T-strand production (Ji *et al.*, 1989; Toro *et al.*, 1988; Veluthambi *et al.*, 1988), as does the presence of a fragment containing the putative nopaline-type *overdrive* in a nopaline-type *vir* environment (Culianez-Macia and Hepburn, 1988). There is also a link between T-strand levels and transformation frequency (as determined by tumourigenesis), as removal of the octopine-type *overdrive* in an octopine-type *vir* environment reduces both T-strand production and subsequent tumourigenesis (Van Haaren *et al.*, 1987b). Furthermore, this link appears to be quantitative, as stepwise decreases in T-strand production resulting from increases in the distance between the right border and the octopine-type *overdrive*, led to stepwise decreases in tumourigenesis (Van Haaren *et al.*, 1987b). Therefore, removing *overdrive* reduces T-strand production, hence less T-strands are available for integration into plant cells. This decreases the likelihood of more than one, or any, T-strand being transferred and integrated into the plant genome, resulting in the subsequent decrease in transformation frequency and T-DNA copy number shown in this Thesis. The putative correlation between T-DNA concentration and insertion frequency is supported by the observation that transformation procedures which transfer DNA directly to plant material, such as biolistics or protoplast electroporation, use high levels of DNA relative to *A. tumefaciens*-mediated transformation and often result in multiple insertion events (Finnegan and McElroy, 1994). An example of this

is provided by Allen *et al.* (1996), who used biolistic techniques to transform tobacco. Of the plants produced, the average copy number of the *gusA* gene was 20.2 copies per plant, with a maximum of 77 copies (as determined by Southern analysis and PCR protocols for copy number quantification).

No previously published study has investigated the link between either T-strand production or transformation frequency, and the T-DNA copy number in resulting plant transformants. Other research, however, does support a link between absence of *overdrive* in binary vectors and decreased T-DNA copy number in plant transformants. Fobert *et al.* (1991) used a binary promoter-trapping vector and a *Nicotiana tabacum* leaf disc transformation method to generate a population of transformants to screen for tagged promoters. Of 51 plants transformed with the promoter-trapping vector, 92% (47 plants) contained a single T-DNA insert, and only one plant had the maximum of three inserts. In contrast, in another population of transformants generated with pBIN19-derived binary vectors in the same set of experiments, less than 50% had single inserts, and some plants contained up to five inserts. No theory was offered to explain the marked differences in both the T-DNA copy number and the range of T-DNA copy numbers generated by the different plasmids. Furthermore, no mention was made of any relative differences in transformation frequency. Analysis of the promoter-trapping vector, however, reveals the absence of any *overdrive*-like region, as the T-DNA right border was synthetic and no flanking sequences were incorporated. The vectors that generated the plant population with the higher T-DNA copy numbers, were pBIN19-derived (as was the pANDY8-pANDY10 plasmid series), and thus contain a nopaline-type right border and flanking sequences that include the putative *overdrive* core. The study reveals, therefore, that although the plasmids used by Fobert *et al.* (1991) were not closely related to each other, there is a link between absence of an *overdrive* region, and an increased proportion of plants containing single T-DNA inserts. This trend mirrors that exhibited by deletions in the *overdrive* region detailed in this Thesis.

The promoter-trapping vector of Fobert *et al.* (1991) represents an ideal negative control for the investigations in this Thesis. This is because all *overdrive*-like regions flanking the right border are absent in the vector of Fobert *et al.* (1991), in contrast to this Thesis where small specific deletions were made in the region flanking the right border. More extensive deletions in the *overdrive* region of the current pANDY8-pANDY10 plasmid series may well result in further decreases in transformation frequency. Correspondingly, the proportion of plants, as generated by the tobacco leaf disc method, that contain single T-DNA inserts may also increase

from the existing 86% (Fig. 32, p. 125) to a value closer to the 92% described by Fobert *et al.* (1991). This is assuming that (as yet) unknown regions exhibiting partial *overdrive* activity still remain in pANDY9 and pANDY10. However, that the differences in T-DNA copy number exhibited by the *overdrive*-deleted system (Fobert *et al.*, 1991) and the *overdrive*-core-deleted system (this Thesis), may be due to the use of different plant cultivars and experimental procedures, cannot be excluded.

Previously published data indicate that the proportion of plants (transformed with standard binary vectors) containing a single T-DNA is variable, and ranges from 5% (Donald Kerr, personal communication; tobacco), 11% (Grevelding *et al.*, 1991; *Arabidopsis thaliana* root explants) 33% (Lindsey *et al.*, 1993; tobacco), 35% (Koncz *et al.*, 1989; tobacco), 38.5% (Deroles and Gardner, 1988a; 1988b; petunia), 54% (Lindsey *et al.*, 1993; *Arabidopsis thaliana*), 64% (Grevelding *et al.*, 1993; *A. thaliana* leaf explants) to 65% (this study; tobacco). All these transformants were generated by plasmids that contained *overdrive*-like sequences, and the proportions containing single T-DNA are much lower than the 86% generated by binary vectors with deletions in the putative *overdrive* core in this thesis. Furthermore, the highest T-DNA copy numbers, range from four to six, which is larger than the maximum of two T-DNA inserts harboured by plants generated by vectors containing deletions of the putative *overdrive* core (this Thesis). Interestingly, the only studies to provide data with values similar to that of this Thesis involved vectors with synthetic borders, hence no *overdrive* sequences were present. Of a population of *Arabidopsis thaliana* transformants, 71% contained a single T-DNA insert, and only one plant of the 66 had the maximum copy number of three inserts (Kertbundit *et al.*, 1991). This is very similar to the T-DNA copy number spread of Fobert *et al.* (1991) where only one plant out of 51 contained the maximum of three T-DNA inserts, although the proportion of plants with a single T-DNA was 92%. This further substantiates evidence of the influence of *overdrive* on T-DNA copy number, and particularly the spread of T-DNA copy numbers.

It is difficult, however, to make valid comparisons with studies in the literature, as not only were different plant species, bacterial strains and plant transformation systems used, but also different methods to determine T-DNA copy number. Each of these variables have the potential to influence T-DNA copy number. Different plant species have different susceptibilities to, or ability to induce *vir* activity of, *Agrobacterium tumefaciens*, depending upon the host range of the strains, thus influencing T-strand transfer and T-DNA copy number. Likewise, the particular transformation system and explant material used has been shown to markedly affect T-DNA copy number. Of

a population of transformants generated from *Arabidopsis thaliana* root explants, 64% contained single T-DNA inserts, whereas only 11% of the transformants generated by an *A. thaliana* leaf disc explant method contained single inserts (Grevelding *et al.*, 1993). Again, this might be due to differences in the susceptibility of the material to *Agrobacterium tumefaciens* infection, or its ability to signal the induction of *vir* activity. T-DNA copy number can be determined by Southern analysis and, in some cases (Lindsey *et al.*, 1993), segregation of a particular plant selectable marker (kanamycin resistance is commonly used). Complications with segregation analysis mainly arise due to multiple insertion events occurring at, or very close to, the same site. These linked inserts usually segregate as a single locus, thus revealing an artificially low number of T-DNA copies. Furthermore, multiple copies may lead to silencing of the selectable marker in the progeny, further complicating the segregation assays.

The results of this Thesis, however, showed that when all other factors (such as explant material, bacterial strain and concentration, binary vector, and the transformation procedure) were kept constant, deletion of a putative core region from a nopaline-type *overdrive* T-DNA transmission enhancer influenced both T-DNA insert number and the spread of T-DNA copy number, most likely due to a reduced amount of T-strands being transferred.

4.3 IMPLICATIONS OF T-DNA COPY NUMBER

4.3.1 T-DNA Copy Number and Transformation Frequency in Plant Transformation Systems

As reviewed by Finnegan and McElroy (1994) and Matzke and Matzke (1995), the presence of multiple T-DNA insertions in transgenic plants has been associated with reduction or suppression of transgene expression. Furthermore, multiple inserts also complicate gene-tagging or enhancer/promoter-trapping due to the presence of extra tags. As yet, the only certain way to overcome these problems is to analyse plants with single T-DNA copies. In fact, Finnegan and McElroy (1994) suggested that plant transformation methods should be developed that ensure single-copy transgene integration. Removal of the nopaline-type putative *overdrive* core from the vectors used in this Thesis halved the incidence of multiple T-DNA insertion events such that 86% of the population of transformants contained single T-DNA copies. Manipulation of the putative nopaline-type *overdrive*, therefore, produced a transformation system in which nearly nine out of ten transgenic plants contained a single T-DNA insert. In spite of the high percentage of plants containing single T-DNA inserts, the transformation frequency of the protocol was also halved. This is not a problem with

plants such as *Nicotiana tabacum*, as even at the reduced rate of transformation large quantities of transformants were generated rapidly. For those plants, however, with a low transformation frequency, a further 50% reduction in transformation frequency is impractical.

The correlations between reduced T-strand production and subsequent transformation frequency (Van Haaren *et al.*, 1987b), and transformation frequency and T-DNA copy number (this Thesis), may be used as a diagnostic tool to develop and optimise *Agrobacterium tumefaciens*-mediated plant transformation protocols. Transformation protocols require efficient regeneration from the explant material, as well as the plant being an efficient host for *A. tumefaciens* strains. If an effective regeneration system has been developed, but the incidence of regenerating transformants is very low, then analysis of the T-DNA copy number of the transformants may provide a clue as to optimising the procedure. If the majority of transformed plants contain a single T-DNA, then it is conceivable that poor T-strand transmission is implicated. The focus should, therefore, be on optimisation of the bacterial/plant interaction which is influenced by factors such as bacterial density, poor induction of *vir* genes by signals from the host plant, suitability of the plant to be a host for *A. tumefaciens*, virulence of the particular *A. tumefaciens* strain, and cocultivation conditions. If the majority of plants have multiple T-DNA inserts, then the focus should be on optimisation of the regeneration process as T-strand transfer is proceeding efficiently. It could then be, that most of the explant cells exposed to *A. tumefaciens* infection are not in the zone of cells that regenerate. Optimisation of the transformation procedure should then focus on the regeneration protocol, and may be based on factors such as: manipulating phytohormones to alter the spectrum of cells that regenerate; exposure of the regenerating cells to *A. tumefaciens* by precise dissection; or ensuring survival of the regenerating cells.

4.3.2 T-DNA Copy Number and Transformation Frequency in Gene-Tagging

The use of binary vectors with deletions in the *overdrive* region also has implications affecting experimental approaches directed at the use of gene-tags or enhancer/promoter-traps derived from T-DNA. Although the great majority of transformants to be screened for tagging events would contain a single T-DNA tag, the decrease in transformation frequency would make generation of a large population of transformants more difficult. Furthermore, the high incidence of plants containing a single T-DNA results in a decrease in the total number of T-DNA tags in the transformed plant population. This means that a much larger population of transformants would have to be screened to find the same number of tagging events

as found in a population of transformants that contained three or four T-DNA inserts per plant. An example of this is provided by Fobert *et al.* (1991) and Koncz *et al.* (1989) who used conceptually similar tagging vectors. When screening plants for expression of tagged gene-fusions, only 5% of the population generated by Fobert *et al.* (1991) expressed in the leaf, whereas 20% of the population generated by Koncz *et al.* (1989) expressed in the leaf. The proportion of plants, however, in the different populations that contain multiple T-DNA copies is 8% and 65% for Fobert *et al.* (1991) and Koncz *et al.* (1989), respectively. The total number of tags in the Koncz *et al.* (1989) study is, therefore, much higher than that of the Fobert *et al.* (1991) study, and if expressed on a per tag basis, the frequency of tagging events in the two studies would be much more similar.

A compromise, therefore, has to be made between a decrease in the frequency of tagging events on a per plant basis, and easier analysis of the tagged genes/promoters due to a high proportion of single T-DNA inserts. In many systems (Fobert *et al.*, 1991; Kertbundit *et al.*, 1991; Koncz *et al.*, 1989; Lindsey *et al.*, 1993), tagging events are detected by expression of a promoterless reporter gene in the T-DNA tag. The presence of multiple T-DNA copies may suppress expression of the reporter gene, thus some tagging events will not be detected during screening. Maybe protocols for the analysis of tagged genes/promoters/enhancers can overcome some of the difficulties of the presence of multiple tags in a plant, but protocols can not overcome missing a tagging event because of reporter gene silencing due to multiple transgene copies.

4.4 FUTURE DIRECTIONS

Larger scale deletions to remove most sequences flanking the nopaline right border in the pANDY8-pANDY10 plasmid series would determine whether sequences remain that exhibit partial *overdrive*-like activity and whether the 5′-CGTGA-3′ sequence is an important factor in putative nopaline-type *overdrive* activity, as determined by transformation frequency and T-strand production assays. The effect of these deletions on T-strand production and T-DNA copy number in plants could confirm a link between reduced T-DNA generation and reduced incidence of multiple T-DNA insertion events. Further work is also required to determine whether VirC1 binds with the putative nopaline-type *overdrive* region in any way. Furthermore, gel retardation assays may determine whether deletion of the putative core region affects binding of factors, such as *vir* proteins to the *overdrive*. No work has yet been performed to ascertain the effect of deletions within either the octopine or nopaline-type *overdrive* regions on binding of *vir* induced factors. This is an essential component of any research aimed at evaluating enhancers that exact their effect through interacting specifically with DNA binding proteins.

4.5 SUMMARY

A series of binary vectors was created from which a 15 bp and a 36 bp portion of sequence containing the putative core region of the nopaline-type *overdrive* had been deleted. The smaller deletion was as effective as the larger deletion in decreasing transformation frequency of *Nicotiana tabacum* leaf discs, which was reduced by 47%. The relationship was observed when using octopine-type host strains of different chromosomal backgrounds, and also when transforming unrelated plant species (*Arabidopsis thaliana*). The deleted putative nopaline-type *overdrive* core was the only one present in a region that has been shown previously to behave as an *overdrive*-like enhancer. The decrease in plant transformation frequency upon removal of this putative core provided strong evidence that it was indeed an *overdrive*-like consensus core. Furthermore, in a *virC2* mutant environment, the plant transformation frequency was reduced markedly for all three plasmids (approximately a 90% reduction compared with the wild-type *vir* environment). However, there was no difference in the plant transformation frequencies of the putative *overdrive*-deleted and undeleted plasmid series in a *virC2* mutant environment. This suggested that the mechanism by which the deletions influenced plant transformation frequency did not act independently of the *virC* operon, which is further evidence of *overdrive*-like activity.

The plant transformation frequency of the wild-type putative nopaline-type *overdrive* plasmid, pANDY8, was very similar whether the host *A. tumefaciens* strain provided an octopine or a nopaline-type *vir* environment (LBA4404 and GV3101, respectively). However, in a nopaline-type *vir* environment, deletions of the putative *overdrive* core had no influence upon plant transformation frequency (in contrast to when the plasmids were in an octopine-type *vir* environment). Previous studies (Bakkeren *et al.*, 1989) have shown that *vir* gene products accumulate to a greater level in *A. tumefaciens* strains harbouring a nopaline-type *vir* regulon compared with those harbouring an octopine-type *vir* regulon. Higher levels of certain *vir* products, such as VirD1 and VirD2 allow for enhanced T-strand production without the requirement of an *overdrive* (De Vos and Zambryski, 1989). Results from this Thesis suggest that the nopaline-type *vir* strains could compensate for the deletions in the putative *overdrive* region compared with octopine-type *vir* strains. This indicates that the nopaline-type *vir* environment may provide a less sensitive system for assaying the influence of such small deletions upon plant transformation frequency.

The putative nopaline-type *overdrive* was also shown to influence T-DNA copy number in transformed *Nicotiana tabacum*. Removal of either the 15 bp or the 36 bp portion containing the nopaline-type putative *overdrive* core reduced the incidence of multiple T-DNA insertion events by 50% such that 86% of the plants had a single T-DNA insert. Furthermore, the spread of T-DNA copy numbers was reduced from more than four to a maximum of two. This is the first time that a link has been made between *overdrive* and T-DNA copy number, and it is possibly related to frequency of T-DNA transfer.

REFERENCES

Albright, L. M.; Yanofsky, M. F.; LeRoux, B.; Ma, D.; Nester, E. (1987). Processing of the T-DNA of *Agrobacterium tumefaciens* generates border nicks and linear single-stranded T-DNA. *Journal of Bacteriology* **169**: 1046-1055.

Allen, G. C.; Hall, G. Jr; Michalowski, S.; Newman, W.; Spiker, S.; Weissinger, A. K.; Thompson, W. F. (1996). High-level transgene expression in plant cells: effects of a strong scaffold attachment region from tobacco. *The Plant Cell* **8**: 899-913.

Ankenbauer, R. G.; Nester, E. W. (1990). Sugar-mediated induction of *Agrobacterium tumefaciens* virulence genes: structural specifity and activities of monosaccharides. *Journal of Bacteriology* **172**: 6442-6446.

Bakkeren, G.; Koukolíková-Nicola, Z; Grimsley, N.; Hohn, B. (1989). Recovery of Agrobacterium tumefaciens T-DNA molecules from whole plants early after transfer. *Cell* **57**: 847-857.

Bergeron, J.; Macleod, R. A.; Dion, P. (1990). Specifity of octopine uptake by *Rhizobium* and *Pseudomonas* strains. *Applied and Environmental Microbiology* **56**: 1453-1458.

Beringer, J. E. (1974). R factor transfer in *Rhizobium leguminosarum*. *Journal of General Microbiology* **84**: 188-198.

Bevan, M. (1984). Binary *Agrobacterium* vectors for plant transformation. *Nucleic Acids Research* **12**: 8711-8721.

Bevan, M. W.; Chilton, M. D. (1982). T-DNA of *Agrobacterium* Ti and Ri plasmids. *Annual Review of Genetics* **16**: 357-384.

Birnboim, H. C.; Doly, J. (1979). A rapid alkaline extraction procedure for screening recombinant plasmid DNA. *Nucleic Acids Research* **7**: 1513-1523.

Boyer, H. W.; Roulland-Dussoix, D. (1969). A complementation analysis of the restriction and modification of DNA in *Escherichia coli*. *Journal of Molecular Biology* **41**: 459-472.

Chalepakis, G.; Beato, M. (1989). Hydroxyl radical interference: a new method for the study of protein-DNA interactions. *Nucleic Acids Research* **17**: 1783.

Chambers, S. P.; Prior, S. E.; Barstow, D. A.; Minton, N. P. (1988). The pMTL*nic*$^-$ cloning vectors. I. Improved pUC polylinker regions to facilitate the use of sonicated DNA for nucleotide sequencing. *Gene* **68**: 139-149.

Chang, C. -H.; Winans, S. C. (1992). Functional roles assigned to the periplasmic, linker, and receiver domains of the *Agrobacterium tumefaciens* VirA protein. *Journal of Bacteriology* **174**: 7033-7039.

Chaudhury, A. M.; Signer, E. R. (1989). Non-destructive transformation of *Arabidopsis*. *Plant Molecular Biology Reporter* **7**: 258-265.

Chen, C. -Y.; Winans, S. C. (1991). Controlled expression of the transcriptional activator gene *virG* in *Agrobacterium tumefaciens* by using the *Escherichia coli lac* promoter. *Journal of Bacteriology* **173**: 1139-1144.

Chilton, M. -D.; Currier, T.; Farrand, S. K.; Bendich, A. J.; Gordon, M. P.; Nester, E. W. (1974). *Agrobacterium tumefaciens* DNA and PS8 bacteriophage DNA not detected in crown gall tumors. *Proceedings of the National Academy of Sciences, USA* **71**: 3672-3676.

Chomczynski, P. (1992). One-hour downward alkaline capillary transfer for blotting of DNA and RNA. *Analytical Biochemistry* **201**: 134-139.

Church, G. M.; Gilbert, W. (1984). Genomic sequencing. *Proceedings of the National Academy of Sciences, USA* **81**: 1991-1995.

Citovsky, V.; Warnick, D.; Zambryski, P. (1994). Nuclear import of *Agrobacterium* VirD2 and VirE2 proteins in maize and tobacco. *Proceedings of the National Academy of Sciences, USA* **91**: 3210-3214.

Citovsky, V.; Zupan, J.; Warnick, D.; Zambryski, P. (1992). Nuclear localization of *Agrobacterium* VirE2 protein in plant cells. *Science* **256**: 1802-1805.

Clarke, M. C.; Wenbin, W.; Lyndsey, K. (1992). High-frequency transformation of *Arabidopsis thaliana* by *Agrobacterium tumefaciens*. *Plant Molecular Biology Reporter* **10**: 178-189.

Close, T. J.; Rogowsky, P. M.; Kado, C. I.; Winans, S. C.; Yanofsky, M. F.; Nester, E. W. (1987). Dual control of *Agrobacterium tumefaciens* Ti plasmid virulence genes. *Journal of Bacteriology* **169**: 5113-5118.

Close, T. J.; Tait, R. C.; Kado, C. I. (1985). Regulation of Ti plasmid virulence genes by a chromosomal locus of *Agrobacterium tumefaciens*. *Journal of Bacteriology* **164**: 774-781.

Culianez-Macia, F. A.; Hepburn, A. G. (1988a). Right border sequences enable the left border of an *Agrobacterium tumefaciens* nopaline Ti-plasmid to produce single-stranded DNA. *Plant Molecular Biology* **11**: 389-399.

De Cleene, M.; De Ley, J. (1976). The host range of crown gall. *The Botanical Review* **46**: 389-466.

Denhardt, D. A. (1966). A membrane-filter technique for the detection of complementary DNA. *Biochemical and Biophysical Research Communications* **23**: 641-646.

Deroles, S. C.; Gardner, R. C. (1988a). Expression and inheritance of kanamycin resistance in a large number of transgenic petunias generated by *Agrobacterium*-mediated transformation. *Plant Molecular Biology* **11**: 355-364.

Deroles, S. C.; Gardner, R. C. (1988b). Analysis of the T-DNA structure in a large number of transgenic petunias generated by *Agrobacterium*-mediated transformation. *Plant Molecular Biology* **11**: 365-377.

Dessaux, Y.; Petit, A.; Tempé, J. (1993). Chemistry and biochemistry of opines, chemical mediators of parasitism. *Phytochemistry* **34**: 31-38.

De Vos, G.; Zambryski, P. (1989). Expression of *Agrobacterium* nopaline-specific VirD1, VirD2, and VirC1 proteins and their requirement for T-strand production in *E. coli*. *Molecular Plant-Microbe Interactions* **2**: 43-52.

Ditta, G.; Stanfield, S.; Corbin, D.; Helinski, D. R. (1980). Broad host-range DNA cloning system for Gram-negative bacteria: construction of a gene bank of *Rhizobium meliloti*. *Proceedings of the National Academy of Sciences, USA* **77**: 7347-7351.

Dixon, W. J.; Hayes, J. J.; Levin, J. R.; Weidner, M. F.; Dombroski, B. A.; Tullius, T. D. (1991). Hydroxyl radical footprinting. *Methods in Enzymology* **208**: 380-413.

Doyle, J. J.; Doyle, J. L. (1987). A rapid DNA isolation procedure for small quantities of fresh leaf tissue. *Phytochemical Bulletin* **19**: 11-15.

Doyle, J. J.; Doyle, J. L. (1990). Isolation of plant DNA from fresh tissue. *Focus* **12**: 13-15.

D'Souza-Ault, M.; Cooley, M. B.; Kado, C. I. (1993). Analysis of the Ros repressor of *Agrobacterium virC* and *virD* operons: molecular intercommunication between plasmid and chromosomal genes. *Journal of Bacteriology* **175**: 3486-3490.

Dürrenberger, F.; Cramer, A.; Holm, B.; Koukolíková-Nicola, Z. (1989). Covalently bound VirD2 protein of *Agrobacterium tumefaciens* protects the T-DNA from exonucleolytic degradation. *Proceedings of the National Academy of Sciences, USA* **86**: 9154-9158.

Fang, G.; Hammar, S.; Grumet, R. (1993). A quick and inexpensive method for removing polysaccharides from plant genomic DNA. *BioTechniques* **13**: 52-56.

Feldmann, K. A. (1991). T-DNA insertion mutagenesis in *Arabidopsis*: mutational spectrum. *The Plant Journal* **1**: 71-82.

Filichkin, S. A.; Gelvin, S. B. (1993). Formation of a putative relaxation intermediate during T-DNA processing directed by *Agrobacterium tumefaciens* VirD1, D2 endonuclease. *Molecular Microbiology* **8**: 915-926.

Finnegan, J.; McElroy, D. (1994). Transgene inactivation: plants fight back! *Bio/Technology* **12**: 883-888.

Fobert, P. R.; Miki, B. L.; Iyer, V. N. (1991). Detection of gene regulatory signals in plants revealed by T-DNA-mediated fusions. *Plant Molecular Biology* **17**: 837-851.

Fuqua, C.; Winans, S. C. (1996). Conserved *cis*-acting promoter elements are required for density-dependent transcription of *Agrobacterium tumefaciens* conjugal transfer genes. *Journal of Bacteriology* **178**: 435-440.

Fuqua, W. C.; Winans, S. C.; Greenberg, E. P. (1994). Quorum sensing in bacteria: the LuxR-LuxI family of cell density-responsive transcriptional regulators. *Journal of Bacteriology* **176**: 269-275.

Fürste, J. P.; Pansegrau, W.; Ziegelin, G.; Kröger, M.; Lanka, E. (1989). Conjugative transfer of promiscuous IncP plasmids: interaction of plasmid-encoded products with the transfer origin. *Proceedings of the National Academy of Sciences, USA* **86**: 1771-1775.

Gamborg, O. L.; Miller, R. A.; Ojima, K. (1968). Nutrient requirements of suspension cultures of soybean root cells. *Experimental Cell Research.* **50**: 151-158.

Garfinkel, D. J.; Nester, E. W. (1980). *Agrobacterium tumefaciens* mutants affected in crown gall tumorigenesis and octopine catabolism. *Journal of Bacteriology.* **144**: 732-743.

Gelvin, S. B.; Thomashow, M. F.; McPherson, J. C.; Gordon, M. P.; Nester, E. W. (1982). Sizes and map positions of several plasmid DNA-encoded transcripts in octopine-type crown gall tumors. *Proceedings of the National Academy of Sciences, USA* **79**: 76-80.

Ghai, J.; Das, A. (1989). The *virD* operon of *Agrobacterium tumefaciens* Ti plasmid encodes a DNA-relaxing enzyme. *Proceedings of the National Academy of Sciences, USA* **86**: 3109-3113.

Gheyson, G.; Villarroel, R.; Van Montagu, M. (1991). Illegitimate recombination in plants: a model for T-DNA integration. *Genes and Development* **5**: 287-297.

Greene, E. A.; Zambryski, P. C. (1993). *Agrobacteria* mate in opine dens. *Current Biology* **3**: 507-509.

Grevelding, C.; Fantes, V.; Kemper, E.; Schell, J.; Masterson, R. (1993). Single-copy T-DNA insertions in *Arabidopsis* are the predominant form of integration in root-derived transgenics, whereas multiple insertions are found in leaf discs. *Plant Molecular Biology* **23**: 847-860.

Guerineau, F.; Woolston, S.; Brooks, L.; Mullineaux, P. (1988). An expression cassette for targeting foreign proteins into chloroplasts. *Nucleic Acids Research* **23**: 11380.

Guyon, P.; Petit, A.; Tempé, J.; Dessaux, Y. (1993). Transformed plants producing opines specifically promote growth of opine-degrading *Agrobacteria*. *Molecular Plant-Microbe Interactions* **6**: 92-98.

Hajdukiewicz, P.; Svab, Z.; Maliga, P. (1994). The small, versatile *pPZP* family of *Agrobacterium* binary vectors for plant transformation. *Plant Molecular Biology* **25**: 989-994.

Hangarter, R. P.; Stasinopoulos, T. C. (1991). Effect of Fe-catalysed photooxidation on root growth in plant culture media. *Plant Physiology* **96**: 843-847.

Herrera-Estrella, A.; Van Montagu, M.; Wang, K. (1990). A bacterial peptide acting as a plant nuclear targeting signal: the amino-terminal portion of *Agrobacterium* VirD2 protein directs a β-galactosidase fusion protein into tobacco nuclei. *Proceedings of the National Academy of Sciences, USA* **87**: 9534-9537.

Hille, J.; Wullems, G.; Schilperoort, R. (1983). Non-oncogenic T-region mutants of *Agrobacterium tumefaciens* do transfer T-DNA into plant cells. *Plant Molecular Biology* **2**: 155-163.

Hirooka, T.; Kado, C. I. (1986). Location of the right boundary of the virulence region on *Agrobacterium tumefaciens* plasmid pTiC58 and a host specifying gene next to the boundary. *Journal of Bacteriology* **168**: 237-243.

Hoekema, A.; Hirsch, P. R.; Hooykaas, P. J. J.; Schilperoort, R. A. (1983). A binary plant vector strategy based on separation of *vir*- and T-region of the *Agrobacterium tumefaciens* Ti-plasmid. *Nature* **303**: 179-180.

Holmes, D. S.; Quigley, M. (1981). A rapid boiling method for the preparation of bacterial plasmids. *Analytical Biochemistry* **114**: 193-197.

Holsters, M.; Silva, B.; Van Vliet, F.; Genetello, C.; De Block, M.; Dhaese, P.; Depicker, A.; Inzé, D.; Engler, G.; Villarroel, R.; Van Montagu, M.; Schell, J. (1980). The functional organisation of the nopaline *A. tumefaciens* plasmid pTiC58. *Plasmid* **3**: 212-230.

Hooykaas, P. J. J.; Beijersbergen, A. G. M. (1994). The virulence system of *Agrobacterium tumefaciens*. *Annual Reviews of Phytopathology* **32**: 157-179.

Hooykaas, P. J. J.; Den Dulk-Ras, H.; Ooms, G.; Schilperoort, R. A. (1980). Interactions between octopine and nopaline plasmids in *Agrobacterium tumefaciens*. *Journal of Bacteriology* **143**: 1295-1306.

Hooykaas, P. J. J.; Schilperoort, R. A. (1992). *Agrobacterium* and plant genetic engineering. *Plant Molecular Biology* **19**: 15-38.

Horsch, R. B.; Fry, J. E.; Hoffman, N. L.; Eichholtz, D.; Rogers, S. G.; Fraley, R. T. (1985). A simple and general method for transferring genes into plants. *Science* **227**: 1229-1231.

Ish-Horowitz, D.; Burke, J. F. (1981). Rapid and efficient cosmid cloning. *Nucleic Acids Research* **9**: 2989-2998.

Jayaswal, R. K.; Veluthambi, K.; Gelvin, S. B.; Slightom, J. L. (1987). Double-stranded cleavage of T-DNA and generation of single-stranded T-DNA molecules in *Escherichia coli* by a *virD*-encoded border-specific endonuclease from *Agrobacterium tumefaciens*. *Journal of Bacteriology* **169**: 5035-5045.

Jen, G. C.; Chilton, M. -D. (1986a). Activity of T-DNA borders in plant cell transformation by mini-T plasmids. *Journal of Bacteriology* **166**: 491-499.

Jen, G. C.; Chilton, M. -D. (1986b). The right border region of pTiT37 T-DNA is intrinsically more active than the left border region in promoting T-DNA transformation. *Proceedings of the National Academy of Sciences, USA.* **83**: 3895-3899.

Ji, J. M.; Martinez, A.; Dabrowski, M.; Veluthambi, K.; Gelvin, S. B.; Ream, W. (1989). The *overdrive* enhancer sequence stimulates production of T-strands from the *Agrobacterium tumefaciens* tumor-inducing plasmid. p. 19-31. In *Molecular Biology of Plant-Pathogen Interactions* (*UCLA Symposia of Molecular and Cellular Biology; New Series Vol. 101*). Edited by Staskawicz, B.; Ahlquist, P.; Yoder, O. New York: Alan R. Riss, Inc.

Jones, J. D. G.; Shlumukov, L.; Carland, F.; English, J.; Scofield, S. R.; Bishop, G. J.; Harrison, K. (1992). Effective vectors for transformation, expression of heterologous genes, and assaying transposon excision in transgenic plants. *Transgenic Research* **1**: 285-297.

Joos, H.; Inzé, D.; Caplan, A.; Sormann, M.; Van Montagu, M.; Schell, J. (1983a). Genetic analysis of T-DNA transcripts in nopaline crown galls. *Cell* **32**: 1057-1067.

Kado, C. I. (1991). Molecular mechanisms of crown gall tumorigenesis. *Critical Reviews in Plant Sciences* **10**: 1-32.

Kado, C. I. (1994). Promiscuous DNA transfer system of *Agrobacterium tumefaciens*: role of the *virB* operon in sex pilus assembly and synthesis. *Molecular Microbiology* **12**: 17-22.

Kerr, D. H. (1996). T-DNA promoter tagging in *Nicotiana tabacum.* Thesis, Ph.D. (submitted), Massey University, Palmerston North, New Zealand.

Kertbundit, S.; De Greve, H.; Deboeck, F.; Van Montagu, M.; Hernalsteens, J. -P. (1991). *In vivo* random β-glucuronidase gene fusions in *Arabidopsis thaliana. Proceedings of the National Academy of Sciences, USA* **88**: 5212-5216.

Koncz, C.; Martini, N.; Mayerhofer, R.; Koncz-Kalman, Z.; Körber, H.; Redei, G. P.; Schell, J. (1989). High-frequency T-DNA-mediated gene tagging in plants. *Proceedings of the National Academy of Sciences, USA* **86**: 8467-8471.

Koncz, C.; Schell, J. (1986). The promoter of the T_L-DNA gene 5 controls the tissue-specific expression of chimaeric genes carried by a novel type of *Agrobacterium* binary vector. *Molecular and General Genetics* **204**: 383-396.

Lessl, M.; Balzer, D.; Weyrauch, K.; Lanka, E. (1993). The mating pair formation system of plasmid RP4 defined by RSF1010 mobilization and donor-specific phage propagation. *Journal of Bacteriology* **175**: 6415-6425.

Lessl, M.; Lanka, E. (1994). Common mechanisms in bacterial conjugation and Ti-mediated T-DNA transfer to plant cells. *Cell* **77**: 321-324.

Lindsey, K.; Wei, W.; Clarke, M. C.; McArdle, H. F.; Rooke, L. M.; Topping, J. F. (1993). Tagging genomic sequences that direct transgene expression by activation of a promoter trap in plants. *Transgenic Research* **2**: 33-47.

Lorow, D.; Jessee, J. (1990). MAX efficiency DH10B™: a new host for cloning methylated DNA. *Focus* **12**: 19-20.

McBride, K. E.; Knauf, V.C. (1988). Genetic analysis of the *virE* operon of the *Agrobacterium* Ti plasmid pTiA6. *Journal of Bacteriology* **170**: 1430-1437.

McNeil, M.; Darvil, A. G.; Fry, S. C.; Albersheim, P. (1984). Structure and function of the primary cell wall in plants. *Annual Review of Biochemistry* **53**: 625-633.

Mantis, N. J.; Winans, S. C. (1992). The *Agrobacterium tumefaciens vir* gene transcriptional activator *virG* is transcriptionally induced by acid pH and other stress stimuli. *Journal of Bacteriology* **174**: 1189-1196.

Martineau, B.; Voelker, T. A.; Sanders, R. A. (1994). On defining T-DNA. *The Plant Cell* **6**: 1032-1033.

Márton, L.; Browse, J. (1991). Facile transformation of *Arabidopsis*. *Plant Cell Reports* **10**: 235-239.

Mattanovich, D.; Rüker, F.; da Câmara Machado, A.; Laimer, M.; Regner, F.; Steinkellner, H.; Himmler, G.; Katinger, H. (1989). Efficient transformation of *Agrobacterium* spp. by electroporation. *Nucleic Acids Research* **17**: 6747.

Matzke, M. A.; Matzke, A. J. M. (1995). How and why do plants inactivate homologous (trans)genes? *Plant Physiology* **107**: 679-685.

Michaels, S. D.; John, M. C.; Amasino, R. M. (1994). Removal of polysaccharides from plant DNA by ethanol precipitation. *BioTechniques* **17**: 274-276.

Mozo, T.; Hooykaas, P. J. J. (1992). Factors affecting the rate of T-DNA transfer from *Agrobacterium tumefaciens* to *Nicotiana glauca* plant cells. *Plant Molecular Biology* **19**: 1019-1030.

Murashige, T.; Skoog, F. (1962). A revised medium for rapid growth and bio assays with tobacco tissue cultures. *Physologia Plantarum* **15**: 473-497.

Nester, E. W.; Gordon, M. P.; Amasino, R. M.; Yanofsky, M. F. (1984). Crown gall: a molecular and physiological analysis. *Annual Review of Plant Physiology* **35**: 387-413.

Oerter, K. E.; Munson, P. J.; McBride, W. O.; Rodbard, D. (1990). Computerised estimation of size of nucleic acid fragments using the four-parameter logistic model. *Analytical Biochemistry* **189**: 235-243.

Ooms, G.; Hooykaas, P. J. J.; Van Veen, R. J. M.; Van Beelen, P.; Regensburg-Tuïnk, T. J. G.; Schilperoort, R. A. (1982). Octopine Ti-plasmid deletion mutants of *Agrobacterium tumefaciens* with emphasis on the right side of the T-region. *Plasmid* **7**: 15-29.

Pansegrau, W.; Lanka, E.; Barth, P. T.; Figurski, D. H.; Guiney, D. G.; Haas, D.; Helinski, D. R.; Schwab, H.; Stanisich, V. A.; Thomas, C. M. (1994a). Complete nucleotide sequence of Birmingham IncPα plasmids: compilation and comparative analysis. *Journal of Molecular Biology* **239**: 623-663.

Pansegrau, W.; Schoumacher, F.; Hohn, B.; Lanka, E. (1993a). Site-specific cleavage and joining of single-stranded DNA by VirD2 protein of *Agrobacterium tumefaciens* Ti plasmids: analogy to bacterial conjugation. *Proceedings of the National Academy of Sciences, USA* **90**: 11538-11542.

Pansegrau, W.; Schröder, W.; Lanka, E. (1993b). Relaxase (TraI) of IncPα plasmid RP4 catalyzes a site-specific cleaving-joining reaction of single-stranded DNA. *Proceedings of the National Academy of Sciences, USA* **90**: 2925-2929.

Pansegrau, W.; Schröder, W.; Lanka, E. (1994b). Concerted action of three distinct domains in the DNA cleaving-joining reaction catalysed by relaxase (TraI) of conjugative plasmid RP4. *Journal of Bacteriology* **269**: 2782-2789.

Pansegrau, W.; Ziegelin, G.; Lanka, E. (1990). Covalent association of the *traI* gene product of plasmid RP4 with the 5′-terminal nucleotide at the relaxation nick site. *The Journal of Biological Chemistry* **265**: 10637-10644.

Pazour, G. J.; Das, A. (1990). *virG*, an *Agrobacterium tumefaciens* transcriptional activator, initiates translation at a UUG codon and is a sequence-specific DNA-binding protein. *Journal of Bacteriology* **172**: 1241-1249.

Peralta, E. G.; Hellmiss, R.; Ream, W. (1986). *Overdrive*, a T-DNA transmission enhancer on the *A. tumefaciens* tumour-inducing plasmid. *The EMBO Journal* **5**: 1137-1142.

Peralta, E. G.; Ream, L. W. (1985). T-DNA border sequences required for crown gall tumorigenesis. *Proceedings of the National Academy of Sciences, USA* **82**: 5112-5116.

Petit, A.; Tempé, J. (1985). The function of T-DNA in nature, p. 625-636. *In* van Vloten-Doting, L.; Groot, G.; Hall, T. (ed). *Molecular Form and Function of the Plant Genome.* Plenum Publishing Corp. N.Y. (cited in Winans, 1992).

Rago, R.; Mitchen, J.; Wilding; G. (1990). DNA fluorometric assay in 96-well tissue culture plates using Hoechst 33258 after cell lysis by freezing in distilled water. *Analytical Biochemistry* **191**: 31-34.

Ream, W. (1989). *Agrobacterium tumefaciens* and interkingdom genetic exchange. *Annual Review of Phytopathology* **27**: 583-618.

Reed, K. C.; Mann, D. A. (1985). Rapid transfer of DNA from agarose gels to nylon membranes. *Nucleic Acids Research* **13**: 7207-7221.

Regensberg-Tuïnk, A. J. G.; Hooykaas, P. J. J. (1993). Transgenic *N. glauca* plants expressing bacterial virulence gene *virF* are converted into hosts for nopaline strains of *A. tumefaciens*. *Nature* **363**: 69-71.

Rogowsky, P. M.; Close, T. J.; Chimera, J. A.; Shaw, J. J.; Kado, C. I. (1987). Regulation of the *vir* genes of *Agrobacterium tumefaciens* plasmid pTiC58. *Journal of Bacteriology* **169**: 5101-5112.

Rogowsky, P. M.; Powell, B. S.; Shirasu, K.; Lin, T.- S.; Morel, P.; Zyprian, E. M.; Steck, T. R.; Kado, C. I. (1990). Molecular characterization of the *vir* regulon of *Agrobacterium tumefaciens*: complete nucleotide sequence and gene organisation of the 28.63-kbp regulon cloned as a single unit. *Plasmid* **23**: 85-106.

Roitsch, T.; Wang, H,; Jin, S.; Nester, E. (1990). Mutational analysis of the VirG protein, a transcriptional activator of *Agrobacterium tumefaciens* virulence genes. *Journal of Bacteriology* **172**: 6054-6060.

Sambrook, J.; Fritsch, E. F.; Maniatis, T. (eds) (1989). *Molecular Cloning - A Laboratory Manual*. 2nd Ed. Cold Spring Harbor Laboratory Press.

Sanderfoot, A. A.; Ingham, D. J.; Lazarowitz, S. G. (1996). A viral protein as a nuclear shuttle. *Plant Physiology* **110**: 23-33.

Sanger, F.; Niklen, S.; Coulson, A. R. (1977). DNA sequencing with chain-terminating inhibitors. *Proceedings of the National Academy of Sciences, USA* **74**: 5436-5467.

Sauerwein, M.; Wink, M. (1993). On the role of opines in plants transformed with *Agrobacterium rhizogenes*: tropane alkaloid metabolism, insect-toxicity and allelopathic properties. *Journal of Plant Physiology* **142**: 446-451.

Savka, M. A.; Black, R. C.; Binns, A. N.; Farrand, S. K. (1996). Translocation and exudation of tumor metabolites in crown galled plants. *Molecular Plant-Microbe Interactions* **9**: 310-313.

Scheiffele, P.; Pansegrau, W.; Lanka, E. (1995). Initiation of *Agrobacterium tumefaciens* T-DNA processing. *Journal of Biological Chemistry* **270**: 1269-1276.

Shaw, C. H. (1993). New insights on T-DNA transfer. *Trends in Microbiology* **1**: 325-327.

Shaw, C. H.; Watson, M. D.; Carter, G. H.; Shaw, C. H. (1984). The right hand copy of the nopaline Ti-plasmid 25 bp repeat is required for tumour formation. *Nucleic Acids Research* **12**: 6031-6041.

Sheikholeslam, S. N.; Weeks, D. P. (1987). Acetosyringone promotes high efficiency transformation of *Arabidopsis thaliana* explants by *Agrobacterium tumefaciens*. *Plant Molecular Biology* **8**: 291-298.

Shurvinton, C. E.; Hodges, L.; Ream, W. (1992). A nuclear localization signal and the C-terminal omega sequence in the *Agrobacterium tumefaciens* VirD2 endonuclease are important for tumor formation. *Proceedings of the National Academy of Sciences, USA* **89**: 11837-11841.

Shurvinton, C. E.; Ream, W. (1991). Stimulation of *Agrobacterium tumefaciens* T-DNA transfer by overdrive depends on a flanking sequence but not on helical position with respect to the border repeat. *Journal of Bacteriology* **173**: 5558-5563.

Singh, A.; Kao, T. -H.; Lin, J. -J. (1993). Transformation of *Agrobacterium tumefaciens* with T-DNA vectors using high-voltage electroporation. *Focus* **15**: 84-87.

Srinivasan; Yanofsky, M. F.; Nester, E. W. (1989). 25-bp long border sequence of T-DNA is sufficient for cleavage by *vir*D endonuclease of *Agrobacterium*. *Journal of Genetics* **68**: 161-170.

Stachel, S. E.; Messens, E.; Van Montagu, M.; Zambryski, P. (1985). Identification of the signal molecules produced by wounded plants that activate T-DNA transfer in *Agrobacterium tumefaciens*. *Nature* **318**: 624-629.

Stachel, S. E.; Nester, E. W. (1986). The genetic and transcriptional organization of the *vir* region of the A6 Ti plasmid of *Agrobacterium tumefaciens*. *The EMBO Journal* **5**: 1445-1454.

Stachel, S. E.; Timmerman, B.; Zambryski, P. (1986). Generation of single-stranded T-DNA molecules during the initial stages of T-DNA transfer from *Agrobacterium tumefaciens* to plant cells. *Nature* **322**: 706-712.

Stachel, S. E.; Timmerman, B.; Zambryski, P. (1987). Activation of *Agrobacterium tumefaciens vir* gene expression generates multiple single-stranded T-strand molecules from the pTiA6 T-region: requirement for 5′ *vir*D gene products. *The EMBO Journal* **6**: 857-963.

Stachel, S. E.; Zambryski, P. C. (1986). *virA* and *virG* control the plant-induced activation of the T-DNA transfer process of *Agrobacterium tumefaciens*. *Cell* **46**: 325-333.

Steck, T. R.; Morel, P.; Kado, C. I. (1988). *vir* box sequences in *Agrobacterium tumefaciens* pTiC58 and A6. *Nucleic Acids Research* **16**: 8736-

Tabor, S.; Richardson, C. C. (1989). Selective inactivation of the exonuclease activity of bacteriophage T7 DNA polymerase by *in vitro* mutagenesis. *Journal of Biological Chemistry* **264**: 6447-6458.

Tinland, B.; Hohn, B.; Puchta, H. (1994). *Agrobacterium tumefaciens* transfers single-stranded transferred DNA (T-DNA) into the plant cell nucleus. *Proceedings of the National Academy of Sciences, USA* **91**: 8000-8004.

Tinland, B.; Koukolíková-Nicola, Z.; Hall, M. N.; Hohn, B. (1992). The T-DNA-linked VirD2 protein contains two distinct functional nuclear localisation signals. *Proceedings of the National Academy of Sciences, USA* **89**: 7442-7446.

Toro, N.; Datta, A.; Carmi, O.; Young, C.; Prusti, R. K.; Nester, E. W. (1989). The *Agrobacterium tumefaciens virC1* gene product binds to overdrive, a T-DNA transfer enhancer. *Journal of Bacteriology* **171**: 6845-6849.

Toro, N.; Datta, A.; Yanofsky, M.; Nester, E. (1988). Role of the overdrive sequence in T-DNA border cleavage in *Agrobacterium*. *Proceedings of the National Academy of Sciences, USA* **85**: 8558-8562.

Valvekens, D.; Van Montagu, M; Van Lisjebettens, M. (1988). *Agrobacterium tumefaciens*-mediated transformation of *Arabidopsis thaliana* root explants by using kanamycin selection. *Proceedings of the National Academy of Sciences, USA* **85**: 5536-5540.

Vande Broek, A.; Vanderleyden, J. (1995). The role of bacterial motility, chemotaxis, and attachment in bacteria-plant interactions. *Molecular Plant-Microbe Interactions* **8**: 800-810.

Van Haaren, M. J. J.; Pronk, J. T.; Schilperoort, R. A.; Hooykaas, P. J. J. (1987a). Functional analysis of the *Agrobacterium tumefaciens* octopine Ti-plasmid left and right T-region border fragments. *Plant Molecular Biology* **8**: 95-104.

Van Haaren, M. J. J.; Sedee, N. J. A.; Krul, M.; Schilperoort, R. A.; Hooykaas, P. J. J. (1988). Function of heterologous and pseudo border repeats in T-region transfer via the octopine virulence system of *Agrobacterium tumefaciens*. *Plant Molecular Biology* **11**: 773-781.

Van Haaren, M. J. J.; Sedee, N. J. A.; Schilperoort, R. A.; Hooykaas, P. J. J. (1987b). Overdrive is a T-region transfer enhancer which stimulates T-strand production in *Agrobacterium tumefaciens*. *Nucleic Acids Research* **15**: 8988-8997.

Veluthambi, K.; Jayaswal, R. K.; Gelvin, S. B. (1987). Virulence genes *A*, *G*, and *D* mediate the double-stranded border cleavage of T-DNA from the *Agrobacterium* Ti plasmid. *Proceedings of the National Academy of Sciences, USA* **84**: 1881-1885.

Veluthambi, K.; Ream, W.; Gelvin, S. B. (1988). Virulence genes, borders, and overdrive generate single-stranded T-DNA molecules from the A6 Ti plasmid of *Agrobacterium tumefaciens*. *Journal of Bacteriology* **170**: 1523-1532.

Vervliet, G.; Holsters, M.; Teuchy, H.; Van Montagu, M.; Schell, J. (1975). Characterization of different plaque-forming and defective temperate phages in *Agrobacterium* strains. *Journal of General Virology* **26**: 33-48.

Vogel, A. M.; Das, A. (1992). Mutational analysis of *Agrobacterium tumefaciens virD2*: tyrosine 29 is essential for endonuclease activity. *Journal of Bacteriology* **174**: 303-308.

Vogelstein, B.; Gillespie, D. (1979). Preparative and analytical purification of DNA from agarose. *Proceedings of the National Academy of Sciences, USA* **76**: 615-619.

Wang, K.; Genetello, C.; Van Montagu, M.; Zambryski, P. C. (1987). Sequence context of the T-DNA border repeat element determines its relative activity during T-DNA transfer to plant cells. *Molecular and General Genetics* **210**: 338-346.

Wang, K.; Herrera-Estrella, A.; Van Montagu, M. (1990). Overexpression of *virD1* and *virD2* genes in *Agrobacterium tumefaciens* enhances T-complex formation and plant transformation. *Journal of Bacteriology* **172**: 4432-4440.

Wang, K.; Herrera-Estrella, L.; Van Montagu, M.; Zambryski, P. (1984). Right 25 bp terminus sequence of the nopaline T-DNA is essential for and determines direction of DNA transfer from Agrobacterium to the plant genome. *Cell* **38**: 455-462.

Waters, V. L.; Guiney, D. G. (1993). Processes at the nick region link conjugation, T-DNA transfer and rolling circle replication. *Molecular Microbiology* **9**: 1123-1130.

Waters, V. L.; Hirata, K. H.; Pansegrau, W.; Lanka, E.; Guiney, D. G. (1991). Sequence identity in the nick regions of IncP plasmid transfer origins and T-DNA borders of *Agrobacterium* Ti plasmids. *Proceedings of the National Academy of Sciences, USA* **88**: 1456-1460.

White, D. W. R.; Greenwood, D. (1987). Transformation of the forage legume *Trifolium repens* L. using binary *Agrobacterium* vectors. *Plant Molecular Biology* **8**: 461-469.

Willmitzer, L.; Simons, G.; Schell, J. (1982). The TL-DNA in octopine crown-gall tumours codes for seven well defined polyadenylated transcripts. *The EMBO Journal* **1**: 139-146.

Winans, S. C. (1992). Two-way chemical signalling in *Agrobacterium*-plant interactions. *Microbiological Reviews* **56**: 12-31.

Yanofsky, M. F.; Porter, S. G.; Young, C.; Albright, L. M.; Gordon, M. P.; Nester, E. W. (1986). The *virD* operon of *Agrobacterium tumefaciens* encodes a site specific endonuclease. *Cell* **47**: 471-477.

Yanisch-Perron, C.; Vieira, J.; Messing, J. (1985). Improved M13 phage cloning vectors and host strains: nucleotide sequences of the M13mp18 and pUC19 vectors. *Gene* **33**: 103-119.

Yusibov, V. M.; Steck, T. R.; Gupta, V.; Gelvin, S. B. (1994). Association of single-stranded transferred DNA from *Agrobacterium tumefaciens* with tobacco cells. *Proceedings of the National Academy of Sciences, USA* **91**: 2994-2998.

Zambryski, P. C. (1992). Chronicles from the *Agrobacterium*-plant cell DNA transfer story. *Annual Reviews in Plant Physiology and Plant Molecular Biology* **43**: 465-490.

Ziegelin, G.; Pansegrau, W.; Lurz, R.; Lanka, E. (1992). TraK protein of conjugative plasmid RP4 forms a specialized nucleoprotein complex with the transfer origin. *The Journal of Biological Chemistry* **267**: 17279-17286.

Zupan, J. R.; Zambryski, P. (1995). Transfer of T-DNA from *Agrobacterium* to the plant cell. *Plant Physiology* **107**: 1041-1047.

APPENDIX 1: BACTERIAL MEDIA

All media were sterilised at 121°C for 15 min. Liquid media were cooled to the desired growth temperature before bacterial inoculation, and the addition of antibiotics and other heat-labile compounds. Solid media were cooled to 50°C prior to the addition of antibiotic and heat-labile compounds, and pouring. For solid media, agar (Germantown) was added, before autoclaving, to a final concentration of 15 g l^{-1}. Prior to use, cool-stored plates were removed from storage for at least one hour and dried for 30 min in a laminar flow cabinet to prevent 'sweating'.

A1.1 AB Minimal Medium

AB medium (Chilton *et al.*, 1974) contained (g l^{-1}): dipotassium hydrogen orthophosphate (K_2HPO_4), 3.0; sodium dihydrogen orthophosphate ($NaH_2PO_4.2H_2O$), 1.3; ammonium chloride (NH_4Cl), 1.0; magnesium sulphate ($MgSO_4.7H_2O$), 0.3; potassium chloride (KCl), 0.15; calcium chloride ($CaCl_2.2H_2O$), 0.0132; ferrous sulphate ($FeSO_4.7H_2O$), 0.0025; and glucose, 5.0. To prevent caramelisation of the glucose due to prolonged exposure to heat, the medium was removed from the heat source immediately after autoclaving, and cooled quickly prior to pouring or storage.

A1.2 LB (Luria-Bertani) Medium

LB medium (Sambrook *et al.*, 1989) contained (g l^{-1}): tryptone (Difco) 10.0; yeast extract (Difco), 5.0; sodium chloride (NaCl), 10.0. Prior to autoclaving, the pH was adjusted to 7.0 with HCl.

A1.3 SOB Medium

SOB medium (Sambrook *et al.*, 1989) contained (g l^{-1}): tryptone (Difco), 20.0; yeast extract (Difco), 5.0; sodium chloride (NaCl), 0.5; potassium chloride (KCl), 0.186. Prior to autoclaving, the pH was adjusted to 7.0 with NaOH. Immediately before use, 5 ml of a sterile 2 M magnesium chloride ($MgCl_2$) solution was added.

A1.4 SOC Medium

SOC medium (Sambrook *et al.*, 1989) was identical to SOB medium, except that after autoclaving, the medium was supplemented with 10 ml of a filter-sterilised (Millipore 0.45 μm membrane filter) 2 M D-glucose solution.

A1.5 TY Medium

TY medium (Beringer, 1974; White, 1987) contained (g l^{-1}): tryptone (Difco), 5.0; yeast extract (Difco), 3.0; calcium chloride ($CaCl_2.2H_2O$) 0.87.

A1.6 YEB Medium

YEB medium (Vervliet, *et al.*, 1975) contained (g l^{-1}): beef extract (Sigma), 5.0; yeast extract (Difco), 1.0; peptone (Difco), 5.0; magnesium sulphate ($MgSO_4.7H_20$), 0.5; sucrose, 0.5.

A1.7 YM Medium

YM medium (Singh, *et al.*, 1993) contained (g l^{-1}): yeast extract, 0.4; mannitol, 10.0; sodium chloride (NaCl), 0.1; magnesium sulphate ($MgSO_4.7H_20$), 0.2; dipotassium hydrogen orthophosphate (K_2HPO_4), 0.5. Prior to autoclaving, the pH was adjusted to 7.0 with HCl.

APPENDIX 2: PLANT MEDIA

Plant media were treated the same way as bacterial media with regard to autoclaving, pouring, drying and storing (Section A1, p. 163). However, for solid media, agar (Difco) was added, prior to autoclaving, to a final concentration of 8 g l^{-1}.

A2.1 GM Medium

GM medium (Valvekens *et al.*, 1988), based upon MS stock solutions (Section A3.3, p. 167), consisted of (ml l^{-1}): each of MS stock solutions A and B, 20.0; each of MS stock solutions C, D, E, F, and G, 5.0; and (g l^{-1}): sucrose, 10.0; MES, 0.5; myo-inositol, 0.1. Prior to autoclaving, the pH was adjusted to 5.7 with 1 M KOH.

A2.2 ARM Media Base

ARM Media Base (Márton and Browse, 1991) was derived from MS stock solutions (Section A3.3, p. 167), except that stock solution G was replaced by Vitamix stock (Section A3.3, p. 167). The ARM Media Base consisted of (ml l^{-1}): each of MS stock solutions A and B, 20.0; each of MS stock solutions C, D, E, and F, 5.0; Vitamix stock, 5.0; and (g l^{-1}): sucrose, 30.0; myo-inositol, 0.2; potassium dihydrogen orthophosphate (KH_2PO_4), 0.18. Prior to autoclaving, the pH was adjusted to 5.7 with 1 M KOH.

A2.3 ARM I Medium

The ARM I medium (Márton and Browse, 1990) was the same as the ARM Media Base (Section A2.2), except the following phytohormone stock solutions (Section A3.2, p. 167) were added, prior to pH adjustment and autoclaving, to a final concentration of (mg l^{-1}): 2,4-D, 0.15; BAP, 0.6. After autoclaving, the following heat-labile phytohormone stock solutions (Section A3.2) were added to a final concentration of (mg l^{-1}): IAA, 3.0; and 2ip, 0.3. Where required, acetosyringone (Section A3.5, p. 168) and the *A. tumefaciens* antibiotic timentin (Section A3.1, p. 167) were also added, after autoclaving, to a final concentration of 200 μM and 100 mg l^{-1}, respectively.

A2.4 ARM II Medium

The ARM II medium (Márton and Browse, 1990) was the same as the ARM Media Base (Section A2.2, p. 165), except that NAA (Section A3.2, p. 167) was added, prior to pH adjustment and autoclaving, to a final concentration of 0.2 mg l^{-1}. After autoclaving, the heat-labile phytohormone stock 2ip (Section A3.2) was added to a final concentration of 4.0 mg l^{-1}. Where required, the medium was supplemented,

after autoclaving, with kanamycin (transgenic shoot selection) and timentin (Section A3.1, p. 167) to a final concentration of 50 μg l^{-1} and 100 mg l^{-1}, respectively.

A2.5 ARM III Medium

The ARM III medium (Márton and Browse, 1990) was the same as the ARM Media Base (Section A2.2), except that, prior to pH adjustment and autoclaving, IBA and IAA (Section A3.2, p. 167) were added to a final concentration of 0.5 mg l^{-1} and 1.0 mg l^{-1}, respectively. After autoclaving, Zeatin (Section A3.2) was added to a final concentration of 0.2 mg l^{-1}. Where required, the medium was supplemented, after autoclaving, with kanamycin (transgenic shoot selection) and timentin (Section A3.1, p. 167) to a final concentration of 50 μg l^{-1} and 100 mg l^{-1}, respectively. antibiotic.

A2.6 ½MS Medium

The ½MS medium was a half-strength derivative of the Murashige and Skoog (1962) MS medium. It consisted of (ml l^{-1}): each of MS stock solutions (Section A3.3, p. 167) A and B, 10.0; each of MS stock solutions C, D, E, F, and G, 2.5; and (g l^{-1}): sucrose, 15.0; and myo-inositol, 0.05. Prior to autoclaving, the pH was adjusted to 5.7 with 1 M KOH.

A2.7 Nic I Medium

The Nic I medium (Horsch *et al.* 1985), was based upon MS stock solutions (Section A3.3, p. 167), except that stock solution G was replaced by the B5 medium vitamin stock, B5-2 (Section A3.3, p. 167). The Nic I medium consisted of (ml l^{-1}): each of MS stock solution A and B, 20.0; each of MS stock solutions C, D, E, and F, 5.0; B5-2 vitamin stock, 1.0; and (g l^{-1}): sucrose, 30.0; and myo-inositol, 0.1. BAP and NAA (Section A3.2, p. 167) were added to a final concentration of 1.0 mg ml^{-1} and 0.1 mg ml^{-1}, respectively. Prior to autoclaving, the pH was adjusted to 5.7 with 1 M KOH.

A2.8 Nic II Medium

The Nic II shoot-initiating medium was the same as Nic I medium (above), except for the addition of kanamycin (transgenic shoot selection) and timentin (Section A3.1, p. 167) to a final concentration of 300 μg l^{-1} and 100 mg l^{-1}, respectively.

A2.9 Nic III Medium

The Nic III root-initiating medium was the same as Nic II medium (above), except that it did not contain phytohormones.

APPENDIX 3: MEDIA STOCK SOLUTIONS

A3.1 Antibiotics

In order to prepare stock solutions of Ap (ampicillin sodium salt), Cb (carbenicillin disodium salt), Km (kanamycin sulphate), Sm (streptomycin sulphate), Sp (spectinomycin dihydrochloride), the antibiotic was dissolved in MilliQ water, made up to volume, then filter sterilised (Millipore 0.45 μm membrane filter). Tc (tetracycline hydrochloride) and Rf (rifampicin) were dissolved in, and made up to volume with, absolute methanol. Tm (timentin) stock solution was prepared from a 15:1 (w/w) mixture of ticarcillin and clavulanic acid (SmithKline Beecham Pharmaceuticals), which was dissolved in MilliQ water and filter sterilised. All antibiotics were stored at -20°C for a maximum of three months.

A3.2 Phytohormones

To prepare phytohormone stock solutions, they were first dissolved in a minimal volume of 1 M NaOH, diluted to volume with MilliQ water, and filter sterilised (Millipore 0.45 μm membrane filter). IAA, IBA, 2ip, Kinetin, and Zeatin stocks were stored at -20°C for a maximum of three months, whereas 2,4-D, and BAP stocks were stored at 4°C for a maximum of three months.

A3.3 MS Stock Solutions

Plant tissue culture growth media based upon MS medium (Murashige and Skoog, 1962) were prepared from the following stock solutions:

A (g l^{-1}): ammonium nitrate (NH_4NO_3), 82.5

B (g l^{-1}): potassium nitrate (KNO_3), 95.0

C (g l^{-1}): boric acid (H_3BO_3), 1.24; potassium dihydrogen orthophosphate (KH_2PO_4), 34.0; potassium iodide (KI), 0.165; sodium molybdate ($Na_2MoO_4.2H_2O$), 0.05; cobaltous chloride ($CoCl_2.6H_2O$), 0.005.

D (g l^{-1}): calcium chloride ($CaCl_2.2H_2O$), 88.0

E (g l^{-1}): magnesium sulphate ($MgSO_4.7H_2O$), 74.0; manganous sulphate ($MnSO_4.4H_2O$), 4.46: zinc sulphate ($ZnSO_4.7H_2O$), 1.71; cupric sulphate ($CuSO_4.5H_2O$), 0.005.

F (g l^{-1}): EDTA (Fe) ($C_{10}H_{12}N_2NaFeO_8$), 8.0

G (g l^{-1}): thiamine.HCl, 0.02; nicotinic acid, 0.1; pyridoxine.HCl, 0.1; glycine, 0.4.

When preparing ARM media base (Section A2.2, p. 165), stock solution G was replaced with Vitamix stock, prepared as shown below:

Vitamix stock (g l^{-1}): thiamine.HCl, 2.0; pyridoxine.HCl, 0.2; nicotinic acid, 0.2; glycine, 0.4; d-biotin, 0.02.

When preparing Nic media (Section A2.7-A2.9, p. 166), stock solution G was replaced with B5 medium (Gamborg *et al.*, 1968) vitamin stock, B5-2, prepared as shown below:

B5-2 (g l^{-1}): nicotinic acid, 1.0; thiamine,.HCL, 10.0; pyridoxine.hcl, 1.0.

All stocks were filter sterilised (Millipore 0.45 μm membrane filter) and stored at 4°C, except for B5-2, which was stored at -20°C. Fresh stocks were made every three months.

A3.4 Acetosyringone

Acetosyringone (3', 5'-dimethoxy-4'-hydroxyacetophenone) (Aldrich Chemical Company) stock solution was prepared by first dissolving the compound in a minimal volume of DMSO, and making it up to volume with MilliQ water. The stock solution was then filter sterilised (Millipore 0.45 μm membrane filter) and stored in the dark at room temperature.

APPENDIX 4: SOLUTIONS AND BUFFERS FOR DNA

A4.1 1 M Tris-HCl, pH 8.0, stock was prepared by dissolving in 100 ml: 12.11 g Tris, and adjusting the solution to pH 8.0 with concentrated hydrochloric acid (HCl) prior to sterilisation by autoclaving at 121°C.

A4.2 0.5 M EDTA(Na_2), pH 8.0, stock was prepared by adding to 100 ml: 18.61 g EDTA(Na_2), and adjusting the solution to pH 8.0 with concentrated sodium hydroxide (NaOH) prior to sterilisation by autoclaving at 121°C.

A4.3 TE Buffer contained 10 mM Tris-HCl, pH 8.0 and 1 mM EDTA. It was prepared by adding to 100 ml: 1 ml 1 M Tris-HCl, pH 8.0 stock (Section A4.1, above); and 0.2 ml 0.5 M EDTA(Na_2), pH 8.0 stock (Section A4.2, above). It was sterilised by autoclaving at 121°C.

A4.4 DNase-Free RNase-A was prepared by dissolving RNase-A (Sigma Chemical Company) in a 10 mM Tris-HCl, pH 7.5, 15 mM NaCl solution to a final concentration of 10 mg ml^{-1}. Any DNases were denatured by boiling the mixture for 15 min prior to dispensing into aliquots and storing at -20°C till required.

A4.5 Cell Resuspension Buffer contained 50 mM glucose, 25 mM Tris-HCl pH 8.0, 10 mM EDTA, 2 mg ml^{-1} lysozyme, and 0.1 mg ml^{-1} DNAse-free RNase-A. It was prepared by adding in a total of 1 ml: 500 µl 20% (w/v) glucose stock; 250 µl 1 M Tris, pH 8.0 stock (Section A4.1, above); 200 µl 0.5 M EDTA(Na_2), pH 8.0 stock (Section A4.2, above); 200 µl 10 mg ml^{-1} lysozyme (Sigma Chemical Company) stock; and 100 µl 10 mg ml^{-1} DNase-Free RNase-A stock (Section A4.4, p. 169).

A4.6 Cell Lysis Solution contained 0.2 M NaOH, and 1% (w/v) SDS. It was prepared by adding in a total of 10 ml: 0.5 ml 4 M NaCl stock; and 1.0 ml 10% (w/v) SDS stock.

A4.7 STET Lysis Buffer contained 8% (w/v) sucrose, 50 mM Tris-HCl, pH 8.0, 50 mM EDTA, 5% (v/v) Triton X-100. It was prepared by adding in a total of 100 ml: 8 g sucrose; 5 ml 1 M Tris-HCl, pH 8.0 stock (Section A4.1, above); and 1 ml 0.5 M EDTA(Na_2), pH 8.0 stock (Section A4.2, above). After sterilising by autoclaving at 121°C, 5 ml of Triton X-100 were added.

A4.8 Equilibrated Phenol was prepared by dissolving 100 g of phenol and 0.1% (w/w) hydroxyquinoline in 250 ml 0.5 M Tris, pH 8 (Section A4.1, p. 169). After stirring for 30 min, the phases were allowed to separate and the aqueous phase discarded. A further 250 ml aliquot of 0.5 M Tris, pH 8.0, was mixed with the phenol for 30 min, and the aqueous phase discarded once again. This procedure was repeated until the pH of Tris solution had risen above 7.8. The phenol was then mixed with 250 ml STET lysis buffer (Section A4.7, p. 169), sucrose and Triton X-100 excluded, and dispensed into aliquots and stored at -20°C.

A4.9 TNE Fluorometry Buffer contained 10 mM Tris-HCl, pH 7.4, 1 mM EDTA, and 2 M NaCl, pH 7.4. It was prepared by adding to 100 ml: 1 ml 1 M Tris-HCl, pH 7.4 stock; 0.2 ml 0.5 M EDTA(Na_2), pH 8.0 stock (Section A4.2, p. 169); and 11.69 g NaCl.

A4.10 DNA Fragment Size Standards were prepared by combining an equal volume of a *Hin*dIII digest of phage λ DNA with that of a *Hin*dIII/*Eco*RI double digest of phage λ DNA. To generate the *Hin*dIII digest, 100 U of *Hin*dIII were added to a total reaction volume of 800 µl containing buffer M (Boehringer Mannheim GmbH) and 60 µg phage λ DNA (Promega). After incubation at 37°C for 2.5 h, the digestion was terminated by the addition of a one tenth volume of SUDS (Section A4.12, p. 170). A 5 µl aliquot was analysed by gel electrophoresis (Section 2.2.9, p. 46) to confirm that the digestion was complete. The *Hin*dIII/*Eco*RI double digestion was generated in the same way except the reaction mix contained 100 U each of *Hin*dIII and *Eco*RI in buffer M (Boehringer Mannheim GmbH). The working solutions of the combined *Hin*dIII plus *Hin*dIII/*Eco*RI standard were prepared by adding 200 µl of each digestion reaction to 600 µl of 10% (v/v) SUDS in sterile MilliQ water. To resolve the DNA standards fully, the working solution was heated to 70°C for 10 min immediately prior to use.

A4.11 TAE Buffer contained 40 mM Tris acetate, and 1 mM EDTA, pH 8.0. A 50× stock solution, stored at 4°C, was prepared by dissolving in one litre: 242.28 g Tris and 18.6 g EDTA(Na_2), and adjusting the solution to pH 8.0 with approximately 57 ml glacial acetic acid.

A4.12 SUDS Reaction-terminating and Gel-Loading Buffer contained 50% (v/v) glycerol, 1% (w/v) SDS, 0.025% (w/v) bromophenol blue, and 0.1 M EDTA, pH 8.0. It was prepared by adding to 100 ml: 50 ml glycerol; 10 ml 10% (w/v) SDS stock; 0.025 g bromophenol blue; and 20 ml EDTA(Na_2), pH 8.0 stock (Section A4.2).

A4.13 GLB Gel-loading Buffer contained 50% (v/v) glycerol, 0.025% (w/v) bromophenol blue, 10 mM Tris-HCl, pH 8.0, and 1 mM EDTA. It was prepared by adding to 100 ml: 50 ml glycerol; 0.025 g bromophenol blue; 1 ml 1 M Tris-HCl, pH 8.0 stock (Section A4.1, p. 169); 200 µl 0.5 M EDTA(Na_2), pH 8.0 (Section A4.2, p. 169).

A4.14 DEAE Elution Buffer contained 1.0 M NaCl, 10 mM Tris-HCl, pH 8.0, and 1 mM EDTA. It was prepared by adding to 10 ml: 2.5 ml sterile 4 M NaCl stock; 100 µl 1 M Tris-HCl, pH 8.0 stock (Section A4.1, p. 169); and 20 µl 0.5 M EDTA(Na_2), pH 8.0 stock (Section A4.2, p. 169).

A4.15 Restriction Endonuclease Dilution Buffer contained 50% (v/v) glycerol, 0.05% (w/v) BSA, 10 mM Tris-HCl, pH 7.4, 0.1 mM EDTA, and 50 mM KCl. It was prepared by adding to 10 ml: 5.0 ml glycerol; 500 µl 10 mg ml^{-1} BSA stock; 100 µl 1 M Tris-HCl, pH 7.4 stock; 2 µl 0.5 M EDTA(Na_2), pH 8.0 stock (Section A4.2, p. 169); and 500 µl 1 M KCl stock. The dilution buffer was stored at -20°C.

A4.16 5× Blunt End Ligation Buffer contained 250 mM Tris-HCl, pH 8.0, 50 mM $MgCl_2$, 5 mM DTT, 250 µM ATP, 125 µg ml^{-1} BSA, and 15% (w/v) PEG 6000. It was prepared by adding to 1.0 ml: 250 µl 1 M Tris-HCl, pH 8.0 stock (Section A4.1, p. 169); 50 µl 1 M $MgCl_2$ stock; 50 µl 0.1 M DTT stock; 2.5 µl 0.1 M ATP stock; 125 µl 1 mg ml^{-1} BSA stock; and 500 µl 30% (w/v) PEG 6000 stock. This ligation buffer was stored at -20°C.

A4.17 2× Cracking Buffer contained 0.2 M NaOH, 0.5% (w/v) SDS, and 20% (w/v) sucrose. It was prepared by adding to 10 ml: 500 µl 4 M NaCl; 500 µl 10% (w/v) SDS; and 2.0 g sucrose.

A4.18 TBE Buffer for Sequencing Gels contained 89 mM Tris, 2.5 mM EDTA, and 89 mM boric acid (H_3BO_3). A 10 times stock, stored at room temperature, was prepared by dissolving in one litre: 108.0 g Tris; 9.3 g EDTA(Na_2); and 55.0 g boric acid.

A4.19 40% Acrylamide Solution contained 40% (w/v) acrylamide: bisacrylamide (19:1 w/w, respectively), and was prepared by dissolving in 100 ml: 38.0 g acrylamide, and 2.0 g bisacrylamide. The solution was stored away from light at 4°C.

A4.20 Nucleotide TLC Phosphate Buffer contained 0.75 M potassium dihydrogen orthophosphate (KH_2PO_4), pH 3.5. It was prepared by adding to 500 ml: 51.03 g potassium dihydrogen orthophosphate (KH_2PO_4), and adjusting the pH to 3.5 with orthophosphoric acid (H_3PO_4) prior to autoclaving at 121°C and storing at 4°C.

A4.21 TE-Equilibrated Sepharose CL-6B Resin was equilibrated in freshly sterilised TE buffer (Section A4.3, p. 169) by adding an equal volume of TE to packed Sepharose CL-6B resin (Sigma Chemical Company), then shaking till a slurry formed, allowing the resin to settle, and pouring off the supernatant. This was repeated at least three times to equilibrate the beads and to elute the preservative from the resin. After the last wash, sufficient TE was retained to provide an equal volume of TE to packed Sepharose resin. The equilibrated resin was stored a 4°C.

A4.22 20× SSPE contained 3.6 M NaCl, 0.2 M sodium phosphate, and 0.02 M EDTA, pH 7.7. It was prepared by adding to one litre: 210.38 g NaCl; 31.20 g sodium dihydrogen orthophosphate ($NaH_2PO_4.2H_2O$); 7.44 g EDTA(Na_2), and adjusting the solution to pH 7.7 with concentrated NaOH. In order to prepare **2× SSPE** and **5× SSPE** solutions, 10-fold and 4-fold dilutions, respectively, were made of the 20× SSPE stock.

A4.23 100× Denhardt's Solution (Denhardt, 1966) contained 2% (w/v) BSA, 2% (w/v) Ficoll, and 2% (w/v) PVP. It was prepared by adding to 50 ml: 1 g BSA (Fraction V); 1 g Ficoll (M_r=400,000); and 1 g PVP (M_r=44,000). The solution was divided into 1.25 ml aliquots, and stored at -20°C.

A4.24 SSPE Hybridisation Solution contained 5× SSPE, 5× Denhardt's Solution, and 0.5% (w/v) SDS. It was prepared by adding to 25 ml: 5 ml 20× SSPE (Section A4.22, p. 172); 1.25 ml 100× Denhardt's Solution (Section A4.23, p. 172); and 1.25 ml 10% (w/v) SDS stock.

A4.25 Fragmented Herring Testes DNA was prepared by adding Herring Testes DNA (Sigma Chemical Corporation) to sterile MilliQ water to a final concentration of 10 mg ml^{-1}. When fully dissolved, the solution was boiled for 10 min, then the DNA was sheared further by passing it rapidly through a 18 gauge hypodermic needle. and dispensed into 1.25 ml aliquots which were stored at -20°C.

A4.26 2× SSPE Wash contained 2× SSPE and 0.1% (w/v) SDS. It was prepared by adding to 100 ml: 10 ml 20× SSPE (Section A4.22, p. 172); and 1 ml 10% (w/v) SDS stock.

A4.27 1× SSPE Wash contained 1× SSPE and 0.1% (w/v) SDS. It was prepared by adding to 100 ml: 5 ml 20× SSPE (Section A4.22, p. 172); and 1 ml 10% (w/v) SDS stock.

A4.28 0.1× SSPE Wash contained 0.1× SSPE and 0.1% (w/v) SDS. It was prepared by adding to 100 ml: 0.5 ml 20× SSPE (Section A4.22, p. 172); and 1 ml 10% (w/v) SDS stock.

A4.29 1 M Disodium Phosphate Buffer, pH 7.2, was prepared by dissolving in one litre: 70.98 g disodium hydrogen orthophosphate (Na_2HPO_4), and adjusting to pH 7.2 with orthophosphoric acid (H_3PO_4) prior to sterilisation by autoclaving.

A4.30 SDS Hybridisation Solution contained 0.5 M disodium hydrogen orthophosphate (Na_2HPO_4), 1.0 mM EDTA, 7% (w/v) SDS, and 1% (w/v) BSA, pH 7.2. It was prepared by adding to 25 ml: 12.5 ml 1 M disodium phosphate buffer, pH 7.2 (Section A4.29); 50 µl 0.5 M EDTA(Na_2) stock, pH 8.0 (Section A4.2, p. 169); 8.75 ml 20% (w/v) SDS stock; and 0.25 g BSA, Fraction V (Sigma Chemical Company).

A4.31 SDS Wash Solution contained 40 mM disodium hydrogen orthophoshate, 1 mM EDTA, and 5% (w/v) SDS. It was prepared by adding to 100 ml: 4 ml 1 M disodium phosphate buffer, pH 7.2 (Section A4.29); 200 µl 0.5 M EDTA(Na_2) stock, pH 8.0 (Section A4.2, p. 169); and 25 ml 20% (w/v) SDS.

A4.32 Genomic Extraction Buffer for plants contained 2.0% (w/v) CTAB, 1.4 M NaCl, 0.2% (v/v) 2-mercaptoethanol, 100 mM Tris-HCl, pH 8.0, and 20 mM EDTA. It was prepared by adding to 100 ml: 40 ml sterile 5% (w/v) CTAB stock; 35 ml sterile 4 M NaCl; 200 µl 2-mercaptoethanol; 10 ml Tris-HCl, pH 8.0 stock (Section A4.1, p. 169); and 4 ml 0.5 M EDTA(Na_2), pH 8.0 stock (Section A4.2, p. 169).

APPENDIX 5: SEQUENCE DATA FROM pANDY4

A5.1 Sequence data from the junction of pMTL25P through the pUC18 mcs to the $P_{mas2'}$ promoter of the mcs-P_{35S}-*nptII* fusion (refer Fig. 16B, p. 91).

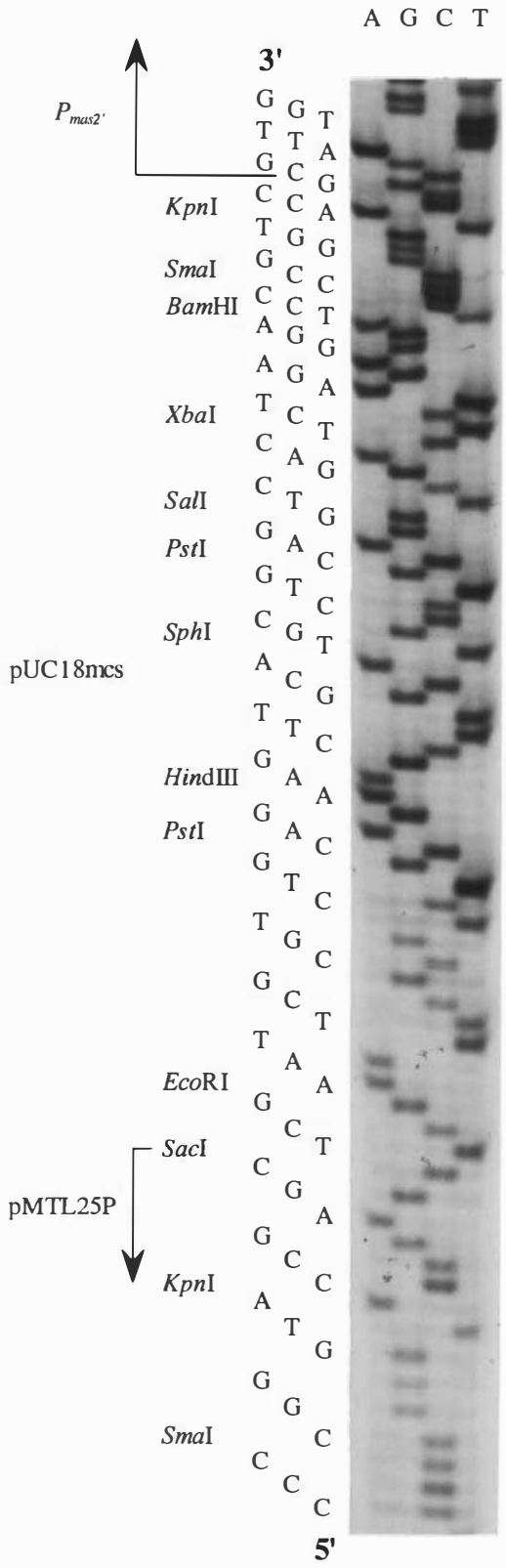

A5.2 Sequence data from the junction of pMTL25P through to the *ocs*3′ terminator of the mcs-P_{35S}-*nptII* fusion (refer Fig. 16C, p. 91).

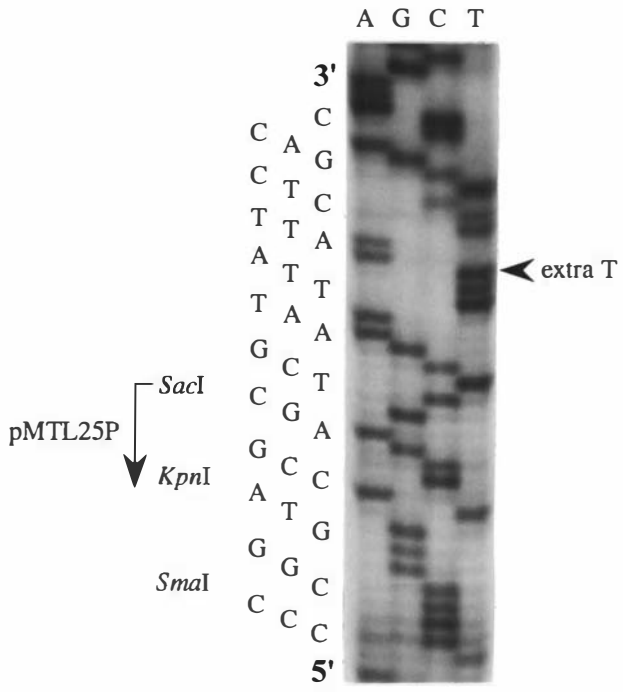

APPENDIX 6: PLASMID MAPS

A6.1 pBIN19/GTG (courtesy of D. H. Kerr (1996))

A restriction map of the binary promoter-trapping vector pBIN19/GTG showing the position (kb) of several restriction sites and the multiple cloning sites at either end of the T-DNA. Features of this plasmid include: a promoterless *gusA* gene adjacent to the right border for promoter-trapping; stop codons in all three reading frames immediately upstream of the translation start sequence of the promoterless *gusA* gene (thus preventing translational fusions if the T-DNA inserts into an active plant gene); both a *bla* bacterial-selectable marker and a pBR322 *oriV* located in the T-DNA for plasmid rescue of flanking plant genomic DNA; the border regions, including the putative *overdrive* region, are derived from the nopaline-type Ti-plasmid, pTiT37. Only one of the six *Eco*RV sites is shown. The marked sites (**bold** *) are those useful in plasmid rescue of plant genomic DNA flanking the right border.

RB=right border; LB=left border; OD=putative nopaline-type *overdrive* core; *oriV*=origin of replication; *bla*=β-lactamase gene; P_{nos}-*nptII*=neomycin phosphotransferase gene driven by *nos* promoter and terminated by *ocs*3′ sequence; *ocs*3′=transcription termination sequence of octopine synthase gene; *gusA*=β-glucuronidase gene; *nptIII*=neomycin phosphotransferase gene.

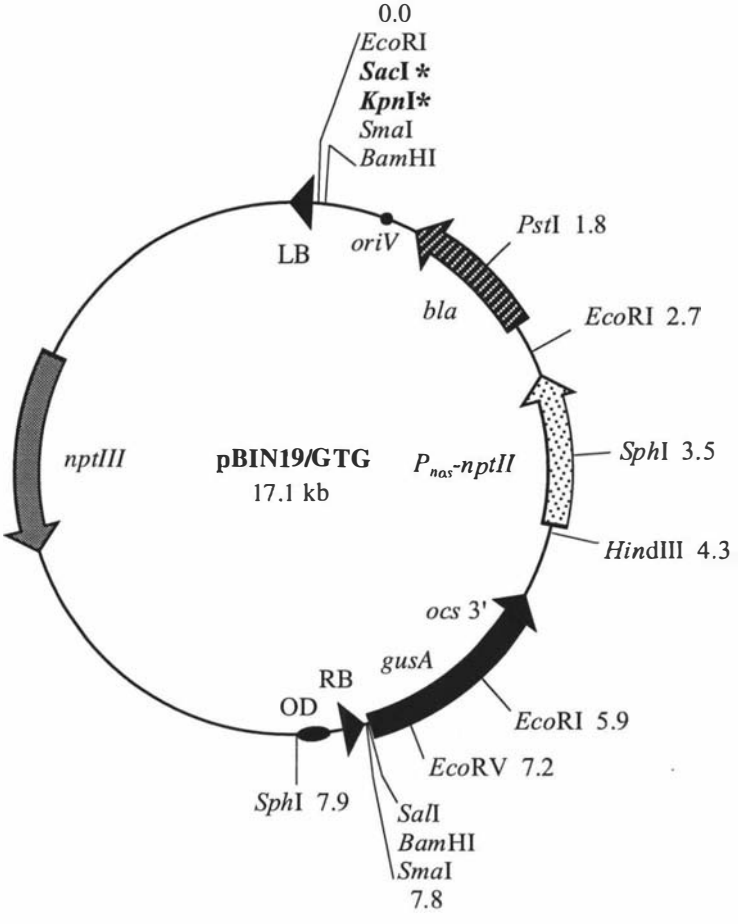

A6.2 pANDY6

A restriction map of the binary vector pANDY6 showing the position (kb) of several restriction sites and the multiple cloning regions present at either end of the T-DNA. Only one of the six *Eco*RV sites is shown. The unique sites adjacent to the left border into which plant-selectable markers may be inserted are highlighted (**bold***).

RB =right border; LB =left border; OD =putative nopaline-type *overdrive* core; *bla* =β-lactamase gene; *gusA* =β-glucuronidase gene; *nptIII* =neomycin phosphotransferase gene; *oriV* =origin of replication; *ocs*3′ =transcription termination sequence of octopine synthase gene.

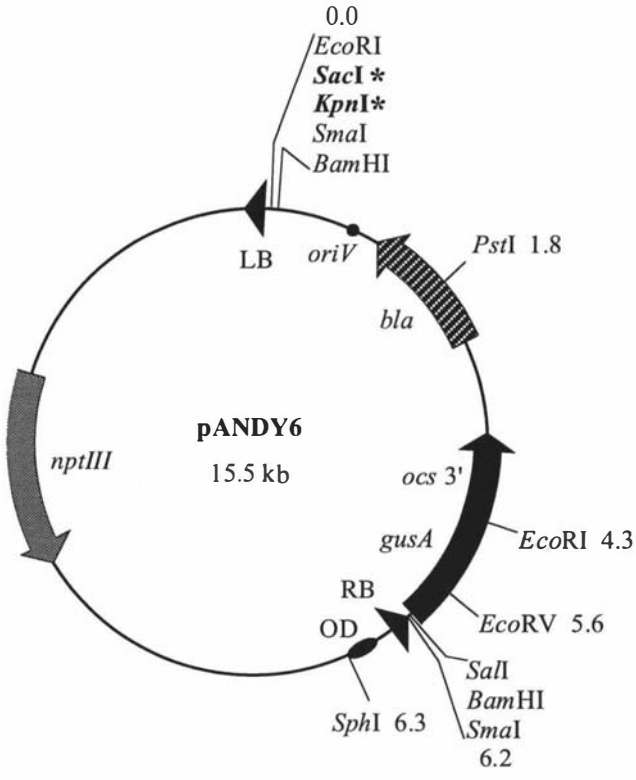

A6.3 pANDYOD⁻2 and pANDYOD⁻3

A restriction map of the binary vectors pANDYOD⁻2 and pANDYOD⁻3 showing the position (kb) of several enzyme sites and the multiple cloning regions present at either end of the T-DNA. Only one of the six *Eco*RV sites is shown. Deletions across the putative nopaline-type *overdrive* region of the two plasmids are compared with that of pANDY6 (below plasmid map). The two unique sites adjacent to the left border into which plant-selectable markers may be inserted are indicated (**bold***).

RB =right border; LB =left border; *bla* =β-lactamase gene; *gusA* =β-glucuronidase gene; *nptIII* =neomycin phosphotransferase gene; *oriV* =origin of replication; *ocs*3′ =transcription termination sequence of octopine synthase gene.

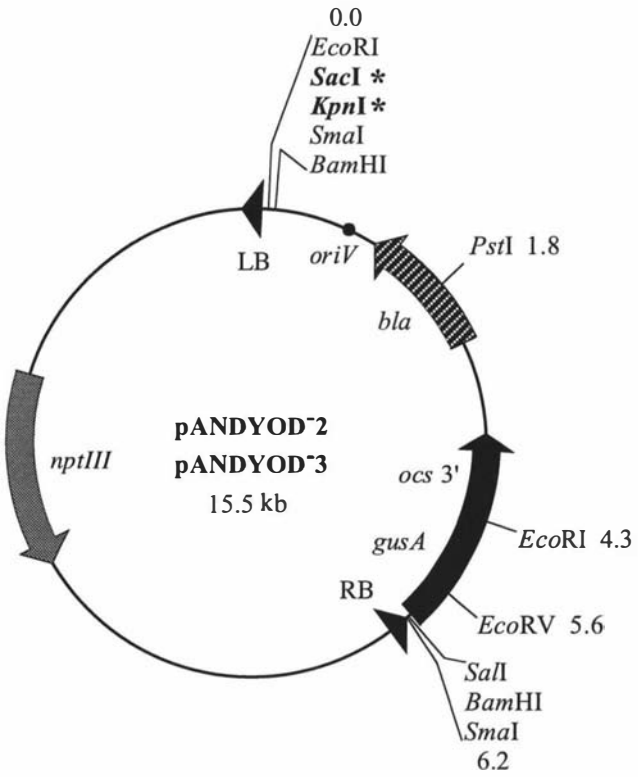

Sequence data showing deletions across the *overdrive* region of pANDYOD⁻2 and pANDYOD⁻3 compared with that of pANDY6.

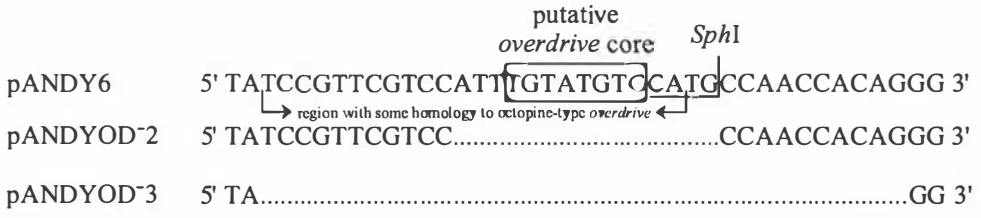

A6.4 pSLJ491

A restriction map of pSLJ491 showing the position (bp) of the sites (**bold**) used to excise the P_{35S}-*nptII* fusion. Some other sites and their position throughout the P_{35S}-*nptII* fusion and the rest of the plasmid are also shown.

RB=right border; LB=left border; $P_{mas2'}$=2′ promoter of the mannopine synthase gene; P_{35S}=promoter of the Cauliflower Mosaic Virus 35S RNA subunit; *nptII*=neomycin phosphotransferase gene; *ocs*3′=transcription termination sequence of octopine synthase gene; Tc^r=gene encoding resistance to tetracycline.

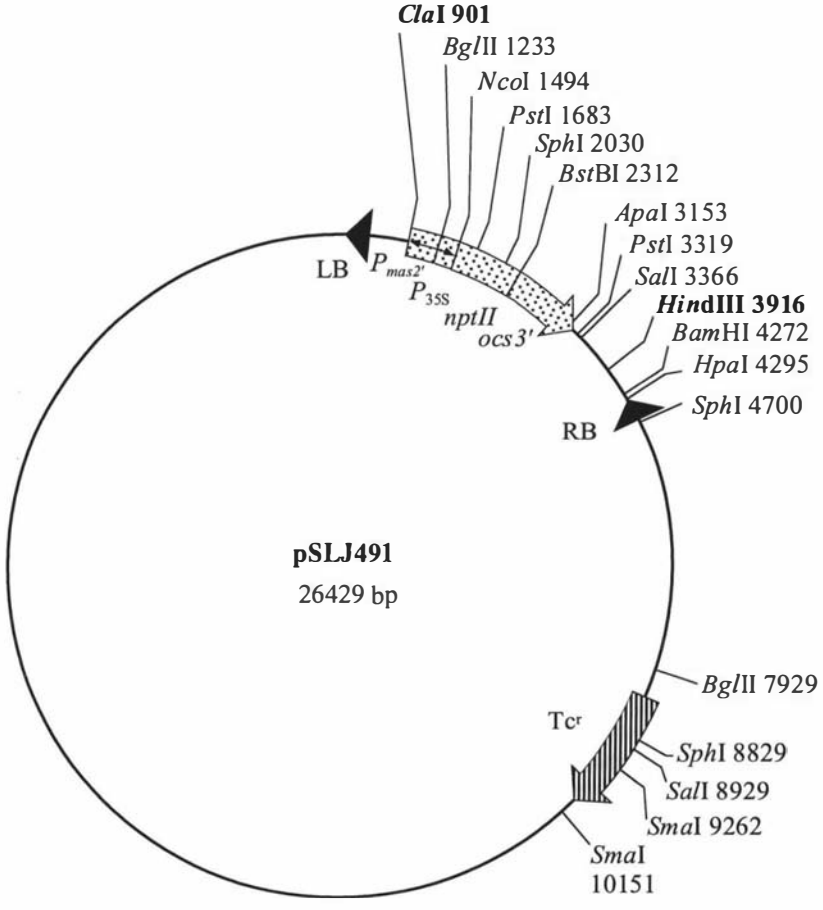

A6.5 pMTL22P

A restriction map of the cloning vector pMTL22P showing the position (bp) of the multiple cloning region and some other enzyme sites throughout the plasmid. The enzyme sites used in cloning steps are indicated (**bold**).

bla=β-lactamase gene; mcs=multiple cloning site; *oriV*=origin of replication; *lacZ'*=portion of the β-galactosidase gene.

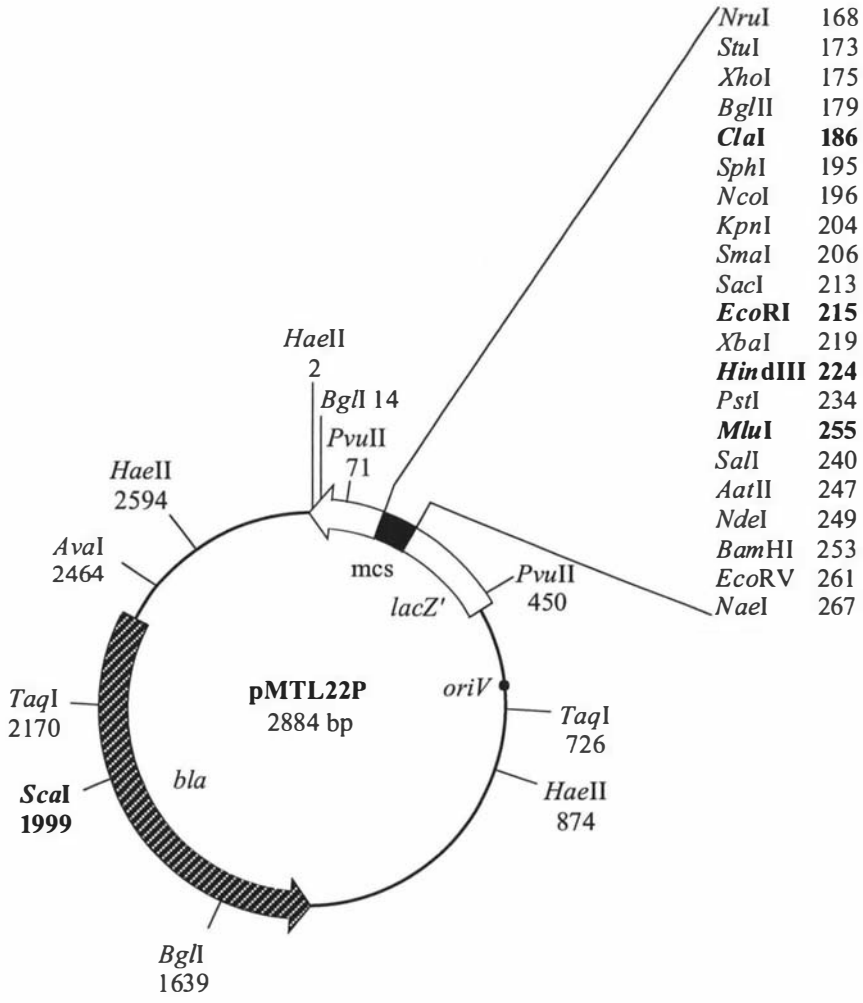

A6.6 pMTL25P

A restriction map of the cloning vector pMTL25P showing the position (bp) of the multiple cloning region and some other enzyme sites throughout the plasmid. The enzyme sites used in cloning steps are indicated (**bold**). The position and orientation of the annealing sites of both the -40 Universal (**Uni**) and the -44 Reverse (**Rev**) sequencing primers is indicated by half arrows.

bla=β-lactamase gene; mcs =multiple cloning site; *oriV*=origin of replication; *lacZ'*=portion of the β-galactosidase gene.

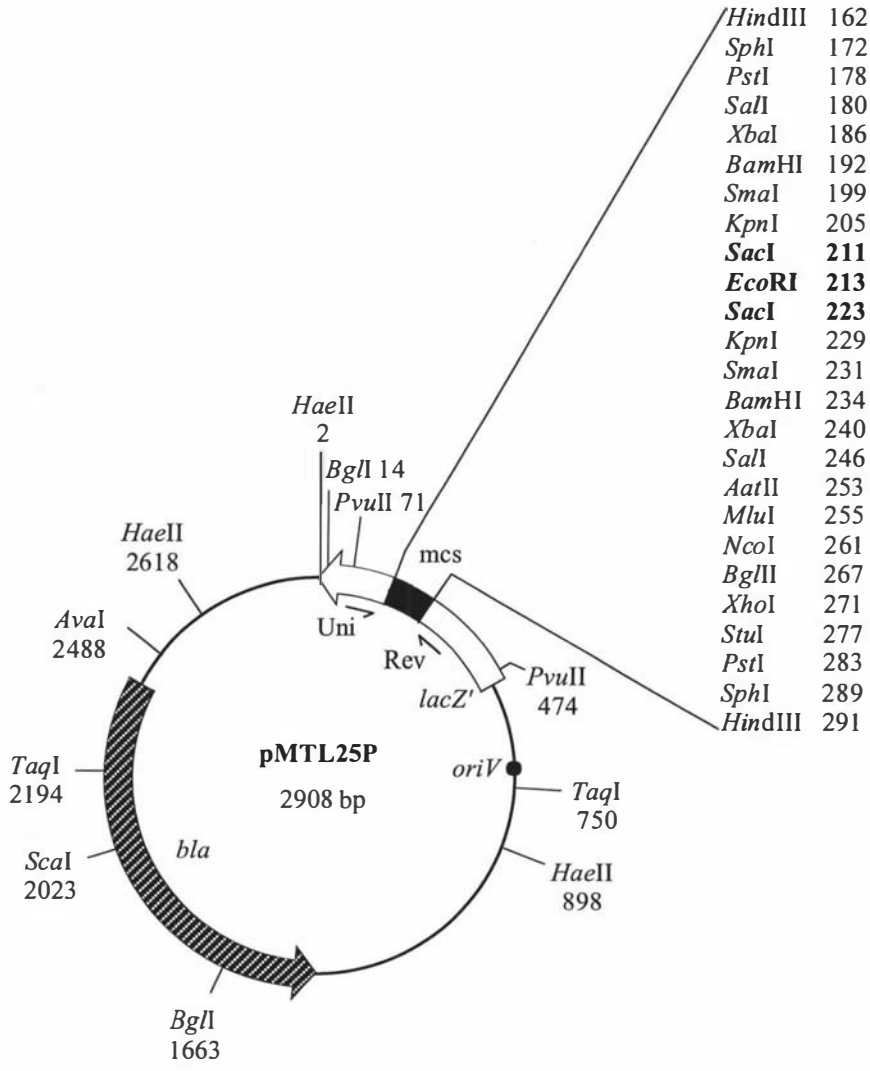

A6.7 pUC18

A restriction map of the cloning vectors pUC18 showing the position (bp) of the multiple cloning region and some other enzyme sites throughout the plasmid. The enzyme sites used in cloning steps are indicated (**bold**).

bla=β-lactamase gene; mcs=multiple cloning site; *oriV*=origin of replication; *lacZ'*=portion of the β-galactosidase gene; *lacI*=*lac* operon repressor gene.

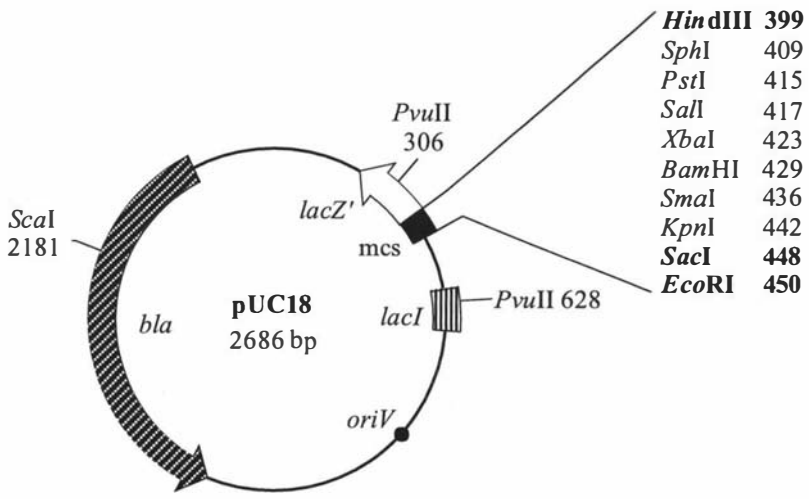

A6.8 pANDY1

A restriction map of pANDY1 showing the position (bp) of several enzyme sites throughout the P_{35S}-*nptII* fusion, the rest of the plasmid, and the multiple cloning regions flanking the fusion. Enzyme sites used in cloning steps are indicated (**bold**). The curve (**bold**) adjacent to the plasmid map represents the 536 bp portion of the *nptII* gene used as a probe in Southern analysis of plants transformed with pANDY8, pANDY9, and pANDY10.

$P_{mas2'}$=2′ promoter of the mannopine synthase gene; P_{35S}=promoter of the Cauliflower Mosaic Virus 35S RNA subunit; *nptII*=neomycin phosphotransferase gene; *ocs*3′=transcription termination sequence of octopine synthase gene; *bla*=β-lactamase gene; mcs=multiple cloning site; *oriV*=origin of replication; *lacZ′*=portion of the β-galactosidase gene.

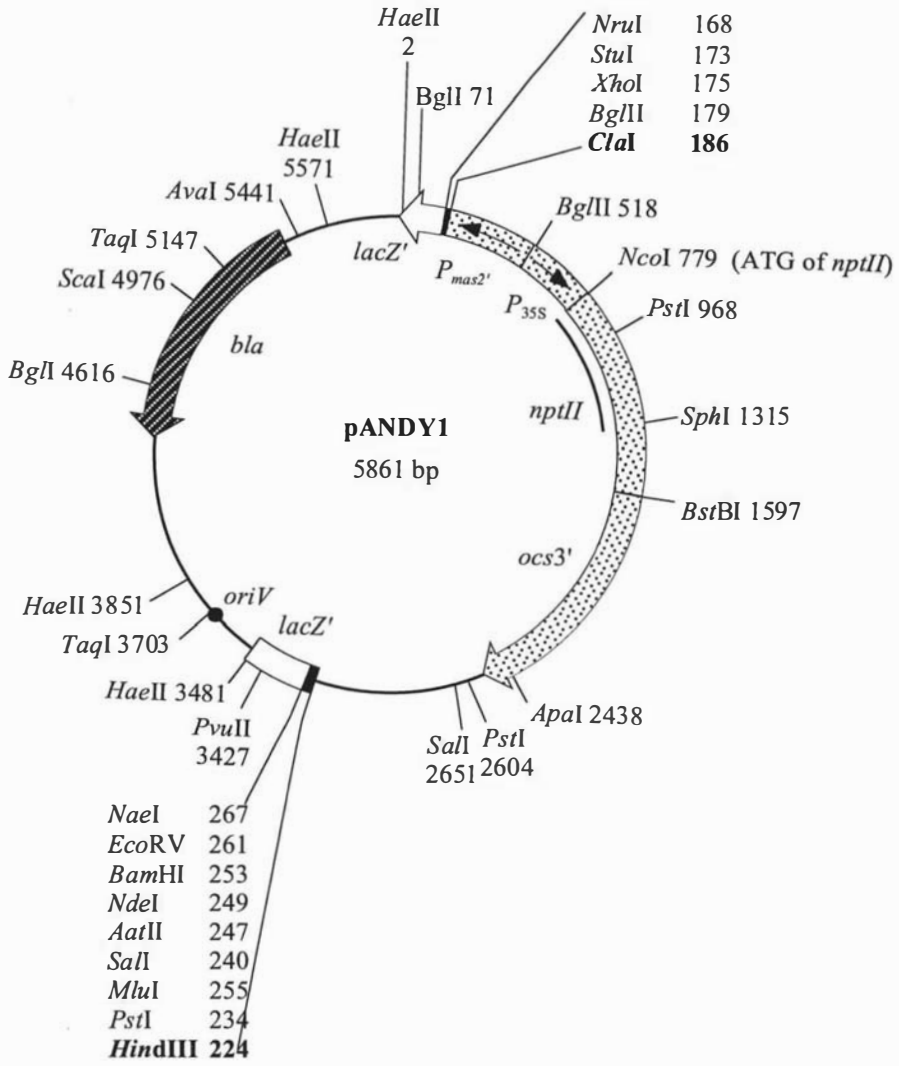

A6.9 pANDY2

A restriction map of pANDY2 showing the position (bp) of several enzyme sites throughout the P_{35S}-*nptII* fusion, the rest of the plasmid, and the multiple cloning sites (mcs) upstream of the fusion. Enzyme sites used in cloning steps are indicated (**bold**).

$P_{mas2'}$=2′ promoter of the mannopine synthase gene; P_{35S}=promoter of the Cauliflower Mosaic Virus 35S RNA subunit; *nptII*=neomycin phosphotransferase gene; *ocs*3′=transcription termination sequence of octopine synthase gene; *bla*=β-lactamase gene; mcs =multiple cloning site; *oriV*=origin of replication; *lacZ′*=portion of the β-galactosidase gene; *lacI*=*lac* operon repressor gene.

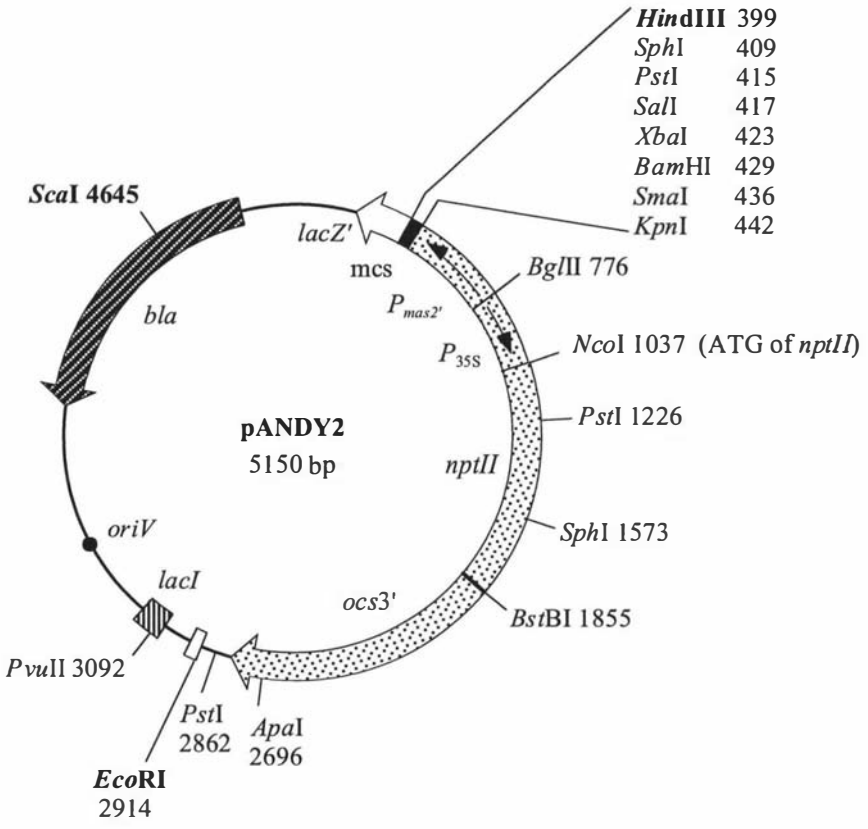

A6.10 pANDY3

A restriction map of pANDY3 showing the position (bp) of several enzyme sites throughout the P_{35S}-*nptII* fusion and the rest of the plasmid. Enzyme sites in **bold** highlight the attached pUC18 mcs upstream of the fusion. Where both an enzyme site and its position are in **bold**, it indicates a site involved in the construction of, or subsequent cloning with, the plasmid.

$P_{mas2'}$=2′ promoter of the mannopine synthase gene; P_{35S}=promoter of the Cauliflower Mosaic Virus 35S RNA subunit; *nptII*=neomycin phosphotransferase gene; *ocs3′*=transcription termination sequence of octopine synthase gene; *bla*=β-lactamase gene; mcs =multiple cloning site; *oriV*=origin of replication; *lacZ′*=portion of the β-galactosidase gene.

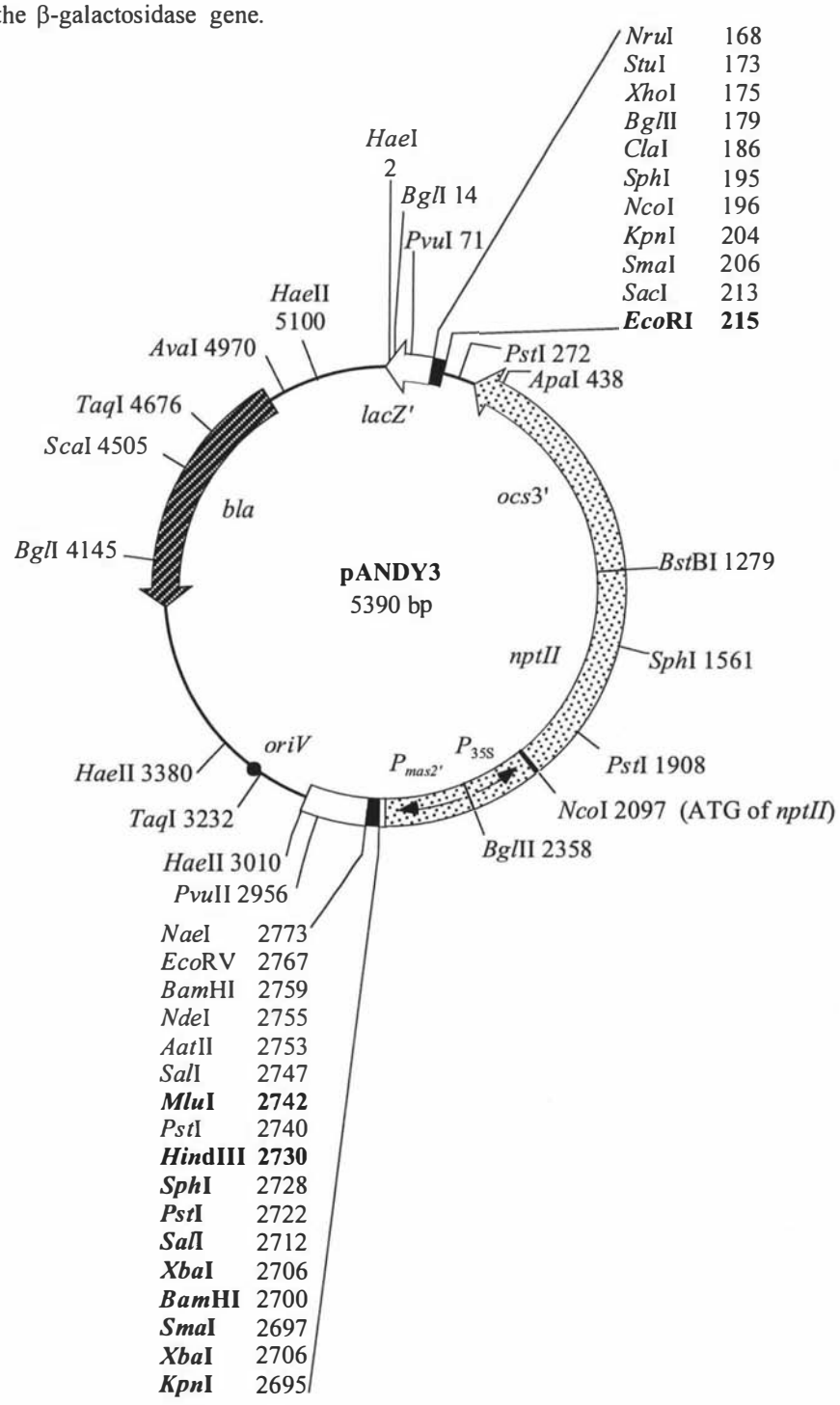

A6.11 pANDY4

A restriction map of pANDY4 showing the position (bp) of several enzyme sites throughout the P_{35S}-*nptII* fusion and the rest of the plasmid. Enzyme sites in **bold** highlight the attached pUC18 mcs upstream of the fusion. Where both an enzyme site and its position are in **bold**, it denotes a site involved in the construction of, or subsequent cloning with the plasmid.

$P_{mas2'}$=2′ promoter of the mannopine synthase gene; P_{35S}=promoter of the Cauliflower Mosaic Virus 35S RNA subunit; *nptII*=neomycin phosphotransferase gene; *ocs*3′=transcription termination sequence of octopine synthase gene; *bla*=β-lactamase gene; mcs=multiple cloning site; *oriV*=origin of replication; *lacZ′*=portion of the β-galactosidase gene.

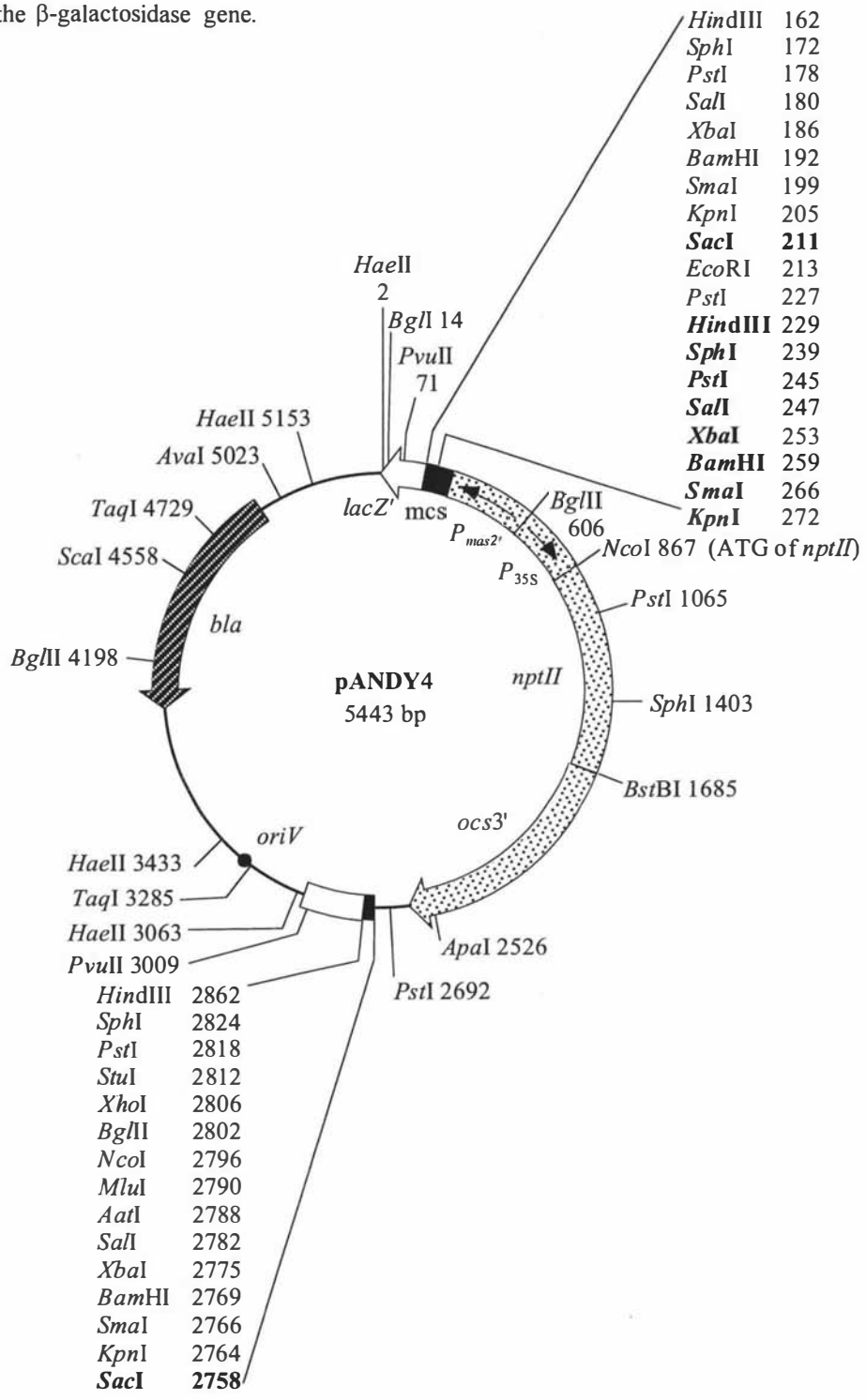

A6.12 pANDY8, pANDY9, and pANDY10

A restriction map of the binary vectors pANDY8, pANDY9, and pANDY10 showing the position (kb) of several enzyme sites and the multiple cloning regions present at either end of the T-DNA. The pUC18 mcs attached upstream of the P_{35S}-*nptII* fusion is also detailed. Deletions across the putative nopaline-type *overdrive* region are highlighted, as are the sites (*) useful in plasmid rescue of plant genomic DNA 5′ of the right border. Only one of the six *Eco*RV sites is shown. The position and orientation of both the -40 Universal (**Uni**) and the **2.1** sequencing primers is indicated by half arrows.

RB=right border; LB=left border; OD=putative nopaline-type *overdrive* core; mcs-P_{35S}-*nptII*=a multiple cloning site from pUC18 attached to a P_{mas2}/P_{35S} dual promoter driving an *nptII* gene; *ocs*3′=transcription termination sequence of octopine synthase gene; *bla*=β-lactamase gene; mcs=multiple cloning site; *oriV*=origin of replication; *nptIII*=neomycin phosphotransferase.

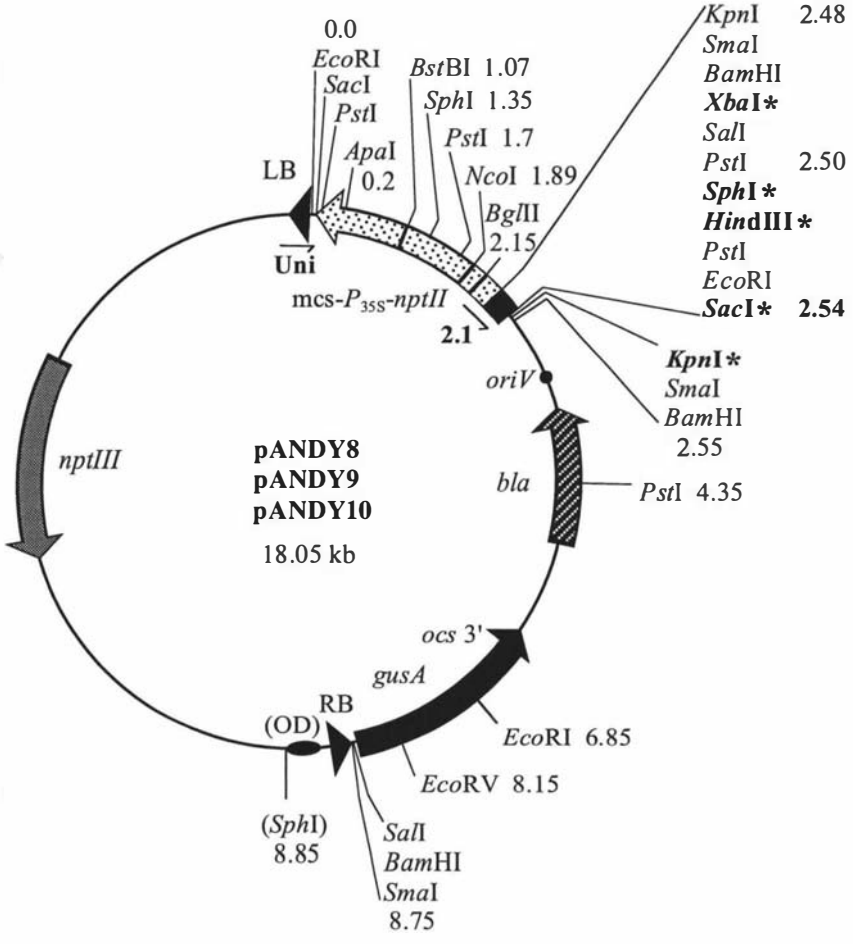

Note: OD and *Sph*I site deleted in plasmids pANDY9 and pANDY10

Sequence data showing deletions across the *overdrive* region of pANDY8, ANDY9, and pANDY10.

putative *overdrive* core — *Sph*I

pANDY8 5′ TATCCGTTCGTCCATTTGTATGTGCATGCCAACCACAGGG 3′

region with some homology to octopine-type *overdrive*

pANDY9 5′ TATCCGTTCGTCC.....CCAACCACAGGG 3′

pANDY10 5′ TA.....GG 3′

A6.13 pJIT166

A restriction map of pJIT166 showing the position (kb) of some enzyme sites throughout the *gusA* gene and flanking promoter and terminator regions. The sites used to excise the *gusA* gene for probe manufacture are marked (**bold**). The curve (**bold**) adjacent to the to the plasmid map represents the 1.9 kb portion of the *gusA* gene used as a probe in Southern analysis of plants transformed with pANDY8, pANDY9 and pANDY10.

$2\times P_{35S}$ =two promoters of the Cauliflower Mosaic Virus 35S RNA subunit; *bla*=β-lactamase gene; *gusA* =β-galactosidase gene; CaMV polyA =transcription termination and polyadenylation sequence from the Cauliflower Mosaic Virus.

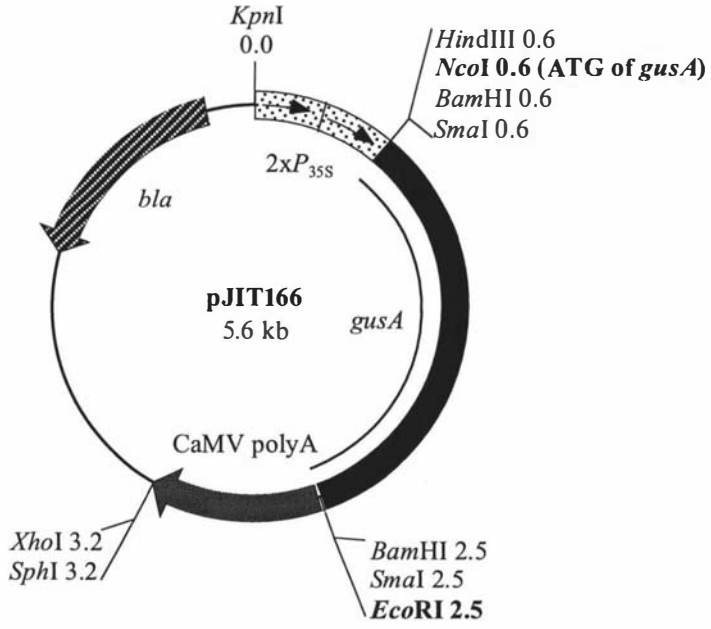

APPENDIX 7: SOUTHERN ANALYSIS DATA

The Southern data gained on every plant analysed was collated and is contained in Tables 2 to 4.

Table 2. Southern analysis using a [^{32}P]-labelled *nptII* left border probe with *Hin*dIII and *Eco*RI-digested genomic DNA from plants transformed with pANDY8.

Plant	*Hin*dIII Digest/Band Size (kb)	*Eco*RI Digest/Band Size (kb)	T-DNA Copies
1	18.3; 9.5; 8.1; 5.6	5.8[1]; 2.5	4
2	2.1	6.9[2]	1
5	4.8	2.5	1[3]
7	5.2	2.5	1
11	4.5	2.5	1[3]
12	13.5; 7.4; 5.2	6.3[1]; 2.5	3
14	6.8	2.5	1
23	4.0	2.5	1
24	3.4	2.5	1
27	6.8	2.5	1
29	9.0	2.5	1
31	5.4; 4.5	2.5	2
32	5.7	8.5[1]; 3.5[2]	1
34	6.1	2.5	1[3]
35	3.2	2.5	1
36	3.4	2.5	1
38	4.8	2.5	1
39	35.0	2.5	1[3]
40	4.1	2.5	1[3]
41	7.4	2.5	1
42	3.6	7.4[1]; 2.5	1
43	10.1; 8.1	6.2[2]; 2.5	2
59	6.0	2.5	1
60	7.4	2.5	1
80	13.3; 4.9	4.0[2]; 2.5	2
81	4.8	2.5	1
82	8.6; 5.5	2.5	2[3]
83	6.7	2.5	1
84	6.2; 5.5; 3.8	5.7[1]; 2.5	3
85	5.8; 5.0; 4.6	4.0[2]; 3.6[2]; 3.1[2]	3

Table 2 continued.

Plant	*Hin*dIII Digest/Band Size (kb)	*Eco*RI Digest/Band Size (kb)	T-DNA Copies
86	3.2	2.5	1[3]
87	12.5	2.5	1[3]
88	14.3; 7.8; 4.3	5.2[1]; 2.5	3[3]
89	6.9[1]; 5.2	2.5	1
90	26; 10.2; 8.6; 3.9	7.4[1]; 2.5	4
91	4.5	2.5	1[3]
104	4.5	2.5	1[3]
106	15.5; 6.7	2.5	2[3]
107	30.0; 9.2	3.2[2]; 2.5	2
108	17.0; 5.2	6.4[1]; 2.5	2
109	6.2	2.5	1[3]
110	11.8[1]; 3.6	7.2[1]; 2.5	1[3]
111	6.2	2.5	1
112	19.0; 11.2; 4.7; 4.3	7.4[1]; 6.4[2]; 2.5	4
113	8.3; 7.3	nd	2
114	4.7	nd	1
116	6.2	2.5	1
117	3.3	7.3[2]	1
118	11.2	2.5	1
119	4.2	2.5	1
120	19.0	9.2[2]	1
121	8.4; 6.0; 4.3	2.5	3
122	19.0; 7.1; 4.3; 4.0	2.5	4
123	5.6	2.5	1
125	5.9	2.5	1
126	8.4; 4.5	2.3[2]	2
127	5.3	2.5	1
128	7.7; 3.9	2.5	2
129	4.8	2.5	1
131	31.2; 8.2; 6.8	2.5	3
136	7.4; 5.5	2.5	2
137	5.1	2.5	1
138	11.7; 10.2; 4.2	2.5	3
139	6.1	2.5	1
140	5.5; 4.2; 3.4	2.5	3
142	7.2; 3.8; 3.4	2.5	3
158	3.9	nd	1
159	5.5	nd	1

Table 2 continued.

Plant	*Hin*dIII Digest/Band Size (kb)	*Eco*RI Digest/Band Size (kb)	T-DNA Copies
160	4.7	nd	1
161	13.3	nd	1
162	11.4; 4.3	nd	2
163	8.2	nd	1

[1]suspected partial digest (usually a faint band relative to others in that lane)

[2]suspected corruption in the T-DNA (usually bands of similar intensity in that lane)

[3]copy number corroborated by *gusA* probing (right border probe) of a *Hin*dIII digest (see Table 5, p. 195).

nd=not determined

Note: 1. T-DNA copy number based upon left border inserts as determined by *nptII* probe.

2. expected band for *Eco*RI digest/*nptII* probe is 2.5 kb.

Table 3. Southern analysis using a [^{32}P]-labelled *nptII* left border probe with *Hin*dIII and *Eco*RI-digested genomic DNA from plants transformed with pANDY9.

Plant	*Hin*dIII Digest/Band Size (kb)	*Eco*RI Digest/Band Size (kb)	T-DNA Copies
3	19.4; 9.9	2.5	2
4	7.4	4.6[2]	1
8	3.7	2.5	1
9	8.9	8.5[2]	1
10	7.7	2.5	1
15	6.0	2.5	1
16	8.0	2.5	1
17	8.5	7.5[2]	1
18	8.0	2.5	1
19	9.4	2.5	1
20	4.2	2.5	1
21	12.7	2.5	1
25	4.0	3.0[2]	1
28	5.4	2.5	1
33	13.7	2.5	1
58	4.5	2.5	1
61	2.8	8.2[1]; 2.5	1
62	5.8	2.5	1[3]
74	5.1	2.5	1[4]
75	3.9	2.5	1[4]
76	4.0	2.5	1
77	4.4	2.5	1[4]
78	40.0	2.5	1[3,4]
79	6.8	2.5	1[3,4]
93	7.3	2.5	1[3,4]
94	8.9	13.6[1]; 5.6[1]; 2.5	1
95	10.6	2.5	1[3]
96	8.3	4.6[2]	1[3]
97	6.6; 5.4	2.5	2[3]
98	17.2	2.5	1[3]
99	6.1	2.5	1
100	4.5	2.5	1[3]
101	27.0	2.5	1[3]
102	6.8	2.5	1[3]
103	11.9	2.5	1[3]

Table 3 continued

Plant	*Hin*dIII Digest/Band Size (kb)	*Eco*RI Digest/Band Size (kb)	T-DNA Copies
115	4.9	2.5	1[3]
132	5.0	2.5	1
133	14.5	2.5	1
134	17.9; 9.1	2.5	2
135	5.7	2.5	1
143	11.2; 7.2	2.5	2
150	4.3	2.5	1
151	4.7	2.5	1
152	12.4; 6.4	2.5	2
153	4.2	2.5	1
154	8.6; 5.3	2.5	2
155	4.6	2.5	1
156	6.7	2.5	1
157	7.2	2.5	1

[1]suspected partial digest (usually a faint band relative to others in that lane)

[2]suspected corruption in the T-DNA (usually bands of similar intensity in that lane)

[3]copy number corroborated by *gusA* probing (right border probe) of a *Hin*dIII digest (see Table 6, p. 196).

[4]copy number corroborated by *gusA* probing (right border probe) of an *Eco*RI digest (see Table 6).

Note: 1. T-DNA copy number based upon left border inserts as determined by *nptII* probe.
2. expected band for *Eco*RI digest/*nptII* probe is 2.5 kb.

Table 4. Southern analysis using a [^{32}P]-labelled *nptII* left border probe with *Hin*dIII and *Eco*RI-digested genomic DNA from plants transformed with pANDY10.

Plant	*Hin*dIII Digest/Band Size (kb)	*Eco*RI Digest/Band Size (kb)	T-DNA Copies
22	6.0	2.5	1
30	3.1	2.5	1
37	23.9	2.5	1
44	6.3	3.2[2]	1
45	20.9; 9.1	2.5	2
46	5.9	2.5	1
47	3.3	2.5	1
48	18.5	2.5	1
49	4.8	2.5	1
50	7.3	2.5	1
51	4.3	4.0[2]	1
52	5.2	9.5[1]; 2.5	1
53	20.8	2.5	1
54	24.0; 13.0	2.5	2
56	3.4	2.5	1
57	5.9	2.5	1
63	3.3	5.2[1]; 2.5	1
65	4.4	8.8[2]	1[3,4]
66	6.6	13.9[2]	1[4]
69	15.3	2.5	1
70	18.3; 8.9	2.5	2[3,4]
71	6.6	6.6[2]	1[4]
72	12.6; 3.4	2.5	2[3,4]
73	26.6[1]; 12.0	2.5	1[3]
92	4.1	2.5	1[4]
144	5.6	2.5	1
148	8.6	2.5	1
149	32.0	2.5	1

[1]suspected partial digest (usually a faint band relative to others in that lane)

[2]suspected corruption in the T-DNA (usually bands of similar intensity in that lane)

[3]copy number corroborated by *gusA* probing (right border probe) of a *Hin*dIII digest (see Table 7, p. 197).

[4]copy number corroborated by *gusA* probing (right border probe) of an *Eco*RI digest (see Table 7).

Table 5. Southern analysis using a [^{32}P]-labelled *gusA* right border probe with *Hin*dIII and *Eco*RI-digested genomic DNA from plants transformed with pANDY8.

Plant	*Hin*dIII Digest/Band Size (kb)	*Eco*RI Digest/Band Size (kb)	T-DNA Copies
5	5.3	nd	1
11	9.9	nd	1
34	6.9	nd	1
39	17.5	nd	1
40	14.2	nd	1
80	17.5	nd	2
81	8.9	nd	1
82	13.3; 8.1	nd	2
83	0	nd	1
84	15.5	nd	2
86	10.2	nd	1
87	21.7	nd	1
88	10.2; 7.8; 6.9	nd	3
90	19.0[1]; 8.9; 5.9; 4.2	nd	4
91	11.8	nd	1
104	10.5	nd	1
106	14.3; 7.3	nd	2
108	17.0; 10.2	nd	1
109	8.6	nd	1
110	17.0[1]; 11.2	nd	1
111	6.7; 6.1; 2.4	nd	1
112	26.0; 13.3; 8.9	nd	4
113	7.6	nd	2
114	0	nd	1

[1]suspected partial digest (usually a faint band relative to others in that lane)

T-DNA copy number in the righthand column was based upon left border inserts as determined by *nptII* probe of *Hin*dIII digested genomic DNA (Table 2, p. 189). In some cases, the number of bands detected using the *gusA* probe did not match those detected using the *nptII* probe (see above).

Table 6. Southern analysis using a [^{32}P]-labelled *gusA* right border probe with *Hin*dIII or *Eco*RI-digested genomic DNA from plants transformed with pANDY9.

Plant	*Hin*dIII Digest/Band Size (kb)	*Eco*RI Digest/Band Size (kb)	T-DNA Copies
62	12.0	nd	1
74	nd	5.6	1
75	nd	14.9	1
76	nd	4.3	1
77	nd	17.4	1
78	40.0	3.4	1
79	14.2	10.0	1
93	8.5	2.0	1
94	31.0; 5.0	13.5[1]; 7.9	1
95	17.1	nd	1
96	7.4	nd	1
97	51.4; 4.4	nd	2
98	27.0	nd	1
99	9.1; 7.9	nd	1
100	51.0	nd	1
101	31.8[1]; 13.5	nd	1
102	18.8[1]; 11.2[1]; 2.4	nd	1
103	23.5	nd	1
115	11.9	nd	1

[1]suspected partial digest (usually a faint band relative to others in that lane)

T-DNA copy number in the righthand column was based upon left border inserts as determined by *nptII* probe of *Hin*dIII digested genomic DNA (Table 3, p. 192). In some cases, the number of bands detected using the *gusA* probe did not match those detected using the *nptII* probe (see above).

Table 7. Southern analysis using a [^{32}P]-labelled *gusA* right border probe with *Hin*dIII or *Eco*RI-digested genomic DNA from plants transformed with pANDY10.

Plant	*Hin*dIII Digest/Band Size (kb)	*Eco*RI Digest/Band Size (kb)	T-DNA Copies
65	12.0	3.4	1
66	nd	27.1	1
69	nd	12.3; 7.9	1
70	nd	17.4; 11.6	2
71	nd	4.6	1
72	8.5; 7.2	7.1; 5.7	2
73	21.0[1]; 13.3	11.6	1
92	nd	2.5	1

[1]suspected partial digest (usually a faint band relative to others in that lane)

T-DNA copy number in the righthand column was based upon left border inserts as determined by *nptII* probe of *Hin*dIII digested genomic DNA (Table 4, p. 194). In some cases, the number of bands detected using the *gusA* probe did not match those detected using the *nptII* probe (see above).